

Materials Forming, Machining and Tribology

Diego Carou
J. Paulo Davim *Editors*


Notes for Manufacturing Instructors

From Class to Workshop

 Springer

Materials Forming, Machining and Tribology

Series Editor

J. Paulo Davim , Department of Mechanical Engineering, University of Aveiro,
Aveiro, Portugal

This series fosters information exchange and discussion on all aspects of materials forming, machining and tribology. This series focuses on materials forming and machining processes, namely, metal casting, rolling, forging, extrusion, drawing, sheet metal forming, microforming, hydroforming, thermoforming, incremental forming, joining, powder metallurgy and ceramics processing, shaping processes for plastics/composites, traditional machining (turning, drilling, milling, broaching, etc.), non-traditional machining (EDM, ECM, USM, LAM, etc.), grinding and others abrasive processes, hard part machining, high speed machining, high efficiency machining, micro and nanomachining, among others. The formability and machinability of all materials will be considered, including metals, polymers, ceramics, composites, biomaterials, nanomaterials, special materials, etc. The series covers the full range of tribological aspects such as surface integrity, friction and wear, lubrication and multiscale tribology including biomedical systems and manufacturing processes. It also covers modelling and optimization techniques applied in materials forming, machining and tribology. Contributions to this book series are welcome on all subjects of “green” materials forming, machining and tribology. To submit a proposal or request further information, please contact Dr. Mayra Castro, Publishing Editor Applied Sciences, via mayra.castro@springer.com or Professor J. Paulo Davim, Book Series Editor, via pdavim@ua.pt


Diego Carou · J. Paulo Davim
Editors


Notes for Manufacturing Instructors

From Class to Workshop

 Springer

Editors

Diego Carou 
Departamento de Deseño na Enxeñaría,
Escola de Enxeñaría Aeronáutica e do
Espazo
Universidade de Vigo
Ourense, Spain

J. Paulo Davim 
Department of Mechanical Engineering
University of Aveiro
Aveiro, Portugal

ISSN 2195-0911 ISSN 2195-092X (electronic)
Materials Forming, Machining and Tribology
ISBN 978-3-031-48467-4 ISBN 978-3-031-48468-1 (eBook)
<https://doi.org/10.1007/978-3-031-48468-1>

© The Editor(s) (if applicable) and The Author(s), under exclusive license to Springer Nature Switzerland AG 2024

This work is subject to copyright. All rights are solely and exclusively licensed by the Publisher, whether the whole or part of the material is concerned, specifically the rights of translation, reprinting, reuse of illustrations, recitation, broadcasting, reproduction on microfilms or in any other physical way, and transmission or information storage and retrieval, electronic adaptation, computer software, or by similar or dissimilar methodology now known or hereafter developed.

The use of general descriptive names, registered names, trademarks, service marks, etc. in this publication does not imply, even in the absence of a specific statement, that such names are exempt from the relevant protective laws and regulations and therefore free for general use.

The publisher, the authors, and the editors are safe to assume that the advice and information in this book are believed to be true and accurate at the date of publication. Neither the publisher nor the authors or the editors give a warranty, expressed or implied, with respect to the material contained herein or for any errors or omissions that may have been made. The publisher remains neutral with regard to jurisdictional claims in published maps and institutional affiliations.

This Springer imprint is published by the registered company Springer Nature Switzerland AG
The registered company address is: Gewerbestrasse 11, 6330 Cham, Switzerland

Paper in this product is recyclable.

Preface

Manufacturing is one of the core topics in most of the undergraduate and graduate engineering courses. Many textbooks have been published dealing with manufacturing processes in general, but also with specific processes in a more comprehensive way. Thus, students and teachers have abundant available literature to learn about the foundations of the processes and learn to apply theories and equations to analyze these processes. Some of these textbooks are being updated from time to time and becoming recommended textbooks in many universities worldwide. Thus, it is possible to recognize a common knowledge on manufacturing that is being transmitted to engineering students.

Traditionally, manufacturing engineering also has included in their programs both lab and workshop sessions. Of course, the extent of these activities greatly depends on the available resources of the schools. In the past, more theoretical approaches have been embraced by educational institutions, in particular universities. However, in the last decades, a shift has been happening from memorization approaches toward learning processes based on the acquisition of competencies by students, aiming to facilitate more meaningful learning experiences. In this context, ‘learning by doing’ methodologies are especially helpful. In manufacturing, labs, and workshops already have a long tradition. There are different ways to approach these activities, but they may help students, among others, to connect theory and practice; to take advantage of technology; to cooperate and learn from peers; to plan, organize, and execute tasks; and to analyze results and deliver reports.

Manufacturing researchers and instructors have driven their attention mainly to the publication of textbooks and research studies, and thus, there is not enough updated literature related to software and lab sessions. It is possible to find information, but it is dispersed through different Internet sites, conference proceedings, journals, etc. Of course, there is a myriad of factors creating this divide, but the truth is that there is still a lack of this type of literature. In this sense, the present book aims at creating a comprehensive study of applied manufacturing engineering. Thus, we have contacted teachers from all over the world to contribute to writing chapters dealing with software and workshop lectures. To do that, we decided to establish a

common structure for all the contributions, not missing key information for readers and aiming at providing a helpful textbook to use mainly at schools.

The book is arranged in a way that software-related chapters appear first. In this sense, human-centered design through additive manufacturing (Chap. [Human-Centered Design Through Additive Manufacturing](#)), materials selection for aerospace engineering (Chap. [Enhancing Materials and Manufacturing Education with Materials Databases: A Case Study in Aerospace Engineering](#)), product design using injection-molding software (Chap. [Understanding the Virtual Injection Molding Product Design](#)), and bulk metal forming analysis using both analytical and numerical methods (Chap. [Bulk Metal Forming Processes: Analytical and Numerical Analysis](#)) are covered. The following Chaps. ([Polymers Injection Molding, Process & Defects—Material Extrusion-Based Additive Manufacturing: Experimental Determination of Process Parameters with Influence on Printing Time, Material Consumption, Surface Roughness and Torsional Strength—Comparison Between the Investment Casting Process \(Lost Wax Casting\) and Machining \(Turning\) in Terms of Dimensional Accuracy and Surface Finish](#) and [Monitoring of Cutting Forces in Turning](#)) focus more directly on the workshop. Thus, next, Chap. [Polymers Injection Molding, Process & Defects](#) deals with the injection process for polymers. The understanding of processes such as material extrusion, investment casting, and turning is covered in Chaps. [Material Extrusion-Based Additive Manufacturing: Experimental Determination of Process Parameters with Influence on Printing Time, Material Consumption, Surface Roughness and Torsional Strength—Comparison Between the Investment Casting Process \(Lost Wax Casting\) and Machining \(Turning\) in Terms of Dimensional Accuracy and Surface Finish](#) and [Monitoring of Cutting Forces in Turning](#). Chapters [Practical Guide of Project-Based Learning \(PBL\) Applied to Manufacturing Technology Subject](#) and [Cavity Manufacturing of Curvilinear Shapes by EDM: Practical Application Through CAM Machining of Electrodes](#) offer comprehensive approaches to the learning process in manufacturing. These chapters allow an understanding of a large range of activities from designing to measuring and including different manufacturing processes. Chapter [Study of Quality Parameters for Abrasive Waterjet Cutting of Metals](#) covers non-conventional machining. In this chapter, the authors analyze the abrasive waterjet cutting process. Inspection of additive manufactured parts through computed tomography is presented in Chap. [Introduction to Computed Tomography: Application to the Inspection of Material Extruded Tensile Testing Specimens](#). Moreover, Chap. [Optimization of the Turning Process by Means of Machine Learning Using Published Data](#) offers an example of using machine learning to optimize the turning process using published data. Finally, the book includes in Chap. [Creating Accessible Interactive Training Materials in Manufacturing Engineering](#) a study on the creation of accessible interactive training materials to use in manufacturing engineering.

We would like to thank all contributors for their involvement in this book and their willingness to communicate and, in this sense, help new instructors and students learn manufacturing engineering with an applied approach.

Aveiro, Portugal

J. Paulo Davim
Diego Carou

Contents

Human-Centered Design Through Additive Manufacturing	1
Elena Arce, Andrés Suárez-García, Rosa Devesa-Rey, and Miguel Álvarez-Feijoo	
Enhancing Materials and Manufacturing Education with Materials Databases: A Case Study in Aerospace Engineering	21
David Álvarez and David López-Adrio	
Understanding the Virtual Injection Molding Product Design	39
Alberto García-Collado and Rubén Dorado-Vicente	
Bulk Metal Forming Processes: Analytical and Numerical Analysis	49
João P. M. Pragana, M. Beatriz Silva, and Bárbara P. P. A. Gouveia	
Polymers Injection Molding, Process & Defects	81
David López-Adrio and David Álvarez	
Material Extrusion-Based Additive Manufacturing: Experimental Determination of Process Parameters with Influence on Printing Time, Material Consumption, Surface Roughness and Torsional Strength	105
Pablo E. Romero	
Comparison Between the Investment Casting Process (Lost Wax Casting) and Machining (Turning) in Terms of Dimensional Accuracy and Surface Finish	117
Irene Buj-Corral and Alejandro Dominguez-Fernández	
Monitoring of Cutting Forces in Turning	131
Branislav Sredanovic and Diego Carou	
Practical Guide of Project-Based Learning (PBL) Applied to Manufacturing Technology Subject	151
Alejandro Pereira and José L. Diéguez	

Cavity Manufacturing of Curvilinear Shapes by EDM: Practical Application Through CAM Machining of Electrodes 185
José L. Diéguez and Alejandro Pereira

Study of Quality Parameters for Abrasive Waterjet Cutting of Metals 221
Bogdan-Alexandru Chirita, Eugen Herghelegiu, Maria-Crina Radu, and Nicolae-Catalin Tampu

Introduction to Computed Tomography: Application to the Inspection of Material Extruded Tensile Testing Specimens 259
Marcos Alonso, Eugenio López, David Álvarez, and Diego Carou

Optimization of the Turning Process by Means of Machine Learning Using Published Data 273
Francisco de Arriba-Pérez, Silvia García-Méndez, Diego Carou, and Gustavo Medina-Sánchez

Creating Accessible Interactive Training Materials in Manufacturing Engineering 289
Şener Karabulut and Şirin Okyayuz

Index 319

Contributors

Marcos Alonso Escola de Enxeñaría Aeronáutica e do Espazo, Universidade de Vigo, Ourense, Spain

David Álvarez CINTECX, Universidade de Vigo, EEI, ENCOMAT Group, Vigo, Spain

Miguel Álvarez-Feijoo Defense University Center, Naval Academy, University of Vigo, Marín, Pontevedra, Spain

Elena Arce Department of Industrial Engineering, Polytechnic School of Engineering of Ferrol, University of A Coruña, A Coruña, Spain

Irene Buj-Corral Department of Mechanical Engineering, Barcelona School of Industrial Engineering (ETSEIB), Universitat Politècnica de Catalunya (UPC), Barcelona, Spain

Diego Carou Departamento de Deseño na Enxeñaría, Escola de Enxeñaría Aeronáutica e do Espazo, Universidade de Vigo, Ourense, Spain

Bogdan-Alexandru Chirita Department of Industrial Systems Engineering and Management, Faculty of Engineering, “Vasile Alecsandri” University of Bacau, Bacau, Romania

Francisco de Arriba-Pérez Grupo de Tecnoloxías da Información, atlantTic, Universidade de Vigo, Vigo, Spain

Rosa Devesa-Rey Defense University Center, Naval Academy, University of Vigo, Marín, Pontevedra, Spain

José L. Diéguez Departamento de Deseño na Enxeñaría, Escola de Enxeñaría Industrial, Universidade de Vigo, Vigo, Spain

Alejandro Dominguez-Fernández Department of Mechanical Engineering, Barcelona School of Industrial Engineering (ETSEIB), Universitat Politècnica de Catalunya (UPC), Barcelona, Spain

Rubén Dorado-Vicente Dpto. Ingeniería Mecánica y Minera, Universidad de Jaén, Jaén, Spain

Alberto García-Collado Dpto. Ingeniería Mecánica y Minera, Universidad de Jaén, Jaén, Spain

Silvia García-Méndez Grupo de Tecnologías da Información, atlantTic, Universidade de Vigo, Vigo, Spain

Bárbara P. P. A. Gouveia IDMEC, Instituto Superior Técnico, Av. Rovisco Pais, Lisboa, Portugal

Eugen Herghelgiu Department of Industrial Systems Engineering and Management, Faculty of Engineering, “Vasile Alecsandri” University of Bacau, Bacau, Romania

Şener Karabulut Department of Mechanical Program, Hacettepe University, Ankara, Turkey

David López-Adrio Deseño na Enxeñaría Department, Universidade de Vigo, EEI, Vigo, Spain

Eugenio López Instituto de Agroecología y Alimentación, Facultad de Ciencias, University of Vigo, Ourense, Spain

Gustavo Medina-Sánchez Departamento de Ingeniería de los Procesos de Fabricación, Universidad de Jaén, Jaén, Spain

Şirin Okyayuz Department of Translation and Interpreting, Hacettepe University, Ankara, Turkey

Alejandro Pereira Departamento de Deseño na Enxeñaría, Escola de Enxeñaría Industrial, Universidade de Vigo, Vigo, Spain

João P. M. Pragana IDMEC, Instituto Superior Técnico, Av. Rovisco Pais, Lisboa, Portugal

Maria-Crina Radu Department of Industrial Systems Engineering and Management, Faculty of Engineering, “Vasile Alecsandri” University of Bacau, Bacau, Romania

Pablo E. Romero Department of Mechanical Engineering, University of Cordoba, Cordoba, Spain

M. Beatriz Silva IDMEC, Instituto Superior Técnico, Av. Rovisco Pais, Lisboa, Portugal

Branislav Sredanovic Faculty of Mech. Engineering, University of Banjaluka, Banja Luka, Republic of Srpska, Bosnia and Herzegovina

Andrés Suárez-García Defense University Center, Naval Academy, University of Vigo, Marín, Pontevedra, Spain

Nicolae-Catalin Tampu Department of Industrial Systems Engineering and Management, Faculty of Engineering, “Vasile Alecsandri” University of Bacau, Bacau, Romania

Human-Centered Design Through Additive Manufacturing



Elena Arce , Andrés Suárez-García , Rosa Devesa-Rey ,
and Miguel Álvarez-Feijoo 

1 Introduction

Engineering Drawing plays a vital role in STEAM disciplines (Science, Technology, Engineering, Arts, and Math) (Perignat & Katz-Buonincontro, 2019). It is a mandatory course typically taught during the first year of engineering programs. Mastery of Engineering Drawing is critical for students to become competent engineers capable of designing innovative solutions to complex challenges. The primary goal of this subject is to equip students with the necessary skills to solve engineering graphic problems, communicate solutions clearly and objectively, and develop spatial visualization abilities, as stated in the teaching guides of STEAM degrees that include this subject in their curriculum. To achieve these goals, teachers are encouraged to design activities that help students learn graphic representation techniques and Information and Communication Technology (ICT) tools. These activities are intended to enhance students' understanding of the subject matter and foster critical thinking, creativity, and problem-solving skills.

Research has demonstrated that students require a combination of both core skills (hard) and transferable skills (soft) in order to succeed academically and professionally (Clarke, 2018). The development of soft skills is considered highly relevant by both the Organization for Economic Cooperation and Development (OECD) and the European Union, given their importance in both the educational system and the labor market (Hurrell et al., 2013; Llamas et al., 2019). As a result, education policies

E. Arce

Department of Industrial Engineering, Polytechnic School of Engineering of Ferrol, University of A Coruña, A Coruña, Spain

e-mail: elena.arce@udc.es

A. Suárez-García (✉) · R. Devesa-Rey · M. Álvarez-Feijoo

Defense University Center, Naval Academy, University of Vigo, Plaza de España S/N, 36920 Marín, Pontevedra, Spain

e-mail: andres.suarez@cud.uvigo.es

at the government level should prioritize the development of soft skills. However, conventional syllabus design methodologies, content, and assessment systems tend to prioritize the development of core skills rather than transferable skills. Therefore, it is imperative that lecturers actively promote the development of both types of skills and focus on designing materials and experiences that prioritize skill development over content. In other words, content should serve as a resource for the development of competencies, rather than the primary focus of learning activities (Rizzi et al., 2020).

Design plays a critical role in engineering by enabling the creation of effective solutions that meet the evolving needs of society (Simon, 2019). To meet the demands of an ever-changing context, learners require flexible methods that foster innovation and enable quick adaptation. Two methodologies that have gained recognition for innovation generation are Design Thinking (DT) and Design Sprint (DS). DT, developed by the Hasso Plattner Institute at Stanford University, prioritizes iterative and user-centered design to enhance problem-solving abilities and follows a cyclical process of inspiration, ideation, and implementation (Plattner et al., 2011). However, due to its relatively lengthy timeframe, Google Ventures combined DT with agile methodologies to create the 5-day DS method, aligning with the product planning using a natural calendar (Knapp et al., 2016). Unlike the “launch and iterate” model popular in Silicon Valley user research projects, the DS model allows for the testing of prototypes without the risk and expense of a full product launch (Google Ventures, 2021). The experience described was carried out in the Engineering Drawing course at the University of A Coruña (Spain). The DS method was chosen over DT to prioritize skill development and avoid costly mistakes inherent in the “launch and iterate” model.

Human-centered design (HCD) is a problem-solving approach that aims to comprehend and cater to the needs, desires, and behaviors of the individuals who will be using the product, service, or system under consideration. This approach entails developing empathy towards users, observing their experiences, creating prototypes, testing solutions, and iterating based on feedback to create effective, usable, and desirable solutions. HCD has been widely adopted in various fields, including product design, user experience design, service design, healthcare, education, and social innovation. Research has shown that this approach is highly effective in enhancing outcomes and user satisfaction across a diverse range of contexts (Lupton & Lipps, 2018; Norman & Verganti, 2014).

HCD and DS are two approaches that can be used in conjunction to design solutions that are effective and user-centered (Pokorni et al., 2020). Design Sprint can be seen as a compressed version of the HCD process. While HCD involves several iterations and can take weeks or months to complete (Zoltowski et al., 2012), a Design Sprint can be completed in as little as five days. Design Sprint uses HCD principles to create a rapid prototype, test it with end-users, and iterate based on feedback to develop a final solution. Thus, Design Sprint can be seen as a focused application of the HCD process that can accelerate the design process and create agile solutions.

Service-learning is an educational approach that combines academic learning with community service to promote civic engagement and social responsibility

(Erickson & Anderson, 1997; Felten & Clayton, 2011). It is a pedagogy that emphasizes experiential learning, in which students engage in community service activities that are directly related to the course material and reflect on their experiences to enhance their learning. Service-learning has been widely recognized as an effective approach to enhancing student learning and engagement. Moreover, it has been found to be particularly effective in STEAM education (Blanco et al., 2022), where it can help students to apply their knowledge and skills to real-world problems and foster their creativity and innovation. Studies have shown that service-learning can enhance student critical thinking, problem-solving and communication skills, as well as their motivation and engagement in learning. The approach also benefits the community by providing valuable services and addressing real-world problems. The Office of Cooperation and Volunteering at the University of A Coruña (UDC) promotes service-learning initiatives that aim to connect academic learning with community service and foster civic engagement among students. The office coordinates and supports service-learning projects in different fields, including STEAM education, health, social work, and environmental sustainability. In this experience, collaboration was done with ASPANEPS (Association of Parents of Children with Psycho-Social Problems, by its Spanish acronym). Particularly, the projects tried to respond to specific needs expressed by the entities themselves and that can be met through the realization of a resource designed ad-hoc and developed through additive manufacturing methods. In this context, a service-learning project was initiated to utilize the power of engineering in solving real-life problems. The project topics were chosen with the goal of connecting with the current reality of the society and highlighting the crucial role of engineering in tackling society issues. The utilization of the HCD-DS methodology proved to be effective in the successful creation of a product for society requirements. This project not only demonstrated the potential of engineering in addressing current challenges, but also served as a reminder of the importance of innovation.

2 Background

The DS methodology, commonly used for software design, can also be applied to product design (Wilkerson & Trellevik, 2021). Human-Centered Design has many applications (e.g. Product design, User experience (UX), Service design, Architecture and urban planning, Social innovation). When implemented in a learning environment, students can acquire both subject-specific and cross-cutting competencies, including creativeness, decision-making, cooperation and communication. The HCD-DS approach, therefore, cultivates both technical and soft skills. By utilizing the HCD-DS method, students were able to complete a comprehensive design task covering all phases and techniques taught in the course, such as sketching, 2D plans, and 3D modeling, under a Challenge Based Learning approach (Fig. 1). Combining these two methodologies, the Human-Centered Design approach is adapted to fit into the Design Sprint process. The Design Sprint process helps to compress the timeline

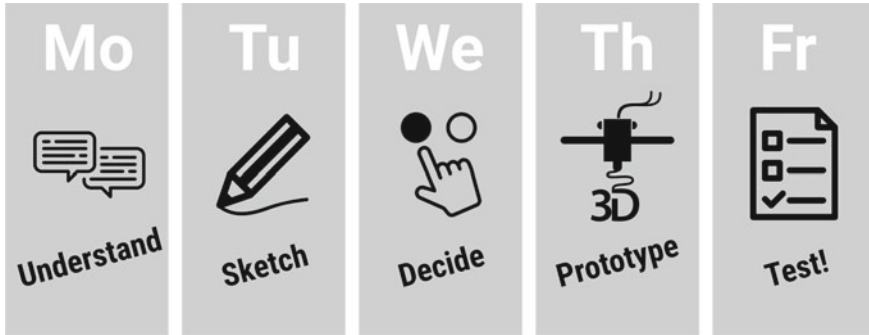


Fig. 1 Design sprint stages

for Human-Centered Design, making it possible to quickly ideate, prototype, and test solutions with users.

The evaluation of the HCD-DS experience was aligned with the 17 Sustainable Development Goals (SDGs) of the United Nations' 2030 Agenda (United Nations. Department of Economic and Social Affairs. Sustainable development, 2020). This initiative contributes to four specific targets: enhancing technical and vocational skills for entrepreneurship and employment, supporting innovation and scientific research, promoting technology development in developing nations, and implementing sustainable consumption and production programs. These targets fall under the Quality Education, Industry, Innovation and Infrastructure, and Responsible Consumption and Production SDGs (as shown in Fig. 2). The integration of Human-Centered Design and Design Sprint projects aims to achieve sustainability by creating tailored solutions that meet user needs while promoting sustainable consumption and production (Target 12). By participating in the HCD-DS activity, students develop hard skills in scientific research, innovation, and value creation associated with Target 9 b. Additionally, the HCD-DS methodology fosters the development of soft skills, which are highly sought after in both the labor market and society (Target 4).

3 Learning Objectives

Bloom's Taxonomy is a framework that classifies educational goals into six levels of cognitive complexity. These levels range from basic thinking skills like remembering and understanding, to more advanced skills such as analyzing, applying, evaluating, and creating (Krathwohl, 2002). When applied to teaching activities, this taxonomy can be used to generate learning objectives that guide instruction and assessment (Forehand, 2005). Bloom's Taxonomy was applied to learning objectives for a Human-Centered Design and Design Sprint project with a service-learning scope:



Fig. 2 Sustainable development goals of 2030 Agenda applied in this experience

- **Remembering:** Students will be able to recall the key principles of Human-Centered Design and Design Sprint methods.
- **Understanding:** Students will be able to explain how Human-Centered Design developed with the focus of Design Sprint with a Service-Learning scope can be used to solve real-world problems and improve people's lives. That is, understand the concept of empathy and how it can be used to design educational resources that meet the needs of children with psychosocial problems.
- **Applying:** Students will be able to apply the concepts and ideas Human-Centered, Design Sprint and Service-Learning principles to develop solutions to real-world problems. In this approach, the students had to develop a prototype of an educational resource for children with psychosocial problems that incorporates their feedback from user testing.
- **Analyzing:** Students will be able to analyze user needs and feedback to refine and improve their solutions. That is, analyze the feedback from user testing to identify strengths and weaknesses of the prototype and make recommendations for improvement.
- **Evaluating:** Students will be able to evaluate the effectiveness of their solutions in meeting user needs and achieving their goals.
- **Creating:** Students will be able to create innovative and effective solutions that address real-world problems and have a positive impact on people lives.

Overall, the learning objectives of a HCD combined with DS project with a service-learning scope aim to develop students' competencies and skills in innovation, entrepreneurship, and social responsibility, while also promoting community engagement and positive social impact.

4 Resources and Organization

To improve the design under development, students are required to create a prototype using FreeCAD, where sketches can be drawn, and files can be exported to *.stl for 3D printing. It is a free and open-source Computer-Aided Design (CAD) software that allows users to create 3D models of physical objects. It is available for Windows, Mac, and Linux operating systems, making it accessible to a wide range of users. The software supports a variety of file formats, including STEP, IGES, OBJ, STL, DXF, and SVG, making it easy to exchange files with other CAD software. FreeCAD uses a parametric modeling approach, which means that the dimensions and parameters of the model can be easily edited and updated. This allows users to quickly make changes to their designs and explore different design options. In addition, FreeCAD has a built-in Python console that allows users to automate repetitive tasks and create complex models using Python scripting. However, FreeCAD can be complex and difficult to learn, especially for users who are new to CAD software.

The monitoring of tutored work can be carried out both in-person and online. In-person monitoring allows for more direct and personal communication, which enables a more detailed and precise review of the work. However, in-person monitoring can be limiting in terms of availability and accessibility of the involved parties. On the other hand, online monitoring allows for greater flexibility and convenience for both parties, as a specific physical space is not required to carry out the tutoring. Additionally, online monitoring can be more efficient in terms of time and resources and allows for the possibility of sharing and reviewing documents in a faster and simpler way. In this experience, the Microsoft Teams platform was used for online monitoring.

Measuring student opinions about teaching–learning activities is important for several reasons. First, it provides valuable feedback that can be used to improve the learning experience. Second, measuring student opinions can help to create a more inclusive and equitable learning environment. By soliciting feedback from all students, including those from diverse backgrounds, instructors can ensure that the teaching–learning activities are accessible and effective for everyone. Finally, measuring student opinions can help to promote student engagement and ownership of the learning process. When students feel that their opinions and feedback are valued, they are more likely to be engaged and motivated in the learning process.

For this purpose, the Net Promoter Score (NPS) survey was applied at the end of the experience. The Net Promoter Score (NPS) is a metric used to measure customer loyalty and satisfaction with a product or service. It is often used in customer satisfaction surveys to gauge how likely customers are to recommend a product or service to others (Palmer & Devers, 2018). To calculate NPS, respondents are typically asked the following single question “On a scale of 0–10, how likely are you to recommend this product/service to a friend or colleague?” Based on their response, respondents are then classified into one of three groups: promoters (score of 9 or 10), passives (score of 7 or 8), or detractors (score of 0–6) (Juntumaa et al., 2020). The NPS is calculated by subtracting the percentage of detractors from the percentage of

promoters, resulting in a score between -100 and $+100$. A positive score indicates that a majority of respondents are promoters, while a negative score indicates that a majority of respondents are detractors.

5 Session Development

Design Sprint, as it was said, consists of five phases: Understand, Sketch, Decide, Prototype, and Test, which include both divergence and convergence cycles (Fig. 3) (Google Ventures, 2019). The Human-Centered Design approach was tailored to fit the stages of the Design Sprint. During the Understand phase, team members use divergent thinking to gather information and identify the problem they need to solve. In the Sketch phase, they generate as many ideas as possible using divergent thinking. Next, in the Decide phase, the team converges on a single solution to prototype. In the Prototype phase, they use divergent thinking again to create multiple versions of the chosen solution. Finally, in the Test phase, they converge again to test the prototype and determine whether it solves the problem. This entire process involves switching between divergent and convergent thinking to efficiently generate and assess potential solutions.

During Stage 1 of the HCD-DS method, Understand, the objective is to comprehend the problem and determine the goal. A real example in a university environment was used to contextualize the process to be followed. So, 12 working groups were formed: 3 groups of 4 members and 9 groups of 3 members. The problem given to the

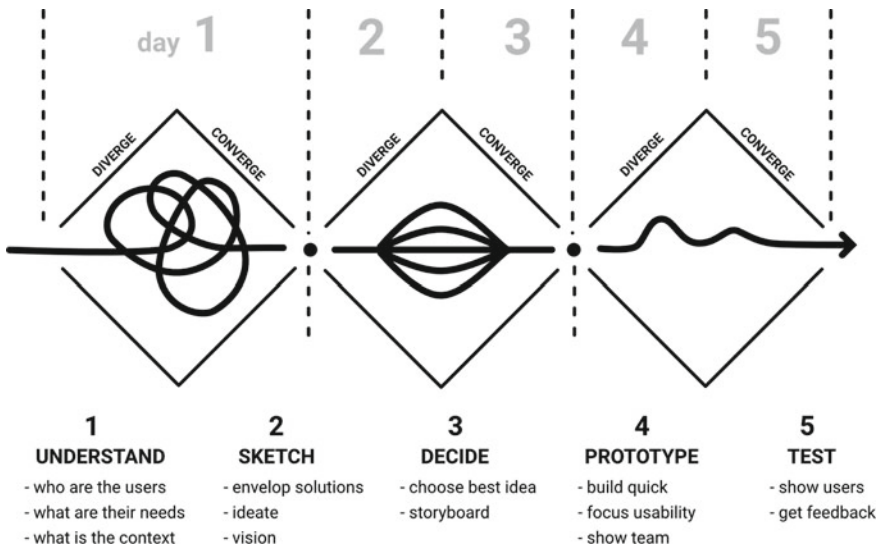


Fig. 3 Design sprint divergence and convergence cycles

students was to design a resource for children in the stage of acquiring reading skills who need to learn how to write from manual exploration to performing the stroke that can be manufactured using a 3D printer. The target user were children (age 6–8 years) with disabilities who attend the ASPANEPS organization. ASPANEPS is a Spanish non-profit organization that provides services and support to children and young adults with disabilities, as well as their families. Founded in 1963, the organization offers a wide range of programs and resources, including educational and therapeutic interventions, leisure activities, and social and occupational training. The main goal of ASPANEPS is to promote the full inclusion and participation of people with disabilities in society, as well as to advocate for their rights and needs. The user conditions include Autism Spectrum Disorder (ASD), Attention Deficit Hyperactivity Disorder (ADHD), and intellectual disability, and in some cases, hypersensitivity to noises and sounds. From the interviews, it was also extracted that primary colors should be used in the resin design for children with visual difficulties. Each group was assigned a workspace and a team leader. The team had to gather all available information about the user profile and the problem. Throughout this stage, the team had to define who will be using the product and how it will solve a problem for them. Students had to share their knowledge about the problem in their groups and constantly ask “How might we...?” to generate ideas.

The Sketch phase is a crucial part of the HCD-DS process. During this phase, students take the knowledge gathered during the Understand phase and use it to generate solutions. The primary goal of this phase is to come up with as many ideas as possible, without being limited by practicality or feasibility. Sketching is a quick and low-fidelity way to generate ideas. The focus is on generating a large quantity of ideas rather than spending time perfecting a single one. The Sketch phase is a highly divergent phase where participants are encouraged to explore a wide range of possibilities. One of the main benefits of the Sketch phase is that it allows participants to approach problems from different perspectives. By using visual representations, participants can easily communicate complex ideas and collaborate with others. It also promotes an open and non-judgmental environment that encourages creativity and innovation. At the end of the Sketch phase, participants should have a range of different solutions to choose from.

During the third phase of the HCD-DS, Decide, the team evaluates all the solutions generated during the Sketch phase and decides which one to move forward with. The goal is to converge on a solution that has the most potential to meet the sprint goal. The team reviews all the sketches and team members select their favorite solution. This process is usually done using a democratic approach such as dot voting; where each member is given a certain number of votes to distribute among the sketches they believe are the strongest solutions. After the votes have been cast, the team discusses the results and any patterns that emerged. They may also discuss any solutions that were not selected but still have potential. A storyboard for the design of the prototype is then created, and the selected sketch has to be fully defined and dimensioned according to UNE 1-039-94 standard.

In the Prototype phase, the team transforms the selected solution sketch into a tangible and interactive prototype. This is a rough representation of the solution,

allowing users to interact with the product and provide feedback. The team can use a variety of tools and techniques, including paper prototyping, digital wire framing, additive manufacturing or even a combination. It is important to keep the design simple and not get bogged down in details. The idea is to create a functional prototype that can be used to test the core functionality and get feedback on its usefulness. Additive manufacturing, commonly known as 3D printing, is a popular method of physical prototyping used during the Prototype phase. This method allows for the quick creation of physical prototypes using various materials, such as plastic or metal. The use of 3D printing allows the team to physically interact with the prototype and test its functionality, identifying any flaws or areas that need improvement. The final selected prototype was exported as STL file and shared with the online community.

Finally, students evaluate the projects in Stage 5 (Test). This phase involved selecting a group of representative users, who will test the prototype and provide feedback on its usability and effectiveness. These users were not related with the evaluated prototype and were asked to provide feedback on the design, such as the visual elements, layout, and overall effectiveness of the design. Feedback may be used to adjust the design before it is finalized and presented to the client or the intended audience. In order to present the prototype, it is recommended an agile presentation format like Ignite format, which consists in a five-minute presentation with 20 slides. Each slide was shown for 15 s, requiring clear communication.

6 Outcomes

In Stage 1 (Understand) students formed working groups and put themselves in the shoes of the user. They made questionnaires with open-ended, yes/no, and Likert-type scale questions. Since it was not possible to directly interact with the children due to being minors, empathetic interviews were conducted with the speech therapy and psychology professionals of the organization. After several iterations, the groups generated a form with the typical user profile. The responses showed that users do not prefer any particular design linked to children's drawings. The resources should be designed for individual and group activities. The most popular "how could we" questions were about creating a product to aid reading comprehension and fine motor skills for children with ASD or ADHD with an attractive design.

Example interview conducted with open-ended responses made by students from speech therapists and psychologists:

Question: Are you looking for a resource related to letters, numbers or strokes in general?

Answer: Yes, letters and/or numbers.

Question: What is the objective you seek with a resource related to letters? Reading / writing / strokes / individual letters?

Answer: We would need visual materials for the children to learn the stroke of writing, such as a board with depth with letters and/or numbers for them to follow the stroke with their finger, manipulative letters with the direction of the stroke, etc.

Question: What is the objective you seek with a resource related to numbers? Writing them / recognizing them / strokes / operations?

Answer: We would need visual materials for the children to learn the stroke of writing, such as a board with depth with letters and/or numbers for them to follow the stroke with their finger, manipulative letters with the direction of the stroke, etc.

Question: What is their favorite color?

Answer: Indifferent, except for red and green for possible color-blind children.

Question: What is your favorite TV show / cartoon / character?

Answer: Since it will be a material that will be used with various groups, favorite cartoons vary among different users. We would prefer not to have cartoons as it could even distract them.

Question: What type of pathology do they have and how does it affect their daily life?

Answer: Difficulties in reading and writing, dyslexia, ADHD, ASD, and intellectual disability.

Question: How can these pathologies affect them in terms of motor skills?

Answer: Currently, the children who would use this material do not have great difficulties at the motor level, but since they are 6-year-old children with limited fine motor skills, it is important to consider that the pieces are of an appropriate thickness for manipulation.

Question: Do the users have any violent tendencies, impulses to swallow or bite things?

Answer: No.

Question: Do sounds or lights cause discomfort to the users or do they help them maintain attention?

Answer: Above all, in cases with ASD and ADHD, it would be good if the materials did not promote loss of attention as they tend to be distracted by small details. Additionally, some children tend to have hypersensitivity to noises and sounds.

In the second stage of the project (Sketch), the students analyzed real-world solutions that had demonstrated success in their respective fields. These products and ideas served as inspiration and were modified for improvement in the subsequent stage of the final design. To accomplish this task, the students consulted various websites such as <https://www.thingiverse.com/>, <https://cults3d.com/>, and <https://free3d.com/es/>. It was expected that the students would apply the theoretical principles of Engineering Drawing that they had learned throughout the course to practical use. At this stage, the lecturer's guidance and tutoring function became increasingly intensive. Following the practical session, the sketches produced were reviewed through individual feedback discussions aimed at identifying areas for improvement. In Fig. 4, an example is shown of a sketch for a design aimed at developing reading and writing skills.

In Stage 3 (Decide), students critically evaluated the proposals generated in the previous stage. A comprehensive analysis of the pros and cons of each proposal was conducted, and the merits of each alternative were specified. The students then engaged in a democratic decision-making process, voting for the proposal they deemed most appropriate for further development in Stage 4 (Prototyping). Ultimately, the alternative that received the most votes was selected for advancement to the next stage. In Fig. 5, an example is shown of a 3D model of a template for letter tracing that allows for the development of fine motor skills and reading and writing

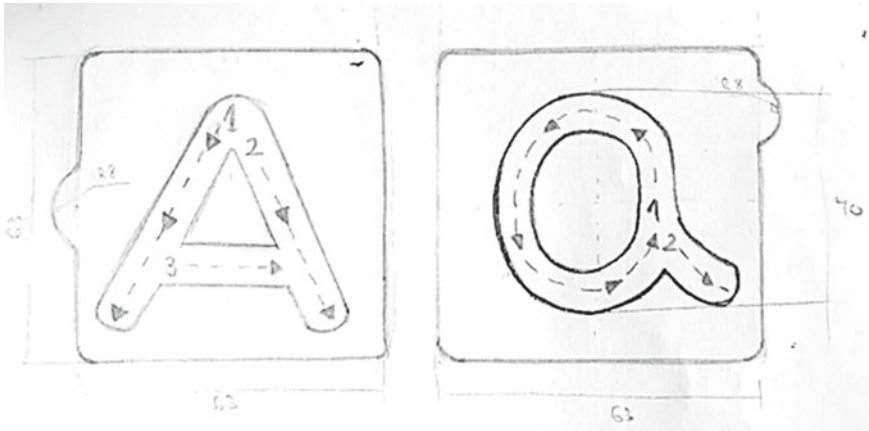


Fig. 4 Sketch of a board with letters (sketch)

abilities. During Stage 4, the 3D modeling process prompted several queries, which necessitated intensive instructional interventions. These concerns were addressed via a Moodle forum, which facilitated the dissemination of information to all course participants. Prior to 3D printing, some student groups created prototypes of their designs to test feasibility. For 3D printing, Chitubox (<https://www.chitubox.com/en>) was the preferred software for preparing *.stl files, owing to its ease of use. Some groups opted for Lychee slicer (<https://mango3d.io/downloads/>) for *.stl file preparation. The final prototype was printed using a Elegoo Saturn printer. The project guidelines informed students of the 3D printer’s model and brand, as this restricted product dimensions and layout in the slicer (maximum print size: 192 × 120 × 200 mm).

In Fig. 6, an example is shown of the support configuration for the slicing of a board for reading and writing activities in the Chitubox environment. In some cases, it was necessary to hollow out the structure so that it could be supported (Fig. 7). It is important for students not only to face the design process but also to have the ability to understand the implications that certain parameters or geometries can have on 3D printing. Although this experience is contextualized in a first-year subject of the degree, students can see the vertical connection that exists in the training program of the degree.

In Stage 5 (Validate), project validation was carried out through an Ignite-style presentation evaluation. Members of the collaborating entities (i.e. ASPANEPS) attended the presentations. Specifically, speech therapists and occupational therapists came to see and test the printed prototypes and provide feedback to the students after the resource presentation. The developed prototypes were shown to the members of the entities (Fig. 8). Co-evaluation was conducted, whereby the students themselves participated in the evaluation of each project.

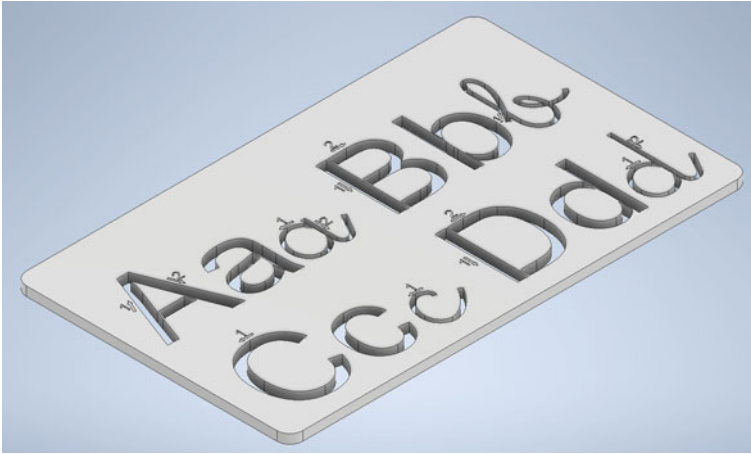


Fig. 5 Modeling letter board to work on literacy and fine motor skills (prototype)

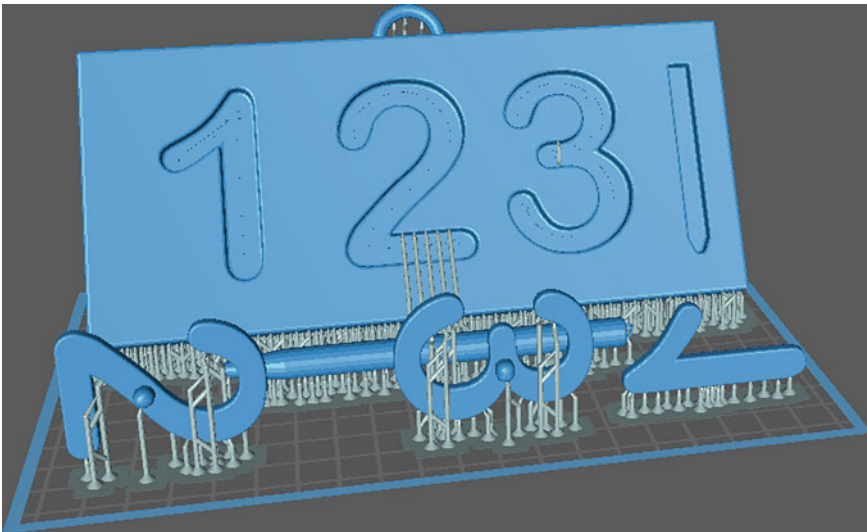


Fig. 6 Slicing configuration in Chitubox environment for a board with letters and numbers (prototype)

7 Deliverables and Assessment

The evaluation methods employed in this study adhered to the guidelines of Biggs and Tang (2011) and employed a constructive alignment approach. This approach ensured a clear alignment between the intended learning outcomes, the assessment system,

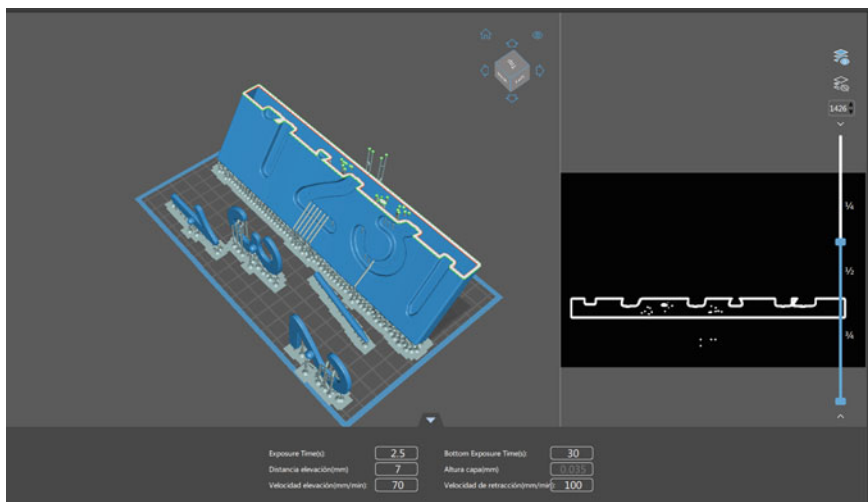


Fig. 7 Structure hollowing and reinforcement placement in the Chitubox environment (prototyping)

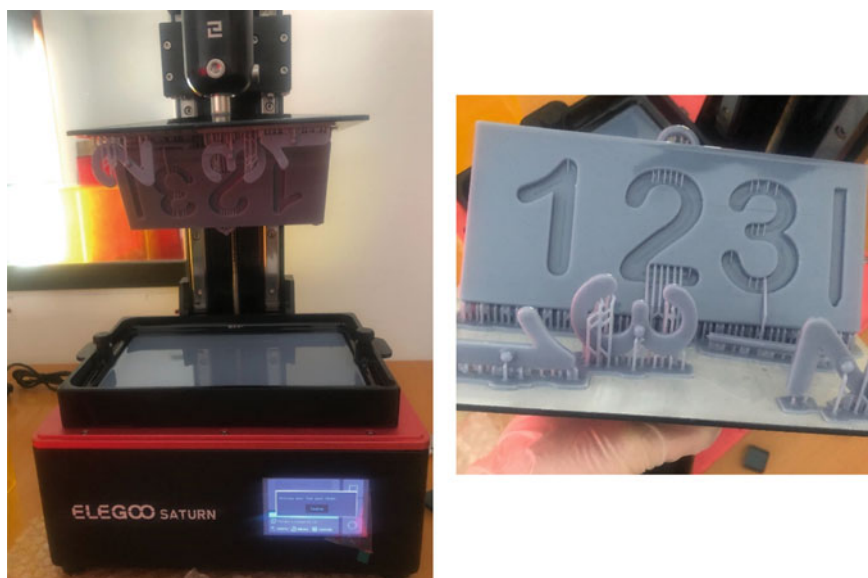


Fig. 8 3D printing of the prototypes (validation)

and the formative activities, specifically focusing on Human-Centered Design and Design Sprint.

To assess student performance in HCD-DS projects, three analytical scoring rubrics were developed: Tables 1, 2, and 3. These rubrics facilitated co-evaluation, hetero-evaluation, and self-evaluation. Each rubric allowed the teacher and student to independently score specific aspects of performance, which were then combined to obtain a total score. Analytical scoring rubrics have the advantage of providing detailed descriptions of expectations at different scoring levels. In this case, a three-level rubric was created, utilizing user-friendly language and criteria derived from Bloom's taxonomy.

The scoring criteria consisted of three levels: Level 1 (Unacceptable), Level 2 (Acceptable), and Level 3 (Excellent). The grading of assignments was based on a

Table 1 Rubric used for peers' assessment (co-evaluation)

	Items	Level 1 (0 points)	Level 2 (1.25 points)	Level 3 (2.5 points)
#1	HCD-DS development	Phases of the HCD-Design Sprint procedure were not elaborated	Phases of the HCD-Design Sprint procedure were partially elaborated	Phases of the HCD-Design Sprint procedure were elaborated
#2	Product	Failure to adapt the product to the target audience	Feasible product developed, but not suitable for the target audience	Feasible and suitable product developed for the target audience
#3	DS description	Design process not explained or justified	Design process explained and justified	Design process explained and justified
#4	3D Model	Unable to generate 3D model or *.stl file	.stl file not generated or partial 3D model	3D model developed, *.stl file generated

Table 2 Rubric used for teacher assessment (hetero-evaluation)

	Items	Level 1 (0 points)	Level 2 (1.25 points)	Level 3 (2.5 points)
#5	Sketch	Sketches not completed, product not defined	Partially dimensioned sketches, partially defined product	Dimensioned sketches, defined product
#6	Dimensions	Incorrect dimensions	Partially correct dimensions	Correct dimensions
#7	Standard	Non-compliance with dimensioning standard	Partial compliance with dimensioning standard	Compliance with dimensioning standard
#8	Part views	Absence of product views in drawings	Inadequate product views in drawings	Sufficient and appropriate product views in drawings
#9	3D model	Numerous errors in the generated 3D solid (and *.stl file)	Some errors in the generated 3D solid (and *.stl file)	Error-free 3D solid (and *.stl file) generated

Table 3 Rubric used for self- evaluation

	Items	Level 1 (0 points)	Level 2 (1.25 points)	Level 3 (2.5 points)
#10	HCD-DS process	Phases of the HCD-Design Sprint procedure were not elaborated	Phases of the HCD-Design Sprint procedure were partially elaborated	Phases of the HCD-Design Sprint procedure were elaborated
#11	Product	Failure to adapt the product to the target audience	Feasible product developed, but not suitable for the target audience	Feasible and suitable product developed for the target audience
#12	3D Model	Unable to generate 3D model or *.stl file	.stl file not generated or partial 3D model	3D model developed, *.stl file generated
#13	Involvement	Limited involvement in one phase of the project	Involvement in multiple phases of the project	Full involvement in all phases of the project

weighting of peer assessment (40%), self-assessment (20%), and teacher assessment (40%). These assignments carried a weight of 7% in the final grade for the subject. The scoring system for the rubrics differed slightly. Items on the co-evaluation and self-evaluation rubrics had a maximum score of 2.5 points (Table 1 and Table 3), while items on the hetero-evaluation rubric had a maximum score of 2 points (Table 2).

The peer review process, also known as co-evaluation, was conducted using the Moodle Workshop module. This module allowed for the monitoring of group progress during the evaluation phases, such as the submission phase and evaluation phase. To ensure consistency and clarity, a rubric was utilized as the grading strategy for the Workshop. The grading evaluation settings were precisely defined, with the grade calculation method comparing assessments to the best one. The submission grade was set at 8, while the assessment grade was set at 2. The final grade was determined as a weighted mean of both the submission and assessment grades. Two types of feedback were provided: an overall feedback mode, where reviewers were required to give a general comment about the submission, and a conclusion section that included teacher comments displayed at the end of the Workshop.

All projects underwent evaluation by other randomly assigned groups three times, demonstrating a high level of consensus among the ratings. During the overall feedback phase, peers primarily focused on suggesting improvements in presentation, addressing security issues with the product, providing activity sheets or usage manuals, and suggesting user profile adaptations. The lecturers’ feedback primarily centered on the dimensioning and perspectives of each design, offering improvement suggestions that required student modifications. Each group was randomly assigned three oral presentation projects to evaluate. The evaluated projects received an average score of 5.92 (*SD* 0.61) out of 8 for the submission grade, and an average score of 1.73 (*SD* 0.13) out of 2 for the assessment grade. The final co-evaluation score was derived from the sum of the submission and assessment grades, resulting

in an average final score of 7.64 points. In the hetero-evaluation conducted by the lecturers, the projects received an average rating of 7.72 points (*SD* 1.73).

In the self-assessment, students evaluated their achievement level in project development and assessed their individual contributions. The lecturers then evaluated the presentation, 3D model, and drawings created using FreeCAD. Self-assessment primarily focused on project development and individual contribution, as shown in Table 1. Students rated themselves with an average score of 8.11 points (*SD* 0.78) in self-evaluation. Several items were common across all three-assessment approaches, allowing for result comparison, such as items #1 and #10, #2 and #11, and #4 and #12.

In general, there is a tendency to score oneself (self-evaluation) higher than co-evaluation and hetero-evaluation. Therefore, the weights (percentages) of each of the three evaluation approaches must be carefully fixed. Otherwise, the final grade could be distorted. If the projects involve significant autonomous workload, it is recommended to conduct a habits test upon completion. The habits test consists of a questionnaire in which students individually answer questions about how they managed the project (e.g. How many times did you meet outside the classroom? Where did you usually meet? How did you communicate to carry out the project?). The questions can be closed or open-ended. The answers can provide information about those students who have not actively participated in the project, as sometimes the group may not manifest the existence of internal problems or uncooperative peers. This questionnaire should be administered in the classroom (using the virtual campus or an online form), under the supervision of the lecturer.

The outcomes of the NPS survey indicated a commendable level of acceptance for the HCD-DS methodology. 38 opinions were registered, with the NPS value indicating 29. Among the respondents, 18 students were promoters, while 13 adopted a passive stance, and 7 were detractors. This outcome is highly favorable, given that NPS scores above zero typically denote satisfactory performance, and those surpassing 50 mean excellence. To substantiate the attainment of a noteworthy NPS value, a comparative analysis was undertaken, juxtaposing the outcome with that of various enterprises (Buell et al., 2015). For instance, Google's NPS score stands at 11, Amazon's at 25, McDonald's at -8, and Facebook at -21. The open-ended question in the NPS survey, "What was the reason for your response?" received an 80% response rate, because it was not mandatory. Student feedback on the HCD-DS method revealed its main advantages as being simple, entertaining, and useful. However, two students mentioned that the method is quite rigid.

8 Further Comments

The traditional pedagogical model, which places the teacher at the center of the teaching-learning process, is becoming obsolete. It is crucial to have active student participation and for the teacher to adopt a facilitator role in learning. Learning is a social process that occurs through interactions with others. Additionally, education

should aim to develop competencies and skills that are not explicitly included in the curriculum but are highly valued by employers (soft skills). To achieve this alignment between competencies, methodologies, and evaluation while maintaining a social perspective, it is recommended to adopt user experience-based methodologies like Human-Centered Design (HCD) or Design Sprint.

The HCD-DS method allows students to engage in interactive learning, where they address various challenges posed by the teacher either individually or in groups. It helps in planning student dedication by outlining expectations at each stage of the project, resulting in a less overwhelming workload and better time management. In this multi-purpose process, applicable to any innovation challenge, the teacher plays the role of a facilitator, despite the focus on product design in this work. The HCD-DS method fosters development in the seven areas of employability skills outlined by the Malaysian Soft Skills Scale while also facilitating links with the 17 Sustainable Development Goals of the 2030 Agenda throughout its five stages. The result is a powerful approach to problem-solving that combines the best of both worlds: the empathy and user-centered focus of Human-Centered Design, and the speed and efficiency of Design Sprint. By putting people at the center of the design process and rapidly iterating on ideas, teams can create innovative solutions that meet real user needs.

9 Conclusions

The present work focuses on using the Human-Centered Design (HCD) and Design Sprint (DS) methodologies to develop an Engineering Drawing classroom experience linked to Service-Learning. The project aims to promote creative and critical thinking in students while solving complex problems. The learning objectives, based on Bloom's Taxonomy, include recalling key principles, understanding the application of HCD and DS, applying concepts to real-world problems, analyzing user feedback, evaluating solution effectiveness, and creating innovative solutions.

The session development followed the five phases of the Design Sprint: Understand, Sketch, Decide, Prototype, and Test. The HCD approach is integrated into each phase, allowing divergent and convergent thinking to generate and evaluate potential solutions. The session included defining the problem, generating ideas through sketching, selecting the most promising solution, creating a prototype (including 3D printing), and testing it with representative users. The resources utilized in the project include FreeCAD, a free and open-source CAD software for creating 3D models, and Microsoft Teams, a collaboration platform for communication and document sharing. The project progress and monitoring can be done both in-person and online, with online monitoring providing flexibility and convenience.

The outcomes of the project showed that users do not have specific design preferences; resources should cater to individual and group activities, and consider the conditions of users with ASD, ADHD, and intellectual disabilities. Primary colors are preferred for better visual perception. The project resulted in valuable insights

for designing resources that aid reading comprehension and fine motor skills for children with ASD or ADHD. Measuring student opinions through the Net Promoter Score (NPS) survey helped to gather feedback to improve the learning experience, create inclusivity, and promote student engagement and ownership.

Overall, the HCD-DS methodology demonstrated its effectiveness in promoting interactive learning, improving time management skills, and creating user-centered solutions. It offers adaptability to various fields and subjects while providing simplicity in its approach.

References

- Biggs, J., & Tang, C. (2011). *Teaching for quality learning at university* (4th ed.). McGraw-Hill education.
- Blanco, T. F., Gorgal-Romarís, A., Núñez-García, C., & Sequeiros, P. G. (2022). Prospective primary teachers' didactic-mathematical knowledge in a service-learning project for inclusion. *Mathematics*, *10*(4), 652.
- Buell, R. W., Raman, A., & Muthuram, V. (2015). *Oberoi hotels: Train whistle in the tiger reserve*. *Harvard Business School Case 615-043*.
- Clarke, M. (2018). Rethinking graduate employability: The role of capital, individual attributes and context. *Studies in Higher Education*, *43*(11), 1923–1937.
- Erickson, J. A., & Anderson, J. B. (1997). Learning with the community: Concepts and models for service-learning in teacher education. Routledge.
- Felten, P., & Clayton, P. H. (2011). Service-learning. *New Directions for Teaching and Learning*, *2011*(128), 75–84.
- Forehand, M. (2005). Bloom's taxonomy: Original and revised. *Emerging Perspectives on Learning, Teaching, and Technology*, *8*, 41–44.
- Google Ventures. (2019). *The design sprint*. Retrieved from <https://www.gv.com/sprint/>
- Google Ventures. (2021). *The GV research sprint: A 4-day process for answering important startup questions*. Retrieved from <https://library.gv.com/the-gv-research-sprint-a-4-day-process-for-answering-important-startup-questions-97279b532b25>
- Hurrell, S. A., Scholarios, D., & Thompson, P. (2013). More than a 'humpty dumpty' term: Strengthening the conceptualization of soft skills. *Economic and Industrial Democracy*, *34*(1), 161–182.
- Juntumaa, J., Laitinen, M. A., & Kirichenko, S. (2020). The net promoter score (NPS) as a tool for evaluation of the user experience at culture and library services. *Qualitative & Quantitative Methods in Libraries*, *9*(2), 127–142.
- Knapp, J., Zeratsky, J., & Kowitz, B. (2016). *Sprint: How to solve big problems and test new ideas in just five days*. Simon and Schuster.
- Krathwohl, D. R. (2002). A revision of bloom's taxonomy: An overview. *Theory into Practice*, *41*(4), 212.
- Llamas, B., Storch, D., de Gracia, M., Mazadiego, L. F., Pous, J., & Alonso, J. (2019). Assessing transversal competences as decisive for project management. *Thinking Skills and Creativity*, *31*, 125–137.
- Lupton, E., & Lipps, A. (2018). *The senses: Design beyond vision*. Chronicle Books.
- Norman, D. A., & Verganti, R. (2014). Incremental and radical innovation: Design research vs. technology and meaning change. *Design Issues*, *30*(1), 78–96.
- Palmer, K., & Devers, C. (2018). An evaluation of mooc success: Net promoter scores. Paper presented at the *EdMedia Innovate Learning*, 1648–1653.

- Perignat, E., & Katz-Buonincontro, J. (2019). STEAM in practice and research: An integrative literature review. *Thinking Skills and Creativity*, 31, 31–43.
- Plattner, H., Meinel, C., & Leifer, L. (2011). *Design thinking: Understand–improve–apply*. Springer Science & Business Media.
- Pokorni, B., Zwerina, J., & Hämmerle, M. (2020). Human-centered design approach for manufacturing assistance systems based on design sprints. *Procedia CIRP*, 91, 312–318.
- Rizzi, V., Pigeon, C., Rony, F., & Fort-Talabard, A. (2020). Designing a creative storytelling workshop to build self-confidence and trust among adolescents. *Thinking Skills and Creativity*, 38, 100704.
- Simon, H. A. (2019). *The sciences of the artificial, reissue of the third edition with a new introduction by John Laird*. MIT press.
- United Nations. Department of Economic and Social Affairs. Sustainable development. (2020). *The 17 goals*. Retrieved from <https://sdgs.un.org/goals>
- Wilkerson, B., & Trellevik, L. L. (2021). Sustainability-oriented innovation: Improving problem definition through combined design thinking and systems mapping approaches. *Thinking Skills and Creativity*, 42, 100932.
- Zoltowski, C. B., Oakes, W. C., & Cardella, M. E. (2012). Students' ways of experiencing human-centered design. *Journal of Engineering Education*, 101(1), 28–59.

Enhancing Materials and Manufacturing Education with Materials Databases: A Case Study in Aerospace Engineering



David Álvarez and David López-Adrio

1 Introduction

Making decisions in real life often requires finding a middle ground between conflicting objectives. People frequently find themselves in the position of making compromises to achieve a balance between a car's performance and its cost. These familiar conflicts also arise when choosing materials.

The objective of material selection is to optimize multiple performance metrics in the product where it will be used. These metrics typically include cost, mass, volume, power-to-weight ratio, and density, among others (Ashby, 2016). Conflicts arise because the choice that optimizes one metric may not necessarily do the same for the others. Therefore, the best choice often involves a compromise that brings all metrics as close to their optima as possible, given their interdependence (Ashby, 2017).

This chapter focuses on multi-objective optimization in material choice. It expands upon established methods for manufacturing process and material selection. These methods are equally applicable to material selection and to the inverse problem of identifying promising applications for new materials. Additionally, it should be noted that the selection of manufacturing processes is also an essential aspect of this decision-making process. The manufacturing process and the selected material are intimately linked due to their interdependence on the performance and properties of the final product (Yavuz, 2019). The choice of material directly affects the manufacturing process, as different materials require specific production methods and techniques (Nayak et al., 2021).

D. Álvarez (✉)

CINTECX, Universidade de Vigo, EEI, ENCOMAT Group, 36310 Vigo, Spain
e-mail: davidag@uvigo.es

D. López-Adrio

Deseño na Enxeñaría Department, Universidade de Vigo, EEI, 36208 Vigo, Spain

The characteristics of the selected material, such as its strength, durability, flexibility, or conductivity, determine the suitability of various manufacturing processes. For example, if a material has high heat resistance, it may be compatible with processes involving high-temperature treatments like casting or forging. On the other hand, materials with excellent formability may be better suited for processes like sheet metal forming or injection molding.

Conversely, the manufacturing process can also influence the material selection. Some processes may impose limitations on the types that can be used effectively. For instance, processes like additive manufacturing or 3D printing often require materials with specific properties, such as powder formability or melt flow characteristics (Arnold et al., 2012). Moreover, the manufacturing process can affect the properties and performance of the final product. Heat treatments, surface coatings, or post-processing techniques employed during manufacturing can modify the crystalline microstructure and enhance its mechanical properties (Ashby, 2016).

Therefore, the selection of the manufacturing process and the material must be considered together as an integrated decision-making process. It is crucial to evaluate the compatibility between the chosen material and the available manufacturing methods to ensure optimal product performance, quality, and cost-effectiveness (Froes et al., 2019; Pollini & Rognoli, 2021).

2 Background

To conduct a practical class on aerospace engineering focusing on material selection and manufacturing processes using the CES EduPack software (CES Edupack has been acquired by Ansys Inc and renamed as Granta Edupack), some background information is necessary. The class should begin with an introduction to the importance of materials and manufacturing processes in aerospace engineering.

Firstly, it is essential to provide an overview of the critical role of materials in aerospace applications. This can include discussing the unique challenges faced by aerospace engineers, such as weight reduction, high-temperature resistance, structural integrity, and performance optimization. Explaining the significance of material selection in meeting these requirements will help students understand the importance of the topic.

Next, introducing the concept of manufacturing processes and their impact on material properties is crucial. Students should be familiarized with various manufacturing techniques used in the aerospace industry, such as casting, forging, machining, and additive manufacturing. Highlighting how each process affects the material's structure, properties, and performance will enable students to appreciate the interdependence between materials and manufacturing methods.

Furthermore, a brief overview of the software should be provided. The software is a powerful tool that assists engineers and designers in material selection by providing comprehensive material property data and performance indices. It allows

users to evaluate and compare different materials based on multiple criteria, including mechanical, thermal, electrical, and environmental properties.

During the practical class, students can be guided through hands-on exercises using the software. These exercises should involve selecting materials for specific aerospace applications and analyzing the trade-offs between different options. Students can explore how different materials and manufacturing processes affect performance, cost, weight, and other relevant factors.

Throughout the class, it is important to encourage critical thinking and problem-solving skills. Students should be encouraged to consider real-world constraints and challenges, such as regulatory requirements, environmental considerations, and cost limitations. This will help them develop a holistic understanding of material selection and manufacturing processes in the aerospace industry.

By providing this background information and incorporating practical exercises using the CES EduPack software, students will gain valuable insights into the complex decision-making process involved in material selection and manufacturing in aerospace engineering. They will understand how to evaluate materials and manufacturing processes to meet the specific requirements, ultimately enhancing their engineering knowledge and skills.

3 Learning Objectives

The learning objectives of the practical class on material selection and manufacturing processes in aerospace engineering can include the following:

- Understand the significance of material selection and manufacturing processes.
- Familiarize oneself with different materials and their properties.
- Gain knowledge of various manufacturing processes commonly employed in the aerospace industry.
- Learn how material properties and manufacturing processes affect the performance and characteristics of aerospace components.
- Develop the ability to evaluate and compare materials based on specific criteria, such as mechanical properties, thermal resistance, and weight.
- Acquire proficiency in using a materials and fabrication process database for material selection and analysis.
- Understand the trade-offs and considerations involved in material selection, including cost, environmental impact, and regulatory requirements. Apply critical thinking skills to make informed decisions regarding material selection and manufacturing processes.
- Enhance problem-solving abilities by analyzing real-world scenarios.
- Collaborate effectively in group activities and discussions.

By achieving these learning objectives, students will be equipped with the knowledge and skills necessary to make objective reports regarding material selection and manufacturing processes. They will be prepared to tackle the challenges and complexities associated with designing and producing aerospace components.

4 Resources and Organization

To conduct the practical class for a group of 10 to 20 students on material selection and manufacturing processes several resources are required. These resources include:

- **Computers:** Each student should have access to a computer equipped with the necessary hardware and software requirements. This will enable them to actively participate in the practical exercises and interact with the software.
- **Projector:** A projector is essential for the instructor to demonstrate the software functionalities and present the theoretical aspects of the class effectively. It allows the entire group to follow along and visualize the concepts being discussed.
- **CES EduPack software licenses:** To utilize all the capabilities of the software, each student will need access to a licensed version. It is important to ensure that there are enough licenses available to accommodate the number of students in the class.
- **Reference materials:** It is beneficial to have additional reference materials available, such as textbooks or online resources, to supplement the class content and provide further insights into material selection and manufacturing processes in the aerospace industry. These resources can serve as valuable references for students during and after the class.
- **Handouts and worksheets:** Providing handouts or worksheets with instructions and exercises related to material selection and manufacturing processes can enhance the learning experience. These resources can guide students through the practical exercises and serve as study materials for future reference.
- **Internet access:** A stable internet connection is necessary to access online resources, software updates, and additional reference materials. It also enables students to explore further information related to the class topics and engage in interactive discussions or research activities.
- **Support from the instructor or teaching assistants:** Having a knowledgeable instructor or teaching assistants available to provide guidance, answer questions, and assist students during the practical class is crucial. They can offer clarification on concepts, address technical issues, and facilitate discussions to enhance the overall learning experience.

By ensuring the availability of these resources and internet access, the practical class on material selection and manufacturing processes in aerospace engineering can be conducted effectively. Students will have the necessary tools to actively participate, explore the software, and gain a comprehensive understanding of the subject matter.

5 Session Development

This practical class aims to provide students with hands-on experience in material selection for aerospace applications. Specifically, the focus will be on selecting aluminum alloys for the fabrication of a liquid oxygen fuel tank. The class will utilize the CES EduPack software to analyze and compare different aluminum alloys, considering their properties, performance, and suitability for the challenging requirements of a liquid oxygen fuel tank.

The objective of this practical class is to enable students to understand the material selection process and apply it to the specific case of an aluminum alloy for a liquid oxygen fuel tank. Students will learn how to evaluate and compare different alloys based on their mechanical properties, corrosion resistance, thermal characteristics, and compatibility with liquid oxygen. By the end of this practical class, students will have gained practical experience in material selection by applying their knowledge to the specific case of selecting aluminum alloys for a liquid oxygen fuel tank. They will have developed skills in evaluating and comparing materials using the software, as well as an understanding of the challenges and considerations involved in aerospace material selection. This practical class will equip students with the necessary tools to make informed decisions in their future careers.

The class structure is described in Table 1.

6 Hands-On Exercise: Material Evaluation with CES EduPack

An Ashby diagram (Fig. 1) is a graphical representation that illustrates the relationships between different material properties. In this case, the Ashby diagram depicts Young's modulus (E) on the vertical axis and density (ρ) on the horizontal axis.

The vertical axis (E) represents Young's modulus, which measures the stiffness or elasticity of a material. Materials with higher values of Young's modulus exhibit greater stiffness and are less deformable under stress, while those with lower values are more flexible.

The horizontal axis represents density (ρ), which measures the mass per unit volume of a material. Materials with lower density are lighter, which can be advantageous for weight-sensitive applications such as aerospace engineering.

The Ashby diagram allows for the comparison of different materials based on their combination of Young's modulus and density. Materials that appear higher on the diagram have higher Young's modulus values, indicating greater stiffness, while those located lower have lower Young's modulus values, indicating more flexibility. Similarly, materials positioned towards the left of the diagram have lower density, indicating lighter weight, while those towards the right have higher density.

The position within the Ashby diagram provides insights into their performance characteristics. For example, materials located in the upper-left region of the diagram

Table 1 Class structure proposed for a three-hour workshop

Topic	Time (min)	Description
Introduction to material selection in aerospace engineering	15	<ul style="list-style-type: none"> • Overview of the importance of material selection in aerospace applications • Explanation of the challenges and considerations involved in selecting materials for aerospace fuel tanks • Introduction to the specific case of an aluminum alloy for a liquid oxygen fuel tank
Properties and requirements of aluminum alloys	30	<ul style="list-style-type: none"> • Discussion on the properties of aluminum alloys, including strength, density, thermal conductivity, and corrosion resistance • Explanation of the specific requirements for a liquid oxygen fuel tank, such as cryogenic compatibility, low thermal expansion, and resistance to ignition • Introduction to relevant aluminum alloy families commonly used in aerospace applications
Hands-on exercise: material evaluation with CES EduPack	60	<ul style="list-style-type: none"> • Demonstration of the software and its functionalities for material selection • Students will access the software on their computers and explore the database of aluminum alloys • Guided exercise on evaluating and comparing aluminum alloys based on relevant criteria, including mechanical properties, corrosion resistance, and cryogenic compatibility • Students will analyze the performance indices provided by the software to assess the suitability of different aluminum alloys for the liquid oxygen fuel tank
Group discussion and analysis	30	<ul style="list-style-type: none"> • Students will discuss their findings and observations in small groups • Each group will present their analysis of the aluminum alloys, explaining their choices and justifications • Facilitated discussion on the trade-offs and considerations in material selection for the liquid oxygen fuel tank • Instructor-led analysis of the optimal aluminum alloy choices based on the specific requirements of the tank
Conclusion and wrap-up	15	<ul style="list-style-type: none"> • Recap of the key concepts covered in the class, including material selection criteria and the importance of considering application-specific requirements • Final remarks on the practical implications of material selection for aerospace engineering • Encouragement for further exploration and research in the field of material selection and manufacturing processes in aerospace applications

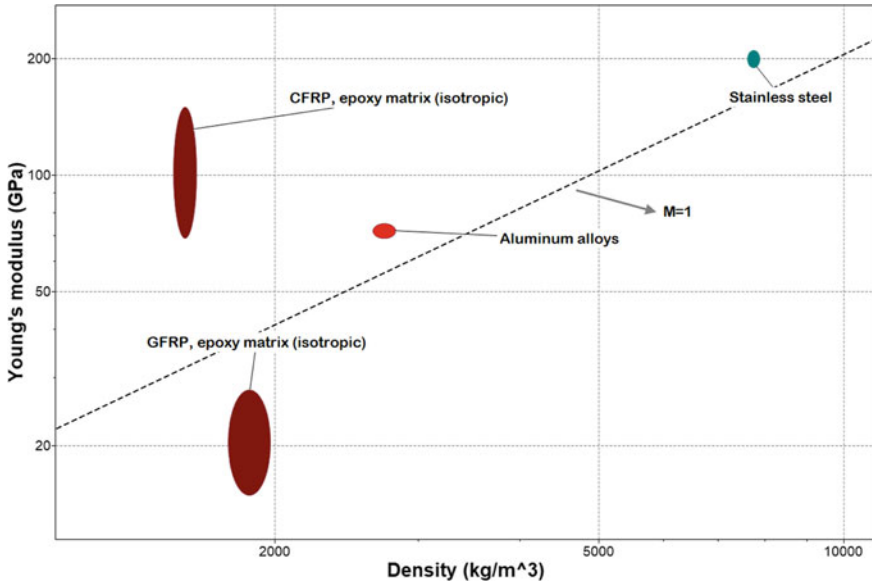


Fig. 1 Ashby plot representing some typical materials employed in the fabrication of pressure vessels

possess high stiffness (high Young’s modulus) and low density, making them ideal for structural applications where strength-to-weight ratios are crucial. Conversely, materials in the lower-right region exhibit lower stiffness (low Young’s modulus) and higher density, making them more suitable for applications where flexibility and weight are less critical.

The process of screening and ranking can be made quantitative by connecting the technical and economic requirements of a design to attribute profiles stored in a database. To establish a robust and systematic ranking procedure, combinations of material properties known as performance indices, as proposed by Ashby, play a vital role. These performance indices encapsulate the performance of a component by considering its functional requirements (F), geometry (G), and material properties (M). The overall performance (P) of the component can often be represented by an equation such as $P = f(F, G, M)$, where $f()$ denotes a function.

Optimum design entails selecting the material and geometry that maximize or minimize the performance metric based on the functional requirements. In cases where the parameters F, G, and M are assumed to be independent, the performance index can be expressed as the product of three separate functions: $P = f_1(F) * f_2(G) * f_3(M)$. The product of $f_1(F)$ and $f_2(G)$ is referred to as the structural efficiency coefficient, capturing the interplay between functional requirements and geometry. On the other hand, $f_3(M)$ represents the material efficiency coefficient.

This simplification allows for the optimization of the overall performance index by selecting a material that minimizes $f_3(M)$, regardless of the specific design details.

As a result, the optimal subset of materials can be identified without the need to solve the entire design problem. While this approach simplifies the fully coupled design problem, it offers valuable insights during the preliminary design phase of a project.

To employ this method, it is essential to define the objectives (maximization or minimization), constraints, and the distinction between specified and free parameters from the outset. By doing so, this powerful and versatile method offers simplicity and can provide substantial insights during the preliminary design stages of various projects. (Froes et al., 2019).

6.1 Level 1 Analysis

The selection of materials for cryogenic tanks (see Fig. 2) involves considering key material indices that address both thermal and mechanical concerns. Ideally, materials with high strength, high fracture toughness, high stiffness, low density, and low gas permeation would be desirable. Therefore, material performance indices are crucial for identifying the most suitable candidates for constructing hybrid tank walls. Among these indices, strength, and density typically dominate the design criteria (Gopal, 2016; Shoji et al., 2022).



Fig. 2 Boeing technicians move the SLS EM1 LH2 hydrogen tank. NASA/Steven Seipel under CC0 1.0 Universal

Table 2 Typical basic performance indices for cryogenic storage tanks

Criteria	Performance index
<i>Thermal</i>	
Minimum heat flux	1/k
Minimum temperature rise	1/a
<i>Mechanical</i>	
Strength-limiting design	σ_f/ρ
Damage-tolerant design	KIc/ρ
Deformation-limiting design	E/ρ

Some of the main performance indices for thermal and mechanical components of cryogenic storage tanks are depicted in Table 2. Here, k represents thermal conductivity, a represents thermal diffusivity ($k/\rho C_p$), ρ denotes mass density, C_p stands for specific heat, α represents the coefficient of thermal expansion, σ_f represents ultimate tensile strength, KIc represents mode I fracture toughness, E denotes Young’s modulus. In this class, the focus will be on exploring mechanical properties to streamline the process of material selection.

In an Ashby diagram, a material index represents a metric or ratio that combines relevant material properties to assess the performance or suitability of materials for a specific application. It allows for a quantitative comparison between different materials based on a single value.

Taking the example of an Ashby diagram depicting Young’s modulus (E) versus density depicted in Fig. 1 Ashby plot representing some typical materials employed in the fabrication of pressure vessels, one can consider the material index E/density. This material index is calculated by dividing Young’s modulus (E) by the density (ρ) of a material.

The material index E/density represents a measure of specific stiffness, which indicates how efficiently a material can resist deformation under load relative to its weight. A higher value of E/density signifies a material that offers a greater stiffness-to-weight ratio, indicating better structural performance. In an Ashby diagram, when the material index E/density is considered, it is represented as a line with a slope of 1. This line represents the ideal trade-off between Young’s modulus (stiffness) and density (weight). It indicates the theoretical upper limit for the combination of these properties, where materials lying on or above this line offer the best possible performance in terms of stiffness-to-weight ratio.

Materials that fall below the performance line have lower specific stiffness and may not offer an ideal balance between stiffness and weight. Conversely, materials positioned above the performance line have higher specific stiffness, indicating better performance in terms of stiffness-to-weight ratio.

In addition to the previously discussed performance index of E/density, other material indices can be used to compare materials in Ashby diagrams. Two common examples are the tensile strength (σ) divided by density (ρ) and the fracture toughness (K) divided by density (ρ) indices (Fig. 3).

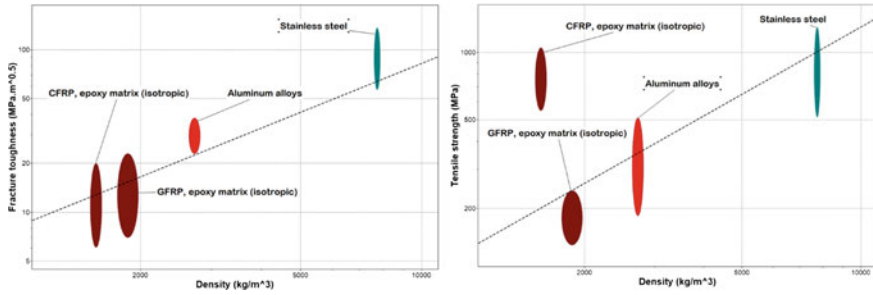


Fig. 3 Ashby plots of K1c versus density and ultimate tensile strength versus density

The tensile strength-to-density index (σ/ρ) represents the material’s ability to withstand applied tensile forces relative to its weight. A higher value of σ/ρ indicates a material that offers a greater strength-to-weight ratio, making it desirable for applications where high strength and low weight are critical.

On the other hand, the fracture toughness-to-density index (K/ρ) relates to a material’s resistance to crack propagation or its ability to resist fracture when subjected to stress. A higher value of K/ρ suggests that the material has better toughness relative to its weight, making it more suitable for applications where resistance to fracture is important.

To compare the cost of a rigid structure and find the most cost-effective option, the appropriate material index to use would be Young’s modulus divided by the product of density and price. The Ashby plot obtained to analyze this aspect is depicted in Fig. 4. The material index, in this case, would be calculated as follows: $\text{Material Index} = (\text{Young’s Modulus [Pa]} / ((\text{Density [kg/m}^3]) * (\text{Price [$/kg]})))$.

This index takes into account the stiffness provided by Young’s modulus, while also considering both the density and price of the material. When Young’s modulus is divided by the product of density and price per cubic meter, a relative measure is obtained, indicating how effectively a material performs concerning its stiffness-to-weight ratio and cost efficiency.

A lower value of the material index indicates that the material offers better performance concerning its density and price. This means that it provides a higher stiffness per unit weight and is more cost-effective for constructing a rigid structure.

When using the material index to compare materials, it is essential to consider other factors as well, such as strength, durability, and manufacturability. The selected material should meet the necessary performance requirements while also offering an optimal balance between stiffness, weight, and cost.

Considering the material indices, aluminum alloys are an optimal material selection for the manufacturing of cryogenic pressure tanks. They offer a favorable combination of strength, fracture toughness, and stiffness, coupled with a low density.

Aluminum alloys possess excellent mechanical properties that make them well-suited for cryogenic applications. Their high strength-to-density ratio, as indicated by indices such as tensile strength-to-density (σ/ρ) and fracture toughness-to-density

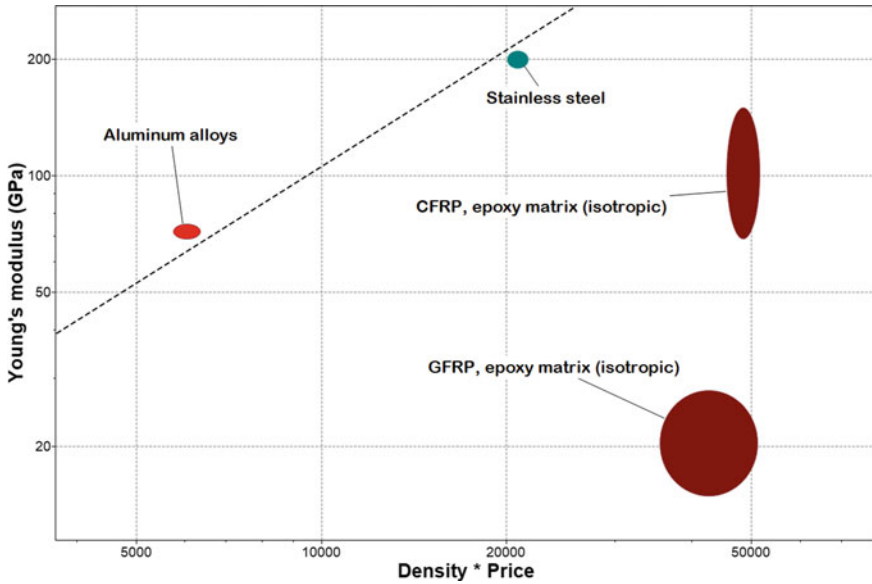


Fig. 4 Ashby plot of young modulus versus density * price (€/kg)

(K/ρ), demonstrates their ability to withstand applied forces while keeping the weight of the structure low. This is particularly advantageous in cryogenic pressure tanks, where minimizing weight is crucial for efficient transportation and operation.

Moreover, aluminum alloys exhibit good fracture toughness, indicating their resistance to crack propagation and ability to withstand impact or sudden load changes. This property is essential for ensuring the structural integrity and safety of cryogenic pressure tanks, which may experience extreme temperature differentials and mechanical stresses.

Aluminum is chosen over carbon fiber for the fabrication of large liquid fuel tanks in space rockets due to its cost-effectiveness and ease of manufacturing. While carbon fiber possesses superior rigidity and resistance, its higher material cost and complex manufacturing processes make it less suitable for large-scale tank production (Higuchi et al., 2005). Continuous fiber-reinforced composite materials will likely incur elevated initial production expenses, and their susceptibility to hydrogen permeation can present a potential complication. Despite aluminum's slightly lower mechanical properties, it still provides sufficient strength and durability to withstand the demanding conditions of rocket launches. Its versatility and familiarity within the aerospace industry, along with its ability to be easily formed and machined into complex shapes, contribute to efficient production processes and a well-established supply chain.

Overall, the combination of high strength, fracture toughness, stiffness, and low-density makes aluminum alloys an excellent choice for the fabrication of cryogenic pressure tanks. Their optimal material properties, as indicated by various material

indices, ensure the tanks can withstand the demanding operating conditions while being lightweight and cost-effective.

6.2 Level 3 (Aerospace) Analysis

After the selection of aluminum using the level 1 database, the subsequent step involves utilizing the level 3 database to identify a suitable aluminum alloy. This progression signifies a refinement in the material selection process, whereby the initial selection of aluminum has narrowed down the options. Accessing the level 3 database offers a more comprehensive array of information on various aluminum alloys, including their composition, properties, and several performance characteristics. This enables a more informed and targeted selection process, aligning the specific alloy with the desired criteria or requirements. The level 3 database serves as a valuable resource in facilitating an optimized decision-making process for selecting the most appropriate aluminum alloy.

In Fig. 5, the Ashby diagram presents a comprehensive overview of aluminum alloys, displaying the alloys suitable for casting in green and the alloys suitable for forging in purple. Overlaid on the graph are two lines with a slope of 1, representing the material indices of specific strength and specific stiffness. These lines provide a visual reference for comparing the performance of different alloys in terms of their strength-to-weight ratio and stiffness-to-weight ratio. By examining the position of each alloy concerning these lines, one can assess their relative performance in terms of these material indices. This additional information enhances the understanding of the alloy selection process, enabling engineers to identify the optimal alloy with the desired balance of specific strength and specific stiffness for the intended application.

In the Ashby diagram of Fig. 6, different alloys are plotted based on their fracture toughness and density values. Higher fracture toughness values indicate improved resistance to crack propagation, while lower density values signify lightweight materials. The position of each alloy on the diagram illustrates its relative performance in terms of fracture toughness and density. By selecting an alloy from regions that offer

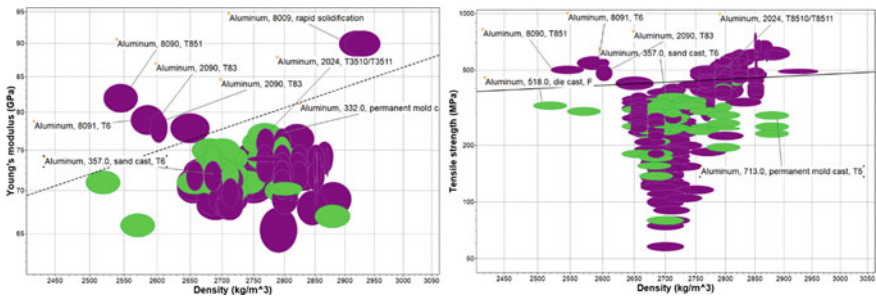


Fig. 5 Ashby diagrams of aluminum alloys (green) and aluminum casting alloys (purple)

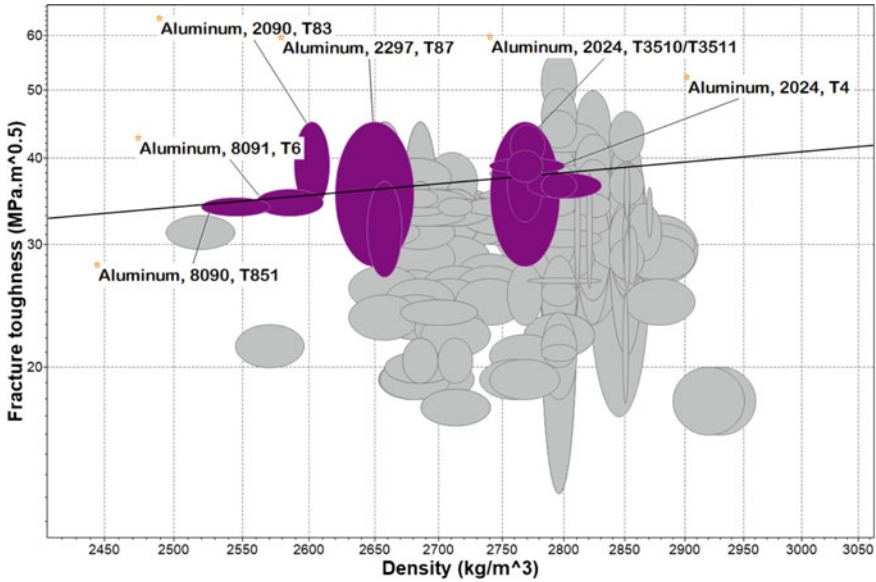


Fig. 6 Ashby plot of fracture toughness versus density

favorable fracture toughness-to-density ratios, engineers can optimize the material choice for achieving the desired performance characteristics.

By maximizing the various material indices discussed earlier, one can narrow down the selection to a group of six materials that maximize the material indices of specific stiffness, specific strength, and fracture toughness divided by density. These materials represent the most favorable combinations of properties, striking a balance between high rigidity, strength, fracture resistance, and low density.

The students can focus their attention on these six materials as potential candidates for applications that require optimal performance in terms of specific stiffness, specific strength, and fracture toughness relative to density. This approach ensures that the material selection process is guided by a systematic and quantitative analysis, leading to the identification of materials that offer the desired combination of properties for the intended application.

The materials resulting from the selection process are as follows:

1. Aluminum, 2024, T3510/T3511
2. Aluminum, 2297, T87
3. Aluminum, 2090, T83
4. Aluminum, 2024, T8510/T8511
5. Aluminum, 8090, T851
6. Aluminum, 8091, T6

These aluminum alloys have been selected based on their high performance in terms of specific stiffness, specific strength, and fracture toughness divided by density

Table 3 Properties of the selected aluminum alloys

Aluminium alloy	Density (kg/m ³)	Tensile strength (MPa)	Young's modulus (GPa)	Fracture toughness (MPa.m ^{0.5})	Specific stiffness ($\frac{E}{\rho}$)	Specific strength ($\frac{\sigma_{1s}}{\rho}$)	Specific toughness ($\frac{K_{1C}}{\rho}$)
AA 8090, T851	2.52e3–2.57e3	480–530	80–84	33–35	0.032	0.198	0.013
AA 8091, T6	2.56e3–2.61e3	505–595	77–81	33–36	0.031	0.213	0.013
AA 2090, T83	2.59e3–2.61e3	441–531	76–79.9	34–45	0.030	0.187	0.015
AA 2297, T87	2.62e3–2.68e3	395–464	76–79.9	28–45	0.029	0.162	0.014
AA 2024, T8510/ T8511	2.75e3–2.78e3	480–530	74–77.8	26–36.4	0.027	0.183	0.011
AA 2024, T3510/ T3511	2.76e3–2.78e3	359–510	74–77.8	38.9–44.6	0.027	0.157	0.015

(Table 3). Each of these alloys offers a favorable combination of properties, making them suitable candidates for applications where a balance between rigidity, strength, fracture resistance, and lightweight design is essential.

Further analysis and evaluation can be conducted on these materials to determine the most suitable choice for the specific requirements of the fabrication of large cryogenic pressure vessels.

In the material database available, students can find extensive information about the manufacturing limitations associated with the selection of each alloy. This includes details on processing techniques, such as casting, forging, drawing welding, and the specific challenges and constraints that arise during each process (Fig. 7). By consulting this database, students can gain valuable insights into the practical considerations and limitations of different materials, empowering them to make informed decisions regarding manufacturing processes and select materials that align with their design objectives.

7 Outcomes

The CES EduPack class on materials selection and manufacturing processes offers students a comprehensive understanding of the principles and techniques involved in choosing suitable materials for engineering applications. By utilizing the powerful materials database, students gain practical experience in analyzing material properties, comparing performance indices, and making informed decisions based on

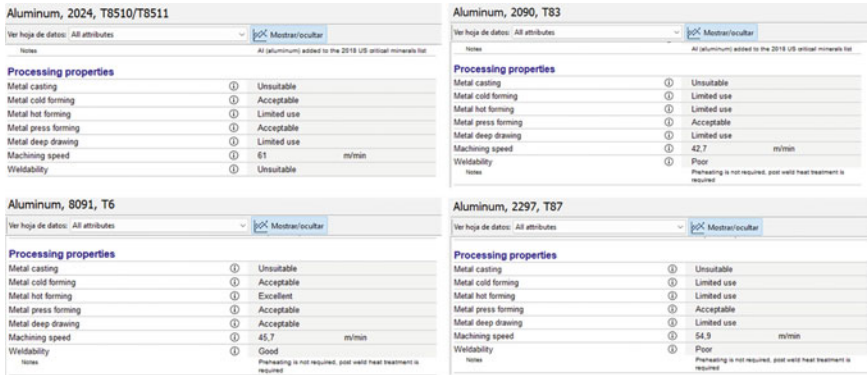


Fig. 7 Screenshots of the technical data about processing properties included in the CES EduPack database

specific design requirements. The main learning outcomes that students can expect to achieve upon completion of the course are:

- **Knowledge of Material Selection:** Through hands-on exercises and case studies, students will acquire a solid foundation in material selection principles. They will learn how to identify and prioritize key design requirements, explore material property databases, and evaluate performance indices to determine optimal material choices for specific engineering applications. This knowledge will enable students to make informed decisions considering factors such as mechanical properties, cost, sustainability, and manufacturability.
- **Familiarity with CES EduPack Software and materials databases:** Students will become proficient in using the software, a powerful tool for material selection and analysis. They will learn how to navigate the software’s interface, access extensive material property databases, and generate informative graphs and charts for visualizing material performance. The hands-on experience with the software will enhance students’ technical skills and enable them to apply the software effectively in their future engineering projects.
- **Understanding of Performance Indices:** The class will emphasize the concept of performance indices as a means of comparing and evaluating materials for specific applications. Students will learn how to interpret and utilize performance indices such as specific stiffness, specific strength, fracture toughness, and others. They will gain insights into the trade-offs and compromises that arise during the material selection process, considering factors such as weight, cost, durability, and environmental impact.
- **Integration of Manufacturing Processes:** In addition to material selection, the class will introduce students to various manufacturing processes and their impact on material properties. Students will explore the relationship between material selection and manufacturing techniques, considering factors such as formability, joinability, and surface finish. They will develop an understanding of how

they can optimize or modify material properties through different processing methods, enabling them to make informed decisions regarding material and process selection.

- **Problem-Solving and Critical Thinking:** The class fosters problem-solving and critical thinking skills in students. Through practical exercises and real-world case studies, students will encounter engineering challenges that require them to analyze data, evaluate trade-offs, and propose optimal material solutions. This experiential learning approach enhances their ability to think critically, solve complex problems, and make evidence-based decisions in the field of materials engineering.

8 Deliverables and Assessment

As a final assignment for the class, students can be tasked with preparing a comprehensive report addressing the material selection process for manufacturing a cryogenic storage tank used in a space rocket. The report should include the following components:

- **Introduction:** Provide an overview of the design requirements, emphasizing the need for a cryogenic storage tank with high performance and reliability in the demanding conditions of space travel.
- **Material Evaluation:** Conduct a thorough analysis of various materials suitable for cryogenic applications, considering factors such as strength, fracture toughness, stiffness, density, thermal conductivity, and permeability to hydrogen. Compare and contrast the advantages and disadvantages of each material.
- **Material Selection Criteria:** Define the specific criteria for selecting the most suitable material for the cryogenic storage tank. This may include factors like weight reduction, cost-effectiveness, manufacturability, and compatibility with other components.
- **Material Selection Process:** Describe the methodology used to evaluate and compare different materials. This could involve the use of material indices, Ashby diagrams, and databases like CES EduPack. Explain the rationale behind the chosen approach and justify its suitability for the given application.
- **Material Recommendations:** Present the recommended material(s) for the cryogenic storage tank based on the evaluation and analysis conducted. Justify the selection by highlighting how the chosen material satisfies the desired performance criteria and meets the unique challenges of space travel.
- **Manufacturing Considerations:** Discuss the manufacturing processes and techniques involved in fabricating the cryogenic storage tank with the chosen material. Address any specific limitations, challenges, or requirements associated with the manufacturing process and propose strategies to overcome them.
- **Conclusion:** Summarize the findings of the material selection process and highlight the significance of the chosen material for the successful design and construction of the cryogenic storage tank in the context of space exploration.

The report should be well structured, supported by scientific and technical evidence, and demonstrate a comprehensive understanding of material properties, performance metrics, and manufacturing considerations. It should also include appropriate references to sources consulted during the research process.

9 Conclusions

The practical class on material selection and manufacturing processes using CES EduPack has proven to be a valuable learning experience for engineering students. By exploring the software's extensive materials database, Ashby diagrams, and material indices, students gained a deep understanding of the complexities involved in choosing the most suitable materials for specific engineering applications.

Through hands-on activities and real-world case studies, students were able to apply their knowledge and develop critical thinking skills when selecting materials for the fabrication of a cryogenic storage tank for space rockets. They learned how to consider multiple factors such as mechanical properties, cost, and manufacturability to make informed decisions. By maximizing material performance indices, students were able to identify a subset of materials that excelled in specific criteria such as specific stiffness, specific strength, and fracture toughness to density ratio.

The integration of CES EduPack in engineering education promotes a deeper understanding of the materials used in various industries and prepares students for the challenges they may face in their future careers as engineers.

References

- Arnold, S. M., Cebon, D., & Ashby, M. (2012). *Materials selection for aerospace systems*, 209.
- Ashby, M. F. (2016). *Chapter 2—What is a “Sustainable Development”?* Butterworth-Heinemann.
- Ashby, M. F. (2017). *Materials selection in mechanical design*. Butterworth-Heinemann.
- Bijeta Nayak, B., Jena, H., Dey, D., et al. (2021). *Materials selection and design analysis of cryogenic pressure vessel: A review*, 47, 6605–6608.
- Froes, F., Boyer, R., & Dutta, B. (2019). *1—Introduction to aerospace materials requirements and the role of additive manufacturing*. Elsevier.
- Gopal, K. V. N. (2016). *14—Product design for advanced composite materials in aerospace engineering*. Woodhead Publishing.
- Higuchi, K., Takeuchi, S., Sato, E., et al. (2005). *Development and flight test of metal-lined CFRP cryogenic tank for reusable rocket*, 57, 432–437.
- Pollini, B., & Rognoli, V. (2021). *Early-stage material selection based on life cycle approach: tools, obstacles and opportunities for design*, 28, 1130–1139.
- Shoji, D., Ogwezi, B., & Li, V. C. (2022). *Bendable concrete in construction: Material selection case studies*, 349, 128710.
- Yavuz, H. (2019). *Materials selection for aircraft skin panels by integrating multiple constraints design with computational evaluations*, 21, 112–119.

Understanding the Virtual Injection Molding Product Design



Alberto García-Collado  and Rubén Dorado-Vicente 

1 Introduction

During the design of a plastic component, the engineer considers both the technical requirements that the component will face during its service life, as well as the mechanical properties of the thermoplastic and the technology used in the manufacturing process. When launching new products, engineers must follow a series of stages, which are highly interrelated, such as the design process of the plastic component to be manufactured and the design of the mold where parts are to be injected.

As injected thermoplastic parts have gained importance in the field of engineering, the requirements they have faced have been increasingly demanding, not only in the design phase but also in the injection process. The distribution of the material inside the mold, as well as the flow orientations, and the different degrees of shrinkage that may result, must be calculated, and if necessary estimated before the manufacturing of the mold. All of this results in the great complexity of the design of injected plastic parts, since any variation in the mold will not only lead to a modification of the component design in a localized area, but it can also affect the rest of the part, reducing reliability and diminishing the mechanical performance.

Today, the Finite Element Method (FEM) is regarded as an indispensable tool during the design phase of both the plastic component and the injection mold. In the sense of engineering education, it is possible to develop methodologies based on training students' skills in commercial FEM software and at the same time use the software to explore complex engineering concepts by means of its powerful simulations. The present chapter describes this type of approach: the use of SolidWorks

A. García-Collado (✉) · R. Dorado-Vicente
Dpto. Ingeniería Mecánica y Minera, Universidad de Jaén, Jaén, Spain
e-mail: acollado@ujaen.es

R. Dorado-Vicente
e-mail: rdorado@ujaen.es

plastic as a tool to understand injection molding processes, and for training students in computer-aided tools to obtain part designs adequate for a manufacturing process.

2 Background

This section is devoted to summarizing the basic concepts regarding injection molding and FEM simulations required to understand the laboratory session. Roughly speaking, an injection molding process is based on the material phase change: a polymer is heated to its melting point and then introduced into a mold till it is filled. After that, the material solidifies with its final shape.

Figure 1 shows the main parts of an injection machine including the mold. The thermoplastic injection process can vary between 2 s and several minutes, depending on the type of part. The stages in which the process is divided are:

- Filling: the plastic is injected at high pressure into the mold.
- Packing: after injection, the material continues to be added to avoid a lack of material or density.
- Cooling: the material is cooled until a significant part of its volume solidifies.
- Extraction: opening of the mold and extraction of the piece.

In this lecture, SolidWorks® Plastics, a FEM application, to perform a simulation of the mold injection process till the packing stage is used. Generally, all injection molding simulation programs have the same internal structure:

- A preprocessor for geometry modeling.
- Databases that store the characteristics necessary for the analysis. Thus, a constant update of the database of commercial polymers, refrigerants, mold materials, and the characteristics of existing injection machines on the market is necessary.
- A series of specific calculation modules for each transformation process.
- A post-processor that friendly presents the results of the analysis.

SolidWorks allows to predict and avoid manufacturing defects in plastic part designs and injection molds, which eliminates costly modifications, improves part quality, and reduces time to market. In addition, it allows to balance channel systems and calculate cycle duration, closing tonnage and injection weight, which allows to optimize the design of the feeding system and avoid the high cost of having to re-make the molds.

Once the mold filling study has been carried out, the solution allows: knowing the best location and the number of material inputs in the mold if there are several inputs, a correctly balanced system will obtain the injection speed profile which minimizes the residual stresses of the component, the minimum mold filling time, evaluation of the welding lines or joint lines and air trapping in certain areas, determining the injection pressure and clamping force for correct sizing of the injection machine and the mold. All this information feeds back into the design phase since it can force a substantial

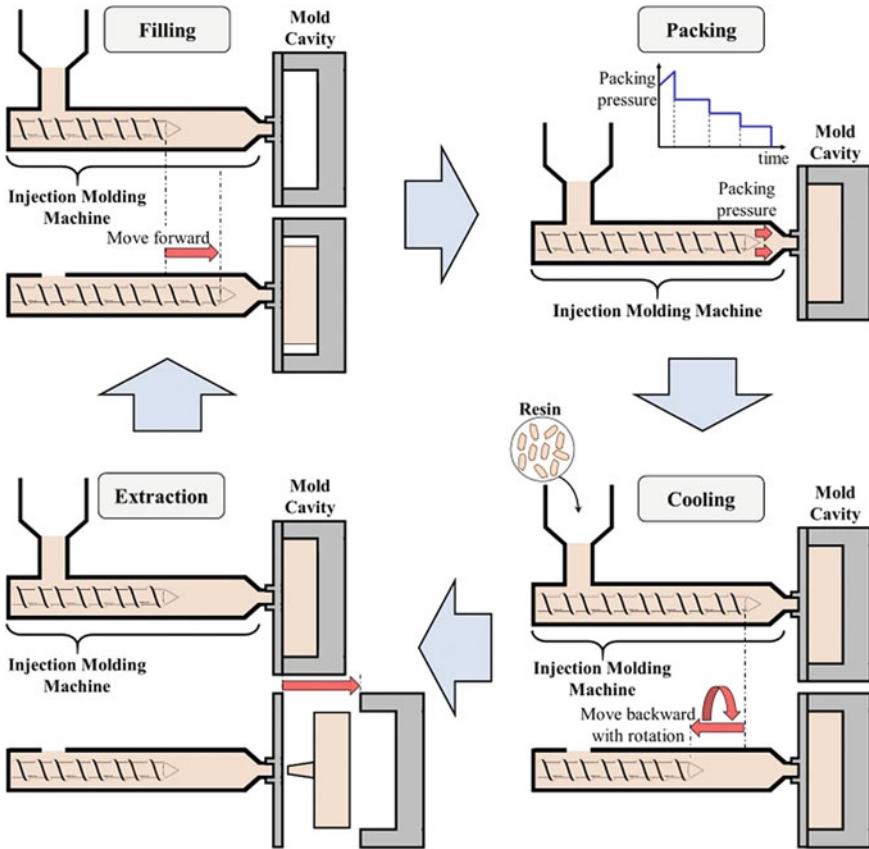


Fig. 1 Injection molding process stages. With permission of Springer. *Source* Jung, J. et. al. Optimization of injection molding process using multi-objective Bayesian optimization and constrained generative inverse design networks. <https://doi.org/10.1007/s10845-022-02018-8>

modification of the original idea of the component. Thermoplastic injection is the plastic molding technique consisting of injecting a molten polymer at high pressure through a nozzle (transferred by a piston mechanism or extruder screw), to fill a mold.

3 Learning Objectives

The following bullets summarize the learning objectives:

- Understand the main phases of the injection molding process.
- Get familiar with software for the analysis of the process.

- Know the process required for the simulation.
- Analyze an injection process determining the relationships between times, temperatures, and pressures.

4 Resources and Organization

To develop the required skills to attain the learning objectives (Sect. 3), the subsequent activities are proposed:

- Face-to-face lecture: a guided example with the commercial software based on the method of finite elements to calculate the feasibility of mold filling in plastic parts. An evaluation of the results of the simulated process, discussing aspects related to the design of the part, always oriented towards manufacturing is also accomplished.
- Homework: an exercise is proposed where students must perform a filling analysis like the guided example.
- Online test of different types of questions to reinforce the concepts taught during the face-to-face activity. This set is implemented in a Moodle-type educational platform.

The first activity is the face-to-face lecture. It is a 2 h session in a room with computers and the FEM software to use. The session development is described in the following Sect. 5.

During the ten last minutes of the face-to-face activity, the instructor explains the homework exercise and how to use the online test to face this work. Students will work in the exercise for one week, and in parallel, with the online test. This test is open one week before the due date for the homework activity. For every attempt, the responses are automatically evaluated, and the feedback is sent to the student.

The lecture is composed of two main activities as shown following:

Activity 1: Feasibility of injection mold evaluation example. Guided by the professor, the students review critical concepts and solve the mold evaluation example described in Sect. 5:

- The basic concepts of plastic injection will be briefly reviewed.
- The student will start working with SolidWorks® Plastics and its basic functions will be described by the instructor at the same time.
- Feasibility of injection analysis will be carried out with the software as an example.

Activity 2: Homework

- A part will be provided by the professor and discussed during the session.
- The part will be imported into SolidWorks plastic simulation, and the filling and packing process will be analyzed. The data collected will be used to complete a report according to the indications found at the end of this tutorial.

5 Session Development

This section is devoted to illustrating a laboratory session: face-to-face activity (Sect. 4). Through the session, it is described a feasibility analysis of injection plastic using SolidWorks® Plastics. Finite element simulation software is essential for designing plastic parts as it helps to obtain the optimal gate location and helps to predict whether there will be weld lines or air traps, sinkholes, and incomplete filling of the part. In this case, a simple 2 mm thick piece with different holes will be used (Fig. 2). The first step is to import the geometry in STEP or IGES format.

Commercial software used for the analysis uses three different ways of meshing a product design. These are Midplane Mesh, Dual Domain Mesh, and 3D Technology. In this case, Tetrahedral elements have been used because the part employed is 3D (Fig. 3).

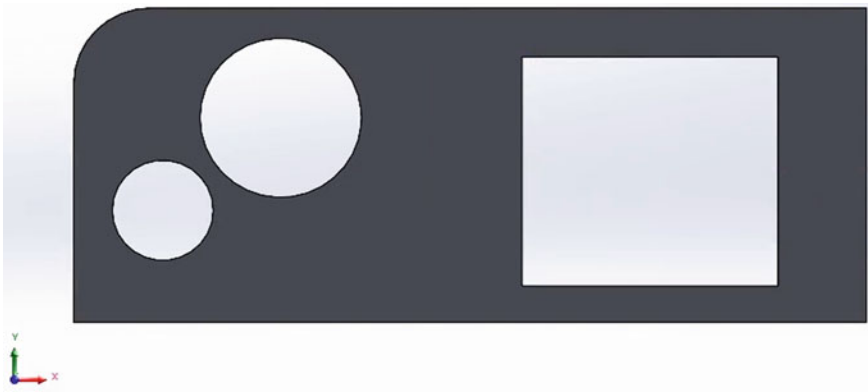


Fig. 2 Part imported from a STEP file

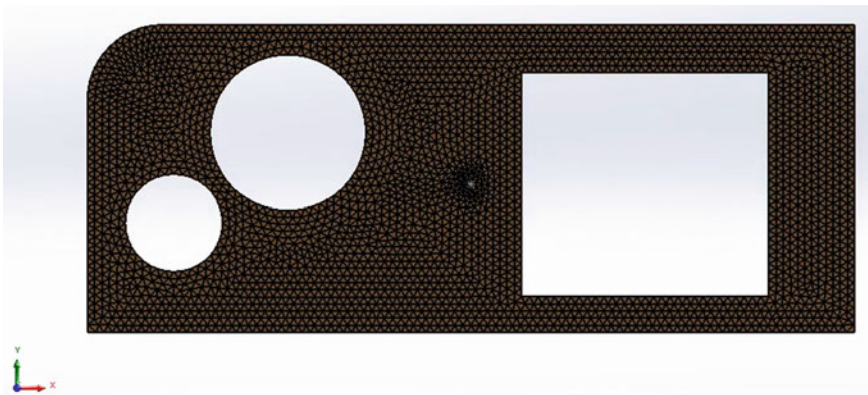


Fig. 3 3D mesh of the part

Optimization of the gate location

To obtain the optimal injection point within the mold cavity, the following will be considered:

- The injection mold geometry.
- An attempt will be made to ensure that the injection point is centered within the mold, to prevent the mold from partially opening during the injection process.
- The position must ensure the complete filling of the part. It will be in areas where the fluid is directed from greater to lesser thicknesses.
- The location must ensure that filling occurs at the same time at all boundaries of the part.

SolidWorks has a tool that helps predict the best entry point location, based on the complete filling of the part and the filling time.

Material and gate dimension

The selection of the material is generally a decision that covers a wide range of possibilities. Today polypropylene is the easiest thermoplastic for the injection process due to its low viscosity, price, low plastic shrinkage, durability, resistance to corrosion, and low water absorption. In this chapter, Generic PP is used, with an injection temperature of 245 °C and a mold temperature of 90 °C.

Not only the entry point of the material into the mold cavity is important, but also the diameter of the gate. Large diameters will fill in less time and with less pressure, but they will leave a visible mark on the piece that can harm its aesthetics. In this sense, a gate of 2 mm is chosen (Fig. 3).

Fill and packing analysis

The main benefit of doing a filling analysis is to predict the fill pattern (Fig. 4). The fill pattern helps identify short shots, which produce incomplete filling of parts. This proves particularly advantageous when dealing with the design of plastic parts featuring varying part thicknesses. Filling pattern analysis also helps to evaluate if the filling process is being carried out in a physical sense. It also partially predicts weld lines and air traps.

Weld lines

Weld line analysis (Fig. 5) is a simple analysis that allows the designer to establish a criterion of whether two plastic faces will form a weak or strong line. Two criteria are generally established:

- The angle at which the encounter occurs. If the two fronts form an angle greater than 135°, it is understood as a welding line; if it is lower, a union line is produced, which has greater mechanical resistance.
- The temperature and pressure at which two plastic fronts encounter occurs. High pressures and temperatures will increase the cohesion of the two plastic fronts, increasing the resistance of the said line.

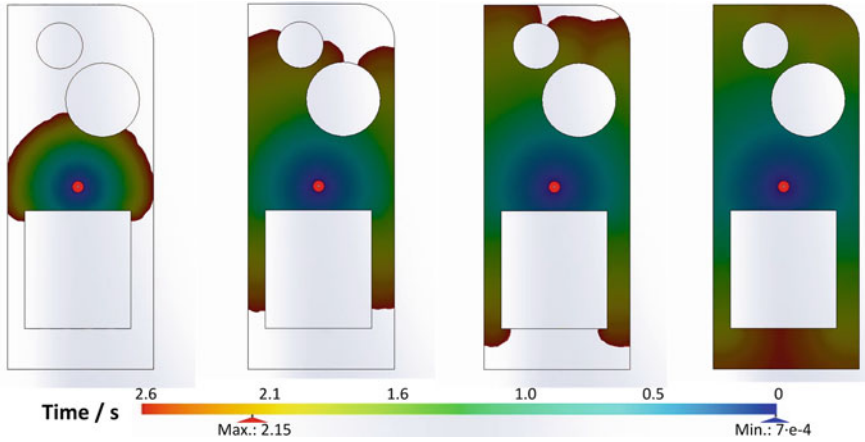


Fig. 4 Fill pattern analysis. The complete filling of the part is done at 2.64 s

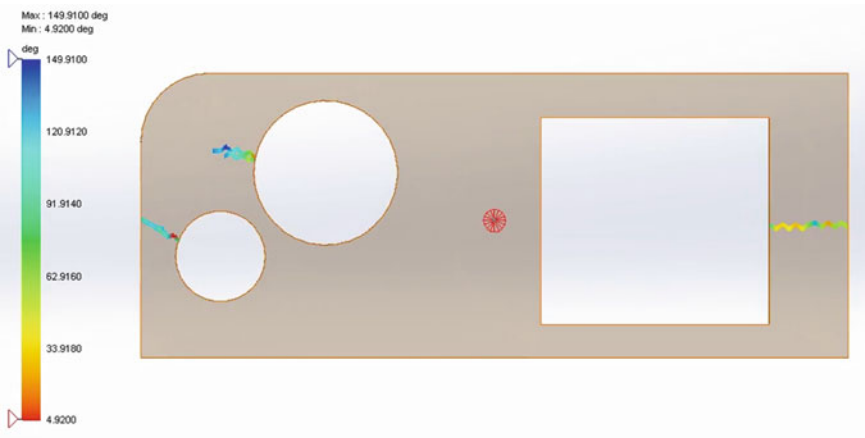


Fig. 5 Weld lines and angles of the plastic fluid fronts

Shrinkage analysis

Although polypropylene has very low typical shrinkage values, it is necessary to analyze them since they can cause important geometric deviations. Shrinkage is the percentage increase in local density from the end of the packing phase to when the part has cooled to the ambient reference temperature (the default value is 25 °C/ 77 °F) (see Fig. 6). Generally, values less than 20% can be admissible.

Clamping force

The clamping force (Fig. 7) is the maximum force required to keep the mold closed during filling. If this is too high or too low, defective parts can result from burners

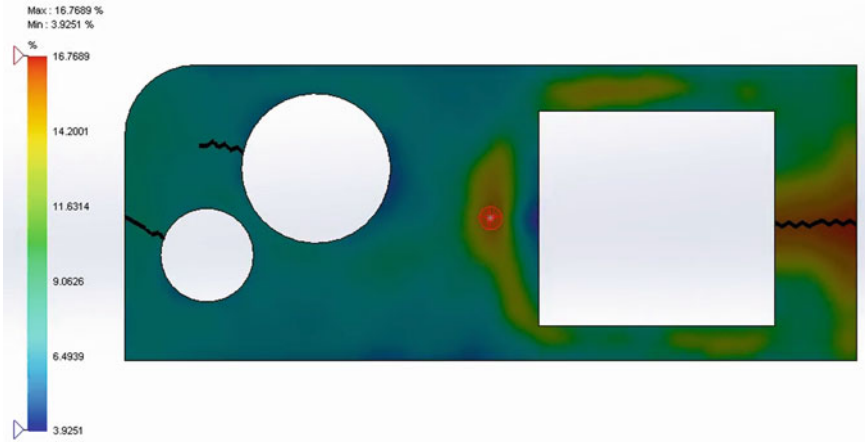


Fig. 6 Shrinkage image after packing

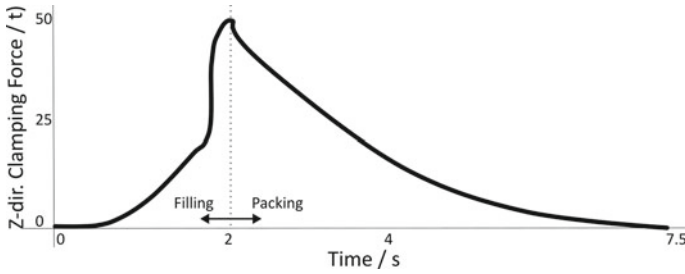


Fig. 7 Clamping force during filling and packing

or burr formation. This force is mandatory to perform an economic analysis of the production. Generally clamping force must be multiplied for 1.2–1.3 times to evaluate the dimension of the injection machine.

6 Outcomes

Expected outcomes of the learning process:

- To identify the important parameters that affect the mold-filling process.
- To understand how the finite element method and its steps can be used to simulate a plastic injection process.
- To be able to design and evaluate the design with a clear orientation towards manufacturing of plastic injected parts.

7 Deliverables and Assessment

Considering the activities described in Sect. 4, each student must submit a report with his/her analysis of the filling exercise. Regarding the assessment, it is proposed a summative evaluation based on the following tools:

- Annotations: participation of the students during the face-to-face activity based on the instructor's annotations. 20% of the score.
- Check list. A checklist is used to evaluate students' reports. 80% of the score.

The report submitted will be evaluated. The main aspects to evaluate are:

- Is the gate location well positioned? Is the part located in the XY plane? Are filling time and full filling of the cavity?
- Evaluation of the feasibility of the injection molding. Is the fill pattern correct? Is the filling time appropriate? Can weld lines be eliminated? and a complete evaluation of the shrinkage.
- Are the clamping force and the packaging well represented?

8 Conclusions

In the analysis of filling feasibility with tools based on the FEM, it is very important to correctly understand the manufacturing process. The simplicity of the analysis can lead the student to think that evaluating the suitability of a part manufactured by injection of thermoplastics is relatively simple. Weld lines, shrinkage, clamping force, and gate location are the most useful outputs for validating the filling process of a plastic part. In this lecture note, a feasibility analysis of mold filling has been proposed, subsequently, outcomes deliverables and assessment are proposed. Students will learn to identify the most important parameters that affect the mold-filling process. In this sense, they will improve their ability in designing plastic parts in injection.

Bulk Metal Forming Processes: Analytical and Numerical Analysis



João P. M. Pragana , M. Beatriz Silva , and Bárbara P. P. A. Gouveia 

1 Introduction

The art of manufacturing as the world knows it has deep roots in technological developments made by craftsmen ever since the dawn of mankind. These developments consisted mostly of progressively improved methods and techniques to provide society with the necessary and desired goods. With time, general demands from consumers grew into more complex and stringent ones and could only be fulfilled through further developments of manufacturing technologies that allowed transforming raw materials into novel quality products of increasingly added value.

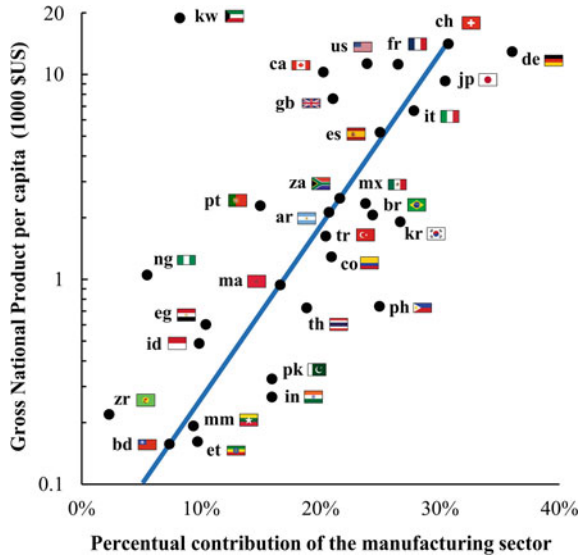
Because of this, country incomes in the form of Gross National Product (GNP) have increasingly been tied to their corresponding engagement in the manufacturing sector as shown in Fig. 1. Data included was compiled from the World Development Report of 1982 (World Bank, 1982) and may at times be biased to industrially developing countries due to their fewer aptitudes and resources for venturing deep into the manufacturing sector. Still, there is a solid correspondence between GNP and manufacturing contributions to the economy of several countries demonstrated by the linear blue-colored trendline of Fig. 1.

Among the current wide range of manufacturing solutions, metal forming composes different processes used for reshaping workpieces through permanent plastic deformation imposed by a rigid set of tools without adding or removing material. From large scale steelmaking and metalworking to micro forming operations on parts smaller than a single grain of rice (Vollertsen, 2013), metal forming has been playing a center role in the prosperity of society ever since the XVIII century with pioneering applications of iron sheets produced in rolling plants (Gale, 1964).

Mechanization of metal forming allowed separating technology from craftsmanship while opening the way for the mass production of components through compact

J. P. M. Pragana · M. B. Silva · B. P. P. A. Gouveia (✉)
IDMEC, Instituto Superior Técnico, Av. Rovisco Pais, 1049-001 Lisboa, Portugal
e-mail: bgouveia@tecnico.ulisboa.pt

Fig. 1 Gross national product per capita as a function of the percentual contribution of manufacturing to the economy of several countries represented by their flag and ISO country code. Adapted from Schey (1999)



multi-stage production lines with synchronous feed, transportation, and monitorization (SCHULER, 1998). Hence, know-how on metal forming plays a key and elementary role in the basic knowledge of engineers in multiple industrial sectors. It provides intricate and essential skills necessary for efficiently and economically assessing project planning and decision-making tasks.

As of today, most modern engineering programs at undergraduate and graduate levels aim at providing students with in-depth analysis of the main fundamentals in the major fields of both sheet and bulk-forming. This vision stands out from that utilized in very descriptive courses focused on materials, tools, machine-tools and products from a general perspective. Inversely, the fundamental (analytical) approach allows students to assimilate prior knowledge of materials science, solid mechanics, physics, mathematics, thermodynamics, and computer science with central aspects in metal forming associated with plasticity, tribology, metallurgy, data processing, among others.

In parallel to the above, the establishment of the finite element method (FEM) for accurately modelling and simulating metal forming operations has also been significant in view of developing new processes and products, optimizing standards techniques, and increasing process know-how (Nielsen & Martins, 2021a). Moreover, finite element computer programs can also be a valuable digital tool for assisting in training junior students and engineers from a user’s perspective by giving a deep visualization of metal flow and corresponding continuum changes in field variables related to displacements, strains, stresses, loads, pressures, and temperatures as a function of the operating parameters. Conversely, comprehension of phenomenological aspects of metal forming is as well needed for users of finite element programs

because it allows them to develop critical skills to thoroughly analyse numerical results while questioning their accuracy and reliability.

Under these circumstances, this chapter presents a combined analytical and numerical lecturing methodology aimed at teaching engineering students from bachelor and master levels regarding the fundamentals of metal forming. The methodology comprises project group assessments based on bulk metal forming problems that students must solve using analytical methods and numerical methods by finite element analysis. Examples of computations and analyses are related to initial workpiece dimensions, strains, force–displacement evolutions, energy consumptions, process efficiency, among others. The presentation is based on the implementation of the proposed methodology to engineering curricula of Instituto Superior Técnico from the University of Lisbon lectured by the authors, which include mechanical engineering, aerospace engineering, materials engineering, and industrial engineering and management.

2 Background

Up to the mid-XX century, most technological developments in metal forming were attained by trial-and-error experimentation without significant support from fundamental concepts related to the theory of plasticity. This tendency started to be inverted after the First World War with the establishment of the slip line field method by Hencky and Feiringer to assess stress and velocity fields (Bruhns, 2014) which was later integrated with the theory of plasticity by Hill (1950). In the second half of the XIX century, continuous proposal of new processing capabilities together with the analysis of metal forming through analytical methods built on representative elements (ideal work and slab method) and energy (lower and upper bound) as well as empirical methods (visioplasticity) were crucial in defining the foundations of modern plasticity-based technology (Fig. 2).

Further developments on computer-aided engineering, design and manufacturing in the metal forming industry allowed process modelling and simulation to be carried out to optimizing the production of sound components (Tao et al., 2011). This trend comprises applications of the finite element method (FEM) to attain an accurate portrayal of the metal flow and workability limits (Pragana et al., 2020) as a function of operating parameters which can be difficult or even impossible to handle wholly through analytical analysis (Kobayashi et al., 1989).

In what follows, brief presentations of calculation methods appropriate for solving bulk metal forming and are within the lecturing scope of the proposed methodology are included. Their application is generally established upon the following assumptions:

- Workpiece material is homogenous and isotropic,
- A rigid-plastic material model is assumed (elastic deformations are neglected),

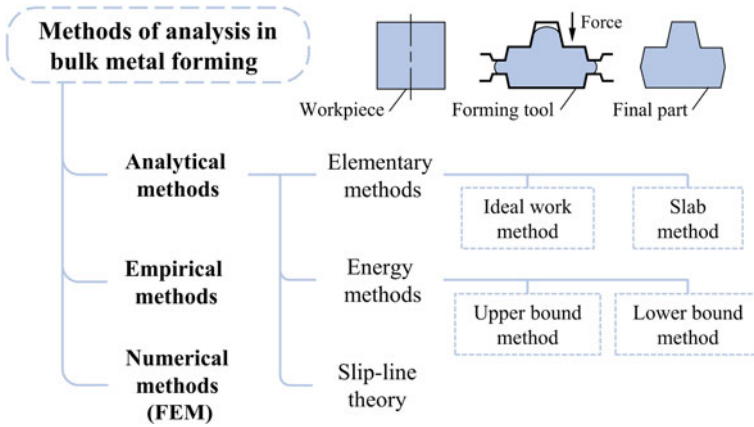


Fig. 2 Flowchart of methods used for solving bulk metal forming problems with special emphasis given to the analytical methods

- Plastic flow is uniform (flat sections maintain their flatness after plastic deformation takes place).

2.1 Ideal Work Method

The ideal work method (also known as work or energy balance method), is based on the balance between the external work W_e and the total work W_t required for a metal forming operation (Hosford & Caddell, 2007),

$$W_t = W_r + W_f + W_i \tag{1.1}$$

where the work parcels W_r , W_f and W_i represent redundant deformation, friction forces between the workpiece and forming tools and ideal work of deformation, respectively. The last parcel accounts for the amount of work required for shaping parts in the absence of friction and inhomogeneous flow. This value is determined by considering the ideal plastic work per unit volume w_i necessary to plastically deform a given workpiece with volume V ,

$$W_i = V w_i = V \int_0^\epsilon \sigma_{ij} d\epsilon_{ij} \tag{1.2}$$

where σ_{ij} and ϵ_{ij} are the stress and strain fields, which can be easily handled by considering the following relationship based on the ideal plastic work per unit of volume w_i ,

$$w_i = \int_0^{\varepsilon} \sigma_{ij} d\varepsilon_{ij} = \int_0^{\bar{\varepsilon}} \bar{\sigma} d\bar{\varepsilon} \quad (1.3)$$

where $\bar{\sigma}$ and $\bar{\varepsilon}$ are the effective (or, generalized) stress and strain that can be used to convert all solicitations imposed on the workpiece into pure uniaxial tension or compression states. This enables the ideal work of deformation to be determined from the material flow curve with or without strain hardening (Sect. 5.1).

However, the ideal plastic work is only a fraction of the total work (Eq. 1.1). Because it is challenging to determine the individual contributions of work from redundant deformation and friction forces between the workpiece and forming tools, the common approach is to consider empirical efficiency values. These efficiency values are determined by the ratio between the ideal work and the total work,

$$\eta = \frac{W_i}{W_t} \quad (1.4)$$

This allows appropriate use of the ideal work method mainly for estimating the required loading or energy to carry out metal forming operations, which in practical terms can be useful for tool design (geometry, dimensions, and materials) and for selecting the appropriate machine-tool.

2.2 Elementary Slab Method

The elementary slab method considers the equilibrium of forces along all axes x , y , z to take place under representative volumes (hereafter designated as slabs) of the deformable workpiece,

$$\sum F_x = \sum F_y = \sum F_z = 0 \quad (1.5)$$

where the directions x , y and z are assumed to be the principal directions.

Throughout plastic deformation, the behaviour of the elements reflects upon the whole workpiece which allows assuming the equilibrium of forces (Eq. 1.5) acting at any instant of deformation. This analysis leads to the formulation of one or more differential equations portraying the relations between stresses, workpiece geometry and friction. With the inclusion of the yield criterion and the boundary conditions, the individual contributions of all slabs can be solved through integration and subsequently summed together for providing the distributions of stresses and force along the contacts between the workpiece and the forming tools (Axmann & Mannl, 1998).

Contrary to the ideal work method, the elementary slab method incorporates the friction shear stresses in the contacts between the workpiece and forming tools, which are typically handled through the Amonton-Coulomb model with a friction coefficient μ or through the Prandtl model with a constant friction factor m (C. V. Nielsen & Bay, 2018). However, the inclusion of friction affects only the force

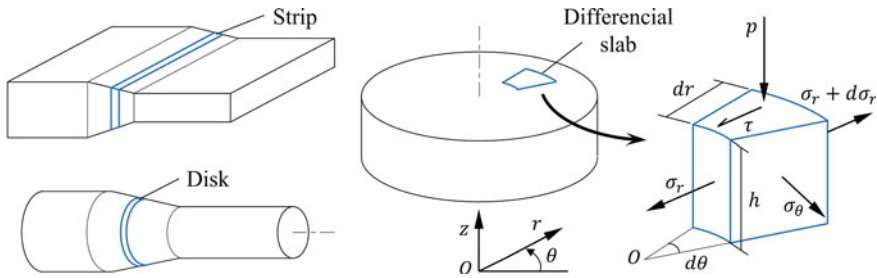


Fig. 3 Elementary slab method in plane strain and axisymmetric conditions with a detailed presentation of the loading diagram in case of a differential slab deformed under upsetting

balance meaning that the method does not account for internal distortions or misorientations of the principal directions generated during plastic deformation either by the friction or by the redundant work. Because of this constraint, slab method results can have significant deviations for higher shear stresses along the contacts between the workpiece and the forming dies.

Elementary slabs may assume different formats and shapes, which are selected concerning the metal forming process under analysis and the geometry of forming tools and workpiece. Moreover, slabs are typically modelled in either plane strain or axisymmetric conditions in order to facilitate handling the differential equations that result from force equilibrium previously presented in Eq. (1.5) (Ghoshchi et al., 2010).

Examples of standard geometries are shown in Fig. 3 with the detailed decomposition of loading for a differential ring slab commonly used for modelling upsetting operations in axisymmetric conditions. The differential slab possesses a radial thickness dr , a height h (equal to the cylinder height) and a sector angle $d\theta$ while being subjected to the upset pressure p , radial stresses σ_r and $\sigma_r + d\sigma_r$, circumferential stress σ_θ and frictional shear stress τ emerge.

3 Learning Objectives

Learning objectives are statements of the expected knowledge, and understanding after a learning process and can be classified according to Bloom's Taxonomy for the cognitive domain (Anderson et al., 2001). Figure 4 illustrates the different learning objectives and cognitive processes organized according to Bloom's Taxonomy into six categories: remembering, understanding, applying, analysing, evaluating and creating.

While the lower cognitive domain includes remembering and understanding information, the higher cognitive domain allows students to develop critical thinking which is recognized by engineering employers and academics as a fundamental

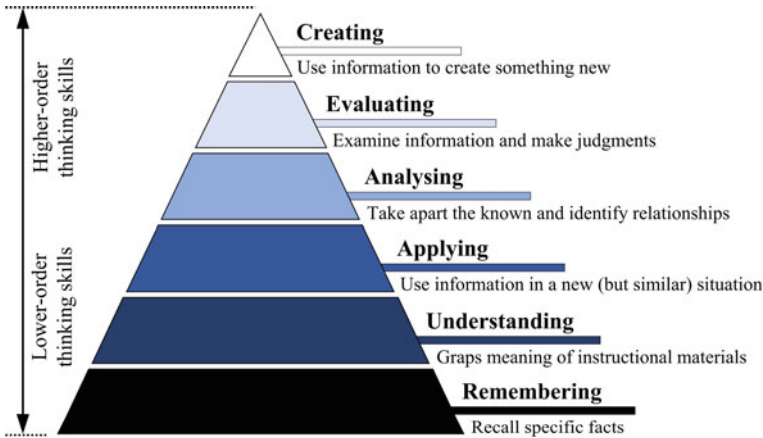


Fig. 4 Bloom's Taxonomy for the cognitive domain. Adapted from (Anderson et al., 2001)

competence (Penkauskienė et al., 2019) for the jobs of the future (World Economic Forum, 2023).

One teaching methodology that allows students deeper learning aligned with the higher-order competencies of Bloom's taxonomy is Project-Based Learning (PBL) in which students are engaged in solving an open-ended problem.

In the PBL approach, students have a leading role while lecturers have a supervision and guiding role in the learning process, and the work is performed in small groups. This diverges from traditional teacher-led classroom activities by allowing students to manage their own time and effort as self-studying while opportunities for critical discussion are offered during project-based classes. The learning objectives promoted in the proposed PBL in bulk forming are the following:

- To promote a strong theoretical basis of the ideal work and slab methods,
- To apply analytical and numerical methods as means for solving a specific problem,
- To compare the application of analytical methods with numerical methods,
- To evaluate the potential and limitations of the problem-solving with each specific method,
- To acquire other competencies, such as communication, collaboration, critical thinking and creativity through the development of the project,
- To provide opportunities for feedback and revision of the work plan and project similar to what occurs in real professional life.

4 Resources and Organization

Implementation of the proposed methodology requires lecturers from manufacturing courses to have a medium to strong pedagogical background on phenomenological concepts of bulk metal forming. These concepts are mainly based on the theory of plasticity involving: (i) stresses and strains, (ii) plastic deformation at micro and macroscopic levels, (iii) flow curve models and strain hardening, (iv) yield plasticity criteria, (v) mechanical testing of metallic materials and (vi) flow rules, constitutive equations, and plastic work. These main concepts are relevant because together they compose the foundation of both analytical and numerical methods capable of analyzing a large spectrum of different metal forming processes.

Adding to the above, other forms of expertise related to numerical methods from a developer's viewpoint, tribology applied to forming, formability of metals, mechanisms of machine-tools and tool design can be of great use to lecturers and junior instructors for complementing plasticity theoretically based concepts with detailed and valuable theoretic and experimental insights. Abilities in proper handling and transferring this know-how to students are typically dependent on the subareas where lecturers develop their scientific work which explains why different intensities in the coverage of each topic can vary across different universities. Still, little or even vague expertise in the aforementioned topics should not hinder the implementation of the proposed methodology whose resources needed for fully preparing lecturers are presented hereafter.

4.1 Analytical Resources

Metal forming courses require concepts transmitted to students to be strongly grounded in some type of available literature in the form of multimedia files, personal notes, and most importantly metal forming handbooks with contents aligned with the teaching objectives of each course (Bhattacharyya et al., 2022).

In several bachelor and master courses spread worldwide, available handbooks such as those of Groover (2011), Kalpakjian and Schmid (2013) and Schey (1999) are useful for providing a solid and general background on manufacturing processes with a good description of science, technology and practice. In what comes to metal forming, mathematical modeling in the aforementioned books is handled in an easily navigable presentation justifying their usability in broad manufacturing courses.

In the case of courses being dedicated to the fundamentals of metal forming, their references must cope with know-how on the theory of plasticity based on applied mathematics and mechanics that constitute the cornerstone of analytical and numerical modeling of plastic deformation processes (Bruhns, 2019). Examples of reference handbooks that completely fulfil these requisites are those of Hosford and Caddell (2007), Lange (1985), and Mielnik (1991), while more modern ones such as that of Klocke (2013) provide partial coverage of phenomenological topics

but complemented with practical insights on forming processes, machine-tools, and tooling. For the proposed methodology, the recommended bibliography is centered on the handbook of Rodrigues and Martins (2010) widely used in bachelor and master engineering courses of Portuguese-speaking universities.

4.2 Numerical Resources

The inclusion of numerical analysis by means of the finite element method in the proposed methodology is aimed at providing students with a comprehensive overview of the interactions between the main plastic deformation process variables and their consequences on metal flow. This computational-based approach serves as a solid complement to other analytical analysis methods. In fact, physical phenomena that constitute metal forming operations are sometimes difficult to thoroughly express using quantitative relationships. Hence, proper handling of nonlinearities in metal forming related to geometry, material properties and boundary conditions only became possible with the widespread use of finite element modelling for the analysis of state-of-the-art industrial processes (Tekkaya & Martins, 2009).

Being the proposed methodology focused on the analysis of bulk metal forming processes where elastic deformations that take place on the workpiece are negligible, computer programs based on the quasi-static flow formulation are the most appropriate ones to be utilized. Commercial programs such as FORGE[®], DEFORM[®], QForm, or eesy-form are among the available options for solving metal forming processes by making use of constitutive equations for rigid-plastic behaviour. In terms of available literature, handbooks from Dunne and Petrinic (2005) or Kobayashi et al. (1989) are good bibliographic sources for courses that convey deeper into finite element formulations applicable to large deformations. More recent handbooks such as that of Nielsen and Martins (2021b) address the aforementioned concepts in detail while also bridging them together with other key topics in metal forming concerned with material formability and tool design.

Implementation of the proposed methodology made use of the in-house finite element program i-form developed by researchers from the University of Lisbon and the Technical University of Denmark (Sampaio et al., 2022a, 2022b). The program allows thermo-mechanical simulation of metal forming operations with given geometries for workpieces and tools, material data, boundary conditions, type of analysis and numerical parameters to provide predictions of force, velocities, stresses, among other field variables (Fig. 5). Details on the theoretical background and numerical implementation of i-form can be found elsewhere (Nielsen et al., 2013).

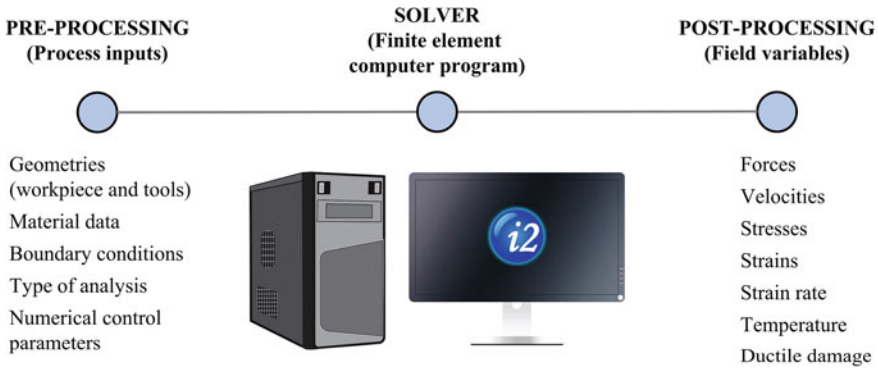


Fig. 5 Finite element environment of metal forming within the computer program i-form

4.3 Organization

The overall structure needed for implementing the proposed methodology makes use of activities scheduled according to two different types: theoretical-practical classes and laboratory classes. All classes are lectured during the semester within a total of 14 weeks under a weekly total student's exposure time of 3.5 h. Details of lectured topics and main milestones during the semester are further disclosed in the timetable presented in Fig. 6.

As seen, theoretical-practical classes are initially focused on lecturing the phenomenological aspects related to the plasticity theory, which are later extended to different metal-forming processes. Both analytical calculation methods are fully covered up to the end of the sixth week of the semester upon which project assignments are delivered to each group composed of a maximum of four students (refer to the milestone on weeks 5–6 of Fig. 6). The remaining theoretical-practical classes convey into some metal forming processes that are further evaluated on mid-term and final written assignments which complements the project-based evaluation (refer to milestones on weeks 7–8 and 13–14 of Fig. 6).

Laboratory classes are divided into two main components. The first component is dedicated to assisting students in installing, using and understanding the framework of the finite element program i-form. These classes are all carried out in a classroom environment (refer to weeks 5–8 and 11–12 of Fig. 6). The second component is focused on hands-on laboratory experiments to provide a more visual perception of different metal forming processes by making use of industrial like equipment (machine-tools, tooling and raw materials). Unlike the first component, the second one is taught in a laboratory environment through experimental demonstrations where students are encouraged to get involved.

The final milestones of the semester are allocated for the submission of the project report, project presentation sessions and lastly for an optional written exam. Further details on the project assignments and corresponding outcomes and expected deliverables will be discussed in the following sections.

Week	Theoretical-practical classes (3 hours per week)	Laboratory classes (0.5 hours per week)	Milestones
1 – 2	Introduction to the course Plasticity theory	Enrollements of student groups for the project	
3 – 4	Analytical modelling with the ideal work method	Compression tests Open & closed die forging	
5 – 6	Analytical modelling with the elementary slab method	Installation and utilization of the finite element program	Project proposal
7 – 8	Forging processes Extrusion processes	Utilization of the finite element program	Mid-term written test
9 – 10	Rolling processes Shearing processes	Shearing and blanking	
11 – 12	Bending processes Deep drawing processes	Utilization of the finite element program	Project deadline
13 – 14	Incremental forming processes	Deep drawing and bending	Project deadline Final written test
Final evaluation period (semester ending)			
15	Preparation week for studying and for presentation and discussion of the deliverables from the project		Group presentation sessions
16	Evaluation week for exams only		Written exam

Fig. 6 Semester-based timetable of the metal forming course

5 Session Development and Outcomes

Knowledge transfer to students under different types of classes (refer to the semester-based timetable shown in Fig. 6) requires the implementation of different teaching methodologies to allow assembling technological, analytical, and numerical learning in each class type.

In what follows, special emphasis is placed on the methodologies used for teaching analytical concepts (theoretical classes of weeks 1–8) and numerical resources (laboratory classes of weeks 5–8 and 11–12) needed for analysing and solving bulk metal forming processes.

5.1 Analytical Methods

The first two weeks of the course are focused on teaching students the fundamental principles of mechanical behaviour in metals and the theory of plasticity. In the subsequent four weeks, the theoretical-practical classes introduce the analytical methods necessary for the project. These classes cover the work balance method followed by

the slab analysis method. During these sessions, both methods and their underlying assumptions are presented to provide students with a comprehensive understanding of their application domains, limitations, and potential errors.

Following the theoretical introduction of each method, practical examples are provided, and students are guided to solve problems using the Portuguese handbook by Gouveia et al. (2011). Moreover, these classes also serve as an introduction to bulk metal forming processes such as extrusion, drawing, rolling, and forging, which are presented with higher depth after the sixth week.

5.1.1 Extrusion Analysis with Work Balance Method

A didactic and comprehensive approach to teaching the utilization of the ideal work method is by applying it to cylindrical forward extrusion or wire drawing operations. This strategy not only helps students understand the mechanics of these manufacturing processes but also facilitates a thorough comprehension of the methodology to derive the force/pressure and energy needed to carry out the metal forming operations through analytical analysis.

Figure 7 illustrates a direct (forward) axisymmetric extrusion of a cylindrical rod with initial D_0 and final diameter D_1 . The conical region is where plastic deformation is imposed by a die leading to an increase in strain up until the rod reaches the die exit. If redundant work and friction are to be neglected, plastic deformation can be assumed as homogeneous reaching a maximum effective strain $\bar{\epsilon}_f$ and effective stress $\bar{\sigma}_f$ at the die exit where $D = D_1$.

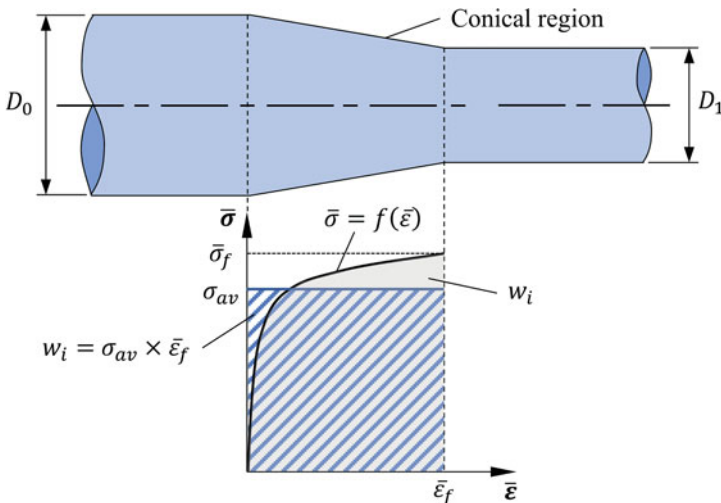


Fig. 7 Schematic representation of a direct extrusion of a rod with the graphical visualization of the average flow stress σ_{av} associated with ideal work w_i and effective strain $\bar{\epsilon}$

In the above circumstances, the energy spent on redundant deformation W_r and friction W_f is neglected. These assumptions result in the total work W_t required for the extrusion operation to be equal to the ideal work for the plastic deformation W_i ,

$$W_t = W_i = V \int_0^{\bar{\epsilon}_f} \bar{\sigma} d\bar{\epsilon} \quad (1.6)$$

where the integral represents the area below the material flow curve (Fig. 7) corresponding to the plastic work per unit volume w_i which allows for determining the average flow stress σ_{av} on the material volume V along the conical region,

$$\sigma_{av} = \frac{w_i}{\bar{\epsilon}_f} = \frac{\int_0^{\bar{\epsilon}_f} \bar{\sigma} d\bar{\epsilon}}{\bar{\epsilon}_f} \quad (1.7)$$

By combining Eqs. (1.6) and (1.7), one can express the ideal work for the plastic deformation W_i as a function of the deformed volume V , the average flow stress σ_{av} and maximum effective strain $\bar{\epsilon}_f$,

$$W_i = V \sigma_{av} \bar{\epsilon}_f \quad (1.8)$$

Additionally, the steady-state regime of extrusion under ideal conditions is imposed by the extrusion force F applied to the initial rod which remains constant along the punch displacement ΔH . Hence, the external work needed to carry out the metal forming operation is given by,

$$W_e = F \Delta H \quad (1.9)$$

By establishing an energy balance between ideal work (Eq. 1.8) and external work (Eq. 1.9), the extrusion force required to plastically deform a given volume V of the workpiece is given by,

$$F = \sigma_{av} \bar{\epsilon}_f \frac{V}{\Delta H} = \sigma_{av} \bar{\epsilon}_f A_0 \quad (1.10)$$

where A_0 is the initial cross-section of the rod. However, Eq. (1.10) is absent from the individual contributions of work related to redundant deformation and friction. This limitation can be addressed by considering empirical efficiency values η based on the ratio between ideal and total work (Eq. 1.4) that allows assessing a better prediction of the extrusion force,

$$F = \frac{1}{\eta} \sigma_{av} \bar{\epsilon}_f \cdot A_0 \quad (1.11)$$

This methodology is applicable for computing the extrusion force in the steady state regime by accounting the effect of friction along the conical region of the workpiece. In case of indirect (backward) extrusion operations, this is generally the case due to low relative sliding between the cylindrical rod and the tool container. In case of direct extrusion, friction plays a more significant role since it opposes the relative motion between the workpiece and the container wall hindering the movement of the punch and increasing its force. Moreover, this phenomenon diminishes along the punch movement due to linear decrease of the contact area between the container wall and the cylindrical rod.

The additional force F_f needed to overcome friction-based shear stresses between the cylindrical rod and the container walls, can be determined by balancing the forces acting on the workpiece inside the container along the axial (movement) direction (Fig. 8). By assuming a constant shear stress τ along the container wall over the unextruded length $(H - \Delta H)$, the additional force F_f is given by,

$$F_f = \tau \pi D_0 (H - \Delta H) \tag{1.12}$$

Summing up Eqs. (1.12) and (1.11) allows assessing the total extrusion force required to plastically deform the cylindrical rod into its final shape and to overcome friction within the container and conical die of the extrusion tool set,

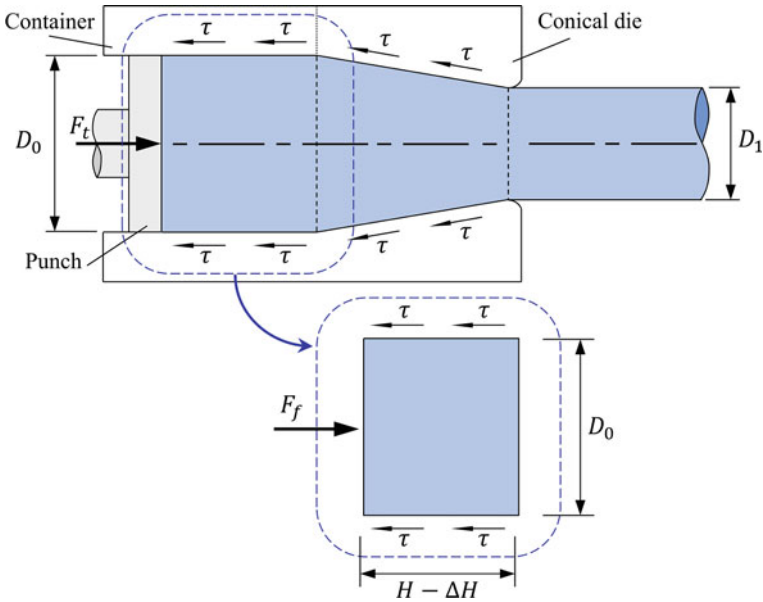


Fig. 8 Schematic representation of a direct extrusion of a rod with special emphasis placed on the friction based shear stresses acting on the contacts between the workpiece and the tool set (container and conical die)

$$F_t = \tau \pi D_0 (H - \Delta H) + \frac{1}{\eta} \sigma_{av} \bar{\epsilon}_f A_0 \quad (1.13)$$

Lastly, the punch pressure p_t can be obtained by dividing Eq. (1.13) by the cross-sectional area of the punch, which is defined by the initial cross-section of the rod A_0 ,

$$p_t = \frac{4\tau}{D_0} (H - \Delta H) + \frac{1}{\eta} \sigma_{av} \bar{\epsilon}_f \quad (1.14)$$

5.1.2 Extrusion Analysis with Slab Method

The slab method is one of the earlier methods of analyzing the stresses and loads of bulk metal forming processes such as upsetting, rolling, extrusion or drawing under plane strain or axisymmetric conditions within steady or non-steady states.

To enable effective teaching and enhance student learning outcomes of this analytical method, the methodology discussed in Sect. 3. can also be applied and built upon the example of a direct extrusion operation of a rod like what was presented for the ideal work method.

Figure 9 depicts an elemental conical frustum in the plastically deformed region during the extrusion through a conical die with a semi-angle α . By considering normal and frictional stresses acting on the elementary slab along the axial direction, the following differential equation can be written,

$$(\sigma_z + d\sigma_z) \frac{\pi}{4} (D + dD)^2 + p \sin \alpha \left(\frac{\pi D dz}{\cos \alpha} \right) + \tau \cos \alpha \left(\frac{\pi D dz}{\cos \alpha} \right) = \sigma_z \frac{\pi}{4} D^2 \quad (1.15)$$

where σ_z is the axial stress, p is the normal pressure and τ is the frictional shear stress. Neglecting the second-order terms, attending to the geometric relationship $dz = dD/(2 \tan \alpha)$ and modelling friction with the Prandtl model $\tau = mk$ where m is the constant friction factor along the contact between the workpiece and the conical die gives rise to the following equation,

$$\sigma_z dD + \frac{D d\sigma_z}{2} + p dD + mk \frac{dD}{\tan \alpha} = 0 \quad (1.16)$$

Computation of the axial stress σ_z from Eq. (1.16) requires knowing beforehand the pressure value p which can be further assessed from force balance along the radial direction of the conical frustum slab,

$$\sigma_r \pi D dz + p \pi D \cos \alpha ds = mk \pi D \sin \alpha ds \quad (1.17)$$

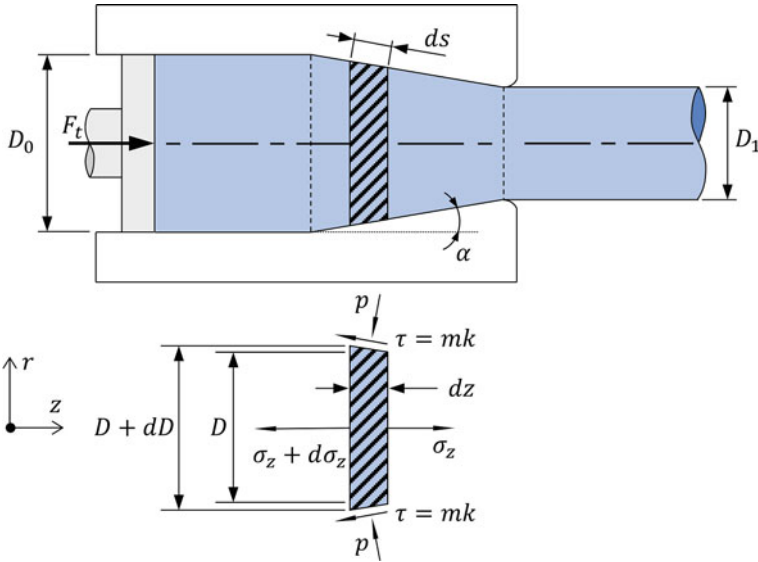


Fig. 9 Schematic representation of a direct extrusion of a rod with a detailed presentation of the loading diagram in elemental (slab) conical frustum slab

This expression can be further simplified by considering the geometric relationship $ds = dz / \cos \alpha$ as follows,

$$\sigma_r = mk \tan \alpha - p \tag{1.18}$$

The axisymmetry of the extrusion operations imposes the radial σ_r and circumferential stresses σ_θ to be equal. Assuming that their values are constant during extrusion allows linking the axial and radial stresses together using the Tresca yield criterion $\sigma_z - \sigma_r = 2k$ where $2k$ is the material yield stress. Combination of this criterion with Eq. (1.18) allows handling the normal pressure p at the conical die,

$$p = 2k + mk \tan \alpha - \sigma_z \tag{1.19}$$

By merging Eqs. (1.16) and (1.19), an expression for calculating the incremental axial stress $d\sigma_z$ can be written in differential form,

$$d\sigma_z = -2k \left(2 + m \tan \alpha + m \frac{1}{\tan \alpha} \right) \frac{dD}{D} \tag{1.20}$$

From hereinafter, the distribution of axial stress on the plastically deformed material inside the conical die can be determined by integrating the individual contributions of all slabs using the boundary condition at the die exit, where $D = D_1$ and $\sigma_z = 0$. Because the material yield stress $2k$ and the friction factor m are constant,

integration of Eq. (1.20) allows computing the following expression of the axial stress depending on the instantaneous diameter D within the conical region,

$$\sigma_z = -2k \left[2 + m \left(\tan \alpha + \frac{1}{\tan \alpha} \right) \right] \ln \left(\frac{D}{D_1} \right) \quad (1.21)$$

The extrusion pressure at the die entrance can be determined as well by considering the boundary condition $D = D_0$ as follows,

$$p_{dieentrance} = 2k \left[1 + \frac{m}{2} \left(\tan \alpha + \frac{1}{\tan \alpha} \right) \right] \bar{\epsilon}_f \quad (1.22)$$

where, $\bar{\epsilon}_f = \ln(A_0/A_1) = 2\ln(D_0/D_1)$ is the effective strain of the extruded material. Inclusion of strain hardening is also possible by replacing the material yield stress, $2k$ with the average flow stress σ_{av} (Eq. 1.7) as previously mentioned in Sect. 2.

One latter adjustment to the last two expressions is based on the influence that friction taking place in the container walls has on extrusion forces/pressures, similar to what was presented for the ideal work method. This is employed by combining the pressure required to overcome friction in the container with the pressure determined using the slab method at the die entrance (Eq. 1.22) giving,

$$p_t = \frac{4\tau}{D_0}(H - \Delta H) + \sigma_{av} \left[1 + \frac{m}{2} \left(\tan \alpha + \frac{1}{\tan \alpha} \right) \right] \bar{\epsilon}_f \quad (1.23)$$

A thorough presentation of both analytical methods for solving bulk forming operations is generally followed by a beneficial strategy of encouraging students to compare results and engage in discussions about the observed differences in the analytically predicted outcomes. This can be effectively implemented during theoretical-practical classes, providing students with the necessary knowledge needed for their first involvement in the Project-Based Learning methodology.

5.2 Numerical Analysis

Sessions of numerical analysis by the finite element method (FEM) for solving bulk metal forming processes are carried out in the laboratory classes under reverse chronology, meaning that students interact first with output data from numerical simulations. This is done to provide students with a general perspective on the main field variables that can be predicted and extracted through numerical post-processing. Under these circumstances, students are able to bridge finite element resources with the phenomenological nomenclature taught in theoretical classes.

For the first class only, examples of 3D model simulations from industrial metal forming case studies can be used for demonstrating the computational and visualization power of finite element computer programs. However, instructors are advised to

only make use of 2D case studies on the project assignments because 3D models may consume a considerable amount of resources in terms of hardware and computation time to solve them (Magrinho et al., 2019).

Pre-processing of numerical simulations is approached and detailed in the second class, which is based on supplying a set of input information required for running the simulations. The third and final numerical class of the semester serves as a tutorial session given to aid students in solving specific issues related to their project assignments. This subsection will focus on the aims and scope of the first and second numerical classes.

5.2.1 Post-Processing

In order to ensure a smooth initial interaction with numerical post-processing, lecturers must supply students with: (i) the installation files needed for setting up the 2D finite element program and (ii) the necessary data for running a model simulation on their personal computers. This model simulation can be of any bulk forming operation without it needing to reassemble any of the problems delivered on the project assignments.

Figure 10 discloses the initial and final model meshes of a cold closed-die forging operation computed in axisymmetric conditions during the first numerical lecture coupled with predictions of certain field variables that will be of use for students to solve the project assignments. These include the distribution of normalized in-plane velocity v_{xy}/v_{die} , distribution of effective strain $\bar{\epsilon}$, calculation of the force–displacement curve, among many others. Other information regarding visualization tools, data exporting and multimedia features are transmitted to students as well for aiding them in preparing their work reports and group presentations.

5.2.2 Pre-Processing

The first stage of numerical analysis used for supplying all input information needed for running the finite element program is carried out from scratch ending once the simulation is fully computed. To do so, the lecturer should exemplify and describe onsite all steps that are implemented on the user interface of the program while students follow the same procedures on their personal computers. In the pre-processing stage, the following input data should be given,

- Geometries of workpieces and tools to be discretized using finite elements,
- Boundary conditions such as process time, tool velocities, friction models, symmetry constraints and applied pressures/constraints,
- Analysis type (quasi-static vs dynamic, type of coupling, isothermal vs. thermo-mechanical analysis),
- Material data related to material behaviour models, plasticity criterion, flow curve, mechanical properties, and thermal properties,

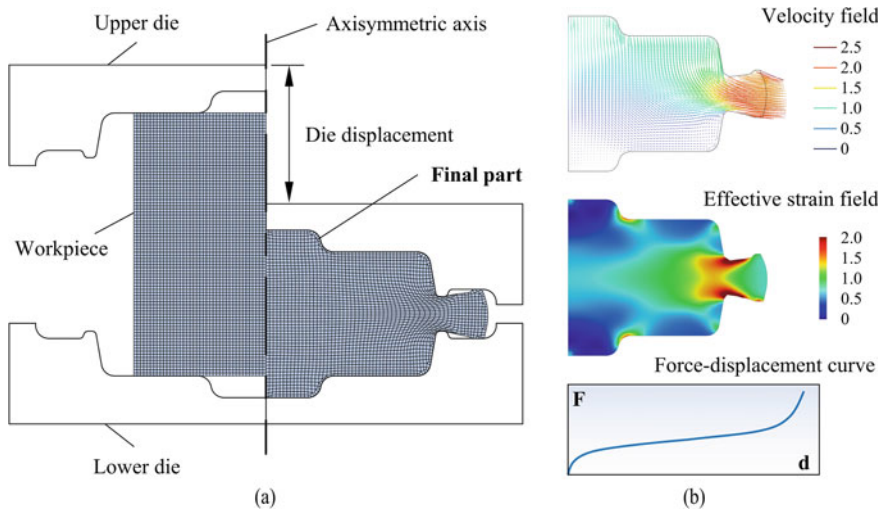


Fig. 10 Post-processing of the 2D model simulation consisting of a closed-die forging operation under axisymmetric conditions. **a** Initial and final computed meshes with captions and **b** Finite element predictions of the normalized velocity field, effective strain field and force–displacement curve at the final step

- Numerical control parameters associated with solution procedures, convergence criteria, time stepping and output requirements.

Figure 11 presents examples of input data related to the first two bullets presented above for running the model simulation of the cold closed-die forging operation. Tool and workpiece geometries are inputted through computer-aided design files (CAD) and subsequently discretized using structured quadrilateral elements (workpiece) and rigid-linear elements (dies). The operation is modelled in axisymmetric conditions, while a tool velocity v_{die} is given for the upper die and constant friction factor m is set for the interfaces of both dies. The analysis is carried out in the quasi-static regime under isothermal conditions and the material data is supplied as a rigid-plastic model with a Hollomon flow curve to be computed under isotropic material flow using the Von Mises plasticity criterion.

Lastly, guidelines for setting numerical parameters such as the time increment of each step, the maximum number of iterations and corresponding residual vectors are given. In addition to the mesh size (i.e., the total number of quadrilateral elements discretizing the workpiece), can be calibrated by students to conduct convergence analyses of the obtained numerical results.

By following the aforementioned steps, students are able to construct the exact numerical model that was analysed in the initial numerical class, and then apply post-processing techniques. In the upcoming weeks leading up to the project deadline, it is expected that students will utilize their acquired knowledge to engage in project assignments as autonomous group work, carried out outside the classroom. However,

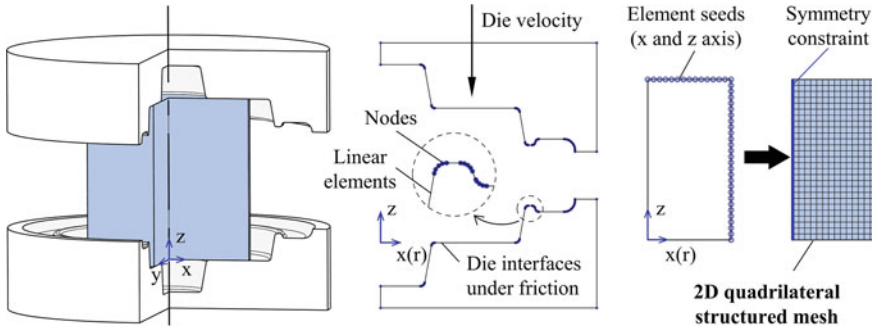


Fig. 11 Numerical input data regarding geometries of the workpiece and tools, and boundary conditions for running the 2D model simulation of a closed-die forging operation

instructors will continue to provide ongoing feedback during office doubt sessions to ensure that students remain focused on the driving metal forming problems and adhere to the core project guidelines.

A detailed overview of the guidelines for using both pre and post-processors of the finite element computer programme can be found in the user manual provided to the students at the start of the semester. Besides describing all features included in the programme, the user guide contains step-by-step examples of elementary metal forming operations that students can carry out autonomously.

6 Deliverables and Assessment

This section provides an overview of the project assignments given to students with further information on the corresponding deliverables (i.e., examples of expected results) and on the assessment criteria used for scoring each work through two components: a written report and an oral presentation.

For this purpose, all the aforementioned topics are detailed according to an example of an implementation of the proposed methodology. The chosen example is that of a cold direct extrusion operation of a cylindrical rod which will be presented and analysed throughout this section.

6.1 Project Assignments

Project assignments delivered to student groups are twofold. In the first section, a bulk metal forming operation is presented with emphasis on the final geometry of a proposed part (Fig. 12a). Here, the geometry and particular dimensions of the final part are given as well as the material data of the workpiece (Fig. 12b). As seen, no

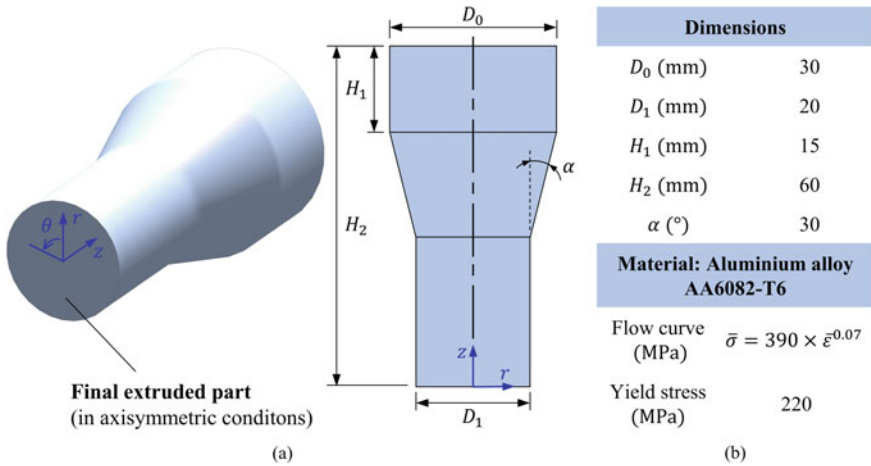


Fig. 12 Example of a first section of a project assignment addressing a direct extrusion operation from an AA6082-T6 aluminium rod. **a** Geometry with added nomenclature of the final part and **b** Dimensions and material data

information regarding the dies (namely, dimensions, geometry and displacement) is given because students are supposed to model them from scratch by analysing not only the dimensions of the final part but also its initial workpiece geometry. In the case of the extrusion operation for producing the part of Fig. 1.12, only two dies are needed: the moving punch at an arbitrary constant velocity and the completely static container featured with the conical die, both subjected to friction.

The second section of the project assignments gives an overview of the deliverables expected from the overall work regarding analytical and finite element calculation methods. For the case of solving the direct extrusion operation of an AA6082-T6 aluminium rod (Fig. 1.12), examples of deliverables are as follows,

- Determination of the initial workpiece geometry and dimensions needed for producing the intended part.
- Calculation of true strains, effective strain, and effective stress at the free length of the extruded part with a friction factor $m = 0$.
- Compare the results from deliverable 2. with those obtained from the numerical analysis.
- Evaluate the load–displacement curves through analytical (slab method) and numerical (FEM) analysis with a friction factor $m = 0$.
- Compare the results from deliverable 4. with those obtained using a friction factor $m = 0.2$.
- Determine and discuss the efficiency of the extrusion operation based on results from analytical and numerical analysis.
- Outline the advantages and limitations of both calculation methods based on results attained from the project.

Additionally, a document template written in line with the above-presented deliverables of the project is supplied to students to assist them in writing the final project report. The available blank space of the template is limited (maximum of 8 pages) to urge students in presenting and discussing the deliverables from the project clearly and succinctly similar to what is carried out in scientific manuscripts.

6.2 Examples of Results

6.2.1 Evolution of Strains

Because extrusion is carried out in axisymmetric conditions, all three true strains taking place at the free length of the extruded part can be calculated with the initial D and final D_1 diameters of the part. Firstly, radial ε_r and circumferential ε_θ strains are the same and obtained as follows,

$$\varepsilon_r = \varepsilon_\theta = \ln\left(\frac{D_1}{D_0}\right) = -0.405 \quad (1.24)$$

The remaining axial strain ε_z can be obtained by considering material incompressibility during forming,

$$\varepsilon_r + \varepsilon_\theta + \varepsilon_z = 0 \Leftrightarrow \varepsilon_z = 0.810 \quad (1.25)$$

As expected, both radial and circumferential strains are compressive at the free length of the extruded part while the positive and higher absolute value of the axial strain displays the increase in length of the part due to the subsequent reduction of its section. This resembles a uniaxial tension state of deformation that allows acknowledging the axial strain ε_z and effective strain $\bar{\varepsilon}$ to be equal according to the Von Mises yield criteria. Hence, the effective stress of the material after being extruded $\bar{\sigma}_f$ can be computed through the material flow curve previously disclosed in Fig. 1.12b, knowing the effective strain $\bar{\varepsilon}_f$ at the die exit,

$$\bar{\sigma} = K \bar{\varepsilon}_f^n = 390 \times 0.810^{0.07} = 384.32 \text{ MPa} \quad (1.26)$$

However, the aforementioned results are valid only in ideal circumstances i.e., if the plastic deformation is uniform. This is rarely the case since the reduction in diameter imposed by the conical die comes at the cost of generating shear stresses that may gain considerable proportions near its inclined interfaces. This phenomenon known as redundant work is present even if no frictional forces are considered and can be thoroughly analysed using finite elements.

Figure 13 presents finite element predictions in frictionless conditions of effective $\bar{\varepsilon}$ and axial strains ε_z as a function of the punch displacement along four elements with different distances to the axis (E1, E2, E3 and E4).

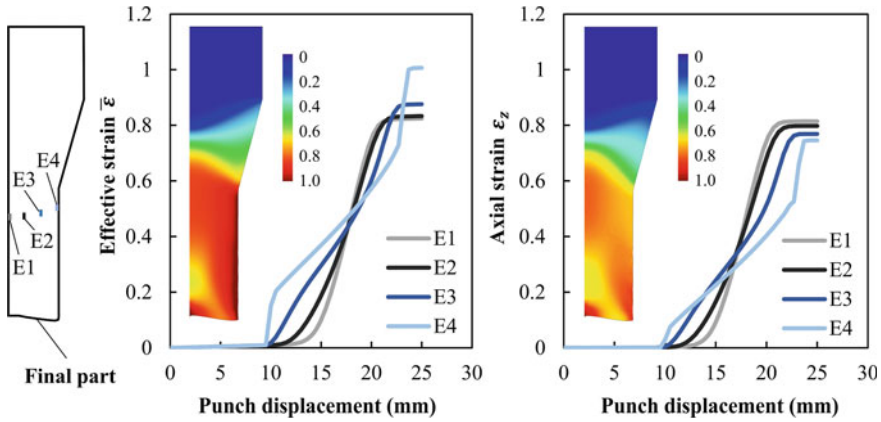


Fig. 13 Finite element predictions of the effective strain and axial strain at four different elements as a function of the displacement from the punch in frictionless conditions

As seen, element E1 adjacent to the axis denotes strain values identical to those calculated with Eq. (1.25). However, moving away from the axis towards the tool surface leads to strains being progressively more affected by the redundant work. This effect is more noticeable for the element E4 adjacent to the container interface where the highest effective strains can be found.

6.2.2 Extrusion Force–Displacement Curve

The calculation of the extrusion forces, in the steady-state stage, as a function of the punch displacement is carried out analytically using the elementary slab method (Sect. 5.1). Assuming that the shear stress due to friction at the interface with the cylindrical container is constant (Prandtl model) the total extrusion pressure using the slab method, can be computed by replacing $\tau = mk$ in Eq. (1.23) as follows,

$$p_t = \frac{4mk}{D_0}(H - \Delta H) + \sigma_y \left[1 + \frac{m}{2} \left(\tan \alpha + \frac{1}{\tan \alpha} \right) \right] \bar{\epsilon}_f \quad (1.27)$$

Because the material exhibits a power law flow curve (Fig. 12), the material strain hardening inside the conical die can be included in the ram pressure calculations by considering the average flow stress σ_{av} (Eq. 1.7) instead of the material yield stress,

$$\sigma_{av} = \frac{K \bar{\epsilon}_f^n}{n + 1} \quad (1.28)$$

where K and n are the material strength and strain-hardening coefficients. This allows expressing the total extrusion pressure applied by the moving punch as follows,

$$p_t = \frac{4mk}{D_0}(H - \Delta H) + \frac{K\bar{\varepsilon}_f^{n+1}}{n+1} \left[1 + \frac{m}{2} \left(\tan \alpha + \frac{1}{\tan \alpha} \right) \right] \quad (1.29)$$

Subsequently, the extrusion force can be obtained by multiplying the corresponding pressure with the initial area of the billet in contact with the punch,

$$F_e = p_t \frac{\pi D_0^2}{4} \quad (1.30)$$

Additionally, it is necessary to predict the instant when the operation reaches a steady state plastic flow which occurs when the material emerges from the die exit. In this non-steady stage of the extrusion, the relation between an arbitrary displacement ΔH from the punch and the instantaneous diameter D_i of the rod within the conical die can be determined by material incompressibility (Fig. 14a) and expressed according to the following equation,

$$\Delta H = \frac{D - D_i}{6D^2 \tan \alpha} (D^2 + DD_i + D_i^2) \quad (1.31)$$

where the instantaneous diameter D_i can be related to the maximum instantaneous effective strain $\bar{\varepsilon}_i$ of the material inside de die as follows,

$$D_i = \frac{D}{\exp(\bar{\varepsilon}_i/2)} \quad (1.32)$$

Equation (1.30) allows plotting the analytical evolution of force as a function of the punch displacement (Fig. 14b) using the elementary slab method. The transition

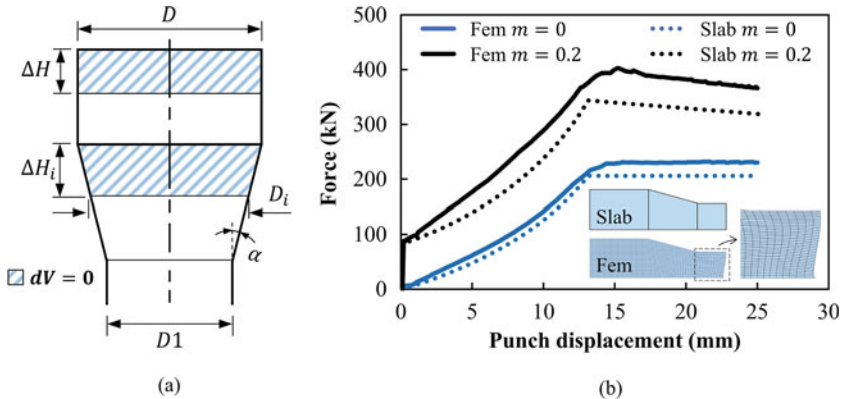


Fig. 14 **a** Schematic representation of the main geometric variables of the extrusion operation **b** Extrusion force as a function of punch displacement obtained through numerical (Fem) and analytical (Slab) analysis with and without friction ($m = 0.2; 0$)

between unsteady and steady states during extrusion is computed by replacing the instantaneous diameter D_i of the rod with its final diameter D_1 , in Eq. (1.31), which gives a punch displacement of $\Delta H = 13.131$ mm. The corresponding numerical simulations with and without the inclusion of friction are plotted as well.

For comparison purposes, Fig. 14b demonstrates that numerically predicted forces are always above those calculated through analytical analysis. This is again due to redundant work taking place at the conical region which is accounted for in finite element analysis, but not in the elementary slab theory which assumes sections of the plane slabs to remain plane throughout deformation. The section detail of the extruded mesh included at the bottom of Fig. 14b allows concluding that the former consideration is not exactly true.

Moreover, the aforementioned effect increases in proportion when constant friction in the container is considered for both methods, as contemplated by the larger deviations in force especially at the steady state stage. However, if no friction is considered, the finite element predicted extrusion force remains constant similar to the assumptions made in the analytical method. Overall, the analytical evolutions of force as a function of punch displacement are shown to be solid predictions.

6.2.3 Extrusion Efficiency

Prior analyses on strains and extrusion forces allowed visualizing the effect of redundant deformation and friction in the overall operation. With this in mind, it is expected that the energy consumption needed to carry out the extrusion operation is affected as well by the same phenomena. Assessing it requires using the ideal work method for estimating the ideal plastic work (i.e., without considering friction nor redundant work). This can be done by substituting the average flow stress, determined by Eq. (1.28), into Eq. (1.8) as follows,

$$W_i = V \sigma_{av} \bar{\epsilon}_f = V \frac{K \bar{\epsilon}_f^{n+1}}{n+1} \quad (1.33)$$

where the volume V_1 corresponds to the extruded region of the part subjected to an effective strain $\bar{\epsilon}_f = 0.810$. By taking into consideration the Hollomon material constants $K = 390$ MPa and $n = 0.07$, Eq. (1.32) provides an ideal work estimation $W_i = 2410.2$ J for the plastic deformation in the steady state regime.

The remaining parcels of the total work can be found from the force–displacement curves acquired from finite element analysis with and without friction. This can be carried out by integrating the curves either through fitting equations that best match the shape of the curves or through computational mathematics techniques such as the trapezoidal rule (Fig. 15a). Because both force and die stroke are discrete data, the trapezoidal rule allows a sound assessment of energy by dividing the curve into several trapezoids and summing together their areas as follows,

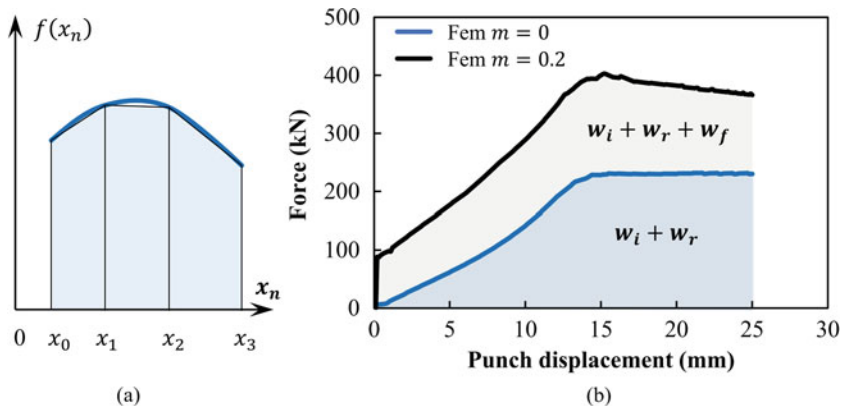


Fig. 15 Determination of the total work from the finite element extrusion forces as a function of die stroke. **a** Implementation of the trapezoidal rule and **b** integration of the force evolutions previously disclosed in Fig. 12b

$$\int f(x)dx = \sum_{n=0}^{N-1} \frac{1}{2}(f_n + f_{n+1})(\Delta x)_n \quad (1.34)$$

Implementation of the trapezoidal rule to the finite element evolutions of force as a function of die stroke (Fig. 15b) allows for determining the total work with and without friction. Knowing the ideal plastic work obtained analytically from the ideal work method, the remaining work parcels related to redundant and friction work can now be individually estimated,

$$W_i + W_r = 3921.2 \text{ J} \Leftrightarrow W_r = 1511.0 \text{ J} \quad (1.35)$$

$$W_i + W_r + W_f = 7399.6 \text{ J} \Leftrightarrow W_f = 3478.4 \text{ J} \quad (1.36)$$

As seen, friction work W_f parcel plays a key role in the extrusion operation under analysis with its value being 44% higher than the ideal plastic work W_i parcel, which is related to the plastic deformation of the workpiece into its final shape. In contrast, the redundant work parcel is the lowest energy contribution for the overall operation being 37% lower than the ideal plastic work parcel.

Lastly, the extrusion efficiency η can be computed using the results obtained from the combination of the analytical and numerical analysis established in Eqs. (1.33) and (1.36),

$$\eta = \frac{w_i}{w_i + w_r + w_f} = 0.326 \quad (1.37)$$

The obtained efficiency value is slightly lower than expected due to the ideal work method accounting only for the energy spent during the steady state regime. Nevertheless, Eq. (1.32) can still be handled to allow assessing the incremental volumes and effective strains within the conical region which in turn would allow attaining a more precise amount of energy consumed during the whole extent of the direct extrusion operation.

6.3 Assessments

Assessment of project group works is based on two main components: (i) a final work report documenting the deliverables of the project (refer to Sect. 6.1) and (ii) an oral presentation from students to lecturers summarizing the main findings of the project.

Project reports are intended to follow a ‘straight to the point’ structure under a maximum of eight pages, meaning that all results found from the analytical and numerical analyses should be briefly and discussed. To do so, students are asked to make use of a document template structured according to the deliverables of the project and formatted as a scientific manuscript. This strategy helps students in getting accustomed to the guidelines of formal writing which will be a valuable asset for their future tasks, e.g., when writing their master thesis.

Oral presentations are used for live assessing the individual knowledge of each student and to evaluate how a group of students can collaborate in order to produce a thorough and cohesive piece of work. As mentioned previously, the presentation should be tailored in line with the deliverables of the project and all group members must actively participate. Each presentation session is given a maximum duration of 30 min where 15 min is for the group presentation and the remaining 15 min is dedicated for discussing about the project results. Other than allowing students to revisit their know-how on metal forming, oral presentations also allow enhancing their communication and teamwork skills.

Table 1 presents the evaluation criteria with corresponding weights used for scoring the final grade of each student group project.

7 Conclusions and Outlook

This chapter was focused on the implementation of the Project-Based Learning methodology aimed at educating students from bachelor and master levels on analytical and numerical methods for analysing bulk metal forming processes. Through numerical analyses using finite element analysis, students can acquire deeper know-how on the combined effects of operating parameters on continuum results related to deformation, velocities, strains, stresses, and loads, among others. However, full

Table 1 Evaluation criteria and weights for assessing student group projects

Evaluation criteria		Weight (%)
1# Report organization	Uniform document design and layout	15
	Clearly identified purpose and approach	25
	Document organization	15
	Arrangement of figures and tables	20
	Formal language	15
	Bibliographic references	10
2# Technical contents	Theoretical results	20
	Analytical results	25
	Numerical results	25
	Critical analysis	20
	Conclusions supporting all results	10
3# Oral presentation	Arrangement of slides	15
	Utilization of multimedia tools	15
	Oral quality	30
	Discussion after presentation	40
Final score	$0.25 \times 1\# + 0.50 \times 2\# + 0.25 \times 3\#$	

Adapted from (Felder & Brent, 2016)

comprehension of the phenomenological aspects of metal forming through analytical analyses is crucial because it allows students to evaluate and discuss numerical results with careful judgment. In terms of general skills, the PBL methodology allows students to further develop their professional aptitudes related to communication, collaboration, creativity, and critical thinking.

All in all, the main conclusions taken by students from the project work are that classical analytical methods (e.g. ideal work and elementary slab methods) are quick and highly accessible to implement, but often need corrections to extend their accuracy (Foster et al., 2009). In contrast, numerical analysis can be highly robust and accurate in high-order, but the convergence of results and initial accessibility issues can be highly time-consuming. Hence, in cases where the convergence of numerical results cannot be assured, analytical methods can be extremely helpful in the first steps toward designing bulk metal forming processes. Additionally, the numerical simulations offer students the possibility of visualizing the forming process, through the observation of the material deformation, and the changes in shape and geometry. This visual feedback allows students to develop an intuitive understanding of the different forming processes, which cannot be obtained experimentally since the material deformation occurs inside the tools.

From experience in implementing the proposed methodology on different metal forming courses, the overall feedback has been positive with students generally understanding the difficulties of both methods of analysis. Still, further progresses

can be achieved from the incorporation of other teaching tools that can elevate the education quality in certain academic topics.

For starters, the possibility of adding experimental analysis of bulk forming processes could be of great interest in conveying students with technical know-how that will accelerate their professional launch into the industry (Martins et al., 2014). Focus can be placed on broader practical aspects related to tool design, project development and experimentation, or on simpler tasks that complement the project work (e.g., obtaining the flow curve of the workpiece material through compression tests). The latter can otherwise be approached using interactive simulation laboratories that overcome the need for capital investment on the resources for real-time laboratory experiments which include but are not limited to raw materials, tools, machine-tools, lubricants and power consumptions (Sharma, 2016).

Adding to the above, the implementation of augmented reality platforms can enhance interactions from students with digital data regarding models, processes animations and simulations using simple equipment (Grodzki et al., 2023). Applications related to deep drawing, bending, extrusion and a novel upset bulk formability test (Sampaio et al., 2022a, 2022b) demonstrate that augmented reality tools can cover a wide range of metal forming operations under an easy-to-use setup by instructors and intuitive use by the student.

Acknowledgements The authors would like to thank Paulo A. F. Martins and Chris V. Nielsen for their kind permission to use the finite element program iform2 in the proposed teaching methodology. Support provided by Fundação para a Ciência e a Tecnologia of Portugal and IDMEC under LAETA-UIDB/50022/2020 and PTDC/EME-EME/0949/2020 is also greatly acknowledged.

References

- Anderson, L., Krathwohl, D., Airasian, P., Cruikshank, K., Mayer, R., Pintrich, P., Raths, J., & Wittrock, M. (2001). *A Taxonomy for learning, teaching, and assessing: A revision of bloom's taxonomy of educational objectives, complete edition* (L. W. Anderson, & D. Krathwohl (eds.); 1st edn.). Addison Wesley Longman.
- Axmann, C., & Mannl, V. (1998). Investigation of metal extrusion and axial compression of compressible media by means of a modified slab method. *Archive of Applied Mechanics (ingenieur Archiv)*, 68(2), 137–146.
- Bhattacharyya, A., Payne, S. W., RoyChoudhury, P., & Schueller, J. K. (2022). An alternative method of teaching the mechanics of bulk metal forming to undergraduates: Newtonian and Lagrangian approaches. *International Journal of Mechanical Engineering Education*, 50(2), 447–492.
- Bruhns, O. T. (2014). Some remarks on the history of plasticity—Heinrich Hencky, a pioneer of the early years. In E. Stein (Ed.), *The history of theoretical, material and computational mechanics—Mathematics meets mechanics and engineering* (1st ed., pp. 133–152). Springer Berlin.
- Bruhns, O. T. (2019). History of plasticity. In *Encyclopedia of continuum mechanics* (pp. 1–61). Springer.
- Dunne, F., & Petrinic, N. (2005). *Introduction to computational plasticity*. Oxford University Press.
- Felder, R. M., & Brent, R. (2016). *Teaching and learning STEM: A practical guide* (1st ed.). Jossey-Bass.

- Foster, A. D., Copeland, T. J., Cox, C. J., Hall, P. W., Watkins, M. A., Wright, R., & Lin, J. (2009). Error analysis and correction in the slab method for determining forming forces. *International Journal of Mechanical Engineering Education*, 37(4), 304–317.
- Gale, W. K. V. (1964). The Rolling of Iron. *Transactions of the Newcomen Society*, 37(1), 35–46.
- Ghoshchi, A. S., Ghoshchi, A. S., Bazargani, S. M., & Emami, S. (2010). Slab method of analysis for three dimensional forward extrusion of squared end section. *ASME 2010 10th biennial conference on engineering systems design and analysis* (vol. 4, pp. 491–495).
- Gouveia, B. P. P. A., Rodrigues, J. M. C., & Martins, P. A. F. (2011). *Tecnologia Mecânica: Tecnologia da Deformação Plástica* (vol. III). Escolar Editora.
- Grodotzki, J., Müller, B. T., & Tekkaya, A. E. (2023). Introducing a general-purpose augmented reality platform for the use in engineering education. *Advances in Industrial and Manufacturing Engineering*, 6, 100116.
- Groover, M. P. (2011). *Introduction to manufacturing processes* (1st ed.). Wiley Global Education.
- Hill, R. (1950). A comparative study of some variational principles in the theory of plasticity. *Journal of Applied Mechanics*, 17(1), 64–66.
- Hosford, W. F., & Caddell, R. M. (2007). *Metal forming: Mechanics and metallurgy* (3rd ed.). Cambridge University Press.
- Kalpakjian, S., & Schmid, S. (2013). *Manufacturing engineering and technology* (7th ed.). Pearson Education.
- Klocke, F. (2013). *Manufacturing processes 4* (1st ed.). Springer.
- Kobayashi, S., Oh, S.-I., & Altan, T. (1989). *Metal forming and the finite-element method*. Oxford University Press.
- Lange, K. (1985). *Handbook of metal forming* (1st ed.). McGraw-Hill.
- Magrinho, J. P., Silva, M. B., & Martins, P. A. F. (2019). A flexible sheet-bulk forming demonstrator. *The International Journal of Advanced Manufacturing Technology*, 103(1–4), 1405–1417.
- Martins, P. A. F., Montanari, L., Cristino, V. A., & Silva, M. B. (2014). Formability and Simulative Tests in Modern Sheet Metal Forming Education. In J. Davim (Ed.), *Modern mechanical engineering. Materials forming, machining and tribology* (pp. 411–447). Springer.
- Mielnik, E. M. (1991). *Metalworking science and engineering* (1st ed.). McGraw-Hill.
- Nielsen, C. V., Zhang, W., Alves, L. M., Bay, N., & Martins, P. A. F. (2013). Coupled finite element flow formulation. In *Modelling of thermo-electro-mechanical manufacturing processes with applications in metal forming and resistance welding* (pp. 11–36). Springer.
- Nielsen, C. V., & Martins, P. A. F. (2021b). *Metal forming: Formability, simulation, and tool design*. Elsevier.
- Nielsen, C. V., & Martins, P. A. F. (2021a). Finite element simulation: A user's perspective. In *Metal forming* (pp. 109–180). Academic Press.
- Nielsen, C. V., & Bay, N. (2018). Review of friction modeling in metal forming processes. *Journal of Materials Processing Technology*, 255, 234–241.
- Penkauskienė, D., Railienė, A., & Cruz, G. (2019). How is critical thinking valued by the labour market? Employer perspectives from different European countries. *Studies in Higher Education*, 44(5), 804–815.
- Pragana, J. P. M., Baptista, R. J. S., Bragança, I. M. F., Silva, C. M. A., Alves, L. M., & Martins, P. A. F. (2020). Manufacturing hybrid busbars through joining by forming. *Journal of Materials Processing Technology*, 279, 116574.
- Rodrigues, J. M. C., & Martins, P. A. F. (2010). *Tecnologia Mecânica: Tecnologia da Deformação Plástica* (vol. I–II). Escolar Editora.
- Sampaio, R. F. V., Zwicker, M. F. R., Pragana, J. P. M., Bragança, I. M. F., Silva, C. M. A., Nielsen, C. V., & Martins, P. A. F. (2022). Busbars for e-mobility: State-of-the-art review and a new joining by forming technology. In *Mechanical and industrial engineering: Historical aspects and future directions* (pp. 111–141). Springer.
- Sampaio, R. F. V., Pragana, J. P. M., Bragança, I. M. F., Silva, C. M. A., & Martins, P. A. F. (2022a). Revisiting the fracture forming limits of bulk forming under biaxial tension. *International Journal of Damage Mechanics*, 31(6), 882–900.

- Schey, J. A. (1999). *Introduction to manufacturing processes* (3rd ed.). McGraw-Hill.
- SCHULER. (1998). *Metal forming handbook*. Springer.
- Sharma, R. S. (2016). Technology enabled learning of metal forming processes for engineering graduates using virtual simulation lab. *International Journal of Mechanical Engineering Education*, 44(2), 133–147.
- Tao, F., Zhang, L., & Nee, A. Y. C. (2011). A review of the application of grid technology in manufacturing. *International Journal of Production Research*, 49(13), 4119–4155.
- Tekkaya, A. E., & Martins, P. A. F. (2009). Accuracy, reliability and validity of finite element analysis in metal forming: A user's perspective. *Engineering Computations*, 26(8), 1026–1055.
- Vollertsen, F. (2013). *Micro metal forming* (F. Vollertsen (ed.)). Springer.
- World Bank. (1982). *World development report*. <https://elibrary.worldbank.org/doi/abs/10.1596/0-1950-3225-X>
- World Economic Forum. (2023). *Future of jobs report*. <https://www.weforum.org/reports/the-future-of-jobs-report-2023/>

Polymers Injection Molding, Process & Defects



David López-Adrio  and David Álvarez 

1 Introduction

This chapter is a guide about teaching the Injection Molding process in technical Bachelor and Master of Science in Mechanical Engineering, Industrial Engineering, or Aerospace Engineering. Contents are designed to be taught in three sessions of two hours with a combination of theoretical and practical skills. These practical seminars are oriented to 20 students and organized in 4 groups of 5 students each.

2 Background

In a world that produces more than 400 million tons per year of polymers (it duplicates in 20 years) and is still growing¹; processes to make pieces from this kind of materials are so important. Polymers production grows because of the unique combination of properties of these products: ease to shape and manufacture, low densities, corrosion resistance, electrical and thermal insulation, and a good rigidity and toughness versus density ratio (Vlachopoulos & Strutt, 2013).

¹ Geyer et al. (2017)—“Global plastics production.” Published online at OurWorldInData.org. Retrieved from: ‘<https://ourworldindata.org/grapher/global-plastics-production>’ (accessed Jun. 23, 2023).

D. López-Adrio (✉)
Deseño Na Enxeñaría Department, Universidade de Vigo, EEI, 36208 Vigo, Spain
e-mail: dlopez@uvigo.es

D. Álvarez
CINTECX, Universidade de Vigo, EEI, ENCOMAT Group, 36310 Vigo, Spain

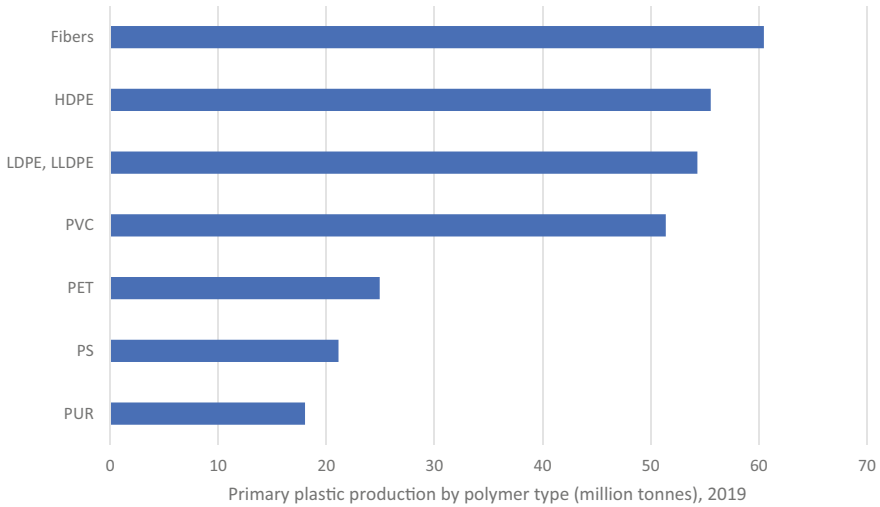


Fig. 1 Primary plastic production by main polymer types 2019, by OurWorldinData.org². PP (polypropylene), HDPE (high-density polyethylene), LDPE (low-density polyethylene), LLDPE (lineal low-density polyethylene), PVC (polyvinyl chloride), PET (polyethylene terephthalate), PS (polystyrene), PUR (polyurethane)

There are many kinds of polymers, but this chapter focuses on the two most common Polypropylene (PP) and Low-Density Polyethylene (LDPE), as shown in Fig. 1. Both polymers are cheap and recyclable with so many applications.

Among the entire polymer processing operations, Injection Molding is the most important along with the extrusion process (Vlachopoulos & Strutt, 2013). Due to its relative ease of use and being able to produce large volumes of pieces with a few manual operations. In addition, this process is very flexible; the same machine could make pieces with completely different geometry or different mechanical characteristics. Only changing the mold or the raw material, in operations that take from minutes to a couple of hours.

This process consists of heating, through a screw-type plunger, a polymer to molten it and force it into a single or multi-cavity mold with the required shape and dimensions. Followed by a very short packing stage necessary to pack more polymer in the mold, and to offset the shrinkage after cooling and solidification. Then the polymer cold down under high pressure until it is solid enough to allow ejection without deformation of the piece.

In this process, the melt path into the mold starts, as shown in Fig. 2, with a sprue and then splits off into runners. Each runner feeds one of the multiple mold cavities through their gates.

² Hannah Ritchie, Veronika Samborska and Max Roser (2023) - "Plastic Pollution" Published online at OurWorldInData.org. Retrieved from: '<https://ourworldindata.org/plastic-pollution>'

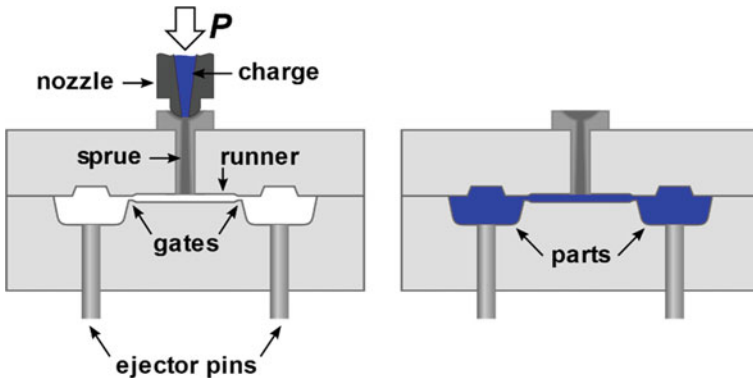


Fig. 2 Simplified diagram of the process by Ariel Cornejo³

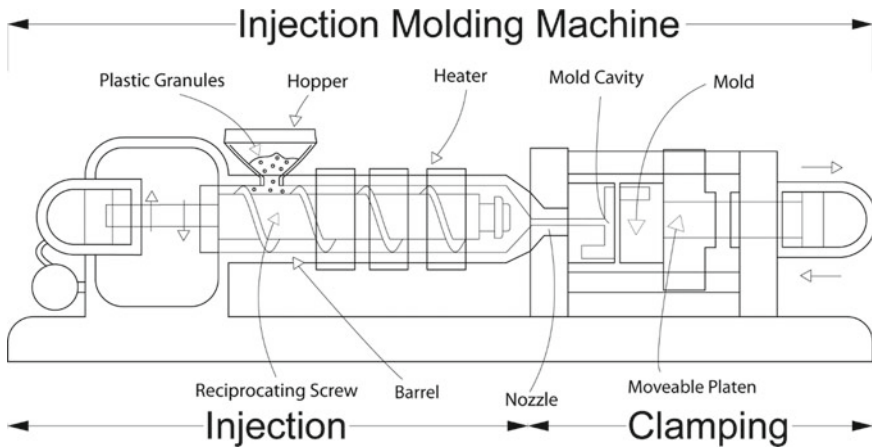


Fig. 3 Injection molding machine scheme by Brendan Rockey, University of Alberta industrial design⁴

To fulfill a good comprehension of this process is important to know the main parts and components of the Injection Molding machine that can be divided into two main sections, as shown in Fig. 3:

- Injection section: where pellets are melted and forced through a nozzle.

³ File: Injection molding diagram.svg—Wikimedia Commons. Published online at Wikicommons under Attribution-ShareAlike 4.0 International (CC BY-SA 4.0) License. Retrieved unchanged from: 'https://commons.wikimedia.org/wiki/File:Injection_molding_diagram.svg' (accessed Jun. 23, 2023).

⁴ File: Injection moulding.png—Wikimedia Commons. Published online at Wikicommons under Attribution 3.0 Unported (CC BY 3.0) License. Retrieved unchanged from: 'https://commons.wikimedia.org/wiki/File:Injection_moulding.png' (accessed Jun. 23, 2023).

- Clamping section: where molds are installed to be used in the machine.

2.1 Injection Section

The injection section is also divided into these main parts:

- Hopper: the way to put plastic pellets inside the machine. This could be standard, as in the image above that must be manually refilled with dry material. Alternatively, it can be a granulate dryer that automatically dehumidifies and feeds the machine with new pellets, stored in an easily refillable container.
- Barrel: inside this part, plastic will be melted by heat and shear stresses generated by the reciprocating screw. In addition, the injection volume is temporally stored on its tip.
- Reciprocating screw: one of the most important parts of the injection molding machine. This is a screw capable not only to rotate but also can translate in its axis direction. Thanks to these movements, this is the part involved in:
 - Transportation of the plastic granules from the hopper to the nozzle with rotational movement.
 - Helping the melting of these pellets due to the shear stresses that the screw generates with its rotation and friction among barrel inner walls, screw flights, and screw spindle; these stresses generate between 60 and 90% of the heat needed to melt the plastic.
 - Dosage of the exact volume of melted plastic controlling the opening of the injection chamber at the nozzle with its translation.

The reciprocating screw is divided into three zones (as shown in Fig. 4). Feed zone, where depth is constant and enough to enable the entry of a good quantity of pellets inside the barrel; this zone is about 50% of the total length of the screw. Compression zone, in this zone the channel depth gets shallower increasing pressure and shear stresses that prevent air between plastic granules and contribute to melting them. This zone is about 25% of the total length of the screw. Metering zone, in this zone, polymer pellets are near to be melted and ready to be mixed and pushed into the mold by the ring plunger (the part that is screwed at the final of the screw); this zone is the final quarter of the screw's total length (including ring plunger) and is the shallowest of the entire screw.

There are various kinds of reciprocating screws; the three most commonly used are:

- General purpose or 3-zone screw as seen in Fig. 4 above. As its name said it is the standard for most polymers and applications.
- Barrier screw (Fig. 5). This kind of screw has an additional flight in its plastication zone called barrier flight. This flight separates the helical mount into two sub-zones, allowing the natural flow of the already melted polymer from the still solid granules thanks to its slightly lower height, as shown in Fig. 6.

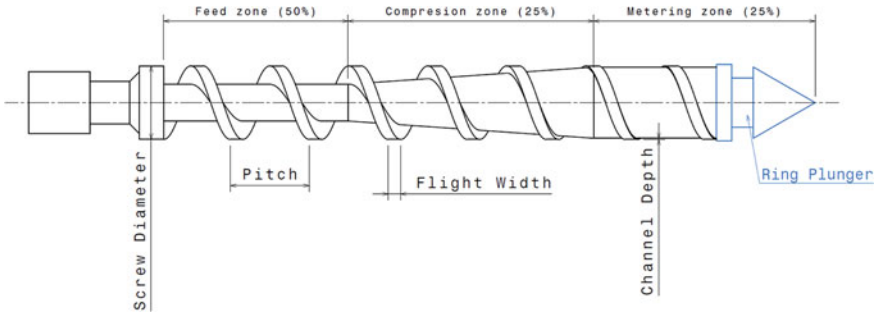


Fig. 4 General purpose reciprocating screw with a description of its main sections, not in scale. By David López-Adrio

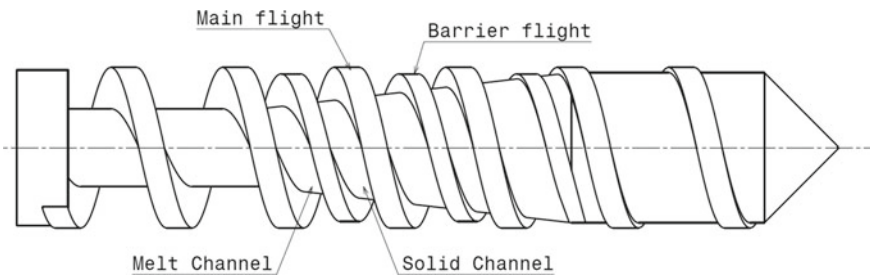


Fig. 5 Barrier reciprocating screw and its main parts, by David López-Adrio

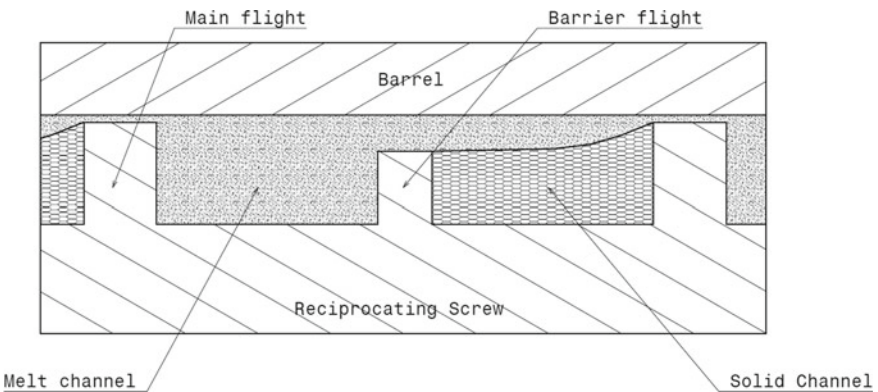


Fig. 6 Barrier screw section, by David López-Adrio

In general-purpose screws, solid granules are surrounded by molten material, so friction and shear stresses have a relatively little effect in the mix. Therefore, heaters are the main cause of melting, which makes plasticizing performance worse. However, the solid channel of the barrier screw allows physical

separation between the melt cushion and the solid bed, increasing melting efficiency by direct friction against the barrel or the screw and eliminating solid breakup, allowing much more control and stability to the mix.

But why barrier screw it is not the standard? Because it is much more expensive and complex to manufacture and has a less controllable melt temperature.

- Degassing screw (Fig. 7). When injecting polymers as recycled PET flakes, that generate high quantities of volatile components, a general-purpose screw cannot separate them from molten material. In consequence, the final piece will have voids that will lead to rejection. In this case, it is required using a special degassing screw. This type of screw has two compression zones with a decreased diameter area (called degassing area) between them, which makes that partially molten plastic can relieve volatile components through an opening in the cylinder.
- Ring plunger: this non-return valve screwed at the end of the reciprocating screw, which is shown in Fig. 8, is responsible to ensure that molten material flows in only one direction. During screw rotation, it allows entry of the plastic to the injection chamber by metering flights of the screw until the material reaches the injection volume. Then, the ring plunger will force molten material thru the nozzle and will prevent the polymer from flowing back over the screw. To accomplish that, the ring plunger has a very close tolerance between its ring and the barrel's inner wall.
- Heaters, thermocouples: heaters are the main way to increase the temperature inside the barrel to maintain melted polymer granules. Thermocouples are measuring instruments that enable gauge and control of the temperature inside

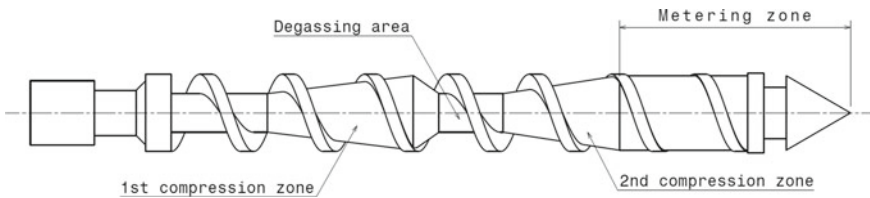


Fig. 7 Degassing screw, by David López-Adrio

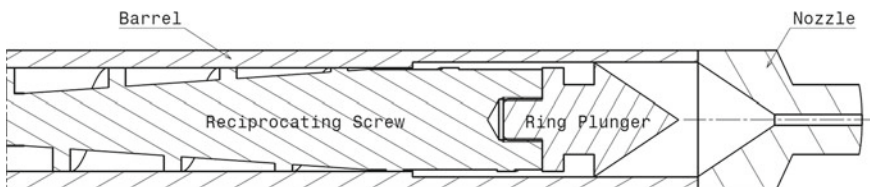
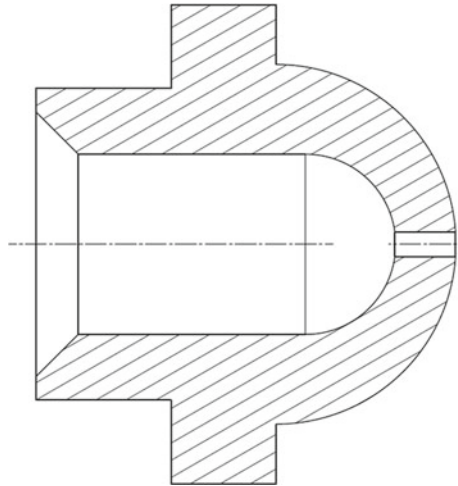


Fig. 8 Ring plunger, reciprocating screw, barrel & nozzle diagram. By David López-Adrio

Fig. 9 General purpose nozzle tip. By David López-Adrio



the barrel doing a close loop control with the heaters and the control system. This allows configuring an individual setpoint per heater.

- Nozzle: through this part, the injection volume of molten material is forced to enter the mold. Its tip design and size are very important to the process behavior. As a small orifice requires higher injection pressure, reducing the available capacity of the machine to fill and pack the mold; but at the same time, can cool the molten material inside the barrel (the tip is in contact with the mold that is refrigerated or at ambient temperature). On the other hand, a wider orifice can make uncontrollable the injection as it can't retain molten material inside it. There are three common types of tips:
 - General purpose: the main flow channel is directed to a small orifice. This kind of tip has a dead spot and it isn't ideal for frequent color or mold changes because molten material can remain in its flow channel, as shown in Fig. 9.
 - Reverse taper: the nozzle tip has a wider orifice that don't freeze quickly, with a separation point (its thinnest section, as shown in Fig. 10) in the middle that makes reversed taper partially frozen and pulled out when the mold opens.
 - Free flow: the diameter inside this tip decreases and leads to a small orifice, as shown in Fig. 11. It eliminates dead spots that the general-purpose tip has in its flow channel.

2.2 Clamping Section

The clamping section is also divided into these main parts:

- Mold: a metal block mechanized to shape molten material in a fixed geometry and dimensions, as shown in Fig. 12. It can be designed to inject one or multiple

Fig. 10 Reverse taper nozzle tip, by David López-Adrio

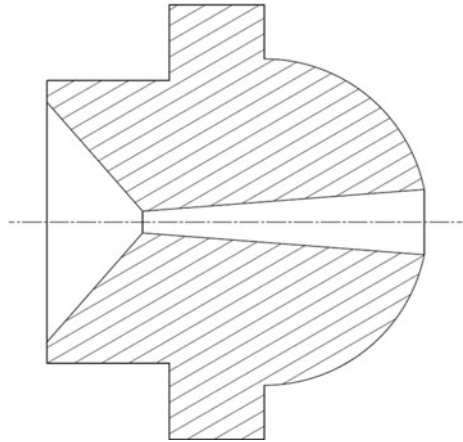
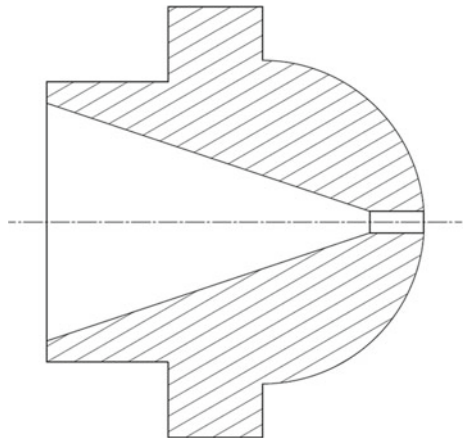


Fig. 11 Free-flow nozzle tip, by David López-Adrio



equal pieces at the same time (up to 100) or designed to inject different pieces. In addition, it can be designed so that only needs a cavity insert change, and then inject a different part. Mold is divided into two main sections by the surface where the cavity and core close, this surface is known as the close or parting line:

- Fixed, Injection or Cavity Side: this side is mounted in the fixed platen of the clamping section. The main components of this side are:
 - Locating ring: where the nozzle enters to center and rests its tip.
 - Sprue bushing: where the nozzle tip rests and molten material starts its path inside the mold. With the runners and gates mechanized in the cavity and core plates, they compound the feed system.
 - Top clamp or setting plate: its only function is to facilitate clamping of the fixed side against the fixed plate of the machine. Usually, the clamp plate is wider than the rest of the plates; but sometimes they are the same wide, in

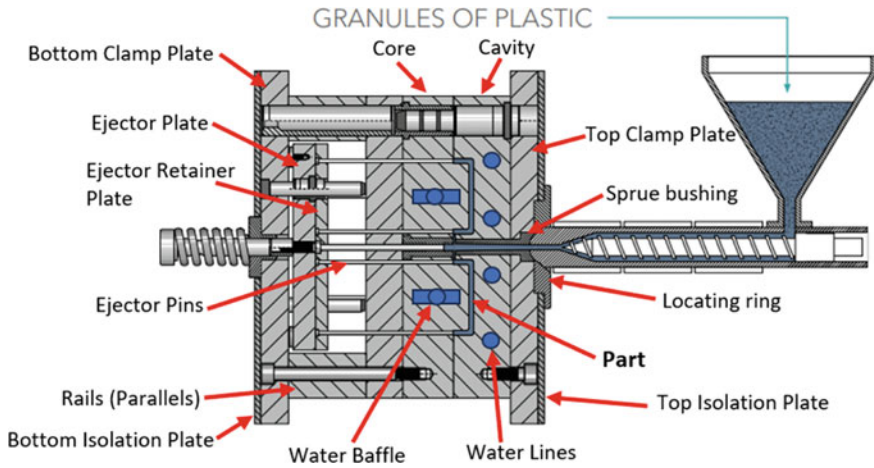


Fig. 12 Mold scheme⁵

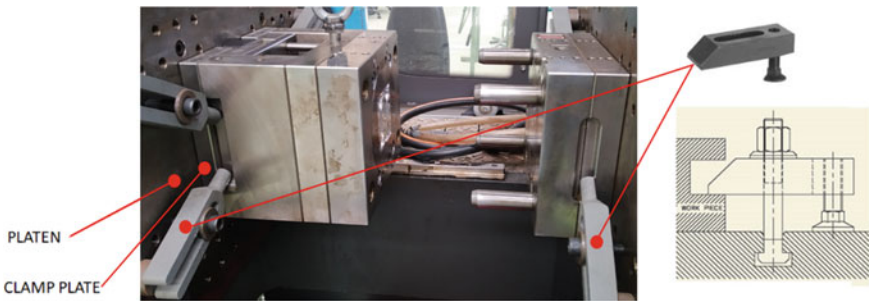


Fig. 13 Mold hold by a mold clamp and its schema, by David López-Adrio

these cases, the cavity plate has clamp slots to allow correct grip as shown in Fig. 13. The mold half can be held with magnets or with mold clamps that use large bolts.

- Cavity plate: in this plate are mechanized the areas of the mold, (Fig. 14) called cavities, where the part is formed into their desired shape. However, usually, cavities are mechanized in inserts that are screwed to the cavity plate to replace them as they become damaged.

These cavities must be a bit bigger than final piece and have a draft angle, since when plastic pieces solidify completely, they shrink a volumetric percentage called coefficient of thermal expansion. The draft angle allows,

⁵ Injection moulding. https://www.meusburger.com/EN/US/media/DOC_PRO_POS_Spritzgiessvorgan_IN (accessed Dec. 14, 2023).

Fig. 14 Feed system, by David López-Adrio

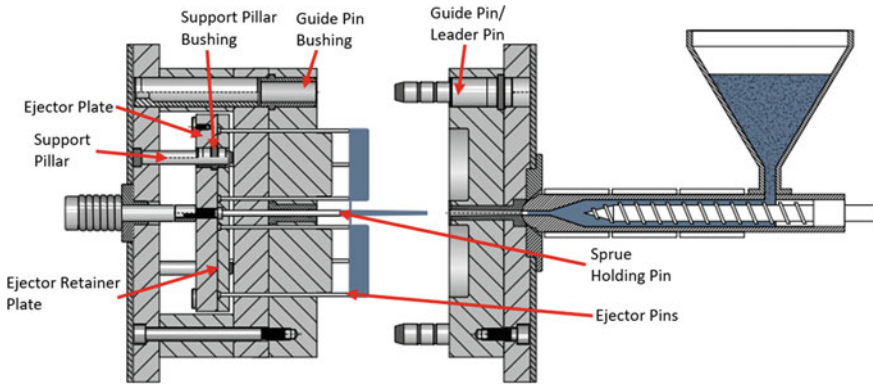
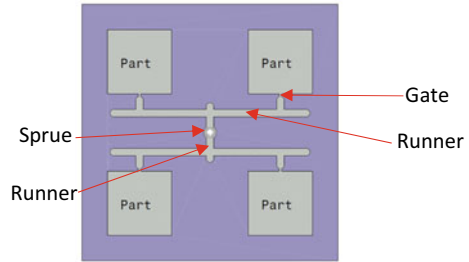


Fig. 15 Open mold and components⁶

during solidification, to create a force against the core that facilitates the ejection of the final piece. Without a draft angle, this force would imprison the piece against the core, making it difficult or impossible to eject.

Also, the cavity plate is drilled with water lines (also known as cooling channels) to allow cooling of the parts (Fig. 12). The cooling system is connected by hydraulic fittings to an external cooling unit, to maintain water temperature constant and close water flow in case needed.

- Guide or Leader pin: four hardened steel pin that prevents mold halves from misaligned with the continuous open and closure cycles, as shown in Fig. 15.
- Moveable, Ejection or Core Side: this side is mounted in the moveable platen of the machine's clamping section and have two common configurations, ejector block or clamping plate plus riser bars (Fig. 15). In the first one ejector and ejector retainer plates are inside a closed plate named ejector box, with the same dimensions as the core plate making inaccessible these plates from the outside. In the second one ejector and ejector retainer plates are between riser bars whose length is equal to the core plate. In this case, both plates are accessible from the

⁶ Injection moulding. https://www.meusburger.com/EN/US/media/DOC_PRO_POS_Spritzgiessvorgang_IN (accessed Dec. 14, 2023).

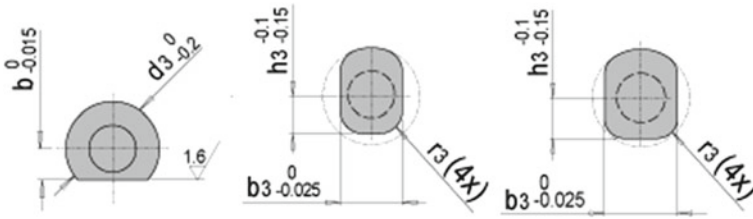


Fig. 16 Different anti-rotation head pin shapes to guarantee pin orientation⁷

outside. The focus is placed on the second type since it is the most frequently used. So, the main components of this side are:

- Core plate: same as cavity plate, but in this case, is usually mechanized to screw core inserts into it to make holes and pockets on the plastic piece. In addition, in this plate, the cooling system is more complex due to the additional thickness compared to the cavity plate, with multi-layer cooling channels and water baffles.
- Guide pin bushing: the components where guide pins enter to prevent mold misalignment.
- Core inserts: removable inserts that perform holes and pockets on the plastic piece.
- Rails or Riser Bars: these bars hold the closure pressure while leaving a constant distance between the core plate and the bottom clamp plate. This allows the movement of the ejector system.
- Ejector system: when plastic parts are already cold, they are pushed off the core using pins or bars integrated with the ejector system.

Ejector plate: this plate must move the entire ejector system forward to eject the final product. It has a bar on it connected to the motors of the machine that allows it to be moved independently of the moveable platen.

Ejector Retaining plate: this plate, screwed to the ejector plate, holds the pins in position. And if the case demands it, their orientation with an oriented geometry as seen in Fig. 16 (e.g., ejector pins mechanized with non-planar tip, sprue holding pin as in Fig. 20).

Ejector pin: they can be of these types⁸:

Ejector pin straight: the standard, Fig. 17.

Blade ejector pin: they are used to push thin walls of the plastic pieces; they do not need an anti-rotation head thanks to their geometry. Fig. 18.

Ejector sleeve (Fig. 19): used to push around an ejector core pin.

⁷ Elementos normalizados|Fabricación de moldes, matrices y utillajes|Meusburger. https://www.meusburger.com/ES/ES/index?gad=1&gclid=EA1aIQobChMI-oG4zqrj_wIVB-3VCh1XJwwyEAYASAAEgKArfD_BwE (accessed Dec. 14, 2023).

⁸ Expulsores y noyos|Elementos normalizados Fabricación de moldes|Meusburger. <https://www.meusburger.com/ES/ES/moldeo-por-inyeccion/expulsores-y-noyos> (accessed Dec. 14, 2023).

Fig. 17 Ejector pin**Fig. 18** Blade ejector pin**Fig. 19** Ejector sleeve

Ejector core pin: they are ejector pins but with another function. In this case, their tips are mechanized to make a hole with a determined shape on the final piece. Besides, they are longer than ejector pins; as they are not going to move with the ejector system, so, they will be held by the bottom clamp plate.

Sprue holding pin (Fig. 20): a special ejector pin that holds the sprue thanks to its geometry.

Return pin: wider ejector pins, responsible of pushing back entire ejector system in case it is left ahead when the mold is going to be closed and preventing ejector pins from being damaged or broken.

Support pillar: steel bars screwed to the core plate. They prevent mold from bending, at the empty area that represents the ejection system, due to the internal pressure generated in the injection process.

- Bottom clamp plate: same as top clamp plate.

Fig. 20 Sprue holding pin, by David López-Adrio

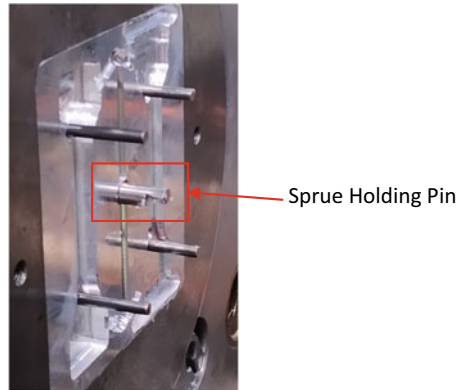
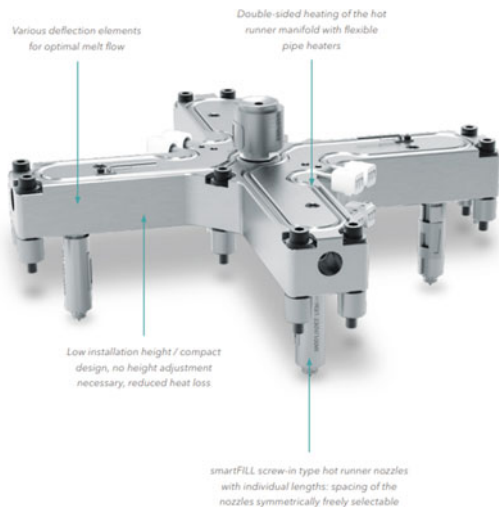


Fig. 21 Hot runner system⁹



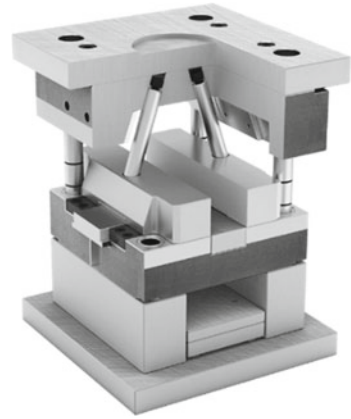
2.3 Other Components

Other additional components of the mold include the following:

- Insulation boards: in case the mold is heated, these boards are screwed to clamp plates to avoid thermal loss.
- Marking stamp: usually, marking stamps are screwed to the core plate. These stamps allow to register the plastic product, manufacturer logo, number of the mold, or date of injection.
- Hot runner systems: a more sophisticated feed system that allows multiple nozzles and flow control by valves as shown in Fig. 21.

⁹ Hot runner systems. Accessed: Dec. 14, 2023. [Online]. Available: www.meusburger.com/hot-runner-systems

Fig. 22 Mold with a double slider system¹⁰



- Slider system: sometimes, plastic pieces have lateral pockets that cannot be performed by the core inserts. In those cases, additional mold movements are needed (frequently perpendicular to the mold open direction) that are realized by slider systems. A mold with this system is shown in Fig. 22.
- Moveable Platen: component of the machine where the moveable half of the mold is clamped. Besides that, the moveable platen is driven by a machine motor to allow the opening and closure of the mold and the movement of the ejector system as independent moves.

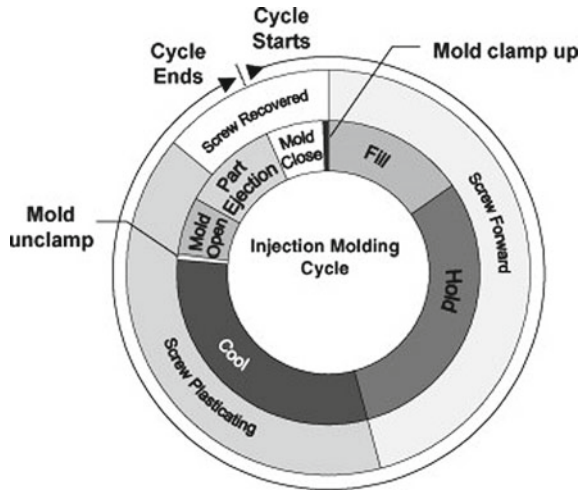
2.4 Process Details

The injection process consists in these stages shown in Fig. 23.

- Mold closure. Close pressure of the mold needs to be controlled to prevent inadvertent mold openings.
- Mold clamp-up: injection unit approach and contact with the mold.
- Filling of the mold. In this step, reciprocating screw moves forward forcing the molten material inside the feed system and cavities of the mold. The injection pressure, injection speed, injection temperature profile, and shot size need to be controlled.
 - Injection pressure: it must provide sufficient force for the molten material to fill the cavities inside the mold, but excessive pressure should be avoided. Otherwise, there might not be enough pressure for subsequent stages. This requirement varies depending on the polymer being injected.
 - Injection speed: so important, this parameter depends on polymer viscosity and gives the fill time value (more speed less fill time):

¹⁰ Sliding core mould. <https://www.meusburger.com/EN/IN/injection-moulding/fb-sliding-core-mould> (accessed Dec. 14, 2023).

Fig. 23 Stages of injection process¹¹



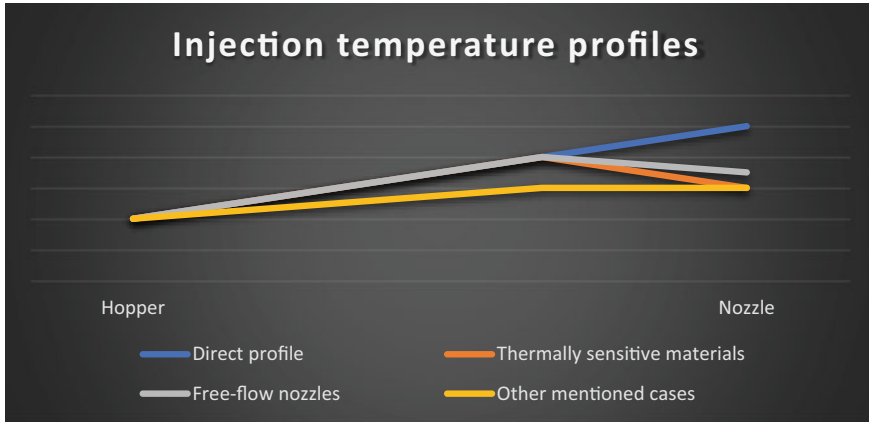
Thin pieces or with long runners must be filled fast.

Increment in injection speed value will have next effects: reduce weld lines, increase surface gloss, decrease fiber and reinforced loads orientation dispersion, increase polymer crystallinity, and increase close pressure needed.

- Injection temperature profile: in the configuration of the process, it is needed to configure the temperature of the different heaters installed on the barrel and controlled by thermocouples; this setpoints are known as injection temperature profile. Commonly this profile will be increasing or direct. This means that the temperature of the heaters will go up from the hopper to the nozzle. Exceptions to general cases are the following cases: thermally sensitive materials, free-flow nozzles, large plastic consumption with reduced cooling times, or reciprocating screw with great depth of pitch. These profiles are shown in Graph 1.

This parameter (in unheated molds and without hot runners), in addition to the spindle speed, are directly related to molten material temperature. If increasing the heaters temperatures or reducing spindle speed, the molten material temperature increases leading to some advantages: weld lines reduction, increased polymer crystallinity, reduction of the viscosity of the molten material, decrease of mold pressure losses, and, in the case of reinforced polymers, reduction of fiber orientation dispersion (this increases the good performance of the reinforcement). Moreover, there are several disadvantages such as: increased volatile and gas generation, which may cause polymer thermal degradation, reduced shear stresses on the molten material, and cooldown time increased by 0.3% per degree.

¹¹ Lim et al. (2008)



Graph 1 Injection temperature profiles, by David López-Adrio

- **Shot size:** the amount of molten plastic between the ring plunger and nozzle that is going to be “shot” inside the mold. This parameter can be controlled directly by setting the injection volume or by adjusting the screw stroke. It is critical, as not only is the volume of the molten material injected into the mold set, but also a slightly larger shot is set to maintain a volume called cushion (between 5 to 10% of the shot size). This cushion acts during hold pressure operation. It is recommended to fill the mold with molten material as fast as possible to 90-95%,¹² then slow injection speed to fulfill the total part volume and continue at a fixed pressure hold phase to start plastic part packaging. In this phase, the screw applies holding pressure through the feed system and molded part, to guarantee final dimensions as the plastic part cools down and contracts volumetrically. This process is only possible with enough molten material remaining in front of the screw to be able to transfer pressure. However, it is a must to minimize the amount of material left in the barrel after each injection cycle. As any remaining material is exposed to constant heat, it could degrade causing problems or mechanical properties loss.

Shot size values are (Figure 24), and being D internal barrel diameter:

- **Optimal Shot Size:** between 1 to $3D$.
- **Exceptional Shot Size:** between 3 to $4D$.
- **Not recommended Shot Size:** below $1D$ and above $4D$.
- **Hold pressure phase:** in this phase the screw applies a constant holding pressure to avoid unwanted dimensional variation on plastic parts. Hold Pressure and hold time are the two parameters to consider in this phase:

¹² Injection Molding FAQ: What is Cushion & why do I need to hold it? <https://www.asaclean.com/blog/injection-molding-faq-what-is-cushion-why-do-i-need-to-hold-it> (accessed Dec. 14, 2023).

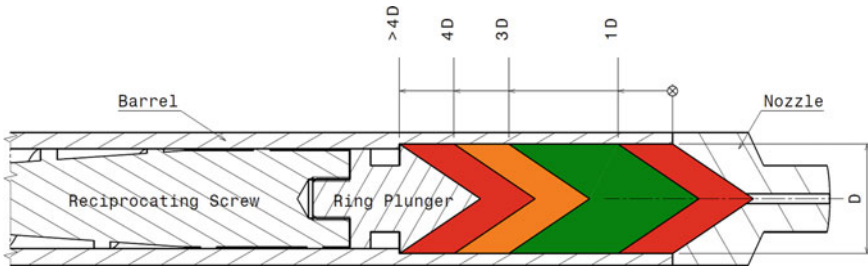


Fig. 24 Recommended shot size, by David López-Adrio

- Hold pressure: it is intimately related to molten material viscosity. If viscosity increases, it worsens transmission of the pressure so its value must be augmented. In the opposite case, hold pressure value must be decreased.
- Hold time: it must be enough to allow the part to cool down sufficiently to keep the final geometry. If it is too long, cooling time and total cycle time will increase; additional molten material is added to the piece.
- Cool phase: in this phase, injection unit goes to its original position. Then, the screw goes backward plasticizing enough polymer to recover shot size and applying back pressure to homogenize molten material properties. In addition, the mold remains closed until plastic pieces solidify completely to not bend it with the ejector system. The only parameter that can be set up in this phase is cool time, which will be reduced with a good cooling system inside the mold.
- Mold open phase: mold opens to its original position.
- Part ejection phase: in the final phase, the ejector system goes forward to expulse the final pieces. They can be removed to a container or extracted by a robot arm with a clamp or vacuum system.

Some recommended injection values to the most common polymers can be found in Table 1.

Part zones:

- Sprue (shown in Fig. 25 as A)

Table 1 Recommended injection values to most common polymers

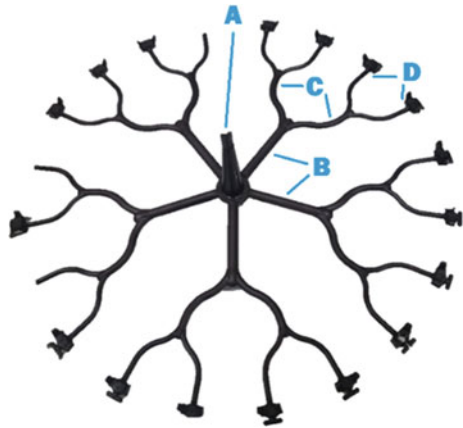
Polymer	Injection temperature (°C)	Injection pressure (Ip) (bar)	Injection speed	Hold pressure	Hold time	Mold temperature (°C)
PP	240–260	90–180	High	40–80% Ip	>50% total cycle time	20–75 (gloss pieces with high temperature)
LDPE	190–240	60	High	30–60% Ip	>50% total cycle time	20–75 (gloss pieces with high temperature)
HDPE	210–260	120	High	30–60% Ip	>50% total cycle time	20–75 (gloss pieces with high temperature)
PVC	170–210	*	Low	Low	Low	25–60
PET	260–280	140	High	5–10 bar	+	60–140
PS	180–250	60–140	Speed needed to gas evacuation	–	Low, with long cooling time	30–65

* Pressure needed to guarantee same injection speed value during injection phase

+ Time needed to avoid shrink formation

– From less to more, be careful, pieces can grow to the point of cannot be ejected

Fig. 25 Sprue and runners¹³



- Runners (shown in Fig. 25 as B & C)
- Gates, marked with an ellipse in Fig. 26
- Parting line, shown in Fig. 27
- Ejector pins marks, highlighted with a circle in Fig. 28

¹³ File: Contoh Dalaman Moulding.png—Wikimedia Commons. Published online at Wikicommons under Attribution-ShareAlike 4.0 International (CC BY-SA 4.0) License. Retrieved unchanged from: https://commons.wikimedia.org/wiki/File:Contoh_Dalaman_Moulding.png (accessed Dec. 14, 2023).

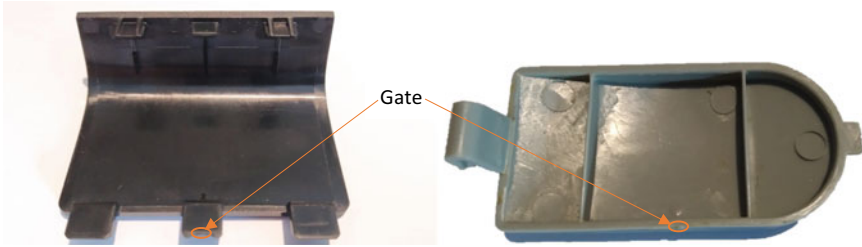


Fig. 26 Gate mark in different pieces, by David López-Adrio



Fig. 27 Parting line, by David López-Adrio

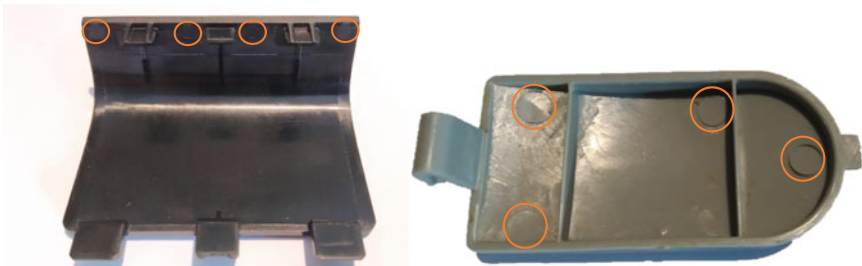


Fig. 28 Ejector pins marks in different pieces, by David López-Adrio

Part defects:

- Blister: elevated or layered zone on the surface part for a problem with the cooling system.
- Burn marks: brown or black areas. Gases and volatiles cannot be evacuated if injection speed is too high. Usually located at the feed system.
- Voids: if injection speed is too slow or injection pressure low, molten material will get cold before cavity mold will be full.

- Flash: if the injection speed is too fast, molten material will solidify in spaces that must be a pocket or in the parting line. This demands more closure pressure.
- Contamination: unwanted materials inside molten plastic or debris from previous injections.
- Air pockets: with elevated initial injection speed, air can be trapped inside the piece.
- Color streaks: localized change of color. Too high injection speed can leave back color additives behind.
- Dieseling: a thin layer of plastic solidifies at cavity walls, but high-speed rips off this layer and burns it. Usually located as far as possible from sprue.
- Flow marks: directional lines with different tones. Injection speed is too fast or molten temperature is too low.
- Sinks: localized depression in thicker zones. Holding pressure or time too low.
- Short shot: the piece is not complete. Lack of molten material volume to be injected. In addition, injection speed or pressure low can provoke it.
- Weld lines: discolored lines where two flow fronts meet. Too low molten material temperature cause this. Material is too cold so flow fronts don't bond together.
- Polymer degradation: polymer oxidation (change of color). High temperature inside barrel, too high spindle speed or excessive time inside the barrel could cause it.

3 Learning Objectives

They are going to be ordered by the seminar session.

Session 1: Theoretical introduction.

- Injection molding machine main components.
- Injection molding process stages.
- Recommended injection values for main polymers.

Session 2: Injection practice.

- Basic handling operations of the injection molding machine.
- Importance of the injection temperature profile.
- Injection volume and cushion volume.

Session 3: Defects visual detection and injected parts main sections.

- Main defects in plastic injected parts and their causes.
- Main sections of the plastic injected parts and visual identification of them.

4 Resources and Organization

To successfully conduct these seminars for a group of 20 students on Polymers Injection Molding, several resources are required.

List of resources needed for the theoretical part:

- Projector: essential for the instructor to share a presentation with all the theoretical foundations.
- Additional reference materials, such as textbooks or online resources, to supplement the theoretical background provided in this chapter as it becomes outdated or incomplete for the instructor's resources.

List of resources needed for the practical part:

- Injection molding machine
- Polyethylene or polypropylene pellets
- Mold for a plastic part: this mold must be tested, and the instructor must know the optimal values of injection parameters. All students must use the same mold to compare their pieces.
- Handouts and worksheets: providing handouts or worksheets with instructions to register the parameters and results of the Injection Molding process can enhance the learning experience. These materials can guide students through the practical seminars and serve as study materials for future reference.
- Support from the instructor or teaching assistants: having a knowledgeable instructor or teaching assistants available to provide guidance, supervision, and assist students during the practical seminar (especially in the session with the machine) is crucial. They can offer clarification on concepts, address technical issues, facilitate discussions to enhance the overall learning experience, and look for the safety of the students during the sessions.

5 Session Development

Session 1: Theoretical introduction.

In this two-hour seminar, all theoretical knowledge will be shown and taught to the students. The structure of this session is shown in Table 2.

Session 2: Injection practice.

Each group of students will make 3–4 injections per temperature in turns, with the temperature values shown below: always with a direct temperature injection profile. The instructor will already set up the rest of the parameters to avoid damage to the machine or accidents, and a non-problematic shot size at the start of each group.

- 10 °C below the minimum recommended temperature.
- Minimum or average recommended temperature.
- Maximum recommended temperature (optional).

Table 2 Session 1 structure proposed for a two-hour seminar

Topic	Time (min)	Description
Introduction to polymers injection molding	15	– Overview of the importance of polymer injection molding
Injection molding machine main components	45	– Explanation of the different sections and their components – Brief explanation of different types of molds
Injection process phases	30	– Explanation of the different process phases – Discussion on the parameters involved in each phase
Recommended injection values to most common polymers	30	– Explanation of recommended injection values

- 10 °C above the maximum recommended temperature.

Objective: each group must find a shot size that allows injecting an entire part without sink defects and cooling time that avoid buckling or deformations on the parts.

Session 3: Part sections and defects visual detection.

In this two-hour seminar, the instructor must develop a brief explanation and then let students apply it. The structure of this session is shown in Table 3.

Table 3 Session 3 structure proposed for a two-hour seminar

Topic	Time (min)	Description
Part sections and defects	45	– Explanation of the different sections of the piece and marks developed by mold mechanisms – Explanation of possible defects and their causes
Group discussion and analysis	60	– Students will discuss and detect the different sections and defects that their pieces present – Each group will present their analysis, explaining which causes provoke defects
Conclusion and wrap-up	15	– Recap of the key concepts covered in the 3 sessions. Including main process phases, main parameters, and defects – Final remarks on the importance of this polymer injection molding for engineering – Encouragement for further exploration and research in this field and micro injection molding to industrial applications

6 Outcomes

The polymers injection molding, process, and defects class offers students a way to comprehend and start in one of the most used industrial processes. One that has an entire industrial sector that demands engineers constantly. The main learning outcomes that students can expect to achieve upon completion of the course are:

- General knowledge about injection machines.
- General knowledge about main mold sections and components.
- Familiarity with injection molding sector terms.
- Understanding of the Injection molding process.
- Defect detection and problem-solving thinking.

7 Deliverables and Assessment

As a final assignment for the class, students can be tasked with preparing a comprehensive report detailing optimal injection values, defects, and causes. The report should include the following components:

- Introduction: provide an overview of the process and its main phases and parameters.
- Optimal values: describe the methodology used to evaluate and determine the different parameters. It must detail optimal injection values determined experimentally as shot size, cushion size, temperature injection profile and cooling time.
- Main pieces sections: show the different sections that their pieces have, and which marks mold stamps on their surface.
- Defects and causes: discuss of the defects present on their pieces, causes and solutions to reach to an optimal final piece.
- Conclusions: summarize findings of the injection molding practice and highlight optimal values reached.

The report should be well-structured, supported by scientific and technical evidence, and demonstrate a comprehensive understanding of polymer injection molding, parameters, and possible defects. It should also include appropriate references to sources consulted during the research process.

Also, this chapter allows the creation of development and test questions for examine students' knowledge about the topics described in it. Some recommendations will be:

- Machine components.
- Process stages.
- Main process parameters.
- Main pieces section identification.
- Defects and causes.

8 Conclusions

This semi-practical class on Polymer Injection Molding has proven to be a valuable learning experience for engineering students. By a theoretical presentation of the process and practical seminar that serve to settle knowledge about the main sections of the machine, phases and parameters of the process, and possible defects and causes that the pieces can suffer; students gained a deep understanding of the complexities of engineering around this widely used industrial process.

Through hands-on activities, students were able to apply their knowledge and develop critical thinking skills when injecting their own pieces. They learned how to consider multiple factors such as injection temperature, shot size, cooling time and understand the influence of others like injection and holding pressure or time. By doing different injections, students were able to identify the most common defects that affect this kind of pieces and their causes, being able to correct them.

The demonstration and direct use of Injection Molding in engineering education promotes a deeper understanding of this process and prepares students for the challenges they may face in their future careers as engineers using or designing plastic parts.

References

- Lim, L.-T., Auras, R., & Rubino, M. (2008). Processing technologies for poly(lactic acid). *Progress in Polymer Science*, 33, 820–852.
- Vlachopoulos, J., & Strutt, D. (2013). Polymer processing. *Materials Science and Technology*, 19(9), 1161–1169.

Material Extrusion-Based Additive Manufacturing: Experimental Determination of Process Parameters with Influence on Printing Time, Material Consumption, Surface Roughness and Torsional Strength



Pablo E. Romero 

1 Introduction

Additive manufacturing (AM) is one of the enabling technologies of Industry 4.0. It allows complex parts to be produced on demand, at an attractive cost for small batches. From a digital model, the 3D printer generates the part layer by layer. Depending on the technology, the parts either are produced directly or require further treatment or processing.

Material extrusion-based additive manufacturing (MEX-AM) is one of the most widely used technologies today. This cost-effective technology, also known as FFF (Fused Filament Fabrication) or FDM (Fused Deposition Modeling), is used intensively to produce prototypes (rapid prototyping), final parts (rapid manufacturing) or tooling (rapid tooling), in sectors as important as the automotive, aeronautical or food industries, among others. For these reasons, in recent years, engineering faculties have progressively incorporated this technology into their syllabuses.

FFF technology is a manufacturing process that has a short learning curve. However, FFF 3D printers allow the tuning of many parameters: nozzle diameter, layer height, infill pattern, infill density, flow, among others. The relationship between these parameters and the printing times, surface or mechanical properties of the printed parts is not always obvious to future engineers. It is often difficult to know a priori which parameter or input variable has the strongest influence on the output variable under study.

P. E. Romero (✉)

Department of Mechanical Engineering, University of Cordoba, Leonardo da Vinci Building, Campus of Rabanales, 14014 Cordoba, Spain

e-mail: p62rocap@uco.es

Design of experiments (DoE) is a widely used tool in industrial processes to determine the influence of various factors (or process parameters) on one or several output variables. One of the most widely used DoE is the response surface method (RSM), introduced by Box & Wilson in (1951). The RSM proposes to use a simple sequence of experiments to generate a polynomial model to obtain an optimal response of the system.

The aim of this practical is to provide students with an experimental approach to FFF technology. In addition to understanding the physics of the process and its strengths and weaknesses, the student will participate in the creation of a DoE with which they will be able to generate a model that allows predicting the printing time, the material consumption, the surface finish, or the mechanical properties of 3D printed parts. In addition, they will understand that not all process parameters have the same influence on the variables to be minimised or maximised.

2 Background

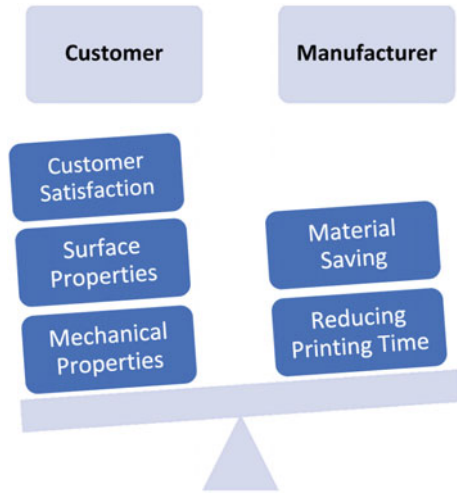
Customers usually demand printed parts that have certain surface properties and suitable mechanical characteristics:

- The surface properties of printed parts are important for certain customers. Surface roughness, for example, affects the tribological behaviour of parts: grippers for a robot may require a high surface roughness, which increases grip (Howard et al., 2021); a diverter on a filling line may require a low surface roughness, to avoid damaging the label on the bottle (Ultimaker, 2023). In some food applications, parts with low wettability and low adhesion surfaces are in demand, as they are less soiled and cleaned more effectively (Romero et al., 2023).
- Most printed parts are subjected to demanding loading situations during their lifetime. To estimate the mechanical capacity of a printed part, standardised mechanical tests of different types (tensile, compression, bending, torsion) are usually used. For this purpose, specimens with the geometry required by each standard are printed and broken in the corresponding testing machine. After breaking a minimum number of specimens as required by the standard, the average values are calculated (International Organization for Standardization, 2019, 2012).

The manufacturer, on the other hand, seeks to reduce the manufacturing cost, saving raw materials and minimising printing time. To manufacture a part at a reasonable cost that is capable of satisfying the customer, the manufacturer has to perform a detailed study of both the part and the manufacturing process. Once this has been done, several prototypes will be manufactured and subjected to tests and metrological checks to ensure that the part meets the customer's minimum requirements (Sartal et al., 2019) (Fig. 1).

Unlike other additive manufacturing technologies, FFF technology allows a large number of process parameters to be modified. An appropriate selection of these

Fig. 1 Customer requirements versus manufacturer’s targets in FFF manufacturing processes



parameters allows parts with better mechanical properties or a better surface finish to be manufactured with less time and material consumption.

Some of the most important process parameters are listed below (Cerro et al., 2021) (Fig. 2): layer height, wall line count (also known as the number of perimeters), infill pattern, infill density and flow compensation (the amount of extruded material is multiplied by this value).

The angles formed by the faces of the printed part concerning the horizontal are known as “built angle”. Although it is not a printing parameter as such, it is a factor to be considered in the process (Garcia-Collado et al., 2022).

Experience, logic, and literature say that layer height, flow and build angle influence the surface finish of the part. However, it is difficult to know which of these has the greatest influence on the surface finish. It is common for an engineer, during his career, to come across similar situations, where he does not know the relationship between the process input variables and the output variables (Montgomery, 2020).

Response surface design (RSM) helps engineers to select, using a reduced number of tests, the process conditions that allow the specifications to be met. To develop the DoE, it is necessary to select the factors (or variables to be studied) and the levels that each factor will take (minimum, average and maximum values). Then, using the Box-Behnken design (Fig. 3), the combinations corresponding to each test are obtained (Kechagias & Vidakis, 2022). Each point in the diagram represents a test; the coordinates of each point coincide with the values to be set in each test for each of the factors. Statistical packages (Minitab, Statsgraphics, among others) are available to help create the DoEs and analyse the results obtained (Khan, 2013).

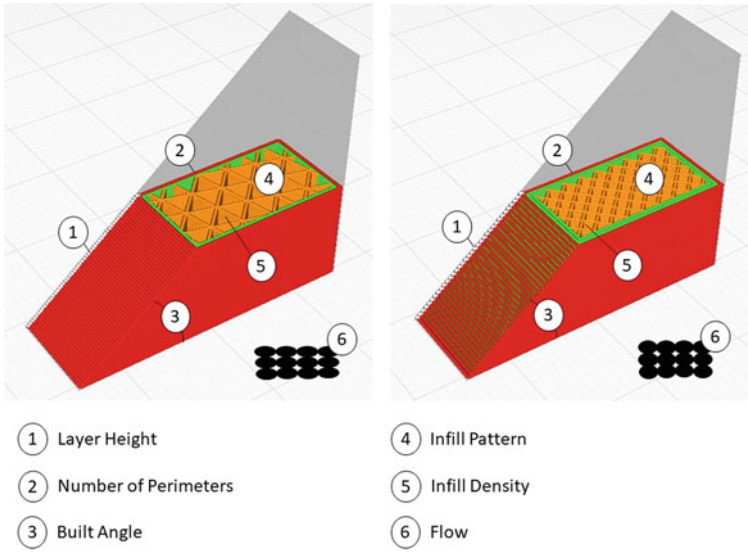
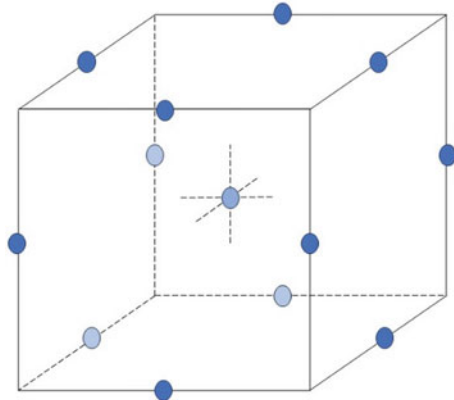


Fig. 2 Parts printed by FFF with the same geometry but different surface and mechanical properties: **a** layer height of 0.2 mm, number of perimeters of 2, built angle of 40°, triangle infill pattern, infill density of 50%, and flow of 90%; **b** layer height of 0.3 mm, number of perimeters of 3, built angle of 40°, grid infill pattern, infill density of 60%, and flow of 110%

Fig. 3 Box-Behnken design for three factors: points on the diagram represent the experimental runs



3 Learning Objectives

The objectives of the workshop are:

- To learn about the different steps necessary to manufacture a part using FFF 3D printing.

- To know the most important printing parameters in FFF and to understand their relationship with the printing time, the surface finish and the mechanical properties of the part.
- Be able to measure the surface roughness of a part autonomously. To know what the “staircase” effect is in FFF.
- To understand the relationship between the internal structure (infill pattern and infill density) of the part and its mechanical properties (in this case, torsional strength).
- To difference between a standardised and non-standardised test and learn how to use low-cost resources to perform initial studies in-house.
- To know the basics of design of experiments and learn to perform simple analyses autonomously.
- Learn to analyse experimental data and draw conclusions.

4 Resources and Organization

For the workshop, the following material is recommended:

- Script.
- Personal computer (PC).
- CAD software.
- Slicing software.
- FFF 3D printer (for every two students).
- PLA filament spool for each printer.
- Can of hairspray.
- Perthometer.
- Digital torque wrench.
- Workbench with a screw.
- A spreadsheet.
- Statistical software.
- Internet connection.

5 Session Development

Preparation of the workshop (at home):

- The student is provided with a script of the practice, where the objectives to be achieved and the material resources to be used are presented. Through this script, the student becomes familiar with the vocabulary and fundamental concepts (fused filament fabrication, surface roughness, mechanical properties, design of experiments, among others).

- In this stage, it is important that each pair of students understands that they are going to print parts with identical geometry to those of their classmates, but with different printing parameters.
- The students are provided with the download link of the Ultimaker CURA software so that they can install it on their personal computer, if they wish to do so.

First session (2 h):

- Students are given two sketches with the dimensions of the specimens. The lecturer assigns each pair the printing parameters that correspond to them, following the DoE:
 - Specimen 1 (Fig. 4 and Table 1): layer height, flow and building angle. In this case, the infill pattern used in all the runs is “triangle”.
 - Specimen 2 (Fig. 5a and Table 2): perimeters, infill density and layer height). In this case, the infill pattern used in all the runs is “cubic”.
- The students model the specimen in 3D using the CAD software.
- Students prepare the printing using the slicer software. At this point, it is important to check that each pair programs the print parameters assigned to them.
- Students record the printing time provided by the slicer software.
- Students upload the print time to a Google Sheets file.

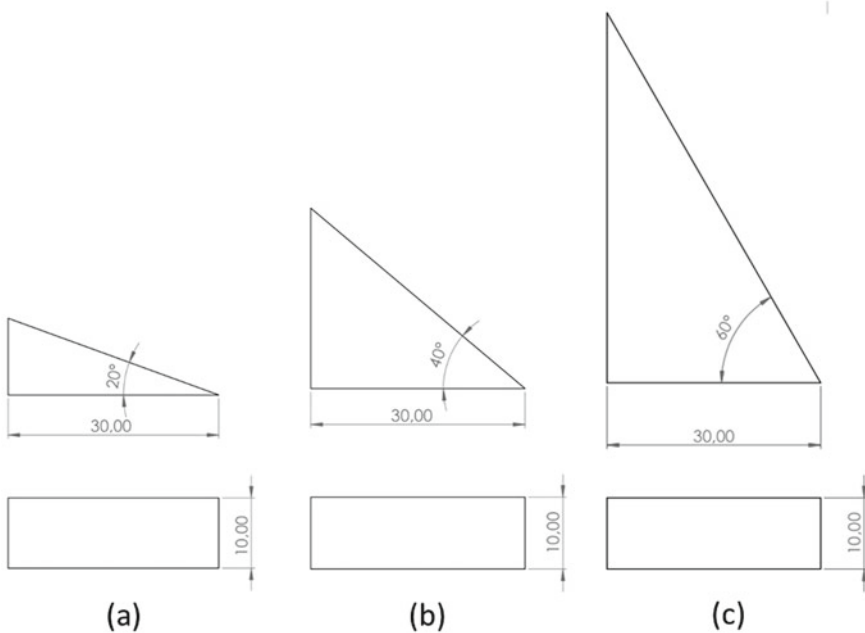
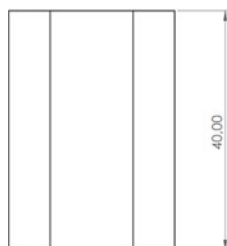


Fig. 4 Specimen 1: geometry of parts used to assess the influence of construction angle on surface roughness

Table 1 Table with the Box-Behnken design of experiments for specimen 1 to be filled in by the students (session 2)

#	LH (mm)	F (%)	WA (°)	Printing Time (min)	Raw Material (g)	Ra (μm)
1	0.3	100	20			
2	0.2	100	40			
3	0.3	110	40			
4	0.1	100	60			
5	0.2	100	40			
6	0.1	100	20			
7	0.2	110	20			
8	0.1	90	40			
9	0.3	90	40			
10	0.1	110	40			
11	0.2	90	20			
12	0.2	90	60			
13	0.3	100	60			
14	0.2	100	40			
15	0.2	110	60			

Each pair is responsible for one run



(a)



(b)

Fig. 5 Specimen 2: dimensions of specimen **a**; digital torque wrench used in the non-standard torque tests **b**

Table 2 Table with the Box-Behnken design of experiments for specimen 2 to be filled in by the students (session 2)

#	Walls	Infill (%)	LH (mm)	Printing Time (min)	Raw Material (g)	Torque (N·m)
1	2	60	0.3			
2	1	40	0.1			
3	2	20	0.1			
4	1	20	0.2			
5	3	40	0.3			
6	1	40	0.3			
7	3	60	0.2			
8	3	40	0.1			
9	2	60	0.1			
10	2	40	0.2			
11	2	40	0.2			
12	3	20	0.2			
13	1	60	0.2			
14	2	40	0.2			
15	2	20	0.3			

Each pair is responsible for one run. The infill pattern used in all the runs is “cubic”

- Students load the filament into the 3D printer.
- Students check that the bed is level.
- Students print specimen 1.

Second session (2 h):

- Students remove the printed specimen 1.
- Students print test specimen 2.
- The students measure the surface roughness of specimen 1 several times, using the perthometer and the holder fabricated for this purpose.
- Students calculate the mean and standard deviation.
- Students apply the Chauvenet criterion to detect aberrant errors.
- Students upload their data to a Google Sheets file.
- Students remove the printed specimen 2.
- Students break specimen 2 using a digital torque wrench and record the value of the peak torque recorded by the wrench at breakage.
- Students upload the peak torque value to a Google Sheets file.

Processing and analysis of the results (at home):

- The students process the created datasheet, using the statistical package. In order not to overload the students, each pair analyses a different output variable (manufacturing time, amount of material, surface roughness, torque). They should obtain the Analysis of Variance (ANOVA) and generate the corresponding graphs.

- Students analyse the results obtained and write a short report. At this point, it is essential that the students assimilate that, normally, the interests of the customers and the manufacturer are opposed to each other. Obtaining parts with excellent surface finishes and high mechanical properties takes time and material. Parts with apparently similar geometry (from an external point of view) will have different costs depending on the programmed printing parameters.

6 Outcomes

During practice, several results are intended to be achieved, each at a different level.

Level 1:

- The student obtains a 3D printed part. Although some students had contact with 3D printing in secondary school, the majority have never had the opportunity to print a part themselves. Consequently, they find the experience highly motivating.
- The student loses the fear of 3D printing. Many students, after the practical sessions, decide to invest their savings and buy a 3D printer to work at home.
- The student interiorises that 3D printing is a manufacturing method used today intensively in companies in different industrial sectors. In fact, during practice, the most advanced students are responsible for designing and printing the supports needed to measure surface roughness. This is known in the argot as “rapid tooling”.

Level 2:

- The student understands the main printing parameters and learns how to use the slicing software (CURA). Furthermore, they can select the appropriate printing parameters to get the part printed in less time, have a better surface finish or have better mechanical properties.
- The student uses the perthometer independently to measure several times the surface roughness of printed parts. In addition, he/she uses the Chauvenet criterion to identify possible aberrant errors. These concepts and instruments have been studied previously but, in this workshop, they must use them in an applied way.
- The student learns to use a digital torque wrench. Furthermore, they understand that, when no other means are available, low-cost resources can be used to carry out non-standardised tests that provide sufficient information to make decisions.

Level 3:

- The student understands the usefulness of experimental designs in engineering. In addition, they learn to use a basic statistical package, with which they can perform the Analysis of Variance (ANOVA), produce graphs, and generate analytical expressions that can be used to estimate the output variables knowing the input variables.
- The student learns to make decisions based on the information generated by the experimental study carried out. In addition, he/she is involved in a situation

in which the customer's requirements (excellent surface finish, high mechanical properties) and the manufacturer's interests (short printing times, saving of filament) are confronted.

- The student understands that apparently similar parts have different costs depending on the manufacturing parameters used. Usually, the manufacturer must optimise the design and manufacturing process to produce parts at the lowest possible cost that meet the customer's specifications. This strategy allows the manufacturer to improve his margins, which are usually small.

7 Deliverables and Assessment

To carry out the practical, students are given:

- A script where they explained in detail what the practice consists of (objectives, development, expected results). The information contained in the script is like that presented in this chapter.
- Sketches with the geometry and dimensions of specimen 1 (Fig. 4) and specimen 2 (Fig. 5).
- Tables with the DoEs to be followed (Tables 1 and 2).
- Run assignment to each of the pairs. This run will be used to set up the print of specimen 1 (surface roughness) and specimen 2 (torque).

The evaluation is carried out in groups and in pairs:

- The group's ability to work is evaluated:
 - Has the working atmosphere during the sessions been adequate?
 - Did the different pairs help each other when they had problems?
 - Did they design and manufacture the necessary tools to carry out the surface roughness measurements?
 - Were they able to complete the table with the results from CURA and the measurements made?
- The report made by each pair is evaluated:
 - Were they able to generate the ANOVA?
 - Is their interpretation of the ANOVA correct, and are they able to identify which factors are most influential?
 - Did they generate the graphs with the response surfaces?
 - Are they able to identify which input values allow them to optimise in each case the printing time, the required filament mass, the surface roughness/maximum torque?
 - What values would you select for the most influential parameters, looking for a balance between customer satisfaction and part cost?

8 Conclusions

The described practice is carried out in a manufacturing subject of the fourth year of the Degree in Mechanical Engineering at the University of Cordoba. The practicum has three main objectives: to introduce the student to additive manufacturing, to understand the power of design of experiments in industry, to realize that there is a relationship between manufacturing process-customer satisfaction-cost.

The proposed methodology is interesting, as it brings students closer to situations that they will have to live during their professional career: every year they will have to face new processes, new machines, etc. but the problems will be similar. The design of experiments and industrial statistics are very powerful tools that the student must know.

The results obtained are excellent. Most of the students pass the test and demonstrate that they have achieved the desired learning results. At the end of the workshop, many students acquire their own low-cost printer to continue learning and printing at home. This is one of the best indicators that the methodology works.

References

- Box, G. E. P., & Wilson, K. B. (1951). On the experimental attainment of optimum conditions. *Journal of the Royal Statistical Society, Series B*, 13(1), 1–38.
- Cerro, A., Romero, P. E., Yiğit, O., & Bustillo, A. (2021). Use of machine learning algorithms for surface roughness prediction of printed parts in polyvinyl butyral via fused deposition modeling. *International Journal of Advanced Manufacturing Technology*, 115(7–8), 2465–2475.
- García-Collado, A., Romero, P. E., Dorado-Vicente, R., & Gupta, M. K. (2022). Studying the effect of short carbon fiber on fused filament fabrication parts roughness via machine learning. *3D Printing and Additive Manufacturing*.
- Howard, D., O'Connor, J., Brett, J., & Delaney, G. W. (2021). Shape, size, and fabrication effects in 3D printed granular jamming grippers. In *2021 IEEE 4th international conference soft robot. RoboSoft 2021* (pp. 458–464).
- International Organization for Standardization. (2019). *Plastics—Determination of tensile properties—Part 1: General principles (ISO 527-1:2019)* (p. 17).
- International Organization for Standardization. (2012). *Plastics—Determination of tensile properties—Part 2: Test conditions for moulding and extrusion plastics (ISO 527-2:2012)*.
- Kechagias, J. D., & Vidakis, N. (2022). Parametric optimization of material extrusion 3D printing process: An assessment of Box-Behnken versus full-factorial experimental approach. *International Journal of Advanced Manufacturing Technology*, 121(5–6), 3163–3172.
- Khan, R. M. (2013). *Problem solving and data analysis using Minitab: A clear and easy guide to Six Sigma methodology*. Wiley.
- Montgomery, D. (2020). *Design and analysis of experiments, 10th*. Wiley.
- Romero, P. E., Barrios, J. M., Molero, E., & Bustillo, A. (2023). Tuning 3D-printing parameters to produce vertical ultra-hydrophobic PETG parts with low ice adhesion: A food industry case study. *Proceedings of the Institution of Mechanical Engineers, Part B: Journal of Engineering Manufacture*, 1–9.

- Sartal, A., Carou, D., Dorado-Vicente, R., & Mandayo, L. (2019). Facing the challenges of the food industry: Might additive manufacturing be the answer?. *Proceedings of the Institution of Mechanical Engineers, Part B: Journal of Engineering Manufacture*, 233(8), 1902–1906.
- Ultimaker (2023). Heineken: Ensuring production continuity with 3D printing. *Success stories*, 2023. [Online]. Available: <https://ultimaker.com/learn/heineken-ensuring-production-continuity-with-3d-printing/>. Accessed December 14, 2023.

Comparison Between the Investment Casting Process (Lost Wax Casting) and Machining (Turning) in Terms of Dimensional Accuracy and Surface Finish



Irene Buj-Corral  and Alejandro Dominguez-Fernández 

1 Introduction

Investment casting was used in ancient times (for at least 6000 years) for artistic purposes, to manufacture, for example, jewels and sculptures (Bouse & Mihalisin, 1989). In the 1940s, it started to be used in the aircraft industry. Today, it is still one of the most employed casting techniques, especially when small parts and/or parts with intricate shapes are required (Pattnaik et al., 2012), for instance for the manufacture of turbine blades and vanes in nickel-base and cobalt-base alloys, which can withstand high temperatures (Rezavand & Behraves, 2007).

Investment casting is a type of casting process in which an expendable pattern is employed, for instance, made of wax. The wax pattern is covered with a ceramic layer, from which the wax is removed. The ceramic layer is later hardened and acts as a mold (Singh et al., 2014). The main steps of the investment casting process are presented in Fig. 1.

One of the main applications of investment casting is the manufacture of jewelry pieces, for example rings, earrings and bracelets, made of precious metals (Ainsley et al., 1978; Ott et al., 1985). Such pieces are usually small, many times with intricate shapes. An alternative way to obtain this kind of parts is machining, which allows obtaining good dimensional accuracy and surface finish. For example, rings can be using of turning operations (Kurnadi et al., 2007). However, when complex shapes are needed for the jewels, the use machines such as five axis machining centers or multiaxis machines is required (Kar et al., 2019; Vardhan & Babu, 2020) and, thus, the manufacturing costs become higher than when simpler machines are employed.

I. Buj-Corral (✉) · A. Dominguez-Fernández

Department of Mechanical Engineering, Barcelona School of Industrial Engineering (ETSEIB),
Universitat Politècnica de Catalunya (UPC), Av. Diagonal, 647, 08028 Barcelona, Spain
e-mail: irene.buj@upc.edu

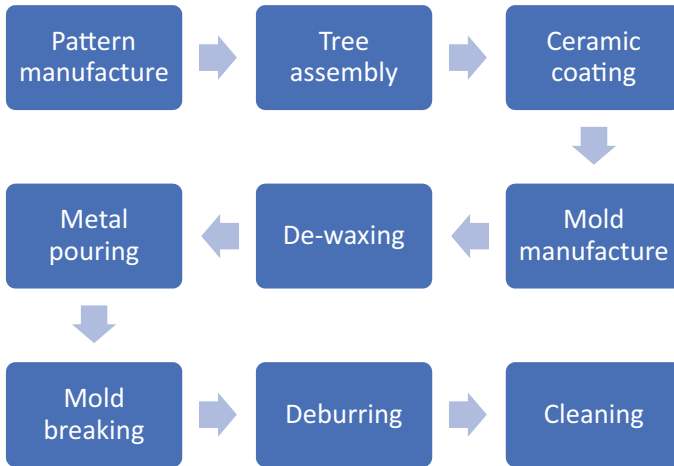


Fig. 1 Main steps of the investment casting process

In the present chapter, the development of a laboratory class about investment casting with 3D printed wax patterns is presented (Cheah et al., 2005; Mukhtarkhanov et al., 2022; Pattnaik et al., 2014). It is focused on the comparison of rings that are manufactured by either turning or investment casting, regarding dimensional accuracy and surface roughness. In addition, the main advantages and disadvantages of each process are discussed.

2 Background

The University Master in Industrial Engineering (MUEI) is taught in the Barcelona School of Industrial Engineering (ETSEIB) of *Universitat Politècnica de Catalunya*, Spain. In the area of Mechanical Engineering, the students can choose among different optional subjects. One of these optional subjects is Part forming systems, in which different manufacturing processes are studied: casting, plastic deformation processes, powder metallurgy, etc. In addition to the theory classes, during the semester four different laboratory classes are developed, which are listed next:

- i. Sand-casting. It consists of manufacturing a sand mould to obtain a tin part.
- ii. Investment casting. It consists of manufacturing a plaster mold with a 3D printed wax tree inside.
- iii. Powder metallurgy. It consists of obtaining a green part from metallic powder.
- iv. Plastic deformation processes. It consists on cutting aluminum disks with a punch/die system.

This chapter deals with the second laboratory class on investment casting processes. The duration of the laboratory class is one hour and a half. It is developed in

the Laboratory of Manufacturing Technologies of the Barcelona School of Industrial Engineering (ETSEIB).

3 Learning Objectives

The main learning objectives of the laboratory class are as follows:

- To know and understand the main steps of the investment casting process.
- To be able to decide for which types of part geometries the investment casting process is preferred over the machining processes.
- To know and understand a specific application of the fused filament fabrication (FFF) technology: the manufacture of wax patterns.
- To be able to calculate the weight of metal to be poured into the investment casting mold.
- To compare the dimensional accuracy and the surface finish obtained in investment casting and turning processes respectively.

4 Resources and Organization

The Laboratory of Manufacturing Technologies of ETSEIB has different equipment that is used in this laboratory class:

- FFF 3D printer.
- 3D printed PLA molds.
- Stove.
- Oven.
- Metallic saucepan.
- Gas heater.
- Precision scale.
- Inside-hole micrometer.
- Contact roughness meter.
- Turning center (Fig. 2).

In addition, consumable materials are required: 3D-printed wax patterns, tin bars, water and plaster powder. Moreover, silver rings made by investment casting, and machined aluminum rings are available.

Fig. 2 Okuma genos L200E turning center



5 Session Development

– First part of the session (30 min): Building a wax tree

At the beginning of the laboratory class, the students are divided into groups of 4–5 people. Each group is provided with previously 3D printed wax patterns of the rings (Fig. 3), as well as with a polylactic acid (PLA) 3D printed mold (Fig. 4).

The main steps to be followed during the laboratory class are:

- To remove the wax patterns from the group.
- To assemble the wax central pillar to the PLA mold base.
- To build a wax tree by joining the ring patterns to the central pillar, using a heat source to melt the wax (Fig. 5).
- To weigh the wax tree on the scale (Fig. 6).

Fig. 3 Group of 3D printed wax patterns of the rings, of decorative motifs and of the central pillar of the wax tree



Fig. 4 PLA 3D printed mold

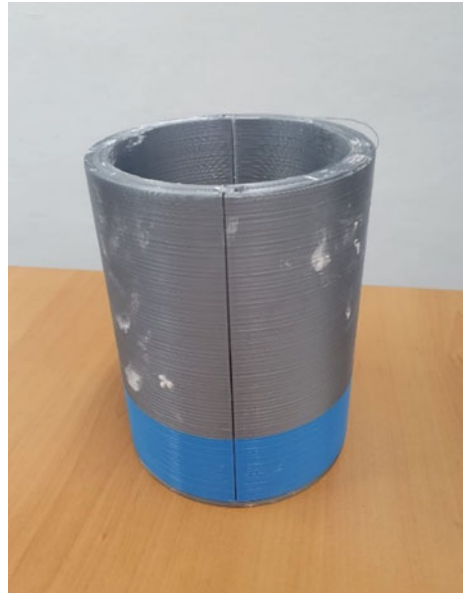


Fig. 5 Building process of a wax tree

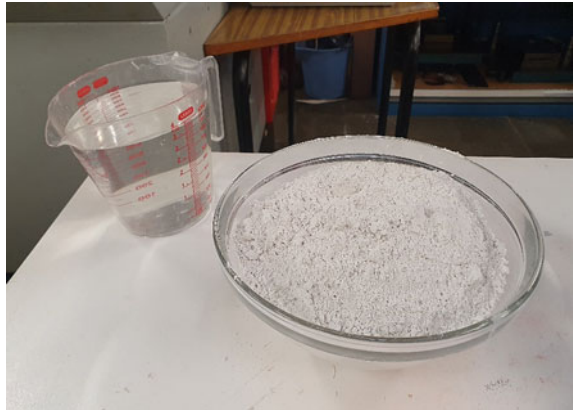


- To calculate the weight of metal that is required to obtain a metal tree, taking into account the wax and the metal (tin) density values.
- To prepare the gypsum plaster by mixing plaster powder and water (Figs. 7 and 8).
- To pour the plaster into the PLA mold containing the wax tree (according to the method employed in this laboratory class, it is not necessary to cover the wax tree with a ceramic layer, since the plaster will act as a mold).
- To heat the mold on the stove to melt and extract the wax from the mold.
- To remove the PLA walls from the plaster mold (Fig. 9).

Fig. 6 Weighing process of the wax tree



Fig. 7 Components of the gypsum plaster



Other processes that are required to obtain the final parts (not carried out during the laboratory class but later) are:

- To heat the mold in the oven for curation.
- To melt the tin bars in the saucepan with the help of the gas heater.
- To pour the tin into the plaster mold.
- To dissolve the plaster mold in water to obtain the metal tree.
- To separate each metallic part from the tree.

Fig. 8 Preparation process of the gypsum plaster



Fig. 9 Plaster mold without PLA walls



– **Second part of the session (30 min): comparison between investment cast and turned rings**

Later, each working group is given 5 silver investment cast rings and 5 aluminum turned rings (Fig. 10).

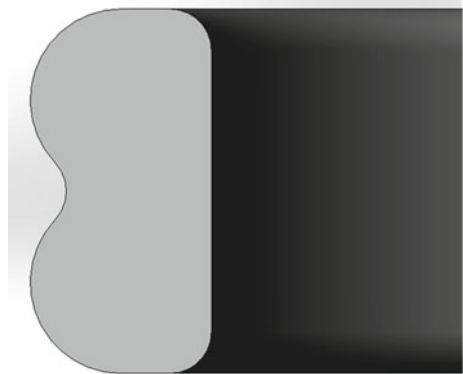
Figure 11 shows a schematic drawing of the cross section of the ring. It is a double row ring, with rounded edges on the external surface. The internal surface is cylindrical with slightly rounded edges.

The students measure the internal diameter of the rings with a Mitutoyo inside-hole micrometer. Surface roughness of the internal area of the rings is measured with a Taylor Hobson Talysurf contact roughness meter, along a generatrix on the

Fig. 10 Investment cast silver ring (left), turned aluminum ring (right)



Fig. 11 Schematic drawing of the ring profile



internal surface of the rings (Fig. 12). Average roughness R_a is considered, which is a common parameter that is used for comparison among different manufacturing processes.

One measurement is taken for each ring, both for diameter and for surface roughness. Then, the average value and the standard deviation is calculated for each group of 5 rings.

6 Outcomes

In the first part of the session, each group of students prepares a wax tree (Fig. 13) inside a PLA 3D printed mold, by local heating and joining of the wax rings to the central wax pillar. In addition, each group obtains a gypsum mold that contains the wax tree.

In the second part of the session, the students measure internal diameters and surface roughness of both the investment cast and the turned rings.

The students can also check a mold in which wax has been removed, and a cured mold, in which sometimes cracks appear from the curing operations in the oven.

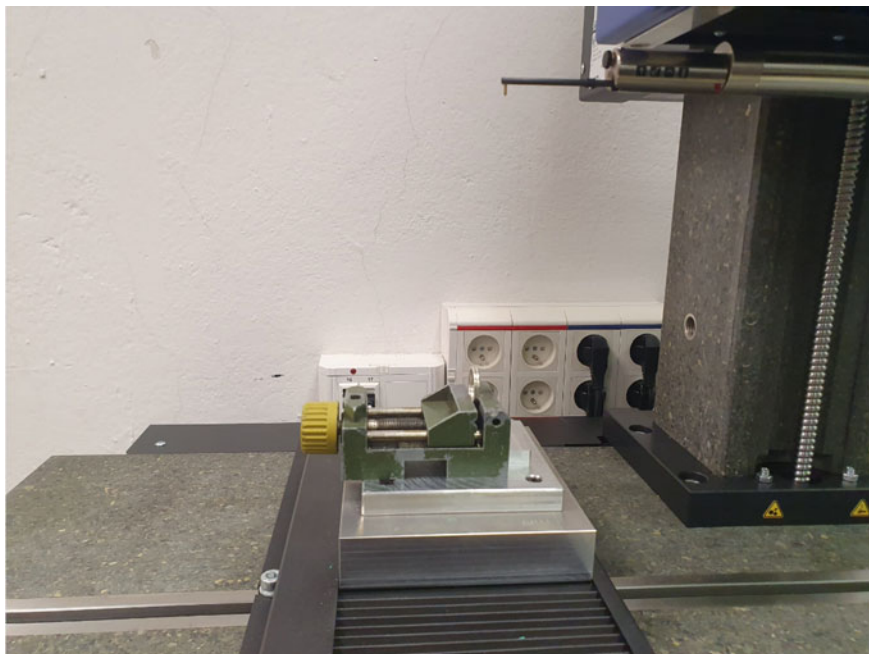


Fig. 12 Roughness measurement process of the rings

Fig. 13 PLA mold with wax tree



7 Deliverables and Assessment

The deliverable of the laboratory class, which is prepared by each group during the last 30 min of the session, contains different questions:

- i. Determine the mass of a wax tree using a precision scale.
Answer: For example, 22.2 g.
- ii. Calculate the mass of a tin tree if wax density is 1.2 kg/dm^3 and tin density is 7.3 kg/dm^3 .
Answer: Equation (1) allows calculating the metal mass.

$$\text{Metal mass (g)} = \text{Wax mass (g)} \frac{\text{Metal density} \left(\frac{\text{g}}{\text{cm}^3} \right)}{\text{Wax density} \left(\frac{\text{g}}{\text{cm}^3} \right)} \quad (1)$$

As for the example defined in question i, the calculations are as follows (Eq. 2):

$$\begin{aligned} \text{Metal mass (g)} &= 22.2(\text{g}) \cdot \frac{7.3 \left(\frac{\text{g}}{\text{cm}^3} \right)}{1.2 \left(\frac{\text{g}}{\text{cm}^3} \right)} \\ &= 135.1 \text{ g} \end{aligned} \quad (2)$$

- iii. Explain the main differences between the two different types of rings (investment casting with polishing operations, and turning), considering their shape, their dimensional error, and their surface finish.

Answer:

(a) Shape.

- In this case, the investment cast part reproduces the shape of the original design. In general, intricate shapes can be obtained with the investment casting process, provided that wax can be melted and extracted from the mold to obtain the cavity prior to metal pouring.
- In this case, the turning process does not provide the shape of the internal rounded edges since the required special tools were not available in the workshop. In general, the investment casting process allows obtaining many special shapes such as buttons, floral motifs, bows, etc., which are characteristic of jewelry parts. Such shapes would be expensive to be machined in the lathe, since special tools, special fixing systems or even a different machine tool would be required, with high cutting times.

(b) Dimensional error.

Table 1 shows the mean and the standard deviation values for the internal diameter of the rings. Similar mean values are obtained in both cases, which are close to the theoretical value of 17.5 mm. Relative dimensional errors correspond to 0.137 % and 0.171 % for investment casting and

Table 1 Dimensions of the rings

Process	Mean value of internal diameter (mm)	Standard deviation of internal diameter (mm)
Investment casting + polishing	17.476	0.064
Turning	17.470	0.007

Table 2 Average roughness Ra of the rings

Process	Mean value of Ra (μm)	Standard deviation of Ra (μm)
Investment casting + polishing	0.09	0.04
Turning	0.79	0.35

for turning respectively. However, higher standard deviation values were reported for the investment casting process than for the turning process.

(c) Roughness.

Table 2 corresponds to roughness results for the rings. It shows that lower mean value of Ra is obtained for the investment casting process + polishing process than for the turning process as expected, given that the investment cast rings have been subjected to a finishing operation. Higher standard deviation values were found for the turning process than for the investment casting + polishing process. Figure 14 shows a roughness profile of an investment cast + polished ring, with an irregular shape that is often obtained in abrasive machining processes. Figure 15 depicts a regular roughness profile of a turned ring.

- (iv) Explain the main reasons for the difference between the cycle time of the rings when each one of the processes is assessed. Cycle time is around 6 h for investment casting and 1.5 min for turning (considering only cutting time).

In the investment casting process, many operations are required: manufacture of the lost wax pattern, manufacture of the plaster mold, wax emptying operation, metal pouring, extraction of the parts from the tree, polishing, etc.

In the turning process, only the machining time was considered (not the preparing, the unproductive nor the tool changing times). The required operations for the ring are as follows: flat turning of the bar’s edge, drilling, profile turning of the external shape, boring and cutting-off of the part.

8 Conclusions

In this chapter, the development of a laboratory class of the subject Part Forming Systems about the comparison between investment casting and turning processes is presented. Main conclusions of the chapter are as follows:



Fig. 14 Example of a roughness profile measured on the internal surface of an investment cast and subsequently polished ring

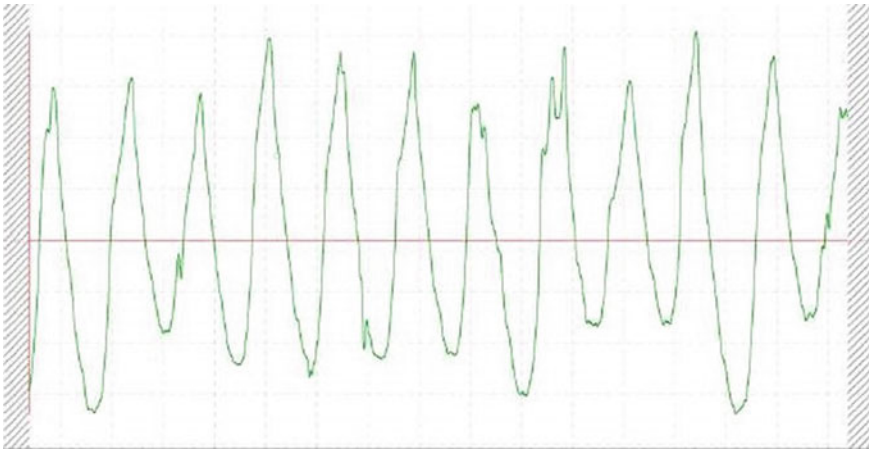


Fig. 15 Example of a roughness profile measured on the internal surface of a turned ring

- It is possible to use FFF 3D printed wax patterns to build wax trees to be used in a laboratory class about investment casting process.
- Both the investment casting process and the turning process allow obtaining metallic rings with simple shapes. However, complex shapes are more easily obtained with the investment casting process than with the turning process.

- The internal diameter of the rings was measured. Both the investment cast and the turned rings provided similar internal diameter mean values, with relative errors of 0.137% and 0.171 % respectively. Thus, the measured values were close to the theoretical one, although the turning process provided lower variability than the investment casting process.
- The investment cast rings, which had been previously subjected to a polishing operation, lead to lower mean surface roughness Ra value (0.09 μm) than the turned rings (0.79 μm).

In the future, the final operations of the investment casting process (mold curing, tin casting, etc.) are to be implemented in the laboratory class of the Parts Forming Systems subject.

Acknowledgements The authors thank Ramón Casado and Arnar Morera from UPC for their help with the manufacture of the rings.

References

- Ainsley, G., Bourne, A. A., & Rushforth, R. W. E. (1978). Platinum investment casting alloys. *Platinum Metals Review*, 22(3), 78–87.
- Bouse, G. K., & Mihalisin, J. R. (1989). Metallurgy of investment cast superalloy components. In *Superalloys supercomposites superceramics*.
- Cheah, C. M., Chua, C. K., Lee, C. W., Feng, C., & Totong, K. (2005). Rapid prototyping and tooling techniques: A review of applications for rapid investment casting. *International Journal of Advanced Manufacturing Technology*, 25(3–4), 308–320.
- Kar, B. C., Panda, A., Kumar, R., Sahoo, A. K., & Mishra, R. R. (2019). Research trends in high speed milling of metal alloys: A short review. *Materials Today: Proceedings*, 26, 2657–2662.
- Kurnadi, M. S., Morehouse, J., & Melkote, S. N. (2007). A workholding optimization model for turning of ring-shaped parts. *International Journal of Advanced Manufacturing Technology*, 32(7–8), 656–665.
- Mukhtarkhanov, M., Shehab, E., & Ali, M. H. (2022). Process parameter optimization for 3D printed investment casting wax pattern and its post-processing technique. *Applied Sciences (Switzerland)*, 12(14).
- Ott, D., Raub, C. J., & Rapson, W. S. (1985). Investment casting of gold jewellery. *Gold Bulletin*, 18(3), 98–108.
- Pattnaik, S., Jha, P. K., & Karunakar, D. B. (2014). A review of rapid prototyping integrated investment casting processes. *Proceedings of the Institution of Mechanical Engineers, Part 1: Journal of Materials: Design and Applications*, 228(4), 249–277.
- Pattnaik, S., Karunakar, D. B., & Jha, P. K. (2012). Developments in investment casting process—A review. *Journal of Materials Processing Technology*, 212(11), 2332–2348.
- Rezavand, S. A. M., & Behraves, A. H. (2007). An experimental investigation on dimensional stability of injected wax patterns of gas turbine blades. *Journal of Materials Processing Technology*, 182(1–3), 580–587.
- Singh, R., Singh, S., & Mahajan, V. (2014). Investigations for dimensional accuracy of investment casting process after cycle time reduction by advancements in shell moulding. *Procedia Materials Science*, 6, 859–865.
- Vardhan, T. V., & Babu, B. S. (2020). Multiaxis CNC programming and machining. In *Modern manufacturing processes* (pp. 167–175).

Monitoring of Cutting Forces in Turning



Branislav Sredanovic  and Diego Carou 

1 Introduction

Monitoring the cutting force values and their behavior is very important in cutting processes. Higher values of cutting forces lead to higher deformation of the cutting tool system and the workpiece (Davim, 2008; Grzesik, 2008). It leads to a deviation from their required relative positions and disrupts the machining kinematics and geometrics (Fig. 1). Consequently, cutting forces, as mechanical loads of the machining system, directly affect the workpiece dimensions accuracy, as one of the most important indicators of the success of the machining (Davim, 2017; Klocke, 2011). An increase in cutting forces value causes an increase in vibrations, especially vibration amplitudes. Increasing vibrations lead to unpredictable movement of the cutting tool tip in relation to the workpiece (Carou et al., 2016). The result of vibration occurring is commonly characteristic marks on the machined surface (craters, plunged materials, surface waviness), which impair the machining quality.

As almost all mechanical energy in cutting processing is converted into thermal energy, high values of cutting forces combined with high values of cutting speed, cause more intensive generation of heat in the cutting zone (Davim, 2017; Klocke, 2011). This puts an additional thermal load on the cutting tool edge, leading to a decrease in its durability (Carou et al., 2017). In addition, a large amount of generated heat can damage the structure and properties of the surface layer of the machined surface.

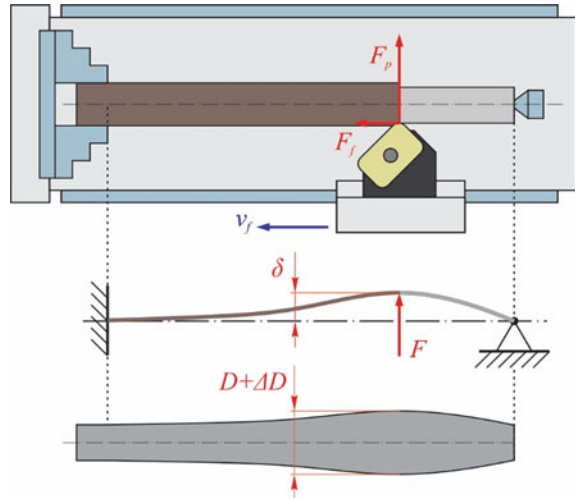
B. Sredanovic (✉)

Faculty of Mech. Engineering, University of Banjaluka, Stepe Stepanovica 71, 78000 Banja Luka, Republic of Srpska, Bosnia and Herzegovina
e-mail: branislav.sredanovic@mf.unibl.org

D. Carou

Departamento de Deseño na Enxeñaría, Escola de Enxeñaría Aeronáutica e do Espazo, Universidade de Vigo, Campus As Lagoas Sn, 32004 Ourense, Spain

Fig. 1 Influence of the cutting force on the workpiece deviation



In the following, the organizational procedure and system for measuring cutting forces during turning will be presented, phase by phase. The method of measuring the workpiece deformation will be presented, to assess the dimensional accuracy. To analyze the signals obtained on the measuring device, the appropriate outcomes as engineering calculations will be performed and presented. The turning process was chosen for the reason that it has a constant chip cross-section geometry. Moreover, the main conclusions can be transferred to other cutting process methods (milling, drilling, etc.).

The objectives of the session are the following:

- Understanding the reasons for the appearance of mechanical resistance during the cutting of metallic parts, based on theoretical background.
- Understanding the physical process and determining its influence on the cutting force values and value behavior, based on theoretical background.
- Willingness to link the effect of cutting force on machining accuracy, surface quality, and energy consumption.
- Learning to arrange the setup, measuring procedures and using the cutting forces measuring sensor system.
- Improving the knowledge of the students to help them to improve the management and development of machining processes.

2 Background

To be able to understand the process of measuring and monitoring cutting forces during turning, and their consequences, it is necessary to present the system of cutting forces in the machining zone. The main movement (rotation of the workpiece), and

the auxiliary movement (straight line or curvilinear movement of the cutting tool) define the relative movement between the workpiece and the cutting tool. During the relative movement, the workpiece and the cutting tool are in the appropriate mutual position, defined by geometric (geometry and dimensions of the workpiece and cutting tool) and process parameters (depth of cut). The kinematics of the relative movement is defined by the feed and cutting speed.

The mutual position and movement of the mentioned elements in the machining system enable constant grabbing of material by the cutting tool and produce the mechanical separation of the material from the workpiece in the form of chips. A certain mechanical resistance occurs during the cutting tool penetration of the workpiece material (Davim, 2017; Klocke, 2011). It represents the resultant cutting force, which is defined by intensity and direction. The resultant cutting force is the sum of all resistances in the cutting zone that are related to:

- Material shearing in the cutting shear plane during chip forming.
- Material deformation in the zone in front of the cutting wedge action.
- Friction of the material plastic flow and chip on the rake side of the cutting tool.
- Friction of the cutting tool clearance side on the machined surface, etc.

Accordingly, the cutting forces primarily depend on the mechanical properties of the workpiece material, the properties of the cutting tool material, process parameters, geometry of the cutting zone, and cooling and lubrication conditions (Sousa et al., 2020; Sredanovic et al., 2011). Based on the theoretical analysis of cutting mechanics, it is concluded that the value of cutting forces increases with the increase in tensile strength and hardness of the workpiece material (Matsubara & Ibaraki, 2009; Thangarasu et al., 2018). Higher stresses appear due to plastic and elastic deformations, material shearing, and chip removal. Different techniques of cooling and lubrication of the cutting zone, and different types of tool materials result in higher or lower friction coefficients in the contact zones between the cutting tool and the workpiece (Davim, 2017; Klocke, 2011). Consequently, the friction coefficients lead to the lowest or higher values of the friction forces in the mentioned contact zones. Note that the frictional and cutting forces can be reduced with an appropriate cooling and lubrication technique.

The value of the cutting forces decreases with the increase of the cutting tool rake angle γ ($^\circ$), because the plastically deformed material flows more easily over the cutting tool rake side, and there are less plastic deformation caused by the cutting tool wedge. An increase in the depth of cut a_p (mm) and feed f (mm), i.e. an increase of cutting thickness h (mm) and cutting width b (mm), cause a larger chip cross-section area. A larger chip cross-section area leads to an increase of shearing and deformation forces and, consequently, to increase of cutting forces. Cutting speed v_c (m/min) plays a complex role. If the cutting speed is higher, then a higher amount of heat is generated in the cutting zone, which leads to material softening, and lower cutting forces. Higher cutting speeds cause greater deformation strengthening of the material, which leads to an increase of tensile strength, and higher cutting forces.

The resulting cutting force can be decomposed into the normal force component on the cutting edge (F_{eN}), which acts towards the tool-cutting wedge, and the force

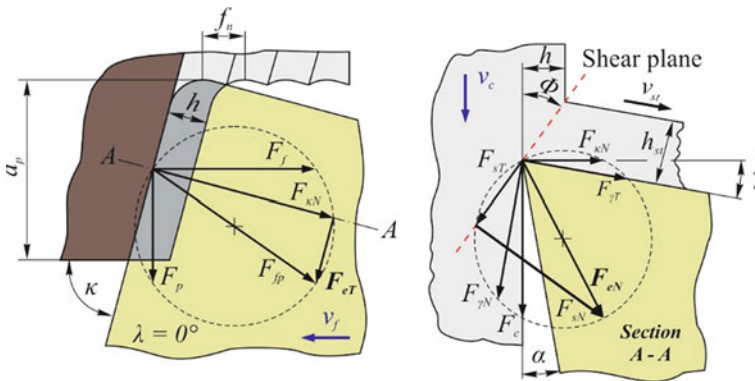


Fig. 2 Cutting force system in the shear plane

component in the direction of the cutting edge extension (F_{eT}), Fig. 2. In addition, the normal force component on the cutting edge can be decomposed into tangential force component in the shear plane (F_{sT}), and normal force component in the shear plane (F_{sN}), i.e. into the normal force component on the rake surface ($F_{\gamma N}$), and tangential resistance on the rake surface ($F_{\gamma T}$).

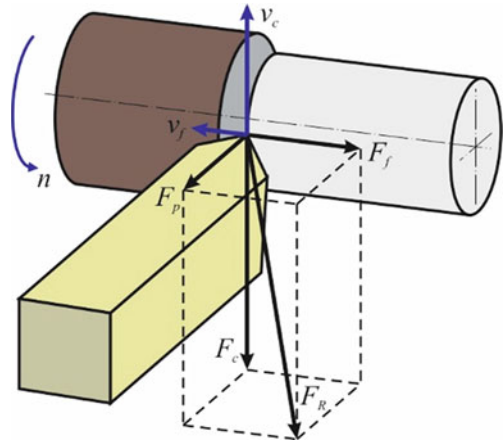
Furthermore, the normal force component on the cutting edge can be divided into resistance to the main movement, i.e. the main cutting force (F_c), and force component normal to the vector of the main movement, i.e. the direction of the cutting edge ($F_{\kappa N}$). The force component normal to the direction of the cutting edge ($F_{\kappa N}$) and the force component in the direction of propagation of the cutting edge ($F_{\kappa T}$) forms the resulting force in the base plane (F_{fp}). The resulting force in the base plane can be decomposed into a component in the direction of auxiliary movement (F_f) and a component normal to the auxiliary movement direction, named passive force (F_p).

In Fig. 3, it is possible to appreciate the decomposition of the resulting cutting force (F_R) into three mutually perpendicular directions. The components correspond to the axes of the workpiece and the machine tool, mutually perpendicular. Thus, the measurable cutting resistances can be identified as follows:

- main cutting force (F_c),
- feed force (F_f), and
- passive force (F_p).

Accordingly, it is possible to use the appropriate procedure and measuring equipment for determining the component cutting force values (Klocke, 2011).

Fig. 3 Observable components of the resultant cutting force



3 Learning Objectives

The purpose of the monitoring procedure is to determine the cutting forces value and its temporal changes to define functional mathematical dependencies that can be used in industrial practice. In addition, it is important to understanding other cutting process performance indicators, and determine the influence of the cutting forces on energy consumption, workpiece dimensional accuracy, machined surface quality, etc. Learning session objectives are:

- Insight into the shape of the cutting forces component measured signals.
- Defining of the graph on cutting force value dependence to technological parameters.
- Measuring of the workpiece deflection.
- Calculation of the required energy to perform the cutting process.
- Calculation of the machining removal rate in the cutting process.
- Defining of graph on energy efficacy dependence to technological parameters.
- Mathematical determining of cutting force formula coefficients.

The cutting force values are most often determined by experimental measurement. The values of the cutting force component can be measured at discrete points in time during machining (Fig. 4). The measured cutting force component signal can show a greater or lesser deviation from the corresponding mean value. Also, the mean cutting force component signal can increase or decrease during the machining time. Greater deviation of the signal from its mean value refers to the existence of significantly high vibrations in machining. This results in poorer machining surface quality and less tool life (Rao et al., 2013; Thangarasu et al., 2018). An increase in the signal may indicate intensive tool wear, deviations in the workpiece shape or material properties.

Based on experimental measuring, it is possible to define the mathematical dependence of the cutting force component mean value. Thus, it is possible to use the *Kinzle* formulation for the main cutting force (Davim, 2008; Grzesik, 2008):

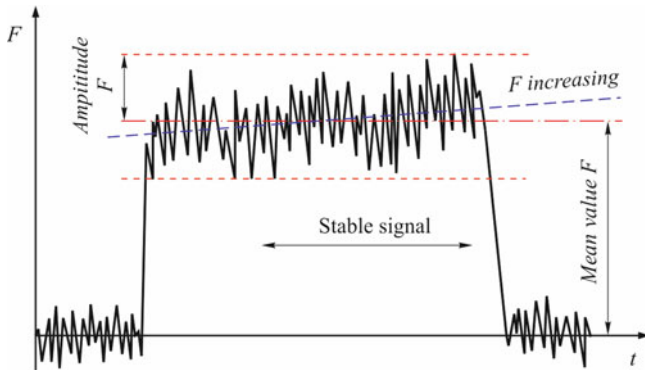


Fig. 4 General cutting force signal shape

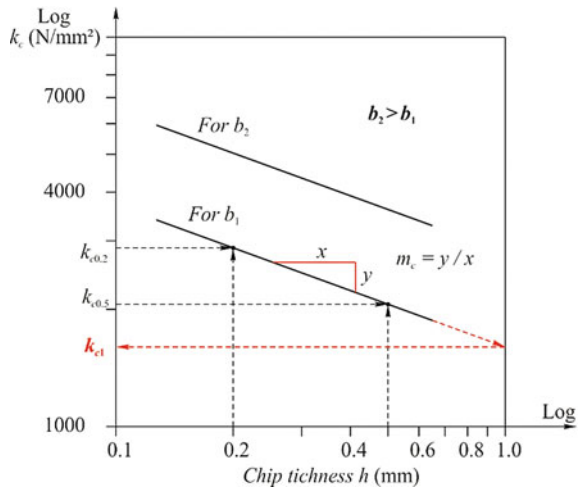
$$F_c = k_c \cdot b \cdot h \tag{1}$$

where h (mm) is cutting thickness, b (mm) is cutting width, and k_c (N/mm²) is specific cutting force, given by the formula (Klocke, 2011):

$$k_c = k_{c1} \cdot h^{-m_c} \cdot \left(1 - \frac{\gamma}{100}\right) \tag{2}$$

In formulation, γ (°) is the cutting tool rake angle. k_{c1} and m_c constants are related to workpiece material properties. The k_{c1} is the main value of the specific cutting force, defined on the cutting of chip cross-section with dimensions $b \times h = 1 \times 1$ mm². The m_c is the direction coefficient of function graph $f(h) = F_c/b$ in a double logarithm coordinate system (Fig. 5).

Fig. 5 Specific cutting force calculation



Cutting thickness and cutting width are related to the chip cross-section geometry. Cutting thickness depends on feed f_n (mm/rev), and tool entering angle κ ($^\circ$):

$$h = f_n \cdot \sin \kappa \quad (3)$$

Cutting width depends on the depth of cut a_p (mm), and tool entering angle κ ($^\circ$):

$$b = \frac{a_p}{\sin \kappa} \quad (4)$$

The productivity of the turning process, defined as the workpiece material removed ratio during machining MRR (cm^3/min), depends on process parameters. It can be calculated by multiplying of depth of cut a_p (mm/rev), feed f_n (mm/rev), and cutting speed v_c (m/min):

$$MRR = a_p \cdot f_n \cdot v_c \quad (5)$$

In the case of turning, the workpiece with the cutting tool entering angle $\kappa = 45^\circ$, values of the other cutting force components can be determined by the *Keckler* ratio (Klocke, 2011):

$$F_c : F_f : F_p = 5 : 2 : 1 \quad (6)$$

The cutting power P_c (W) necessary to overcome the workpiece material mechanical resistance during cutting tool movement, i.e. cutting forces, can be calculated as a multiplication of the main cutting force value F_c (N) and cutting speed v_c (m/min) (Klocke, 2011):

$$P_c = \frac{F_c \cdot v_c}{60} \quad (7)$$

The cutting energy E_c (Ws or J) is the energy required in the turning operation. It can be calculated as the multiplication of the cutting power and the machining time t (min):

$$E_c = \frac{P_c \cdot t}{60} \quad (8)$$

The machining time in turning can be calculated based on the turning length L_c (mm), as the length of the cutting tool traveling path, and the auxiliary movement speed v_f (mm/min). Auxiliary movement speed is the multiplication of feed f_n (mm/rev) and the spindle speed n (rev/min), or $v_f = n \cdot f_n$. Machining time t (min) is the quotient between turning length and auxiliary movement speed $t = L_c/v_f$, or:

$$t = \frac{L_c}{f_n \cdot n} \quad (9)$$

The most unfavorable situation during machining can be analyzed, which is related to problems with dimensional accuracy. It is caused by the workpiece bending due to the action of the cutting force components (Rao et al., 2013). If the workpiece is fixed by a clamping device on one side and supported by a pin on the other side, an unfavorable situation corresponds to the cutting tool position on the 2/3 of the workpiece length. When turning an unsupported workpiece at one side, an unfavorable situation corresponds to the cutting tool position on the free end of the workpiece. In fact, workpiece deflection is caused by the action of passive forces (Klocke, 2011). The maximum workpiece axis bending deviation δ_{max} (mm) can be calculated by:

$$\delta_{max} = \frac{0.4 \cdot \mu \cdot k_c \cdot b \cdot h \cdot L^3}{E \cdot I} \quad (10)$$

where μ is the coefficient of the workpiece fixing case ($\mu = 1/3$ for one free end workpiece side, $\mu = 0.0091$ for one workpiece side fixed by pin), l (mm) is workpiece length between fixturing points, E (MPa) workpiece material elastic module, and I (mm⁴) workpiece cross-section moment of inertia. For a cylindrical part, the moment of inertia is $I \approx 0.05 D_c^4$, where D_c (mm) is the diameter of workpiece.

4 Resources and Organization

Next, there will be noted and explained the general issues, safety issues, measuring system and organization per workplaces and tasks.

General issues. All actions related to measurement must be done under the supervision of laboratory assistants and instructors, who are instructed in the ways of handling equipment in the laboratory.

Safety issues. During the activities, there is a risk of injury from moving elements of the tool machine and touching tools and chips. There is a possibility of electric shock when connecting measuring devices. Moreover, after machining, the workpiece is hot, and there is a risk of burns. In addition, fragments and chips fly out of the cutting zone during machining that can injure a person. It is necessary to provide adequate protection for the eyes and gloves for the hands.

Measuring system. The measuring system consists of *Kistler* device for cutting forces measuring, and *Mitutoyo* device for dimensional measuring (Fig. 6).

The cutting force measuring device consists of a piezoelectric dynamometer, a special signal conductor cable, a signal amplifier, an A/D converter, and a PC software card mounted on the PC slots (KISTLER, 2023). The dynamometer (type 9257B) works on the principle of piezo-elements loading. It provides the appropriate voltage in proportion to the mechanical load. The dynamometer has six piezo-sensors and measures the force in three mutually perpendicular directions. It is mounted on the tool machine support for the auxiliary movement in the x-axis and z-axis (tool turret), which makes the measuring directions coincide with the directions of

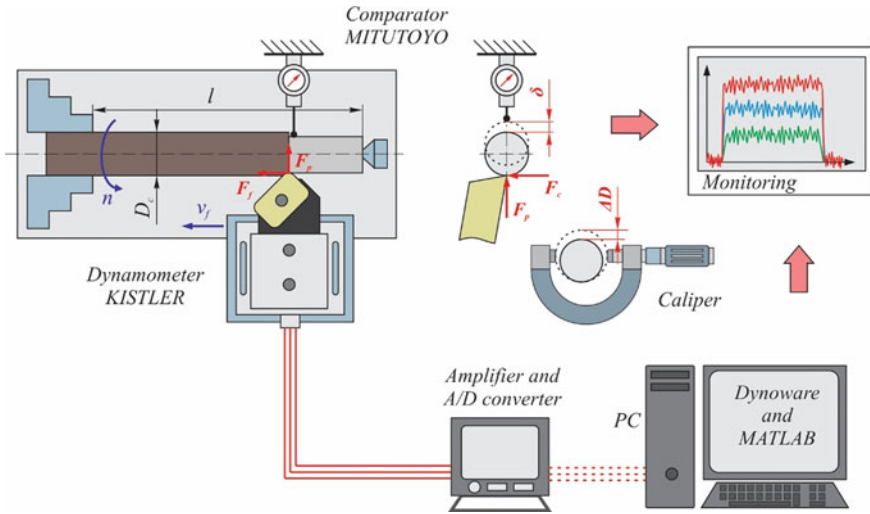


Fig. 6 Schema of the cutting force measuring system

movement of the tool machine and tool tip. It has a tool holder and an element for mounting on the tool machine. The obtained analog electrical signals from the dynamometer are amplified and converted into digital signals in an amplifier device (type 5070A). For this purpose, the amplifier device must be calibrated beforehand, according to the manufacturer’s instructions on the calibration document. Digital signals are transmitted to the PC by a special computer card. It allows measured signal processing, soft computing, and displaying.

Measurement of workpiece dimensional deviation caused by its deformation due to mechanical loading during machining can be measured in two ways: indirect or direct. The first is related to workpiece bending during machining. It is performed by placing the analog or electronic precise comparator measuring head tip on the workpiece nominal surface (before turning) and setting it to zero. The comparator stand must be mounted on a tight tool machine element connected to the cutting tools support (tool turret). The comparator measuring head tip must be placed perpendicular to the machined surface, directly on the other workpiece side regarding the action point of the cutting tool tip. The recording of the comparator head tip moving, i.e. the workpiece bending amount, must be noted during machining. However, there is a risk of unwanted measuring head tip damage. The second way is related to the direct measuring of the dimensional accuracy. Thus, it is calculated the difference Δ (mm) between the measured nominal workpiece diameter and the obtained workpiece diameter. It is performed by using a precise device (digital micrometer). The nominal diameter is the diameter of the workpiece at the action point of the cutting tool before machining. The actual diameter is the diameter at the action point of the cutting tool after machining.

Organization per workplaces and tasks. The optimum size of the learning group is from 7 to 9 students. Tasks can be divided into three students can be involved in setting the measuring device on the turning machine. Moreover, two students can work on setting the PC software and A/D connection with the measuring devices. Another two students can deal with PC software and cutting force signals acquisition. In addition, finally, one student can monitor and note all other details related to the measurement process.

5 Session Development

The necessary time and procedure for setting up the workpiece, setting the machining conditions, domain and variation levels of process parameters, and the way of performing measurements are next described (Monroy Vazquez et al., 2014; Montgomery, 2005). However, the mounting of the previously described measuring device on the tool machine takes about half an hour and must be performed before the session to save time.

Workpiece setting. The workpiece in turning is a cylindrical part made of certain metallic material with a defined diameter and length and without deviations in straightness and cylindricity. It must be prepared for adequate clamping in the lathe fixturing jaws on one side (check fixturing jaw diameter), and fixturing pin on the other side (check length of machine working area). Mounting and preparation workpiece on the tool machine can take about five minutes of session time. For example, typical cylindrical workpieces used have as dimensions: diameter $D_c = 40$ mm and length $L = 480$ mm (Fig. 7). The material is steel 34Cr4 (EN 1.7033, AISI 5132). It is low alloyed chromium carbon steel, with tensile strength $R_m = 890$ MPa, and hardness 240 HB.

Cutting tool setting. The cutting tool should match the target turning operation and workpiece material. According to the workpiece geometry and fixturing, it is recommended to use the right-hand turning indexable cutting tool, which enables external longitudinal turning operation. The cutting tool must be mounted in a dynamometer holder, in the radial direction to the workpiece rotation axis. Preparation and assembling of the tool holder, cutting insert and cutting tool mounting on the device can consume about five minutes of the session. As example, there are used layered cutting tools with material grade PM 4225, by the Sandvik Coromant. Tool holder is PSDNN 2525 M12, and cutting insert is SNMG 1204 08, which enables rake angle of 4° , and an entering angle of 45° .

Process parameters definition. The values of the cutting parameters must correspond to the type and shape of the cutting insert, the cutting insert material grade, the workpiece geometry (L/D ratio and fixing conditions), and the workpiece material. It is recommended to use cutting parameter value domains for fine or rough machining, but not combined. Parameter domains must be kept within the value limits given by the cutting tool manufacturer. Since the most influential cutting parameters on cutting



Fig. 7 Measuring setup on the universal lathe

force are depth of cut a_p (mm) and feed f_n (mm/rev), these two are taken as key parameters. Their values are varied on three levels. Spindle speed (number of revolutions per minute) is kept at a constant level. In this example, the spindle speed is 467 rev/min and the cutting speed for the diameter of $D_c = 40$ mm is $v_c = 84$ m/min. This value is adopted according to the cutting tool manufacturer’s recommendation on workpiece material, and tool machine stability.

Measuring runs. The measuring runs refer to turning with different combinations of varied process parameters (Bera et al., 2018; Hajdu et al., 2023). If it is assumed that the depth of cut varies on three levels, and the feed varies on three levels, it is possible to perform nine combinations (nine runs). During turning, the same place of cutting tool tip action on the workpiece must be taken. Measuring runs must be performed on a certain workpiece length. It must be taken into account that when turning with larger feed values, the machining time of the same length will be shorter. For each run, it is necessary to set the appropriate parameters combination on the tool machine control unit. It is recommended to determine the machining time for each measuring run, and it can enter into the calculation of the total session time, together with the session preparation time. It is necessary to consider that during the measurement there may be a need to adjust the workpiece surface alignment, for correctly setting the process parameters for the next run.

Cutting force and workpiece deflection measuring. Immediately before starting the turning, the measuring cutting forces device must be referenced and switched on (Projoth et al., 2021). In addition, the maximum workpiece deflection must be monitored and noted. In the user environment of the software that acquires the cutting

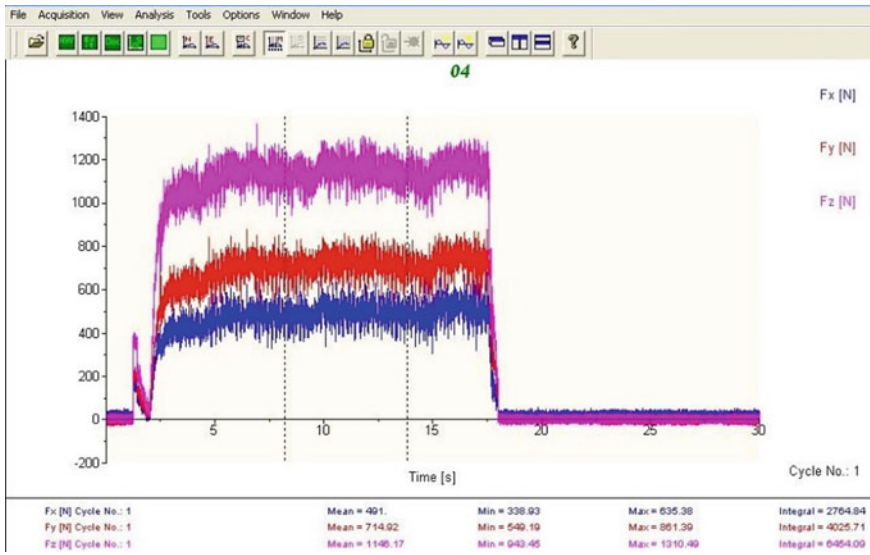


Fig. 8 Cutting force signal on device monitor

force signals, the appearance of the measured signals during time can be obtained and observed. In the user environment, it is necessary to determine the domain in which the signal mean value, maximum, and minimum value are extracted. Vertical cursor lines for the domain boundary must be placed at both ends of the signal stable part, after which the cutting force components mean values are read (Fig. 8).

6 Main Outcomes

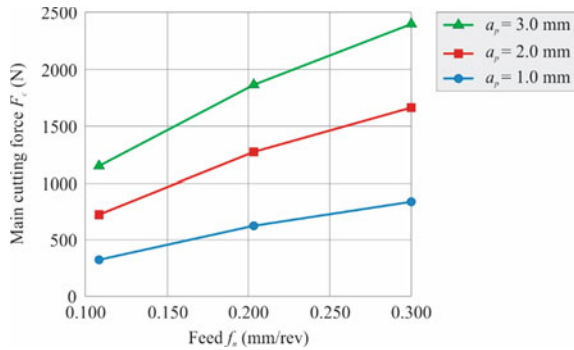
The measurement results for every run with different cutting parameter combinations can be entered in Table 1. However, for each measurement run, different cutting force component mean values and signal behavior are expected. The extracted amplitude values for each component of the cutting force can be entered in the table. In addition, it is necessary to enter the values of the measured workpiece deflection, measured for each run. Cutting forces component, and other outputs of the machining process, measured on given example conditions and procedure, are given in Table 1.

Based on the obtained results, it is possible to draw a diagram of the evolution of each of the cutting force components. For a better understanding, it is necessary to use appropriate feed values on the horizontal axis, and three dependencies in the diagram in accordance with the depth of cut. For each combination, it is possible to enter the appropriate value of the cutting force (Fig. 9). Based on the diagram, it is possible to identify an increase in the cutting force component with the increase in both depth of cut and feed.

Table 1 Measurement and calculation results

Run	Input process parameters		Measured cutting force component			Measured workpiece deviation	Calculated productivity and energy	
	a_p (mm)	f_n (mm)	F_c (N)	F_f (N)	F_p (N)	δ (mm)	MRR (cm ³ /min)	E_c (Ws)
1	1.0	0.108	325	214	159	0.006	9.12	2.626
2	1.0	0.203	622	365	237	0.009	17.14	2.674
3	1.0	0.300	837	542	328	0.013	25.33	2.435
4	2.0	0.108	719	460	292	0.010	18.24	5.810
5	2.0	0.203	1271	744	473	0.018	34.29	5.464
6	2.0	0.300	1661	997	812	0.023	50.67	4.832
7	3.0	0.108	1146	715	419	0.015	27.36	9.260
8	3.0	0.203	1862	1109	652	0.022	51.43	8.004
9	3.0	0.300	2399	1528	897	0.029	76.00	6.978

Fig. 9 Diagram for cutting force behavior analysis



To assess the energy efficiency of the cutting process, it is necessary to define a diagram that shows the ratio between the consumed cutting energy and the material removal rate (E_c/MRR) (Fig. 10). The diagram shows how efficient the cutting parameter combinations are in terms of saving electricity on the tool machine. A lower value of the ratio indicates a better energy efficiency of the cutting process. The conclusion is that the cutting process that takes place at higher cutting parameter values is more efficient.

Next, the method for determining the specific cutting force will be explained (Kaymakci et al., 2012; Lalwani et al., 2008). The procedure for calculating and analyzing the cutting energy value, which used to overcome the cutting forces and the workpiece material resistance in turning. A procedure will be given to the instructor, which can be used to relate the value of the cutting force and the workpiece deflection values. The main cutting force can be calculated as:

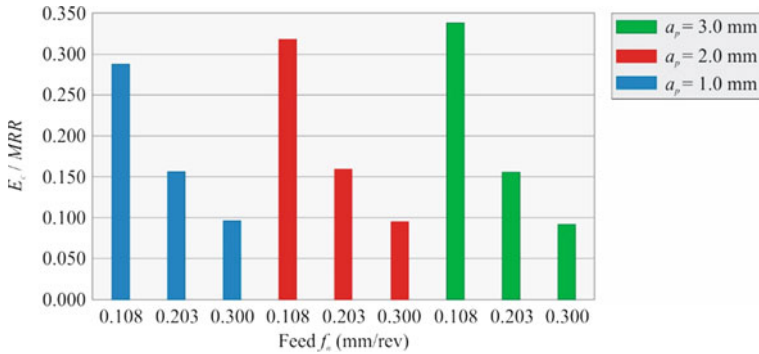


Fig. 10 Diagram for observing of energy efficiency

$$F_c = k_{c1} \cdot h^{-m_c} \cdot \left(1 - \frac{\gamma}{100}\right) \cdot b \cdot h \quad (11)$$

As it is very difficult to determine m_c and k_c graphically, as shown in Fig. 6, there can be used numerical calculation, which will lead to their appropriate values. The previous formulation can be transformed into the following:

$$\frac{F_c}{b \cdot \left(1 - \frac{\gamma}{100}\right)} = k_{c1} \cdot h^{(1-m_c)} \quad (12)$$

To proceed, it is necessary to replace the left side of the equation as follows:

$$\overline{F_c} = k_{c1} \cdot h^{(1-m_c)} \quad (13)$$

In order to linearize the previous expression, the natural logarithm of the left and right sides of the expression is introduced:

$$\ln(\overline{F_c}) = \ln(k_{c1} \cdot h^{(1-m_c)}) \quad (14)$$

It can further be written in the form:

$$\ln(\overline{F_c}) = \ln k_{c1} + (1 - m_c) \cdot \ln h \quad (15)$$

The previous expression can be represented as a linear function, or dependence with the corresponding coefficients A and B.

$$Y = B + A \cdot X \quad (16)$$

The Eq. (16) is suitable for solving by the least squares method (Montgomery, 2005). The method is based on measurement results. If the measurements are displayed in a two-dimensional rectangular Cartesian coordinate system where the

i-th measurement result corresponds to the *i*-th point coordinates (*x_i* and *y_i*), the equation of the linear function $Y = AX + B$, which best corresponds to the measurement results, can be found using this expression. In this case, the calculated natural logarithmic values of the input cutting parameters and the output values of the cutting force component must be used.

By the least squares method, the values of the function coefficients *A* and *B* can be calculated using the expressions:

$$A = \left(n \cdot \sum_{i=1}^n x_i \cdot y_i - \sum_{i=1}^n x_i \cdot \sum_{i=1}^n y_i \right) / \left(n \cdot \sum_{i=1}^n x_i^2 - \left(\sum_{i=1}^n x_i \right)^2 \right) \tag{17}$$

and

$$B = \frac{1}{n} \cdot \sum_{i=1}^n y_i - \frac{A}{n} \cdot \sum_{i=1}^n x_i \tag{18}$$

where the value of *x_i* corresponds to calculated value $\ln h_i$, and the value of *y_i* correspond to the calculated value $\ln (\overline{F_c})_i$, Table 2. Value *n* corresponds to the number of experiment runs, so *n* = 9.

Based on the logarithmic values, and using the previous expressions, a linear dependence is obtained:

$$Y = 7.713 + 0.830 \cdot X \tag{19}$$

Using the obtained linear dependence, the exponent *m_c* in the form of the main cutting force can be calculated using:

$$B = (1 - m_c) = 0.830 \tag{20}$$

Table 2 Recalculation of inputs and outputs data

<i>i</i>	Chip cross section		Cutting force component		Logarithmic values	
	<i>h</i> (mm)	<i>b</i> (mm)	<i>F_c</i> (N)	$\overline{F_c}$	$\ln \overline{F_c} = y_i$	$\ln h = x_i$
1	0.076	1.414	325	239.385	5.47807	-2.5722
2	0.144	1.414	622	458.146	6.12719	-1.9411
3	0.212	1.414	837	616.509	6.42407	-1.5505
4	0.076	2.828	719	264.797	5.57896	-2.5722
5	0.144	2.828	1271	468.090	6.14866	-1.9411
6	0.212	2.828	1661	611.721	6.41628	-1.5505
7	0.076	4.243	1146	281.370	5.63967	-2.5722
8	0.144	4.243	1862	457.164	6.12504	-1.9411
9	0.212	4.243	2399	589.010	6.37844	-1.5505

and finally:

$$m_c = 1 - 0.830 = 0.170 \quad (21)$$

Similarly, comparing the transformed expression with the resulting linear dependence, it can be seen that the specific cutting force can be obtained using the equation:

$$A = \ln k_{c1} = 7.713 \quad (22)$$

Thus:

$$k_{c1} = e^{7.713} = 2238 \quad (23)$$

By including the obtained exponent and the obtained value of the specific cutting force in the initial form for the main cutting force before the mathematical transformation, the following is obtained:

$$F_c = 2238 \cdot h^{-0.170} \cdot \left(1 + \frac{\gamma}{100}\right) \cdot b \cdot h \quad (24)$$

Finally, any combination of input cutting parameters can be included in the obtained previous expression to determine the deviation of the calculated value from the measured value of the main cutting force. This can be shown through the relative error value calculation, by $Error = |(F_{measured} - F_{calculated})/F_{measured}| \cdot 100\%$. It can be noted that the maximum relative error in absolute values of 10.5% is obtained for the first combination of parameters. Other relative errors are under 5%. However, the mean relative error for nine calculated values is only 3.6%.

7 Assessment and Knowledge Check

The evaluation of the acquired student's knowledge about cutting mechanics and cutting force is performed using the questions given below. The evaluation can be organized as a ten-minute knowledge test.

- Q1. What causes workpiece material resistance to cutting tool movement and penetration during the cutting process?

Answer: Resistance to tool movement occurs as a result of workpiece material shearing in the shear plane, plastic-elastic deformation of the material in the zone in front of the cutting tool wedge, friction of the chips plastic flow over the tool wedge rake side, friction of the tool wedge clearance side on the machined surface, resistance to additional chips deformation and breaking.

- Q2. How do the process parameters affect the cutting forces?

Answer: By increasing the depth of cut and feed, the cutting forces increase, due to the larger chip cross-section. An increase in cutting speed generates a great amount of heat in the cutting zone. It contributes to the workpiece material softening, and reduction of tensile strength and cutting force. High values of process parameters can cause a large material deformation and deformation straightening, and increase in cutting forces.

Q3. How are cutting force values most often measured and monitored?

Answer: During the measurement of cutting forces, the model of three cutting force components is most often applied. It includes the definition of three mutually perpendicular components, as follows: the cutting force (it coincides with the direction of the cutting speed vector), the feed force (it coincides with the direction of the axis of rotation), and the passive force (perpendicular to the axis of rotation). Determining of cutting forces is carried out by dynamometers that enable the measurement of the mechanical loads.

Q4. What empirical formulation is used to calculate cutting forces?

Answer: One of the mathematical formulations that describes the dependence of the cutting parameters on the cutting force value is based on the multiplication of the specific cutting force and the chip cross-section area. The specific cutting force (k_c) is calculated based on the main value of the specific cutting force (k_{c1}), defined for infinite chip cross-section, and the direction coefficient of cutting thickness—force function logarithm graph (m_c).

Q5. How is the evaluation of the measured cutting force component signals performed?

Answer: Special software associated with measuring devices is often used to display the values and behavior of cutting force signals. The measured signals are used to read the cutting force component value by selecting the machining and measuring time domain with the steady measured signal. Within the defined domain, the mean value of the cutting force component can be automatically calculated. For the mean value calculation, it is used the measured cutting force signal values over time, and the number of discrete time moments during the measurement.

8 Conclusion

This chapter presents the session and procedure for cutting force measuring and analyzing, calculating, and understanding their impact in machining. Turning was chosen due to the simple workpiece-cutting tool kinematic system. The procedure consists of a theoretical background for a better understanding of the load source and cutting forces in the cutting zone. In addition, there are theoretical explanations of the cutting forces' impact on the dimensional accuracy, machined surface quality, and energy efficiency of the process. The cutting forces system in the cutting zone is represented as a system of three mutually perpendicular cutting force components, which can be measured with a dynamometer.

The mathematical model and formulation of the cutting force components are based on Kinzle's formula. The most usual graphical procedure of Kinzle's formula coefficients defining is presented. The laboratory session shows the setting of the cutting tool, workpiece setting, and measuring equipment on the turning machine, as well as the procedure of data signal measurement and processing. The reading and graphical representation of the cutting force-measured signals were performed in special PC software. In addition to the measurement instructions, there are guidelines for the session organization in terms of time limit, student group size, tasks, and safety regulations. Based on the measured values of the cutting force components, the calculation of other variables and indicators was performed. The analysis of the obtained values was given on a graphical basis. In contrast to the graphical method, the analytical calculation of Kinzle's formula coefficients is shown and applied. Therefore, linearization and the least squares method were used. At the end, there is a section for student's acquired knowledge checking, and summarizing the learning session results.

References

- Bera, T. C., Manikandan, H., Bansal, A., & Nema, D. A. (2018). Method to determine cutting force coefficients in turning using mechanistic approach. *International Journal of Material Mechine Manufacturing*, 6, 99–103.
- Carou, D., Rubio, E. M., Herrera, J., Lauro, C. H., & Davim, J. P. (2017). Latest advanced in the micro-milling of titanium alloys: A review. *Procedia Manufacturing*, 13, 275–282.
- Carou, D., Rubio, E. M., Lauro, C. H., & Davim, J. P. (2016). The effect of minimum quantity lubrication in the intermittent turning of magnesium based on vibration signals. *Measurement*, 94, 338–343.
- Davim, J. P. (2008). *Machining—Fundamentals and recent advances*. Springer.
- Davim, J. P. (2017). *Sustainable machining*. Springer.
- Grzesik, W. (2008). *Advanced machining processes of metallic materials: Theory, modelling and application*. Elsevier B. V.
- Hajdu, D., Astarloa, A., Kovacs, I., & Dombovari, Z. (2023). The curved uncut chip thickness model: A general geometric model for mechanistic cutting force predictions. *International Journal of Machine Tools and Manufacture*, 188, 104019.
- Kaymakci, M., Kilic, Z. M., & Altintas, Y. (2012). Unified cutting force model for turning, boring, drilling and milling operations. *International Journal of Machine Tools and Manufacture*, 54–55, 34–45.
- KISTLER. (2023). Measuring device manufacturer. <https://www.kistler.com/DE/en/cutting-forces-in-turning-operations/C00000103>. Accessed December 14, 2023.
- Klocke, F. (2011). *Manufacturing processes 1: Cutting* (RWTH). Springer.
- Lalwani, D. I., Mehta, N. K., & Jain, P. K. (2008). Experimental investigations of cutting parameters influence on cutting forces and surface roughness in finish hard turning of MDN250 steel. *Journal of Materials Processing Technology*, 206, 167–179.
- Matsubara, A., & Ibaraki, S. (2009). Monitoring and control of cutting forces in machining processes: A review. *International Journal of Automation Technology*, 3(4), 445–456.
- Monroy Vazquez, K.P., Giardini, C., & Ceretti, E. (2014). Cutting force modeling. In L. Laperrière, & G. Reinhart (eds.), *CIRP encyclopedia of production engineering*. Springer.
- Montgomery, D. C. (2005). *Design and analysis of experiments*. Wiley.

- Projoth, T. N., De Pours, M. V., & Nanthakumar, P. (2021). Analysis and prediction of cutting force through lathe tool dynamometer in CNC turning process. *Material Today: Proceedings*, 46(9), 4174–4179.
- Rao, C. J., Nageswara Rao, D., & Srihari, P. (2013). Influence of cutting parameters on cutting force and surface finish in turning operation. *Procedia Engineering*, 64, 1405–1415.
- Sousa, V. F. C., Silva, F. J. G., Fecheira, J. S., Lopes, H. M., Martinho, R. P., Casais, R. B., & Ferreira, L. P. (2020). Cutting forces assessment in CNC machining processes: A critical review. *Sensors*, 20, 4536.
- Sredanovic, B., Globocki-Lakic, G., Cica, D., Borojevic, S., & Golubovic-Bugarski, V. (2011). Modelling of cutting forces with artificial neural network. In *Proceedings of 4th international conference on manufacturing engineering ICMAN 2011*. Aristotle University of Thessaloniki, October 3–5, 2011.
- Thangarasu, S.K., Shankar, S., Thomas, T., & Sridhar, G. (2018). Prediction of cutting force in turning process-an experimental approach. *IOP Conference Series: Materials Science and Engineering*, 310, 012119.

Practical Guide of Project-Based Learning (PBL) Applied to Manufacturing Technology Subject



Alejandro Pereira and José L. Diéguez

1 Introduction

The computer and lab sessions presented are part of a subject taught in an advanced manufacturing course in the final semester of the Mechanical Engineering bachelor, specializing in Design and Manufacturing, at the Industrial Engineering Faculty of the University of Vigo. The objective of this subject is to acquire knowledge of product development and the necessary tools, considering all the phases involved in the manufacturing process.

Students divided into groups carry out the main activities. Each group of students starts with a creative conceptual design phase, where they are trained to improve a product or the necessary tools. Once the concept is determined, the detailed design, manufacturing planning, manufacturing programming, prototype product development and verification, and quality control of the final product are carried out. The methodology is based on product development applying Project-Based Learning (PBL) by utilizing available tools such as PLM platforms like Catia V5-6 from Dassault Systèmes or NX from Siemens company. Moreover, groups can use the manufacturing resources available in the manufacturing workshop (casting furnaces and tools, prototyping machines, CNC machining machines, industrial robots, Coordinate Measuring Machines (CMM), etc.), depending on availability.

A. Pereira (✉)

Departamento de Deseño na Enxeñaría, Escola de Enxeñaría Industrial, Universidade de Vigo,
36310 Vigo, Spain
e-mail: apereira@uvigo.es

J. L. Diéguez

Departamento de Deseño na Enxeñaría, Escola de Enxeñaría Industrial, Universidade de Vigo,
36208 Vigo, Spain

2 Background

Conventionally, teaching methodologies are based on a model in which the instructor presents knowledge in a classroom and the learner tries to assimilate it in the best possible way, which is the passive method of learning.

In recent decades, with advances in learning theories, methodologies have shifted from a focus on teaching to a focus on learning. In this sense, Active Learning Methodologies are developed to increase the student's motivation. Through the development of skills and abilities, learners acquire the ability to solve problems methodologically and autonomously (Konopka et al., 2015).

Project-Based learning (PBL) is a learning strategy that encourages students to solve real problems organized in working groups. This methodology focuses on the student both as an individual and as a member of a working group and considers learning as a communication process.

Standridge (2000) developed and implemented a case-based approach for introducing discrete event simulation to undergraduate and graduate manufacturing engineering students. Students learn only the simulation methods necessary to support the case studies. Case studies are derived from topics of interest to practicing manufacturing engineers. They include four modules: basic systems organizations, systems operating strategies, material handling, and supply chain management. Course instruction is based on active learning. Tutorials and laboratories assist students in comprehending the simulation methods. Courses are taught in a computer-aided teaching studio so that the mix of passive and active learning can be adjusted as appropriate to each class meeting way (Lamancusa et al., 2008).

The work by Jonassen (2015) on problem-solving and constructivist learning environments has influenced the development of PBL techniques, including their application in manufacturing education.

Lorenzo-Yustos et al. (2010) present complete product developments that have been undertaken by teams of students, to the practical application of design and manufacturing concepts. The use of additive technologies has enabled prototypes to be manufactured, which means the pre-production stage has been attained. Important information for improvements has been obtained from students' surveys and the correspondence between students' dedication and the European Credits assigned to the subject is very satisfactory.

Vila et al. (2017) present a structured integrated vision of tools, such as Product Lifecycle Management (PLM) and computer-aided applications (Cax), which support engineering content creation and the associated learning process. PBL is proposed as a learning approach suitable to provide a learning experience that facilitates the development of Industry 4.0 skills and competencies.

Sola-Guirado et al. (2022) studied the feasibility of the teaching proposal for the management of CAD /CAM/CAE tools using a PBL method in a distance-learning environment. The courses have been carried out thanks to the operation of the PLM platform software by means of virtual machines. The practice has given very good

pedagogical results in the work of competencies related to the field of design and industrial manufacturing.

Fernandes et al. (2020) describe step-by-step the PBL approach applied, as well as the objectives and constraints related to the computer-aided design, engineering, and manufacturing (CAD /CAE/CAM) technologies employed in the case studies. They also design the evaluation process, as well as the quantitative results, and the results obtained from the questionnaires answered by the students at the end of the PBL experience.

Angrisani et al. (2020) designed a course based on a “small learning enterprise” integrated with an academic FabLab, applying active learning methodologies, Project-Based and Scenario-Based Cooperative. The educational activity is based on the learning factories concept focused on process innovation, and small enterprises of the fourth industrial revolution, using the Internet of Things (IoT) and additive manufacturing.

Bahha et al. (2019) design learning modules related to casting and product assembly processes and tolerance analysis topics. The learning outcomes of the application of the design-based teaching approach are reflected through the students’ successful completion of the project activities, in addition to acquiring lifelong learning and communication skills through the preparation of micro-lectures and presentations. Moreover, students learned how to use a computer-aided design (CAD) package to perform advanced design and manufacturing analysis.

In recent years, the application of PBL, using additive manufacturing technologies in engineering curricula, has started to expand exponentially as it enables cross-disciplinary learning, as demonstrated by various published studies (Angrisani et al., 2020; Ansaf & Jaksic, 2019; Ellis & Graveson, 2022; Gatto et al., 2015; Pereira et al., 2022; Prabhu et al., 2020; Stern et al., 2019). In the specific case of the Universidade of Vigo, PBL has been applied in manufacturing process engineering since 2007. However, this work is based on a novel approach to the development of practical cases of tooling and real parts to optimize the use of lab resources, applied since 2017.

3 Learning Objectives

In general, the application of PBL in the teaching of manufacturing achieves the following general objectives:

- Significant increase in student motivation.
- Improved creativity in the search for problems and solutions to them.
- Increased group participation.
- Optimization of the learning of applied manufacturing technologies.

In the example provided by the selected group, the following specific objectives have been set:

- Obtaining selected product design (4-stroke engine piston).
- Obtaining process planning training of the final part/assembly (including casting process, additive manufacturing, and machining processes).
- Knowledge of casting technologies, including materials and tooling design.
- Design and manufacture of patterns, cores, molds, and core boxes, applying additive manufacturing to manufacture patterns and core boxes.
- Increase of design capabilities in available PLM platforms (Catia V5 and NX Siemens).
- Increased CAM programming capabilities in turning and milling.
- Verification and quality control training.

4 Resources and Organization

To carry out the PBL practices, the following resources are required:

- Software:
 - Free design: Inkscape, vector graphics editor, openBoard.
 - Detailed design: general-purpose parametric 3D platform PLM.
 - PLM Catia V5-6 (Dassault Systemes[®]) (www.3ds.com).
 - PLM Siemens NX (<https://plm.sw.siemens.com>).
 - Specific slicer for additive manufacturing: Idea Maker 4.2 (Raise 3D Technology Inc.) (www.raise3d.com).
- Laboratory equipment:
 - Foundry.
 - Material extrusion printer: Raise Pro 3D.
 - Manual Pinacho lathe.
 - Vertical machining center with CNC Fagor 8065 control.
 - Lathe with Fagor 8030 control.
 - Tools and fixtures.

The organization of this practice will be:

- Introductory sessions to teach the basics of computer design and manufacturing processes and PBL methodology.
- Creation of groups composed of three to four students.
- Guidance of the activities selected by the student's groups.
- Design and develop of the activities in computer labs.
- The availability of the resources might limit the development of practical activities.

In this chapter, the discipline chosen is manufacturing technologies in which free works are developed, with very variable themes and considering different manufacturing processes in each work. This varied character of subjects and technologies is the innovative case of applying PBL to the student's curriculum. The specific case that has been selected includes free design technologies, detailed CAD design, process planning, and the use of different technologies in the manufacturing process, such as additive manufacturing, casting process, CAM programming, turning, and milling process and quality inspection. The subject consists of 6 ECTS (European Credits Transfer System), which corresponds to 48 h of face-to-face instruction, 60 h of student work, and 10 h of evaluation. The first week is established as an introductory one. The following weeks take place directly in the laboratories and CAD/CAM classroom. The arrangement consists of practical sessions of 2-h practical sessions, three days a week, totaling 48 h of face-to-face instruction.

5 Session Development

The flowchart presented in Fig. 1 explains the PBL methodology to follow. The instructor will explain this chart in the first session. It can be noted that the first row includes the titles composed using "What's and how's ..." questions, the technological resources, the targets, and the objective documentation. The columns include the different steps of each of the titles of the first row, specifically:

- The What and How questions, the different steps composed by the idea, conceptual design, detailed design, the process planning, the programming, the execution of programs in the CNC machines, and the quality control, which include the inspection metrology and functional verification.
- The technology and resources include group formation and problem-solving techniques such as brainstorming, Ishikawa diagrams, etc. (Akay et al., 2008; Ubaidullah et al., 2021). PLM platforms, lamination software for additive manufacturing, AM machines, CNC and conventional machining machines, injection machines, casting resources, metrological devices, and CMMs.
- The third column indicates the targets of each step including the initial sketches, the numerical definition in 3D, the detailed drawings, the process sheets, the quality sheets, and the CAM programs to execute. After establishing the targets, the students obtain the parts and need to apply the quality inspection. The target in this case is the report of quality inspection according to the quality sheet previously designed.
- The last column includes the documentation to be evaluated. Finally, the students must present the work in public in a time of 10 min, with a maximum of 5 min for debate (UVigoTV, 2023).

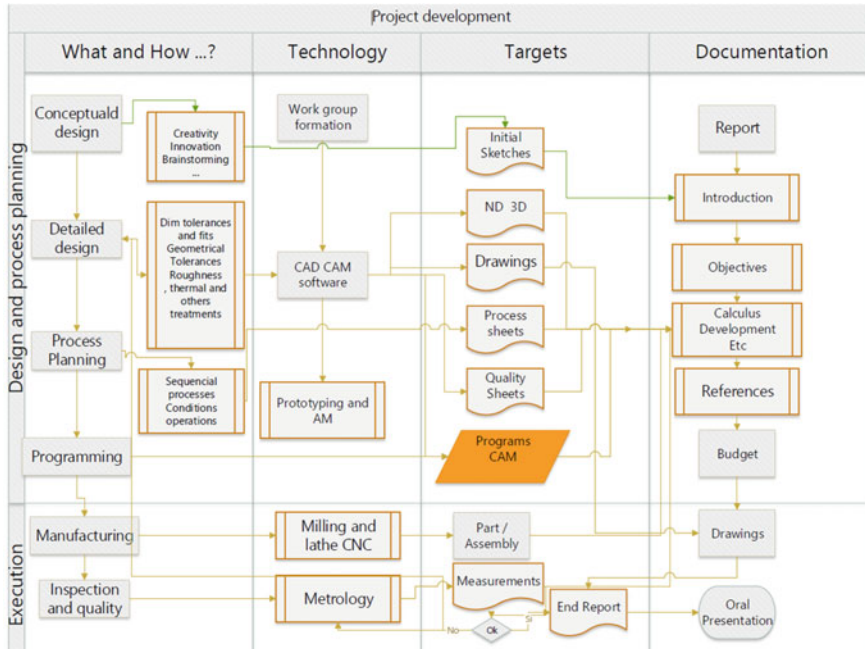


Fig. 1 Flowchart of PBL methodology applied to manufacturing engineering

6 Outcomes

A group of three students has carried out the selected case during the course. The title is “Design and manufacture of a 2-stroke piston”. Figure 2 shows the methodology according to the initial sessions of the instructor. The objective of the case was the design and manufacturing of a 2-stroke piston in AA6030 by casting and machining processes.

6.1 Conceptual Design

The group of three students spent approximately 4 h defining the conceptual design of a 2-stroke piston, defining the specific structure and features of a piston used in a 2-stroke engine. They define the next characteristics of the 2-stroke piston:

- Cylinder fit: the piston is designed to fit tightly within the cylinder to create a combustion chamber. It forms a seal against the cylinder wall to prevent any leakage of gases during the power stroke. The instructor needs to define the maximum range of the dimensions to handle the post-manufacture. Figure 3a shows the initial sketch

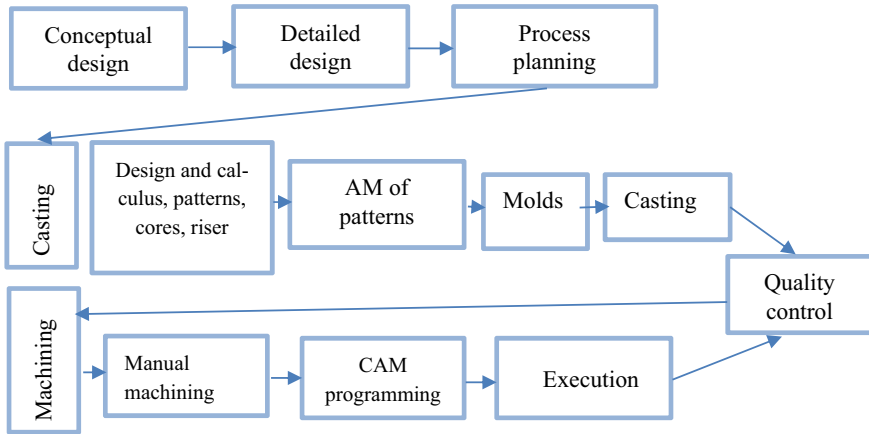
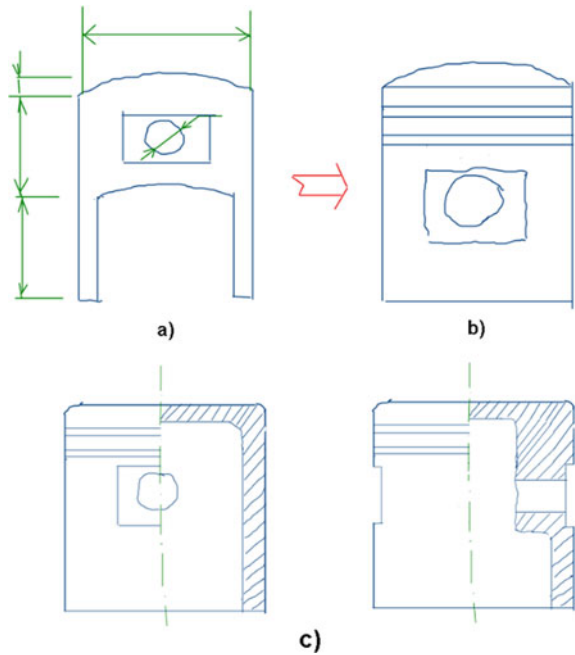


Fig. 2 Specific methodology of the selected case

Fig. 3 a Initial sketch b skirt modification c head modification and inside of cylinder



- Skirt: the skirt is the portion of the piston that extends down the cylinder. It helps guide the piston and maintains alignment within the cylinder. The skirt may have a taper or profile to reduce friction against the cylinder wall and improve overall engine efficiency. In this practical case, the instructor advised reducing the skirt

and making the cylinder lighter on the inside. Figure 3b shows the modification of the skirt.

- Head: typically, it has a slightly concave shape to promote efficient combustion. The design of the crown influences the swirl or turbulence of the air–fuel mixture, optimizing the combustion process. To simplify the manufacturing process, the students define a surface plane as head.
- Ring grooves: these grooves hold the piston rings, which seal the combustion chamber and prevent the escape of gases. They define two-ring grooves.
- Pin bosses: the piston features pin bosses or wrist pin bosses, which are openings on the sides of the piston. These bosses house the wrist pin or piston pin, which connects the piston to the connecting rod.

Figure 3c presents the final conceptual design of the piston. The openboard web platform was used to create the different sketches.

6.2 Detailed Design

The detailed design of the 2-stroke piston involves specific dimensions, tolerances and fittings, characteristics, and materials used in its construction. The student group spent approximately 16 h developing the required activities. The main decisions at this stage involve the following:

- Piston material: the material recommended for the piston was 6030 aluminum alloy due to its lightweight and strength-to-weight ratio.
- Dimensions, tolerances, and fittings of different parts.
 - Piston and head: total tolerance of 0.05 mm and flatness of 0.1 mm.
 - Ring grooves: the tolerance is 0.1 mm, centered ± 0.05 mm.
 - Skirt: the same as in the piston.
 - Pin bosses: the dimension and tolerance of the hole are $\text{Ø } 10 \text{ H7}$. The axis alignment of the holes has geometrical tolerances of perpendicularity regarding the cylinder's axis.
 - Interior: the functionality consists of the lightening of the piston, the separation of the planes, to ensure the positioning of the connecting rod, and the inner clearance to ensure the coaxiality of the outer and inner shafts.

The numeric definition (ND) of a 2-stroke piston was optimized through PLM Catia v5-6 and was analyzed using CAE testing to meet specific performance goals and reliability requirements. Because of this activity, under the instructor's supervision, a detailed drawing was obtained. Figure 4 presents the 3D tolerance annotations, made with the 3D Functional Tolerance & Annotation module of Catia v5-6.

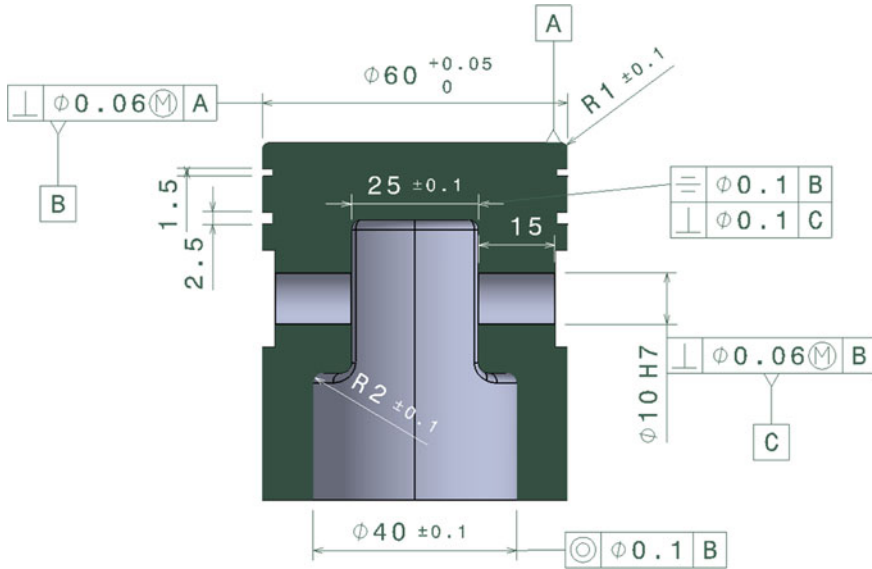


Fig. 4 3D tolerances annotations

6.3 Process Planning

The process planning for casting an aluminum 2-stroke piston involves several steps to ensure the accurate and efficient manufacture of the piston. The key aspects of this activity for casting an aluminum piston involve three fundamental phases, the casting process, the manual turning process, and CNC turning and milling process.

- Casting process
 - a. Design of pattern, cores, and box cores. It is also mandatory to design the feeders and pouring distribution system. The design of the pattern must include machining allowances, contraction dimensions, and the demolding angle. The gating system includes channels and runners that guide the molten metal into the mold while allowing gases to escape.
 - b. Pattern construction: the pattern, distribution system, and core boxes were made from PLA using material extrusion.
 - c. The mold preparation includes the cope (top mold), the drag (bottom), and the core preparation. The molds are made with sand based on a mixture of clay sand. The cores were made in the core box with core sand. In the end, the assembly of different parts and cores conform to the cavity. Figure 5 shows the components of the molds, the feeder system (pouring cup, sprue and sprue well, riser, runner, gates), and mold cavities.
 - d. Melting: the aluminum is melted in a furnace, ensuring it reaches the desired temperature for casting.

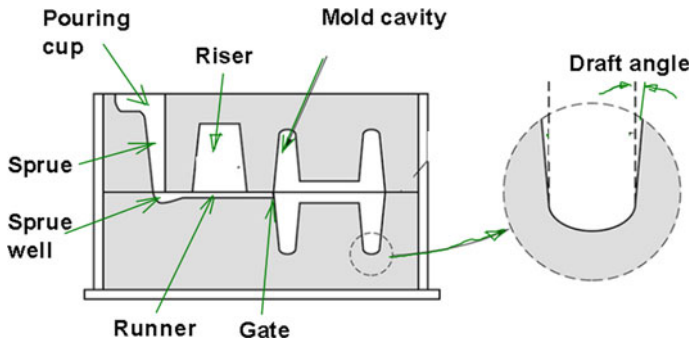


Fig. 5 Sand mold components

- e. The cooling time is controlled to ensure proper solidification and minimize defects such as porosity or shrinkage.
 - f. Shakeout and cleaning: once the piston has solidified, it is removed from the mold by shaking or vibrating the mold.
- Manual machining process: the manual turning planning process for a casting piston involves several steps to ensure accurate CNC machining operations. Here is a general overview of the process:
 - a. Select the manual Pinacho lathe. It must consider factors like manual chuck size, spindle speed, cutting tool capacity, and the ability to accommodate the casting part securely.
 - b. Analyze the machining operations needed to achieve the preform to machine in the CNC lathe. Determine the best way to hold the casting part securely during the post-CNC turning operations. Tool and cutting conditions selection. These parameters include cutting speed, feed rate, and depth of cut.
 - c. Deburring feeder system and turning feeder to use for clamping the part in the CNC machine.

Figure 6a shows the result of the casting process. Figure 6b presents the deburring process to remove the feeder system and, in Fig. 6c, the manual turning to obtain the CNC preform is presented.

- CNC turning process: the piston requires additional turning operations to obtain the outer and inner dimensions. The output of this process is the document that contains the phase (different machines) the sub-phase (change of fixturing), the sequential operations, sketches of operations, used tools, and process conditions (cutting speed, feed per flute, and revolution and axial depth). For instance, the CNC turning process-planning sheet could be shown in Fig. 7. In this document, the numbering of the sequential operations is indicated, considering the clamps (indicated as different sub-phase). Moreover, the different operations, the tools and their ISO geometry, and, finally, the cutting conditions are also presented.

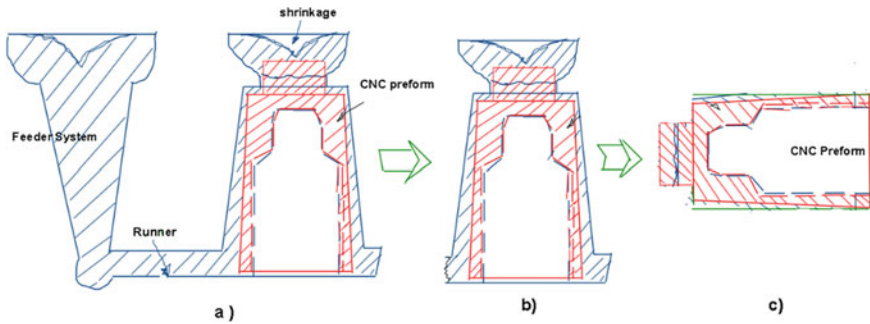


Fig. 6 Manual machining of casting process. **a** casting result, **b** deburring feeder system. **c** turning of CNC preform

- The process sheet made by the group of students is shown in Fig. 8. In the process sheet, it should be noted that there are four sub-phases, meaning four changes of origin. This is due to using a CNC milling machine with only three axes (xyz). In each sub-phase, the setup for positioning the workpiece and taking offsets is performed, which must be added to the additive code in CNC Fagor 8065, G158, to translate the machine origin (G54) and align it with the workpiece origin in the CAM program. The four sub-phases consist of the head piston facing, the two grooving operations on each side of the hole seat and, finally, the machining of the inner planes. In each operation, the tool and cutting conditions, which include cutting speed, feed per revolution, axial and radial depth of cutting are indicated.
- Quality control and inspection (Fig. 9): in this case of study, the quality inspection of the casting process has been visual. In the case of the machining process, this stage of inspection sheet planning is the final step in process planning. According to the experience gained over the years, very few groups of students manage to stay within the course schedule because they get lost in the details and start wanting to manufacture directly without planning the inspection. In this case, the instructor prepared the sheet. This phase involves a dimensional, and geometrical checklist and is documented in the quality and verification sheet.

6.4 Execution of the Casting Process

Initially, the group discusses the process of casting and the way they need to resolve the different activities to make the mold. The guidance of the instructor helps students to identify the following parameters to design the pattern, the feeder system, the core and the core box. These main parameters are:

- Solid contraction of the aluminum of 6.7%.
- Machining allowances of 5%.
- Draft angle of the pattern according to EN 12,890 (EN 12890 2000) of 2°.

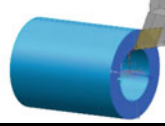
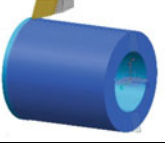
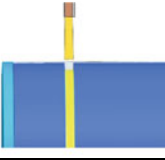
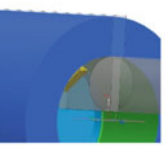
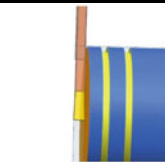
Numbering			Operation sequence	Tool geometry	Cutting conditions			
N Process			Part Piston	Material	Aluminum			
Phase	SP		Description	Sketch	Tool	Vc (m/min)	fz (mm/rev)	ap (mm)
CNC Lathe	Clamp from Machined riser	0	Setup	Preparation of casting preform. Position in machine, and selection of origin				
		1	Facing		T3. DNMG 150404	190	0.15	1
		1,1	Roughness machining					
		2	Turning		T3. DNMG 150404	190	0.15	0.5
		2,1	Roughness machining					
		2,2	Finishing machining					
		3	Grooving ring groove x 2		T3. DNMG 150404	190	0.15	2
		3,1	Roughness machining					
		3,2	Finishing machining					
		4	Interior turning		T10 TCMT 090204	150	0.10	0.5
		4,1	Roughness machining					
		4,2	Finishing machining					
		5	Cutting		T11. N151.2 -400	120	0.08	30
		5,1	Cutting					

Fig. 7 CNC turning planning process sheet

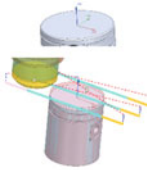
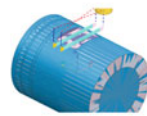
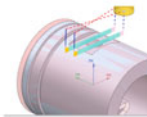
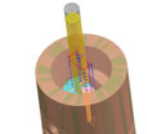
N Process			Part Piston Drawing N		Tool			Material Aluminum							
Phase	SP	O	Description	Sketch	Type	Ø mm	flutes	Vc (m/min)	fz (mm/rev)	ap (mm)	ae (mm)				
CNC Milling	Clamp 1	0	Setup		Comparator. Position in machine.										
		1	Facing												
		1.1	Roughness		T2 SEE13T3	50	4	250	0.15	1	50				
		1.2	Finish									250	0.08	1	50
	Clamp 2	2	0 Setup		Selection of origin										
		2	1 Groove_1		T11	12	4								
		2.1	Roughness					150	0.1	0.8	12				
		2.2	Finish					150	0.06	0.4	12				
		2	3 Drilling		T21 Drill	9.9	2	45	0.15	0.15	9.9				
		2	4 Reamer		T22 Reamer	10	6	50	0.1	0.05	10				
	Clamp 3	3	0 Setup		Selection of origin										
		3	1 Groove_2		T11	12	4								
		3.1	Roughness					150	0.1	0.8	12				
		3.2	Finish					150	0.06	0.4	12				
	Clamp 4	4	0 setup		Selection of origin										
		4	Interior milling		T16	8	2								
		4.1	Roughness					50	0.08	0.6	0.3				
		4.2	Finish					50	0.05	0.4	0.3				

Fig. 8 Process sheet of CNC milling process of manufacturing of piston

- The feeder system consists of an initial cone, channels, three gates, and a feeder to prevent shrinkage in the piston.

Design of pattern, cores, box cores and feeder system.

The students design the pattern in the PLM platform, considering the parting line of the mold and the recommendations of the instructor. Figure 10 depicts the result of the pattern design.

The design of the core is made using a boolean operation for removing an internal cylinder within the piston. The dimensions must be increased the 6.7% of shrinkage. The core box is created by removing the core from a cylinder and parting by a plane that contains the central axis (Fig. 11).

The next step is to design the feeder system that is composed of the riser, pouring cup, runners, and gates. Moreover, all the parts need to be properly assembled with the pattern.

The function of the riser is to feed the part and avoid shrinkage. Thus, the time to cool the riser must be greater than the time for the solidification of the part.

Chvorinov’s rule allows for estimating the time required for solidification in the casting processes. It assumes that the solidification time is proportional to the square

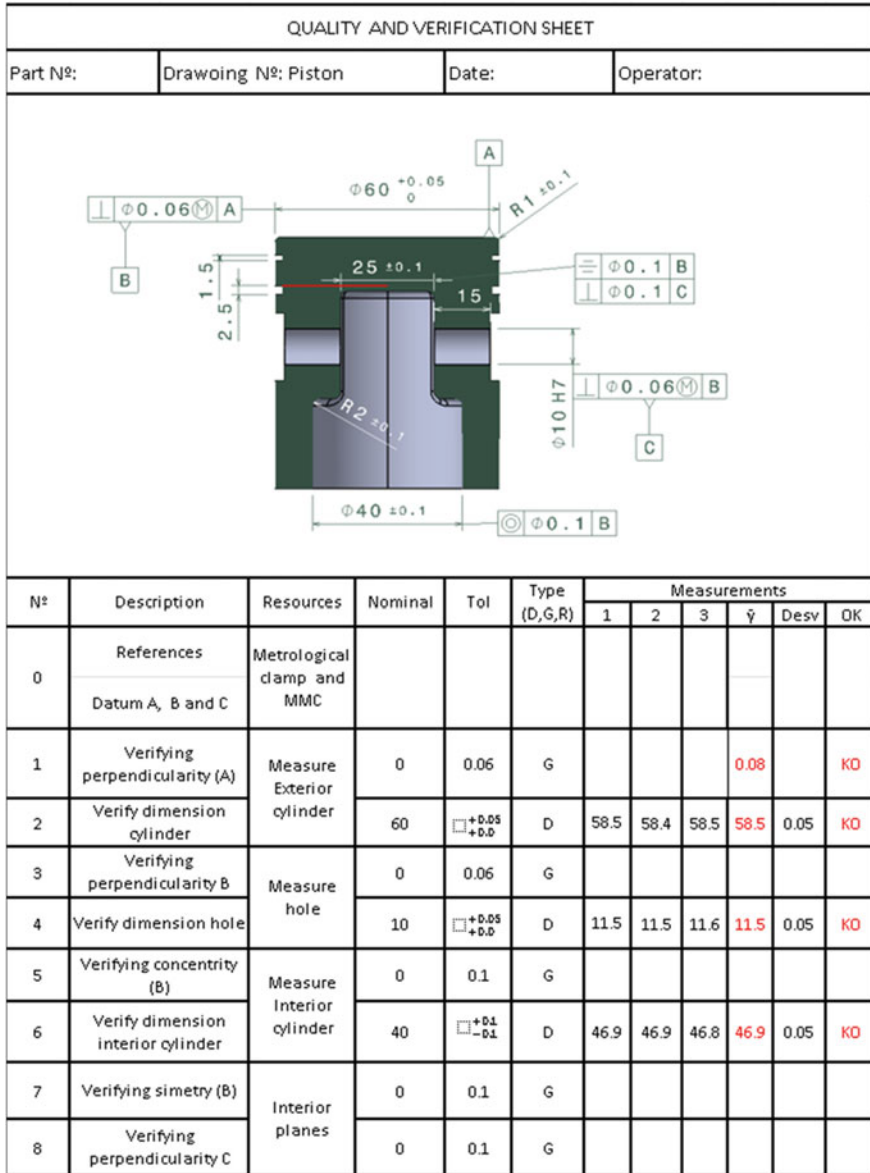


Fig. 9 Quality inspection process sheet of the piston

Fig. 10 Design of pattern

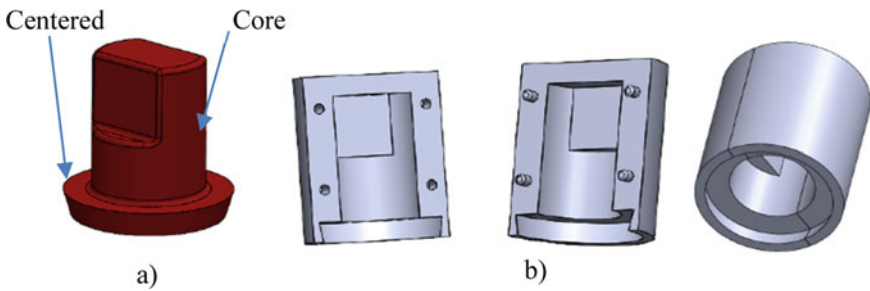
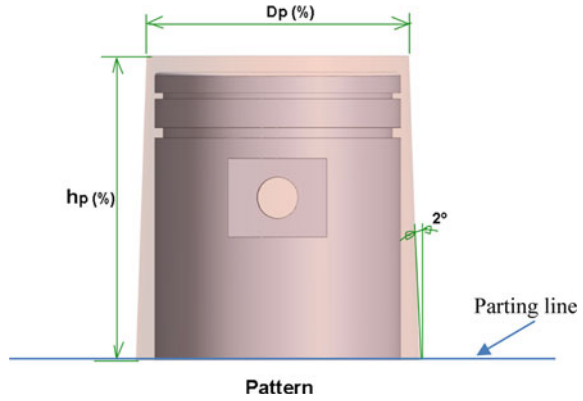


Fig. 11 a Core 3D, b core box

volume-to-surface area ratio of the casting. The formula for Chvorinov’s rule is as follows:

$$t_s = K \left(\frac{V}{S} \right)^2 = KxM^2 \tag{1}$$

where:

t_s = solidification time, min.

V = volume piston, cm^3 .

S = surface of piston, cm^2 .

K = Empirical constant, min/cm^2 . For aluminum, K is equal to $3 \text{ min}/\text{cm}^2$.

M = Thermal module, cm.

The module of the riser must be greater than the module of the part. A semispherical riser was chosen and the volume and surface of each one has been obtained as shown in Fig. 12.

$$M_p (\text{piston module}) = 133 \text{ cm}^3 / 273 \text{ cm}^2 = 0.49 \text{ cm.}$$

$$M_r (\text{riser module}) = 55.6 \text{ cm}^3 / 86.9 \text{ cm}^2 = 0.64 \text{ cm.}$$

Then $M_r > M_p$.

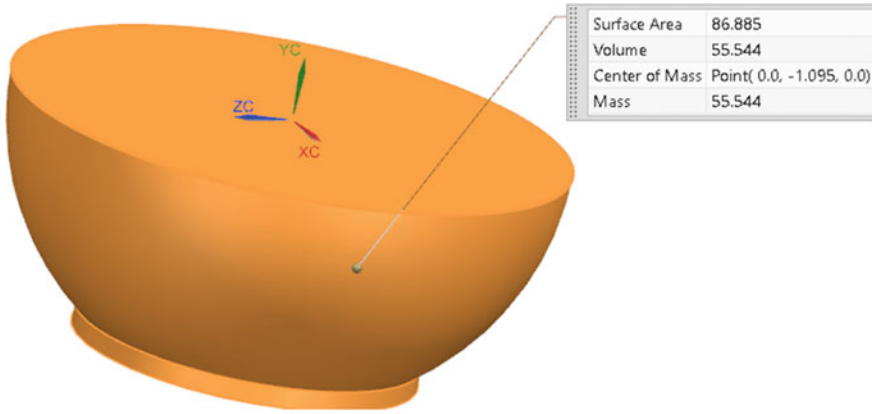


Fig. 12 Measurement of surface and volume of riser design

To know the minimal section of the sprue (S_s) using the flow rate (F) of the molten material must be calculated using Eq. 2.

$$F = \frac{V_m}{t_s} = \alpha \times v_s \times S_s \quad (2)$$

$$S_s = \frac{V_m}{t_s \times \alpha \times v_s} = \frac{F}{\alpha \times v_s} \quad (3)$$

where:

F = flow rate.

V_m = molten volume.

α = fluid pressure loss.

v_s = speed of molten fluid at bottom sprue.

S_s = section of the sprue.

To calculate the speed of the molten fluid, the height of the sprue must be known. Then:

$$v_s = \sqrt{2 \times g \times h} \quad (4)$$

where:

v_s = speed of molten fluid at bottom sprue.

g = gravity.

h = height of sprue.

As it can be shown in Fig. 13, the total height is $h = h_1 + h_2 = 100$ mm.

The calculations are shown in Table 1 considering the Eq. 3 and Eq. 4 and the minimal section of sprue $S_s = 8$ mm².

In this case of study, according to Campbell (Casting Practice, 2004), recommendations for defining the feeder system from the sprue section S_s/S_s : S_r/S_b : $S_g/$

Fig. 13 Height of sprue

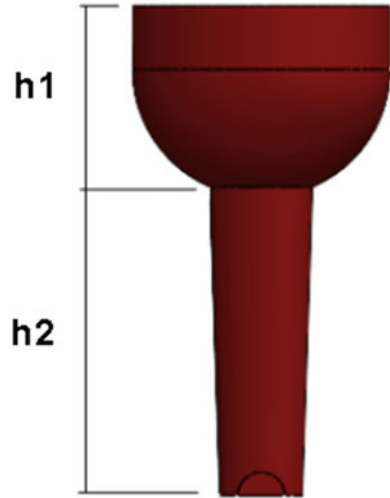


Table 1 Calculation of the feeder system

	Sprue	Piston	Riser
Volume (cm ³)	4.4	133.0	55.6
Surface (cm ²)	20.0	273.0	86.9
M (cm)	0.22	0.49	0.64
K (min/cm ²)	3.00	3.00	3.00
Ts (min)	0.15	0.71	1.20
H mean (mm)	100.0		
Speed (m/s)	1.4		
Flow (cm ³ /min)	264.8		
Section (mm ²)	8		
Ø Circular (mm)	3		

Sb: Sg/Sb, the ratios are assumed to be 1:2:2. Thus, the running section, at least, will be double the one of the sprue and the gate section are double of the sprue section.

Figure 14 shows the complete feeder system, pattern and riser needed to create the molds.

The parameters selected used to design the feeder system are shown in Table 2.

Feeder system, core box and pattern construction by additive manufacturing

The methodology to manufacture the parts is shown in Fig. 15. The software used to create the 3D file is the PLM platform and, according to the recommendations of the instructor, the students must save the file using the 3mf format. The group of students apply this methodology to all the parts of the feeder system. In this guide, only the process with the core box is presented.

Fig. 14 3D Feeder system, pattern and riser

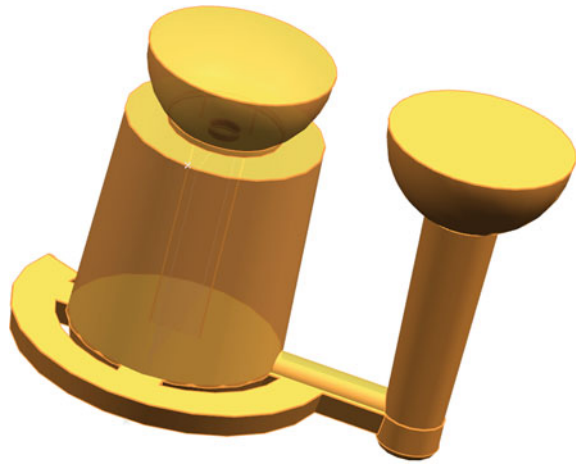


Table 2 Parameters design of feeder system

	Sprue	Runner	Gates
Maximum Ts (min)	0.71		
Speed (m/s)	1.4	0.7	0.7
Minimal section (mm ²)	8	16	16
Minimal Ø diameter (mm)	3	6	6

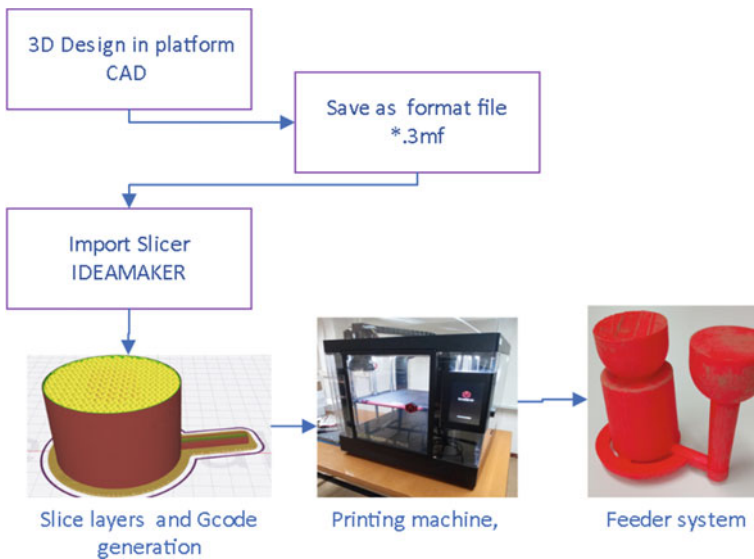


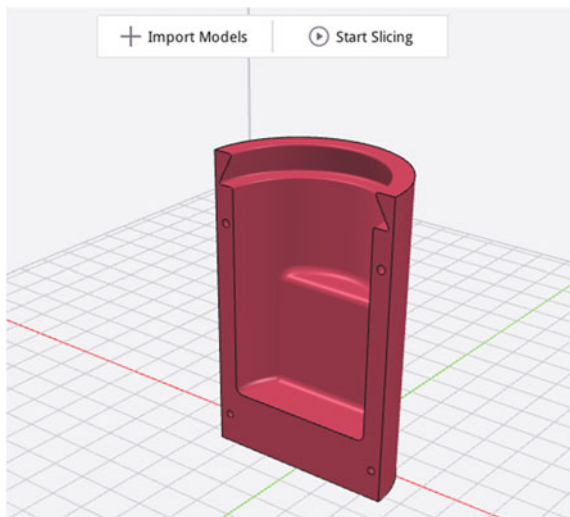
Fig. 15 Methodology to manufacture the feeder system

Figure 16 shows one-half of the core box and the macro to show the way to export the format and the control parameters, such as chordal and angular tolerances. The 3mf file is imported into the slicer program. In this specific project, students used the IDEAMaker software, from the company RAISE, but it is possible to use other slicer programs like Prusa, Cura, Orcaslicer, etc. The next step is positioning the part to be printed with minimal support requirements, especially for horizontal walls. By doing so, the printing process becomes more efficient and may result in better print quality. Figure 16 shows the positioning of the core box part. Before inserting the part, the CAD file must be converted to a format allowed by the slicer, such as stl, or 3mf, as shown in Fig. 17. In this macro of NX it is possible to introduce parameters of quality (chordal and angle tolerance) of the format file 3mf.

When slicing a pattern file there are several important parameters to consider. Some of them appear in the window when starting to slice:

- Layer height: it determines the level of detail and smoothness of the final print in the Z axis. Smaller layer heights generally result in higher quality prints, but they increase printing time. In this case, the layer height was 0.2 mm.
- Printing speed: this parameter determines how fast the extruder moves while extruding the filament. The recommendations of the instructor are using 50 mm/s as the default speed, and less speed of 25 mm/s for the outer and inner shells.
- Infill density: it provides structural support, and it can be adjusted to optimize strength or reduce material usage. The percentage used was 20%.
- Infill patten type: the selected infill pattern has been the gyroid type. It is characterized by a complex lattice-like design that resembles a series of interconnected tubes or tunnels. It has unique properties, including high strength and lightweight characteristics.

Fig. 16 Import and positioning file corebox.3mf



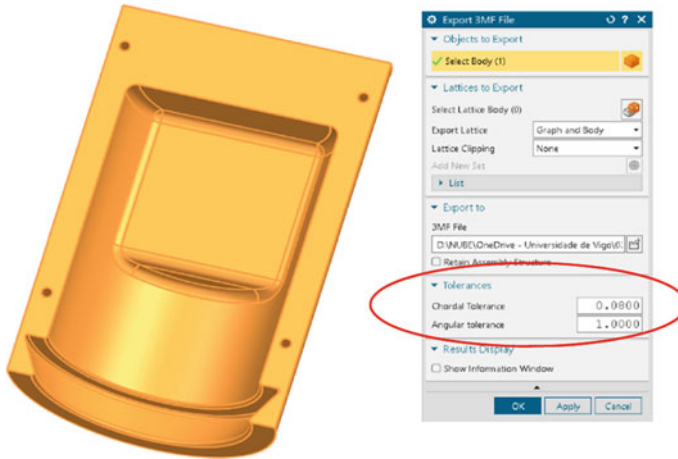


Fig. 17 Export 3D CAD format to “3mf” format

- Support structures: if the pattern file contains overhangs or complex geometries that cannot be printed without support, enabling support structures is crucial. These structures provide temporary support during printing and are usually removable after printing is complete. In this case, there is only touch platform support.
- Bed and extrusion temperature: this parameter depends on the filament material. The students chose PLA filament, and the printing temperature is 205 °C. The recommended bed temperature is 60 °C.
- Print orientation: the orientation of the object on the print bed can affect print quality, strength, and the need for support structures. In this case, it is taking account of the initial positioning.
- Cooling: cooling settings control the fan speed or airflow during printing.

Figure 18 shows the macro where all the parameters are selected.

Figure 19 shows the preview, where it is possible to see the different layers and positions of the extruder, according to the gcode program. It can be noted the gyroid infill pattern, the outer thickness, and the skirt that indicates the extension of the part and base support.

The mold preparation and melting once the feeder system has been manufactured by additive manufacturing, the next step is to prepare the cope and drag parts of the mold. The cope is made as shown in Fig. 20. First, it is required to position the frame mold over a table. The second step consists of positioning the pattern and the feeder system. Then, it is time to prepare the mixture of sand with clay and water and start filling the mold with the positioning patterns (Fig. 21). The sand is then left to dry and the patterns are removed, depending on their angle of exit. This is the justification for splitting the pattern and the riser because each part has a different exit angle.

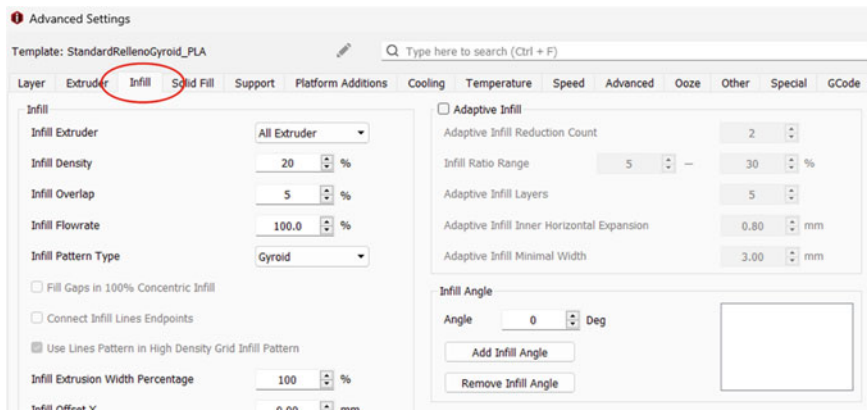


Fig. 18 Advance settings of Ideamaker slicer software

Fig. 19 Preview of the layers of the gcode program

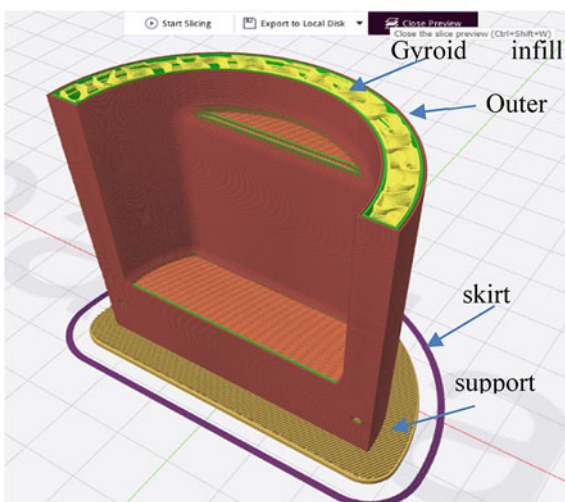


Fig. 20 Manual compression of sand



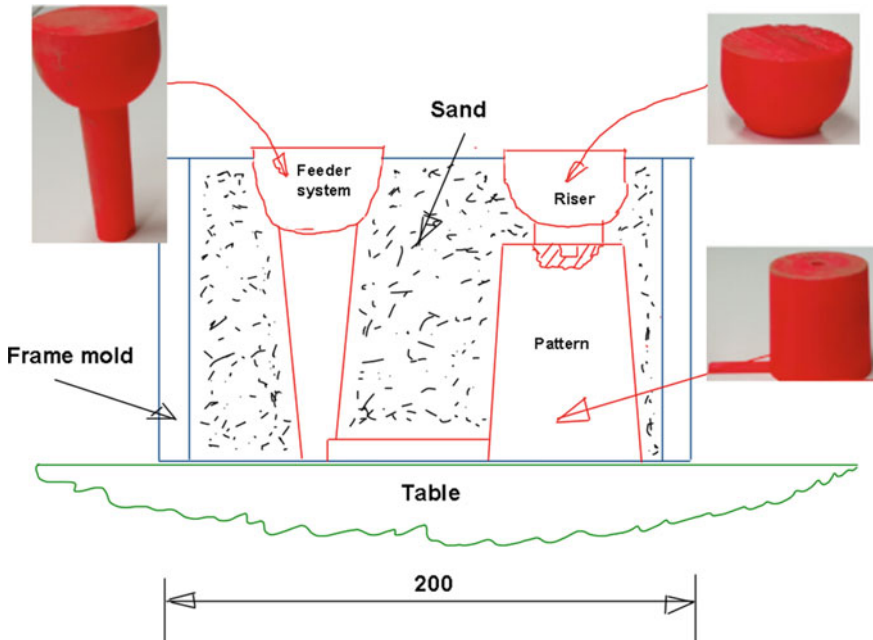


Fig. 21 Cope mold mounting

The drag part is made the same way but only with the sprue well, runner, and gates. Figure 22 shows the three parts of the mold, the cope, the drag without the patterns, and the core box filled with core sand. Core sand is a mixture of sand and a binder material, such as resin to create cores in metal casting processes. Here is a general outline of the core sand production process: high-quality silica sand is used and the binder material used is resin in proportion to three parts of resin and one catalyst. After assembly of the mold, the mold was left to dry for 48 h.

The next step is to heat the pot with the aluminum material inside the furnace to a temperature of 700 °C. Figure 23 shows the process of heating the aluminum and the melting process into the mold.

Shakeout and cleaning

After waiting for the required cooling time, the next step was the shakeout and cleaning of the casting. The sand of the core was hard and needed special cleaning operations. Figure 24 shows the result of the casting process.



Fig. 22 Drag, core box, and inferior cope

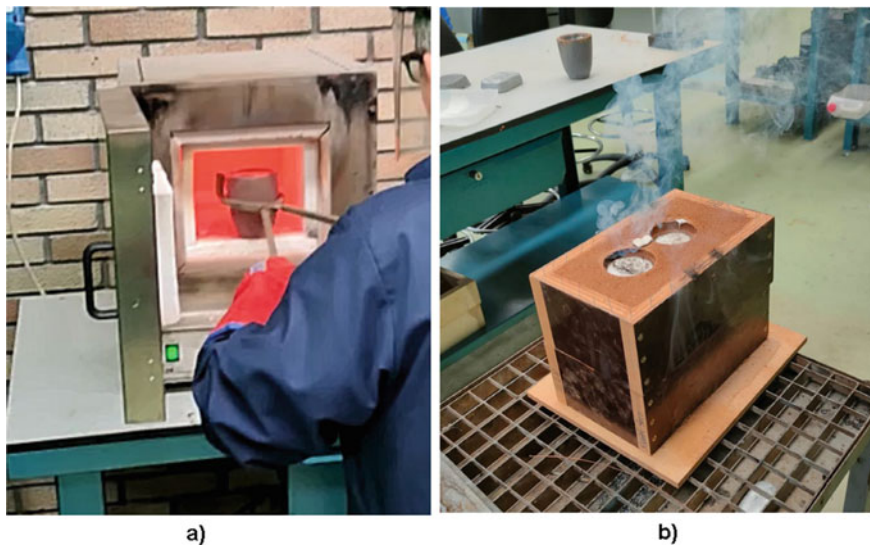


Fig. 23 a heating of pot with aluminum. b Aluminum melted into the mold

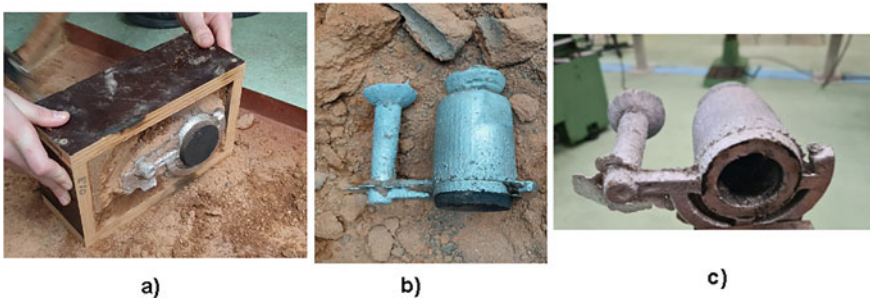


Fig. 24 Result of casting process **a** into the frame mold, **b** with the core, **c** the casting result without sand core

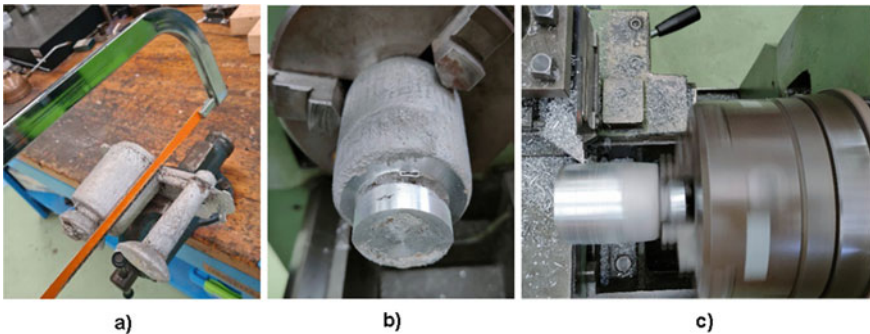


Fig. 25 Manual machining processes **a** sawing the feeder system **b** turning riser **c** rough turning piston

6.5 Conventional Machining Process

The manual operations (Fig. 25) performed include, firstly, removing the feeder system by sawing through the workpiece entry door and, secondly, turning the riser and performing the initial turning to prepare the workpiece for the CNC turning stage.

6.6 CNC Machining Process

The CNC machining process includes CNC programming on the Siemens NX platform, both turning and milling. The instructor has given the methodological indications of CAM programming, which include the following activities to be carried out by the group according to the process planning. The CNC process in NX CAM software involves the following steps:

- **Geometry import:** the initial step is to import the 3D model, from Catia V5, into NX CAM. The students need to select the machining origin and select the raw material and part to machine.
- **Tool selection:** the group chooses the appropriate cutting tools from the available tools in the machines (CMZ 450TBI and Microcut CNC), considering factors like tool diameter, length, and tool material.
- **Toolpath generation:** NX offers a range of toolpath strategies such as contouring, pocketing, and drilling. The students must select the appropriate strategy based on the part's geometry and machining requirements.
- **Parameters setup:** the user defines various parameters such as feed rate, spindle speed, axial and radial depths of cut, and stepovers to optimize the process.
- **Toolpath simulation:** before machining, the software simulates the toolpath to detect any potential collisions or issues that may arise during the process, ensuring safe and efficient operations. The user reviews the simulated process and makes necessary adjustments to optimize machining.
- **Post-processing:** once the toolpath is generated and validated, the software generates machine-specific CNC code, commonly referred to as G-code, which is tailored to the specific machine controller. One of the advantages of NX is that it offers the possibility to create and modify the postprocessor using the postprocessor generator module. In this case, the instructor modifies the postprocessor for a lathe with a CNC Fagor 8055 control and modifies the postprocessor for the milling machine with a CNC Fagor 8065.
- **Output and execution:** once the CNC program is completed, it can be transferred to the CNC machine for execution. First, the instructor or the machine operator places the billet in the appropriate position and establishes the origin according to the programming part origin. After that, the operator must run the simulation in the CNC machine and, finally, execute the program.

CNC turning

Figure 26 shows the CAM programming of the internal turning operation, according to the planning process (operation 4.1, in Fig. 7).

After CAM programming and considering the preparation of the manual turning result, the post-processed programs are executed in G format. In the same program, the facing, turning, and grooving operations of the ring seats are carried out. Figure 26

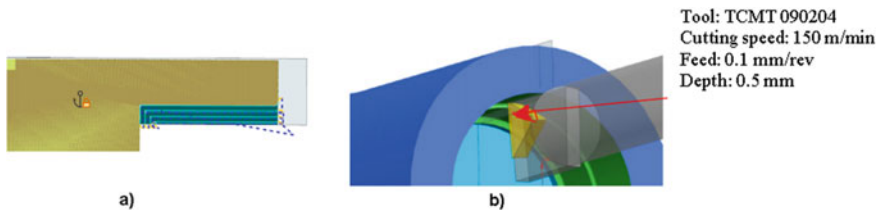


Fig. 26 a NX Cam programming of interior turning. b details of the simulation of the internal turning

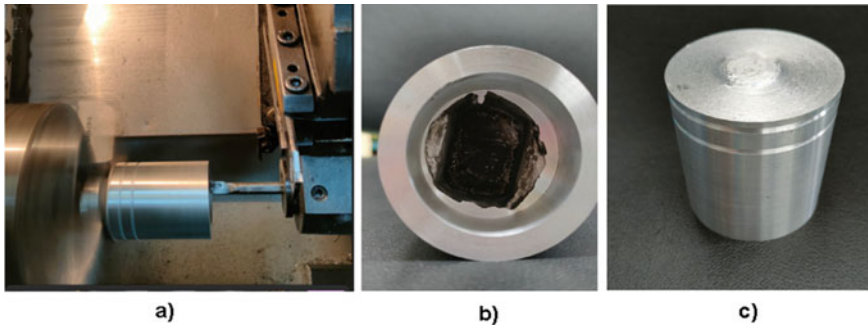


Fig. 27 a) CNC internal turning with tool TCMT090204 b) internal result c) CNC turning result

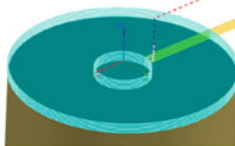
shows the results of the CNC turning phase (CMZ 450TBI lathe). Figure 27a shows the internal turning operation in progress. In Fig. 27b the result of this operation can be seen. In Fig. 27c the part can be seen at the end of the CNC turning operations.

CNC Milling

After obtaining the turned part, the part was moved to the CNC milling, three-axis Microcut CNC machine. In this new stage, it is required to perform 4 sub-phases, six operations in total. These operations, according to Fig. 8, include planing, grooving, drilling, reaming, slotting, and internal milling. The starting point was a height of 70 mm at the highest part and 60 mm of external diameter. The part was positioned using V-bearing and gauges.

Figure 28 shows the procedure followed in the CNC milling process, in which CAM programming has been carried out, as shown in Fig. 28a). Once the CAM program has been post-processed, it is sent to the machine, and the part is positioned, centered in clamps, using a dial gauge to find the center (Fig. 28b). Figure 28c) shows the finished part at this stage.

Facing Tool with 4 inserts
SEE13T3
Cutting Speed : 250m/min
Feed: 0.15mm/rev
axial depth: 1mm
radial depth: 30mm



a)



b)



c)

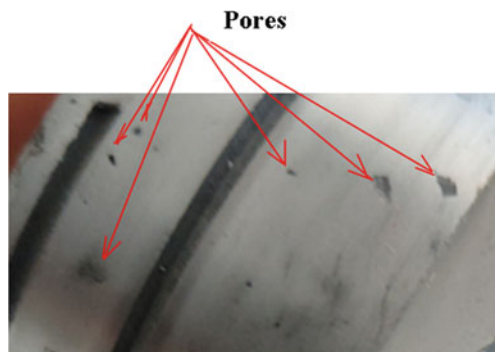
Fig. 28 a) CAM programming of facing operation b) positioning of piston with V-blocks c) result of CNC milling process

6.7 Inspection Process

According to the indications mentioned above in the process planning (6.3) the students have included a qualitative visual inspection for each of the processes, the results of which are as follows:

- Casting process.
 - Failure of sand loosening in the core, after the extraction from the core box. This failure was attempted to be corrected with clay backfill.
 - Failure of dimensions in the piston head, with not enough material for machining. The recommendation to solve this problem was to decrease the functional dimensions by two millimeters.
 - The interior of the casting was not concentric to the external diameter due to an error in the positioning of the core. To solve this problem, it was centered by the manual and CNC turning processes.
- Machining process:
 - The surface finish of the head was rough after cutting the riser. It was recommended to solve in the CNC facing milling process.
 - After facing and turning some pores appeared in the exterior surface of the piston as can be seen in Fig. 29.
 - No suitable 1.5 and 2.5 mm wide grooving tools were available on the CMZ lathe to make the ring seats. To resolve it, a 1 mm deep indentation was made with a T3 DNMG150404 tool.
 - An 11.5 mm tool has replaced the tool for the 2.3 drilling operation in the CNC milling process because there was no tool of the corresponding diameter mounted on the machine.
 - The 2.4 reaming operation, also in the CNC milling process, was not carried out because the corresponding reamer was not available.
 - The internal milling (4.4 operation in Fig. 8) of the side walls was not carried out because there was no 8 mm tool available in the Microcut center with the

Fig. 29 Exterior surface of the piston



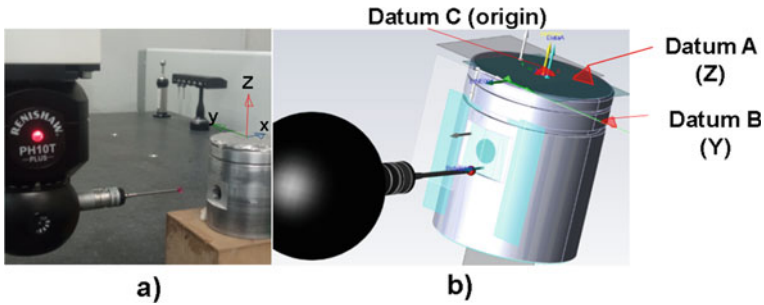


Fig. 30 a Part positioning and alignment b datums obtained for alignment

necessary 55 mm long overhang without interfering with the upper surface of the piston.

Qualitative measurements of dimensions, tolerances, and geometric dimensions have been planned, according to the instructor's initial specifications and recommendations. The instructors carried out the measurements using the CMM (Nikon Altera 15-7-6 CMM), following the quality and inspection sheet (Fig. 9).

The main steps in the methodology for CMM measurement are the following:

- **Alignment:** fixtures ensure stability and repeatability during measurement. In this case, there is only one prototype, so the methodology uses the conventional plane A (head of the piston), line B (projected hole support plane on Plane A), and point C alignment strategy (intersection of the axis of external cylinder with plane A), according to the datums A, B, C in the inspection sheet. Datum A, as a head plane is measured with 4 points, Datum B, in this case, is the line projected of the support plane of the hole, and C is the projection of the axis of the external cylinder measured with 10 points. Figure 30 shows the positioning of the piston and the alignment in the software CMM Camio.
- **Measurement execution:** Once the measurements are made, for instance, the diameter from the external cylinder is obtained. The measure of the cylinder of the hole is made with 10 points and the diameter established on the sheet can be obtained using the CMM.
- **Verification and reporting according to the inspection sheet:** validate the measurement results by comparing them to known reference values. Figure 31 shows some measurements out of tolerances. The software Camio can make the report according to the requirements of the control quality sheet. Figure 32 shows this report.

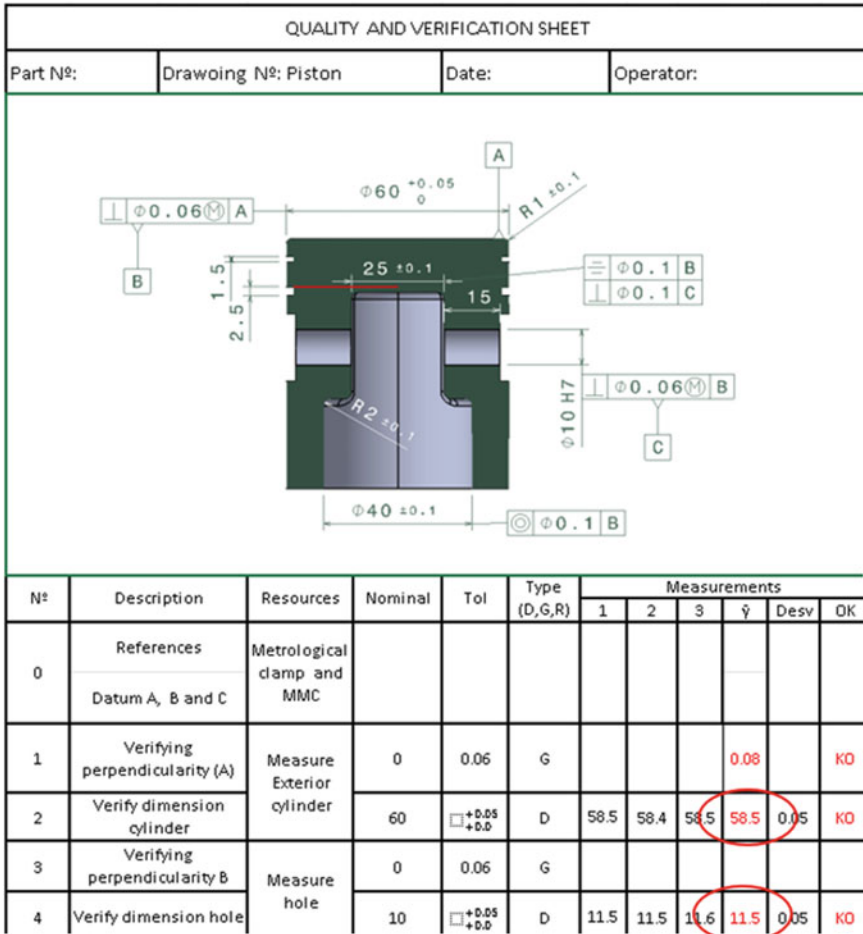


Fig. 31 Inspection sheet with measurements and nonconformities

7 Deliverables and Assessment

In the PBL projects, as shown in Fig. 1, the deliverables that the instructor must assess are the manufactured product, the documentation, and the oral presentation of the group. In this case:

The manufactured product: the objective of this deliverable is to evaluate the knowledge and abilities of the students. The assessment of the manufactured part counts for 40% of the total assessment. Many parameters can modify the assessment, for example, the creativity and level of innovation, the complexity of the part, the number of processes to manufacture the part, the number of parts to design, the different technologies, and the complexity of technologies. In this case study,

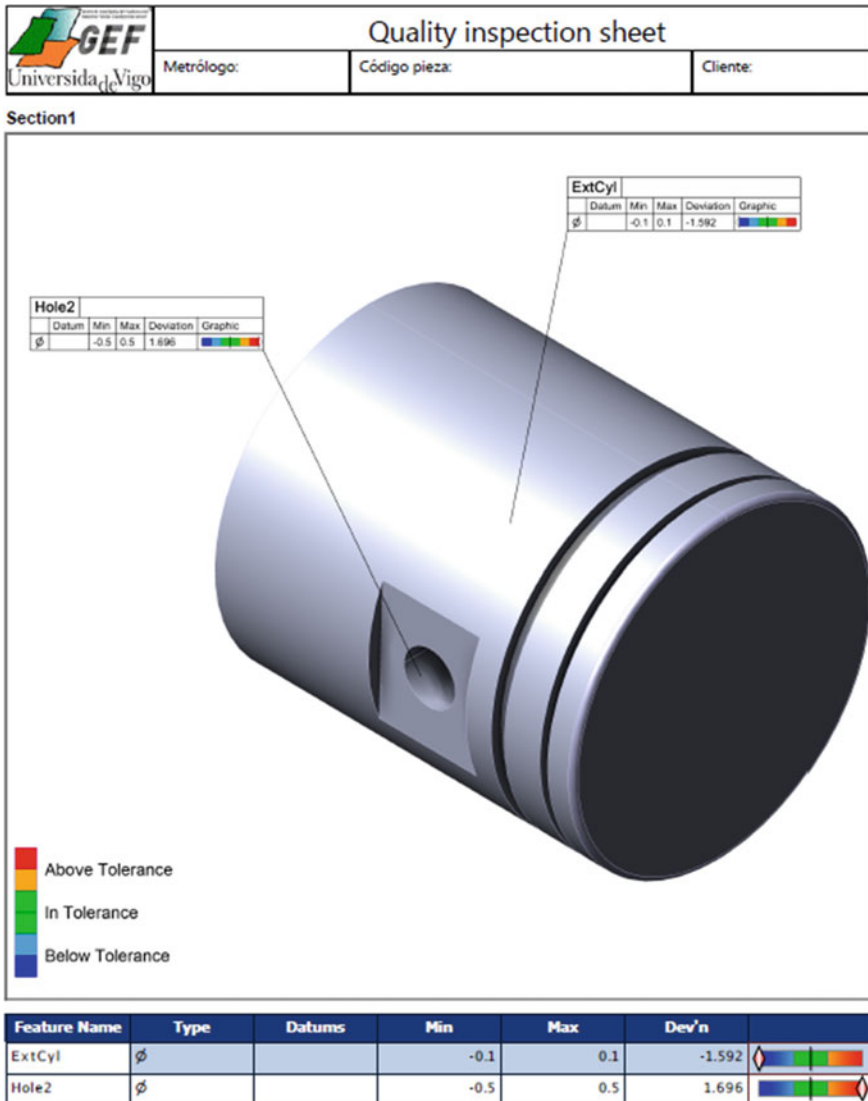


Fig. 32 Report made after the measurements in the Nikon Altera CMM, with Camio software

creativity is not an important parameter, nevertheless, there are many processes, such as casting, creation of molds, manual machining, CNC machining, and inspection process. The instructors, considering this case, have evaluated the manufactured object with a mark of 8 out of a maximum of 10. This evaluation is difficult because different projects are carried out by different groups and is therefore difficult to compare and assess, as some criteria must be qualitative.

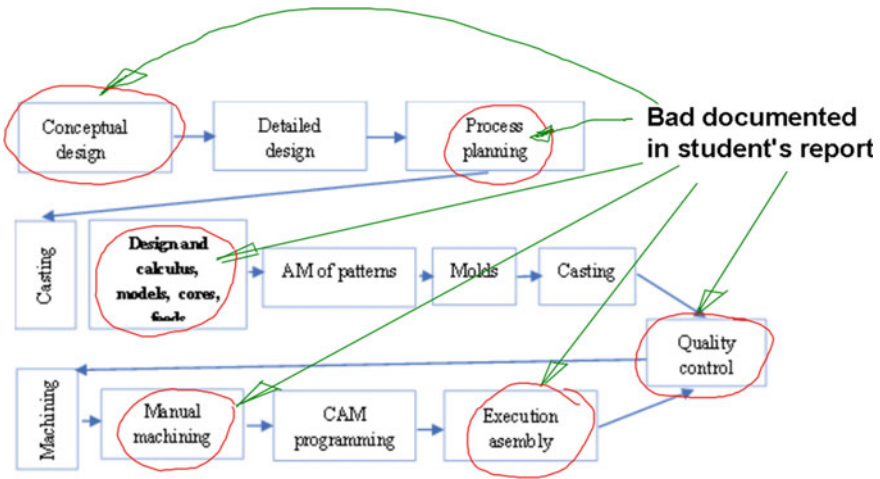


Fig. 33 Flow chart of development of project

The documentation contains the main report, the budget, and the drawings as shown in Fig. 1. The objective of this activity is to evaluate the student’s skills in creating technical documentation and explain the different techniques and calculations used. In this case study, the different steps of the report are shown in Fig. 33. Highlighted in red are the bad deliverables in this stage made by the group of students. In this report, the mark of the assessment was 6 (maximum 10). The assessment of the report counts for 40% of the total mark.

The final item of the assessment of the project of students is the oral presentation. It counts the 20% of the total mark. The instructors explained at the beginning of the project the importance of communication and the ability to synthesize to express the advantages and qualities of the work developed. The presentation should be developed in a maximum of 15 min, explaining the fundamental parts of the work developed. The instructors have 5 min to ask questions to the students in each group. In the academic year 2022–2023, the oral presentations have been recorded by the TV service of the University of Vigo (UVigo TV 2023). In this case study, the two instructors considered that it was a good presentation, but they forgot to show some parts such as the patterns and the core box to make the molds and core. The mark obtained was 8.

The final score of the students was equal to 7.2 (maximum 10).

8 Conclusions

The present chapter presented an example of Project-Based Learning (PBL) in manufacturing. All steps from conceptual design to quality inspection were introduced. PBL allows students to understand the complete manufacturing process from theoretical to practical aspects in an improved learning environment. Moreover, working in groups is also of great importance, not only for the quality of the learning process itself but also for acquiring general competencies that will be valuable for their future.

Acknowledgements The authors would like to thank the students of the case study group, Miguel Serantes, Brandon Otero, and David Moledo, for their commitment and activities. The authors are also particularly grateful for the participation of the workshop teacher, Alfonso Covela, who has always assisted the students and solved the problems that have arisen.

References

- Akay, D., Demiray, A., & Kurt, M. (2008). Collaborative tool for solving human factors problems in the manufacturing environment: The theory of inventive problem solving technique (TRIZ) method. *International Journal of Production Research*, *46*(11), 2913–2925.
- Angrisani, L., Arpaia, P., Bonavolontá, F., Moccaldi, N., & Moriello, R. S. L. (2020). A “learning small enterprise” networked with a FabLab: An academic course 4.0 in instrumentation and measurement. *Measurement (London)*, *150*, 107063.
- Ansaf, B. I. K., & Jaksic, N. I. (2019). *Teaching undergraduate manufacturing course using design-based teaching approach*. ASEE Annual Conference and Exposition, Conference Proceedings. Castings Practice. (2004). *The ten rules of castings*. John Campbell. Elsevier.
- Ellis, B. D., & Graveson, J. (2022). Teaching design and strength of materials via additive manufacturing project-based learning. *Advance in Engineering Education*, *10*(3), 19–5.
- EN 12890. (2000). *Founding—Patterns, pattern equipment and coreboxes for the production of sand*.
- Fernandes, F. A. O., Júnior, N. F., Daleffe, A., Fritzen, D., de Sousa, R. J. A. (2020). Integrating CAD/CAE/CAM in engineering curricula: A project-based learning approach. *Education Science (Basel)*, *10*(5), 125.
- Gatto, A., Bassoli, E., Denti, L., & Luliano, L. (2015). Multi-disciplinary approach in engineering education: Learning with additive manufacturing and reverse engineering. *Rapid Prototyping Journal*, *21*(5), 598–603.
- Jonassen, D. H. (2015). Engineers as problem solvers. In: *Cambridge handbook of engineering education research*.
- Konopka, C. L., Adaime, M. B., & Mosele, P. H. (2015). Active teaching and learning methodologies: Some considerations. *Create Education*, *6*, 1536–1545.
- Lamancusa, J. S., Zayas, J. L., Soyster, A. L., & John, S. (2008). The learning factory: Industry-partnered active learning. *Journal of Engineering Education*, *97*, 5–11.
- Lorenzo-Yustos, H., Lafont, P., Lantada, A. D., Navidad, A. F.-F., Sanz, J. L. M., Muñoz-Guijosa, J. M., Muñoz-García, J., & Otero, J. E. (2010). Towards complete product development teaching employing combined CAD-CAM-CAE technologies. *Computer Applications in Engineering Education*, *18*, 661–668.
- Pereira, A., Lastra, R., Acevedo, J. M., & Diaz-Cacho, M. (2022, March). *PBL strategy for learning maintenance engineering*. IEEE Global Engineering Education Conference, EDUCON 2022, pp. 1316–1321.

- Prabhu, R., Miller, S. R., Simpson, T. W., & Meisel, N. A. (2020). Complex solutions for complex problems? exploring the role of design task choice on learning, design for additive manufacturing use, and creativity. *Journal of Mechanical Design, Transactions of the ASME*, *142*(3), 031121.
- Sola-Guirado, R. R., Guerrero-Vacas, G., & Rodríguez-Alabanda, Ó. (2022). Teaching CAD/CAM/CAE tools with project-based learning in virtual distance education. *Education and Information Technologies*, *27*, 5051–5073.
- Standridge, C. R. (2000). Teaching simulation using case studies. In IEEE (Ed.), *2000 Winter simulation conference proceedings (Cat. No.00CH37165)* (Vol. 2, pp. 1630–16340).
- Stern, A., Rosenthal, Y., Dresler, N., & Ashkenazi, D. (2019). Additive manufacturing: An education strategy for engineering students. *Additive Manufacturing*, *27*, 503–514.
- Ubaidullah, N. H., Mohamed, Z., Hamid, J., & Sulaiman, S. (2021). Discovering the role of problem-solving and discussion techniques in the teaching programming environment to improve students computational thinking skills. *International Journal of Information and Education Technology*, *11*(12), 615–623.
- UVigoTV. (2023). *Presentación de Proyectos por estudiantes*. Tecnologías de Fabricación de EEI. <https://tv.uvigo.es/series/643fb3f1b5099d34f569bf13>. Accessed 14 December 2023.
- Vila, C., Ugarte, D., Ríos, J., & Abellán, J. V. (2017). *Project-based collaborative engineering learning to develop industry 4.0 skills within a PLM framework*. *Procedia Manufacturing*, *13*, 1269–1276.

Cavity Manufacturing of Curvilinear Shapes by EDM: Practical Application Through CAM Machining of Electrodes



José L. Diéguez  and Alejandro Pereira 

1 Introduction

In manufacturing studies within engineering, the integration of design and manufacturing is a critical activity. Moreover, the integration of open-source software into Electro Discharge Machining (EDM) and Computer Aided Manufacturing (CAM) processes has gained significant attention, providing manufacturers with accessible and cost-effective alternatives to proprietary software.

This chapter serves as a gateway to exploring the synergies between EDM, CAM, and open-source software, uncovering the immense potential they hold for enhancing manufacturing capabilities.

The primary objective of this chapter is to explore the integration of open-source software in the design of the EDM electrode and CAM processes to manufacture it. By examining the benefits, challenges, and potential applications, the objective is to provide valuable insights for manufacturers seeking to leverage these technologies.

The chapter is structured as follows. The first part is the introduction to the activity with a background of the problem, learning objectives, resources, and organization needed, how the sessions must be developed, the outcomes, and finally the deliverables and assessment of this practice. The second part is the development of the practice, starting with a free-hand design, the bitmap process, and its trace to obtain the initial CAD design. After the CAD design is validated, the CAM process begins to obtain a machined electrode valid to do the cavity in the EDM machine. Finally, it is possible to obtain the conclusions of this activity.

J. L. Diéguez (✉) · A. Pereira
Departamento de Deseño na Enxeñaría, Escola de Enxeñaría Industrial, Universidade de Vigo,
Vigo, Spain
e-mail: jdieguez@uvigo.es

A. Pereira
e-mail: apereira@uvigo.es

2 Background

Within the process of product development, to integrate into the current industry, a student must be able to master the processes that lead from a design to the creation of the first prototypes before the product launch.

The example proposed in this practice highlights the training in the creation of a first prototype based on an artistic design that will have to be machined in a mold through the EDM process. This allows training in graphic design processes, different machining processes, metrology, and material removal.

In the material removal processes, the excess material is removed in shaping operations that can be done in some different ways:

- Conventional machining is a mechanical cut of the material performed with a sharp cutting tool.
- Nontraditional machining uses other mechanisms to remove material involving electrical, thermal, chemical, or mechanical energy. EDM is one of the most popular thermal processes. Two types of EDM processes, die-sinking and wire EDM, are generally used in industry. In this chapter, focus is placed on die-sinking EDM.

In this practice, these two techniques that remove excess material are combined with the design process.

3 Learning Objectives

In this practice, students can learn to:

- Basics of processing images in bitmap format.
- Familiarity with solid modeling of workpieces.
- Vector graphic design fundamentals.
- Essential principles of parametric 3D computer-aided design (CAD) modeler.
- Acquaintance with computer-aided manufacturing methods.
- Development and design of tools and equipment to realize the machining process.
- Measurements and alignment rules.

4 Resources and Organization

To carry out the practice, the following resources will be used:

- Software: always free and open-source computer programs:
 - GIMP, GNU Image Manipulation Program.
 - Inkscape, vector graphics editor.

- FreeCAD, a general-purpose parametric 3D CAD and CAM program.
- Laboratory equipment:
 - Desktop scanner, digital camera, or mobile phone.
 - CNC vertical machining center.
 - EDM machine.
 - Lathe.
 - Tools and fixtures.

The organization of this session is as follows:

- Individual work to carry out the first steps for designing and manufacturing.
- Two groups to develop the machining process:
 - One group will use the CNC vertical machining center.
 - Another one will work in the EDM machine.

The last two sessions will be developed simultaneously; one group will mill the electrode, while the other works in the EDM machine, and in the next session, the roles of the groups will be changed. The time will be two hours per practical session, working in a group of 20 students, divided into subgroups of 10.

5 Session Development

The development of the session includes several steps introduced by the instructor. Thus, the activity is a completely guided exercise in which the students will learn all the processes using a complete example. Following, the different stages are presented in detail.

5.1 *Initial Design Example*

The design chosen (Fig. 1) to illustrate the process corresponds to the RS (Racing Sport) letters. The sequence can be found in vehicles and it would require manufacturing a mold for plastic injection. The starting point is a freehand design made on a sheet of paper, but the design could also be obtained using reverse engineering from a photograph or scanning an existing design.

The design is a rough drawing and, thus, it is not the finished one. In this sense, it is the starting point for the image treatment that will be shown next. Each of the students will be asked to create a similar design to develop the following steps.

Fig. 1 Freehand design on paper



5.1.1 Bitmap Image Processing

For processing bitmap images, the GNU Image Manipulation Program (GIMP) software is used. GIMP is a free and open-source raster graphics editor that can be used for image manipulation (retouching) and image editing or free-form drawing.

To obtain the image, a desktop scanner will be used. Using GIMP, an image is obtained using the following path: File > Create > Scanner/Camera.

The resolution used was 300 ppi due to it was not a demanding design. In any case, a “dirty” image is obtained (Fig. 2 up) that has to be polished to easily define what will be the paths of the tool in the machining process. One way to clean the image is to use the following: Tools > Selection Tools > Fuzzy Select.

All clear backgrounds were selected and the threshold was modified to select all gray points. In this case, a threshold of 60 for the maximum color difference on a scale between 0 and 255 is used. After the selection, “Del” allows cleaning the selected area. The next step will be to reverse the selection to delete the drawn area using: Select > Invert. It is needed to delete the drawn area with “Del”, obtaining a total blank drawing, but with the area drawn selected.

The next step will be to use the “Bucket Fill Tool” to fill in black the original hand-drawn design: Tools > Paint Tools > Bucket Fill. An opacity of 100% is used. The result is shown in Fig. 2 down.

In Fig. 2 down, it is possible to appreciate how the edge of the image is not perfectly defined. Options such as Erase, Select or Filters can help redefine the edge of the image. Now, the bitmap image is finished (Fig. 3) and can be exported to file formats such as JPG or PNG.

5.1.2 Tracing the Bitmap Image

To convert the bitmap image into a vector format and, therefore, be easily scalable, the Inkscape software is used. This software is a free and open-source vector graphics editor used to create vector images, primarily in the scalable vector graphics (SVG) format. Other CAD software will easily recognize this format.

The processing in Inkscape will be minimal. First, the JPG file is opened in Inkscape. Once the image is selected, the vectorization is performed by Path > Trace

Fig. 2 Images of the processing of the images: **Up** detail of the scanned image, **Down** detail of the preprocessed image

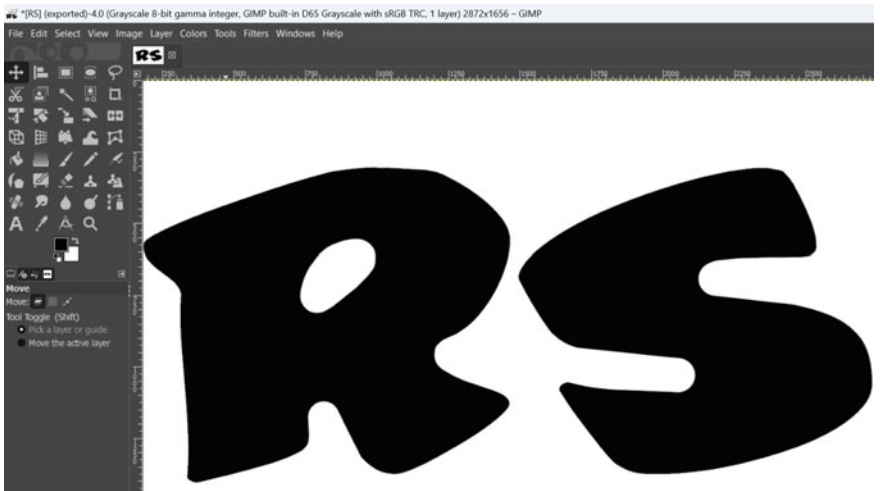


Fig. 3 Detail of the bitmap final design

Bitmap. It is possible to vary the threshold level, but because the image was created in black and white, there should be no problems in obtaining well-defined edges.

It is noteworthy to use the maximum of the Optimize parameter (5 in the scale) to try to optimize paths joining adjacent Bezier curve segments. This will reduce the number of curves. Now, the design is very large (Fig. 4) and needs to be reduced to fit the specifications of the cavity to be made.

Another parameter that may be interesting may be the “Smooth corners” to smooth out corners of the trace. Once you press “Apply”, you will have two objects, the original bitmap and the new object plotted as shown in Fig. 5.

The bitmap object is deleted and the plotted object is saved in the native Inkscape format, Scalable Vector Graphics (SVG). This image can be retouched in the Bezier curves, but to preserve the original design further changes will be minimal.

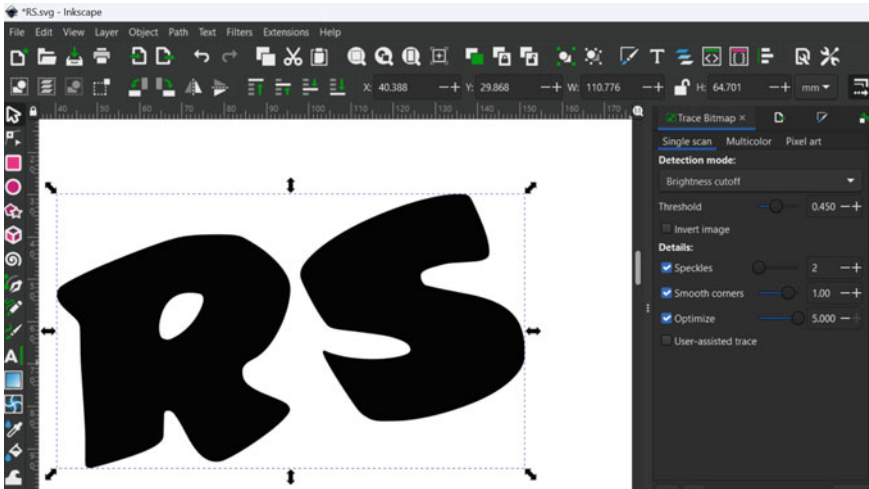


Fig. 4 Trace process on inkscape

Fig. 5 Two objects after the trace process



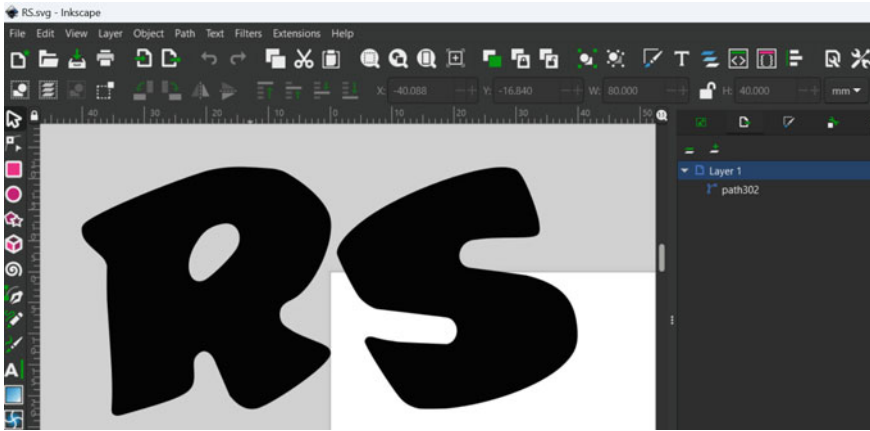


Fig. 6 Resize and move the objective to fit it close to the zero point

The image size is still very large. Thus, the values of 80×40 mm are applied, and it is placed with the center of the design in the top corner of the opened page. This point represents the 0.0 coordinate system used in the machining (Fig. 6). In this way, a first positioning of the design is done. By saving the SVG file and closing Inkscape, this stage is finished.

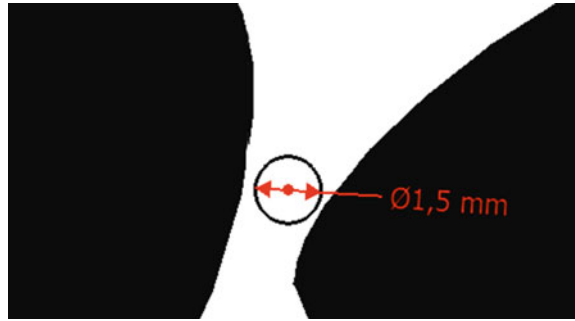
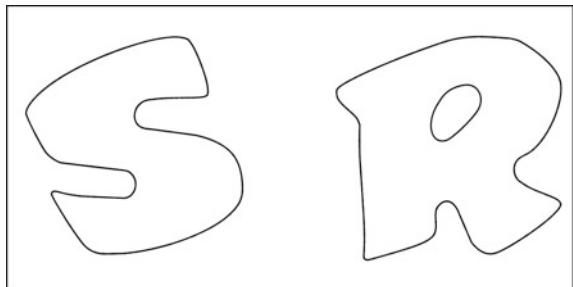
5.2 *Electrode Design*

5.2.1 **Determination of the Electrode Model**

A first consideration to discuss is whether one must perform the design to create a positive or negative (reverse image) part. To understand the problem, it is needed to reflect on the issue that a forward design produces a negative (reverse) cavity that requires a forward workpiece. Once this issue is solved, the following problems for the manufacturing of the electrode are encountered:

- The design is quite large, 20.4 cm^2 of the front surface, which limits the cleaning of the cavity during the EDM process.
- The two letters that are intended to be made are very close together, which makes it necessary to use a very small diameter tool to grind between the two. A cutter of approximately 1.5 mm is needed to remove the material between the two letters as shown in Fig. 7.

Based on the previous, the ideal solution would be to manufacture the two cavities separately. However, this solution would force to carry out two times centering procedures in the machine, for which reason the design depicting the two letters on

Fig. 7 Gap between letters**Fig. 8** Letters position

the same base plate is intended specifically to streamline the alignment process in the EDM machine to just one step as shown in Fig. 8.

The letters need to be inverted due to when the “R cavity” is performed, the “S” geometry will find no obstacles when descending and vice versa as shown in Fig. 9.

5.2.2 Die Sinking Restrictions

The EDM conditions influence the size of the electrode to be made since it is required reducing its size to compensate for the gap in the process. It should be considered that:

- The EDM machine is an ONA model Compact 2.
- A cavity with a 2.5 mm depth with the same electrode without performing a previous roughing operation will be made.
- The gap cleaning will be performed using an external flow.
- The electrode material will be electrolytic copper.
- The electrode is machined in a single process without subsequent polishing.
- The surface finish to be obtained corresponds to the N9 roughness grade number, which corresponds to $Ra = 6.3 \mu\text{m}$ (average roughness).

Considering the previous restrictions, the machine manufacturer’s manual (ONA, Tecnología Compact-2) offers the manufacturing conditions displayed in Table 1.

Fig. 9 Tool motions to create the cavities: **Up** first tool motion to create the “R” cavity, **Down** second tool motion to create the “S” cavity

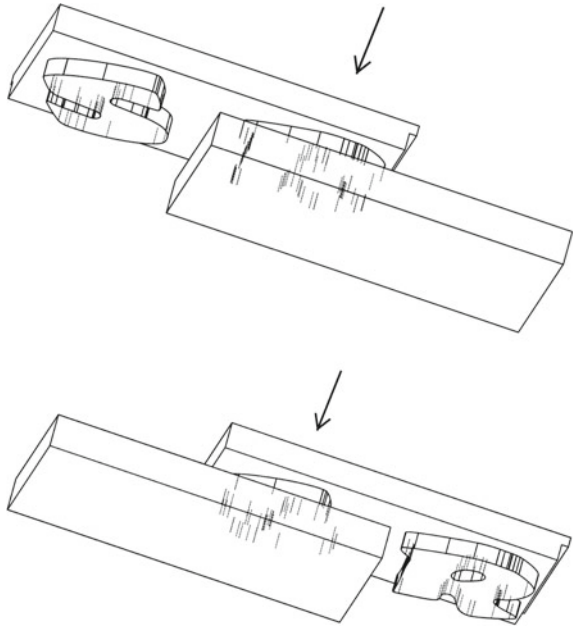


Table 1 Material removal conditions

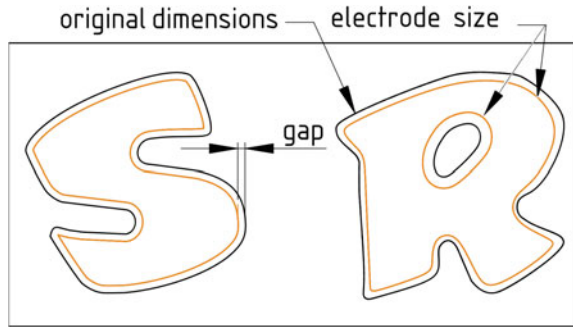
Parameter	Designation and units	Value
Impulse time	t_i (μs)	100
Pause time	t_o (μs)	10
Intensity	I (A)	10
Voltage	V (V)	200
Gap	G (μm)	105
Electrode wear	V_e (%)	0,6
Material removal rate	V_w (mm^3/min)	51

At this stage of the electrode design, the value of 105 μm is important, which affects the perimeter reduction of the dimensions of the electrode and the increase in the dimensions in the “R” cavity. The gap influence in the electrode design in Fig. 10 is shown, drawing not to scale.

5.3 Solid Modeling of the Electrode




For the CAD/CAM processing, FreeCAD 020.1 version is used, which is a general-purpose parametric 3D CAD modeler and has a Path workbench to obtain a CAM




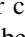
Fig. 10 Original dimensions of the cavity and electrode size due to gap



process of solid and surface objects. One advantage of this software is that FreeCAD recognizes SVG files.

5.3.1 First Steps

A new file must be opened in FreeCAD, in the workbench called “Part design”. It is needed to press the icon “Create part”  and then the icon “Create body” . Now, in the file there is a part with one body. To observe the origin, the “Toggle axis cross” in the “View” menu  needs to be selected.

The next step is to create a sketch clicking ; this sketch will be the rectangular base of the electrode/tool (Fig. 11). Selecting the XY plane, a rectangle is drawn using the “Centered rectangle” tool . First, selecting the origin, and then drawing the rectangle. With the “Sketcher constraints” vertically  and horizontally , the measures of the rectangle can be added. In this case, 100×50 mm. Then, the sketch can be closed and the file saved.

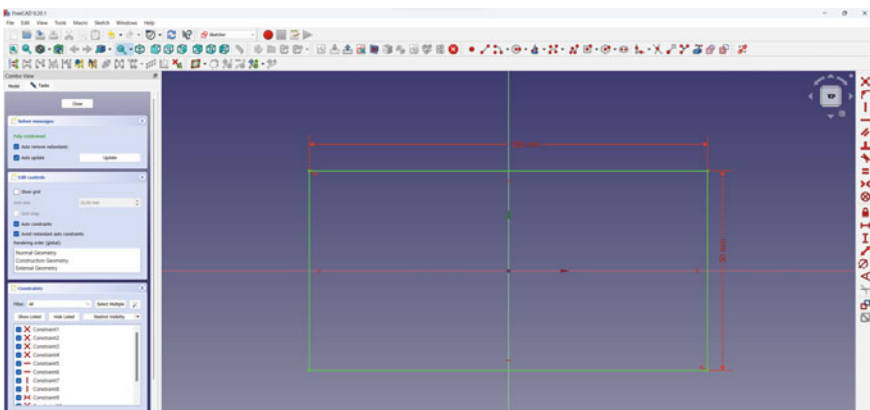


Fig. 11 First sketch

In the Panel “Combo view” and in the “Model” label, this tree structure is visible (Fig. 12).


Selecting the Sketch and using the “Pad” tool , a first block is designed with the parameters shown in Fig. 13. The result to create is a block between the dimensions Z-10 and Z-5.

Fig. 12 Model combo view

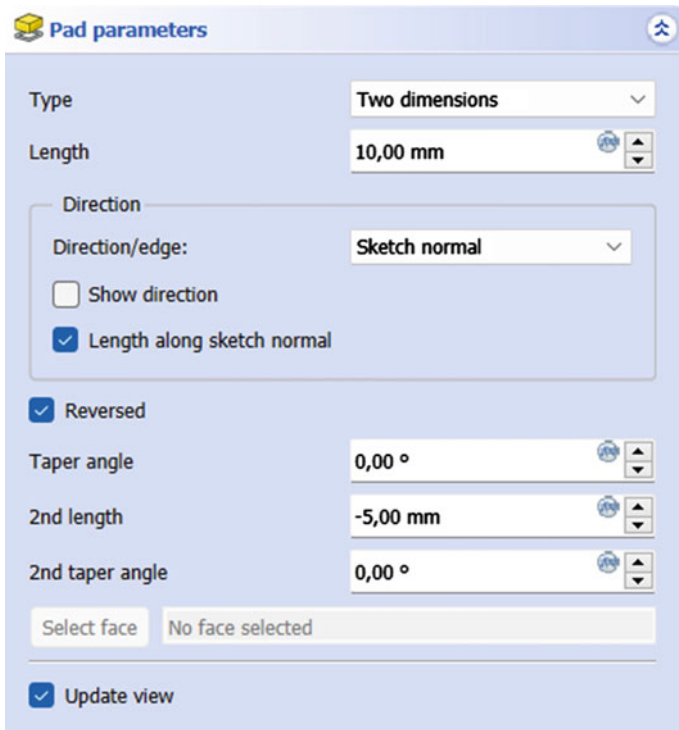
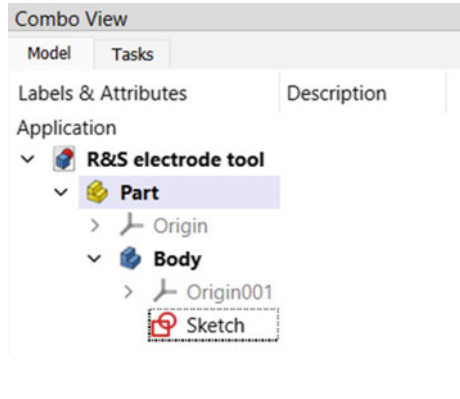


Fig. 13 Pad parameters

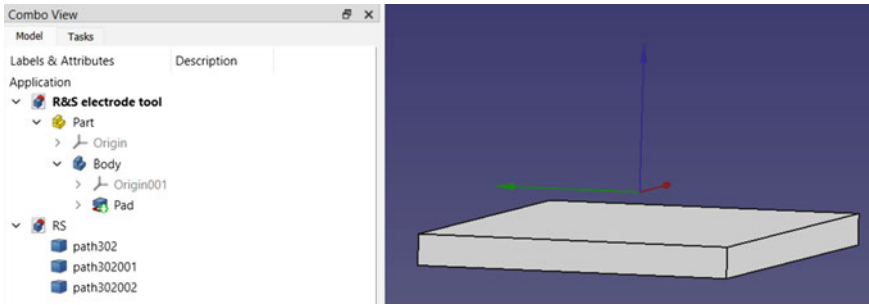


Fig. 14 Base block position and imported design in the model view

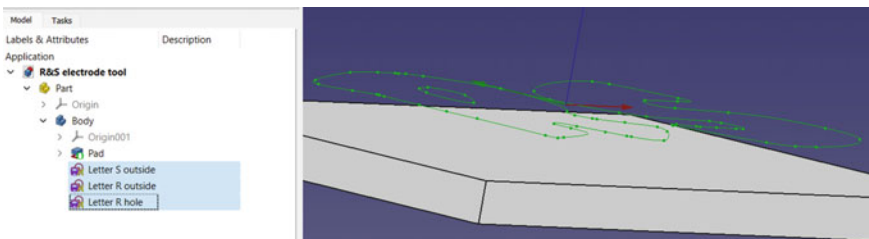



Fig. 15 Renamed sketches in the active body

5.3.2 Import Vectorial Drawing Design

To import the *.SVG file created with Inkscape, it is needed to open it as geometry in FreeCAD. Now, two files can be observed in the Model View, the original (saved as R&S electrode tool) and the imported design (called RS) (Fig. 14).

The imported design appears as three paths, one for the outside edge of the “R” letter, another for the inside hole of this letter, and the last for the outside border of the “S” letter. These imported paths can be easily converted into sketches. Using the Workbench “Draft”, in the “Modification” menu, an option called “Draft to sketch”  can be used to create the sketches. With this conversion in sketches, curves can be easily modified and extruded with the “Pad” option.

To move the created sketches to the active design where the block was created, it is possible to “drag and drop” sketches or to “copy and paste”. It is possible to rename these sketches using the contextual menu or pressing the F2 key as shown in Fig. 15.

5.3.3 Sketch Repositioning

As shown in Figure 16, the letters must change their order. To move the sketches, it is necessary to select the sketch; then, in the Panel Combo View, the Property is shown.

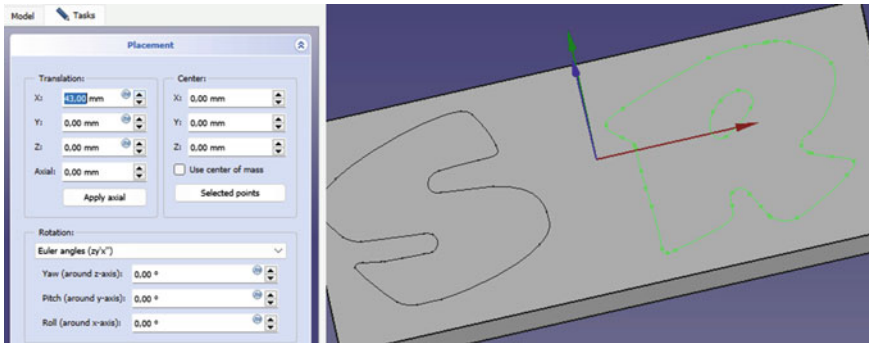






Fig. 16 Repositioning the sketches

The three dots displayed in the “Placement” property allow it to move as shown in Fig. 16. Only the X positions should be modified to achieve the desired positions.

5.3.4 Sketch Offset

To apply the gap restriction of the EDM process, the sketch must be modified with the option to offset planar shapes  as shown in Fig. 17 up. This tool is available in the “Part” workbench. The gap previously defined is introduced as an offset value, negative for the outside edges and positive for the inside edge of the “R” letter. Figure 17 center shows the offset applied to the designed sketches but shows it out of scale to highlight the operation. The three offset operations created can easily be converted into new sketches using the operation “Draft to sketch” . The new sketches must be moved (drag and drop) to the active body, and the result will be renamed the created new sketches as shown in Fig. 17 down. In Fig. 17 down, the offset operations were deleted after the new sketches were moved to the active body.

5.3.5 Pad Operation

Using the offset sketches, in the workbench “Part Design”, it is possible to give volume to the letters using the Pad command  for the outside offsets and the Pocket option . It is important to activate the “Reversed” option because the zero level is defined in Plane XY, and all the workpieces are under this plane in negative Z coordinates. The result of the operation can be seen in Fig. 18.

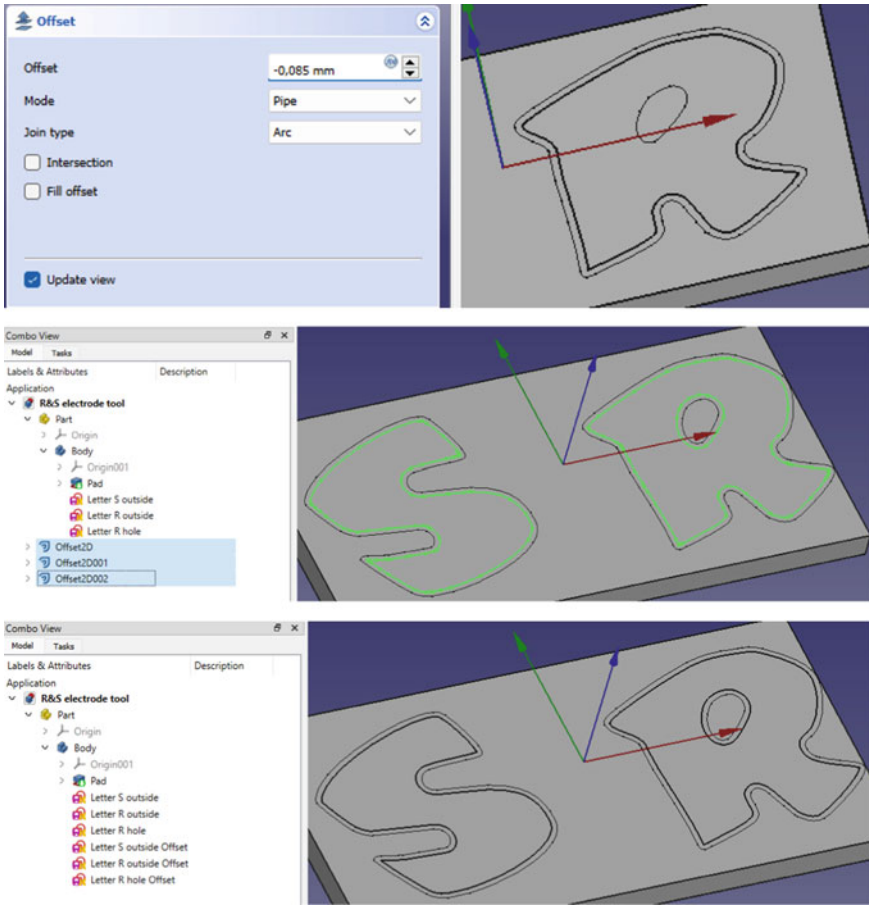


Fig. 17 Sketch offset procedure: **Up** setting offset values, **Center** offset applied to the designed sketches, **Down** original sketches and offset sketches

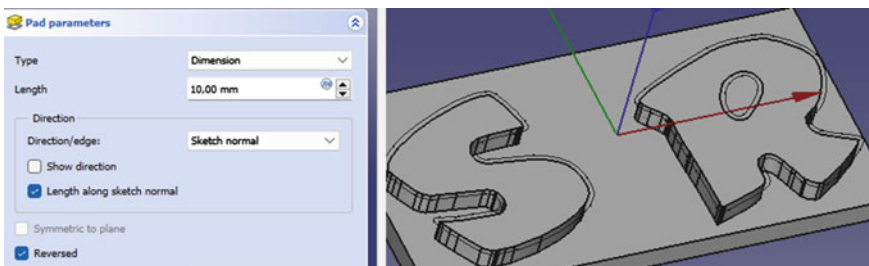


Fig. 18 Pad operation

5.3.6 Profile Alignment

Correct alignment of this tool/electrode is necessary to create a side profile on two sides. This profile is created with a new sketch (Fig. 19) and pad operation. The pad was created with a length of 15 mm, reversed mode, and a second length of -10 mm. Figure 20 shows the final solid geometry, still showing the original sketch design. From this point, these sketches can be hidden using the hide item command in the contextual menu over the object. In the image, the offset sketch has a huge value, out of scale, to be able to observe it clearly.

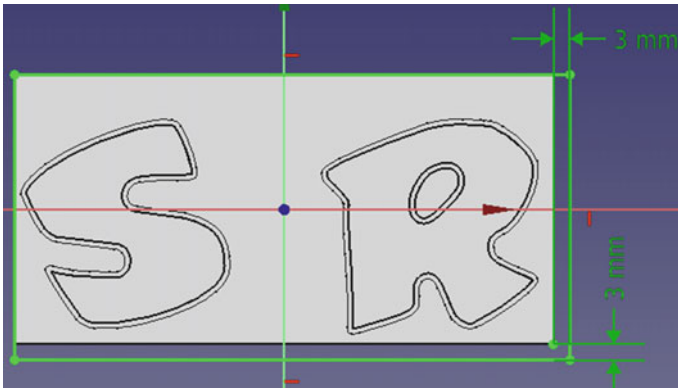
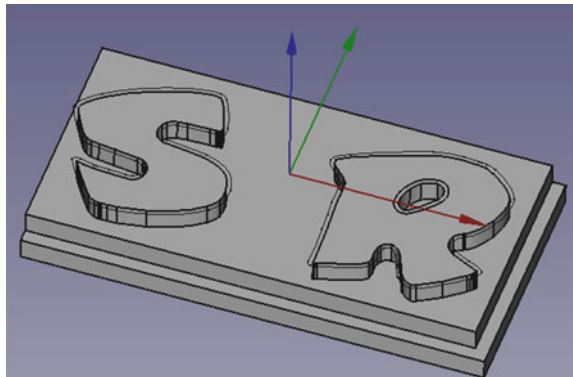


Fig. 19 Profile added on two sides

Fig. 20 Final solid design



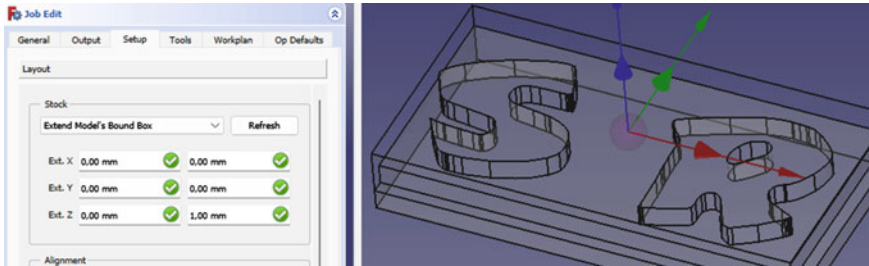



Fig. 21 Main values of stock layout definition


5.4 Manufacturing Processes of the Electrode

The Path workbench of FreeCAD will be used to perform the Computer Aided Manufacturing (CAM) processes required for obtaining the gcode (CNC code). The steps for doing that are presented next.


5.4.1 CAM Initial Stages

In the workbench “Path”, the early step is to create a new “Job”  using the part. In the setup label that appears after accepting the part, the layout of the stock used to perform a CAM simulation (Fig. 21) can be configured. Pressing OK, the main values of the job are defined. It will be necessary to Edit again this Job to define other parameters.

5.4.2 Tools Definition

In the Path menu, it is possible to find the “Tool bit library editor”  as shown in Fig. 22.

The tools needed to machine the part (Create Toolbit button) using the default shapes of FreeCAD are created; in this case, the endmill.fcstd shape template is used as shown in Fig. 23.

After the tools were created in the “Tool bit library editor”, these tools can be shown in the “Toolbit Dock” with the same icon  as the bit library in the Path menu as shown in Fig. 24 up. A $\varnothing 40$ Face Mill with inserts to perform a face milling operation over the stock and two end mills ($\varnothing 16$ and $\varnothing 4$) to make the rough pocket shape and to fish the profile of the letters will be used. Selecting these tools and pressing the “add to Job” button in this Tool Selector, these tools will be added to the job (Fig. 24 down).

In Fig. 24 down, it is possible to appreciate how milling conditions such as feed speed (mm/min) for horizontal and vertical movements and spindle speed (rpm) can be defined.

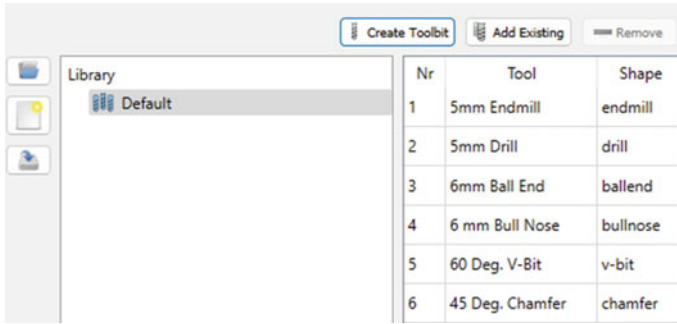


Fig. 22 Tool bit library editor menu with some default tools

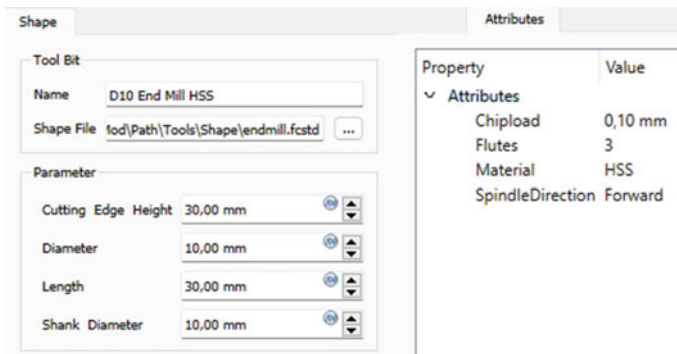
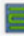


Fig. 23 Shape and attributes of a new tool in the ToolBit library editor

A quick summary of the tool selection is as follows:

- Create the tools in the “Tool bit library editor”.
- Add the tools to the Job from the “Toolbit Dock”.
- Edit tools in the Job adding the cutting conditions.

5.4.3 Face Milling

Face milling of the whole workpiece will be the first operation of the workplan. All the operations appear in the workbench “Path” and in the Path menu. In this case, the “Face”  must be selected. A window requires to “Choose a Tool Controller”, and the ø40 Face Mill is selected. The task window shows the MillFace options. The first label is the “Base Geometry”. The base surface between the letters to extend the face milling operation to over the hole stock face is selected, and this surface is added to the base geometry parameters as shown in Fig. 25.

The next label is “Depths”. The surface selected is placed at level $Z = -5$. The face milling must be $Z = 0$, and the parameters must be the ones displayed in Fig. 26.

Fig. 24 Tool selection: **Up** ToolBit Dock with the tools needed and their numbers in the milling center, **Down** tools added to the Job

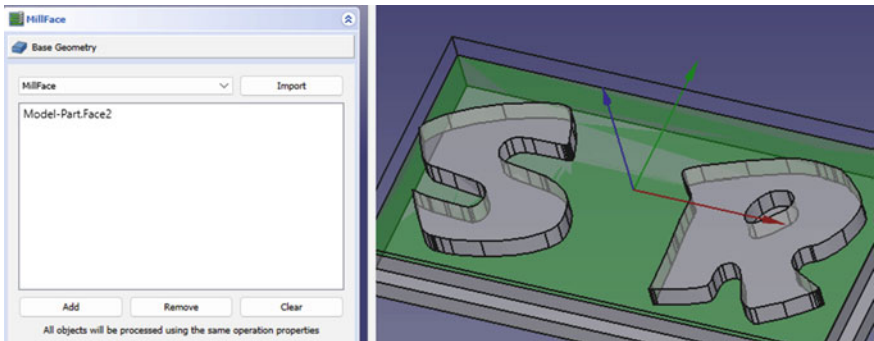
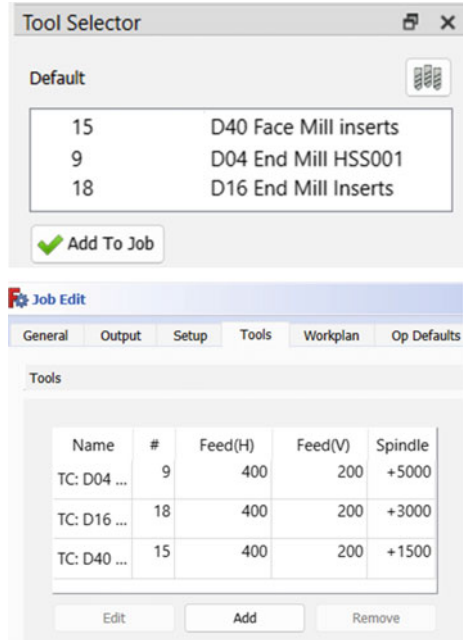


Fig. 25 Base face added to the base geometry

To change a value, a surface with the same depth value is selected. By pressing the blue arrow, this depth is entered. Another alternative is clicking the small blue circle close to the expression, and the “Formula editor” will open in another window to modify the depth value.

The label “Heights” allows modifying the safe and clearance heights of the operation. The values selected can be seen in Fig. 27.

Finally, the “Operation” label allows changing some tool and cutting parameters (Fig. 28). The “Boundary Shape” is important because it specifies if the actual shape of the selected face should restrict the facing or if the bounding box should be faced

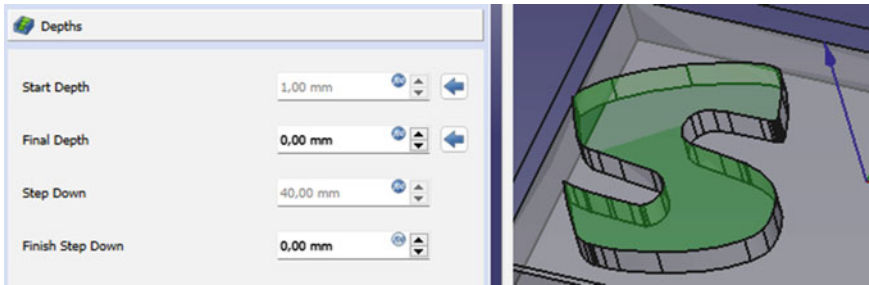


Fig. 26 Start and final depth of face milling operation

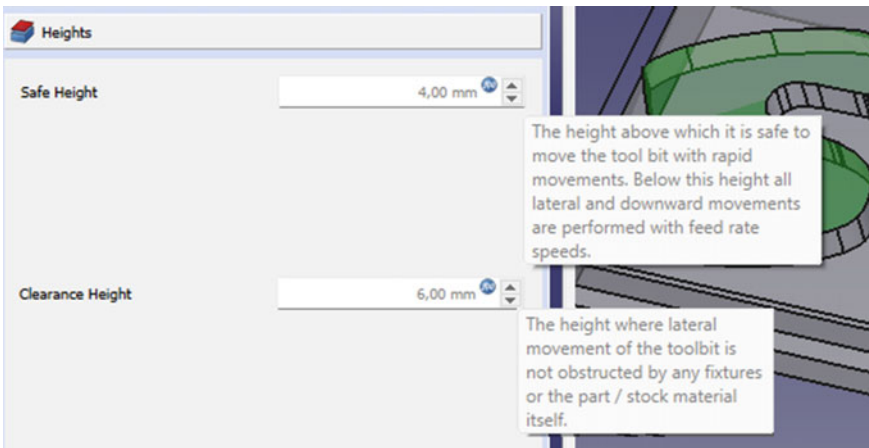



Fig. 27 Safe and clearance heights

off. The “pattern” is important to define how the tool bit is moved in to clear the material out. This face milling operation is simply milling with only one vertical step over, and one should ensure that no material is left behind that should be left by other operations. Pressing the “Apply” button, the tool paths shall be calculated.

5.4.4 Rough Pocket Shape

The next milling operation will be rough milling around the letters of the design. This option is also available in the Path menu and is called “Pocket Shape” . The tool used for this operation of the workplan is the $\varnothing 16$ end mill. The “Base Geometry” shall be the same as the one previously defined. The next label in this milling operation is “Extensions”. It is necessary to enable the extensions of the surface defined as a base geometry as shown in Fig. 29. The box “Default Length” allows setting the extent of

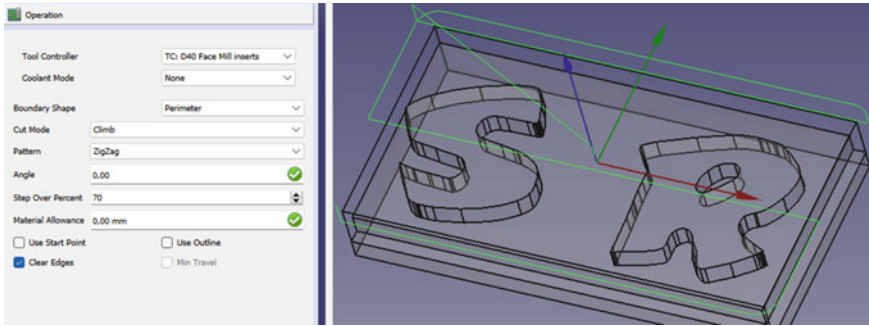


Fig. 28 Face milling operation parameters

the dimension of existing edges detected in the tree “Model-Part”. The default value is half the tool diameter.

Similarly, as it was done in the case of the face milling operation, the next step is to define the “Depths” values (Fig. 30). A milling between $Z = +1$ and $Z = -5$, with a “step Down” of 1.5 mm is established. It is not necessary to “Finish Step Down” because the final level does not need a specific roughness value. The “Step Down”, the depth of each milling pass, was set at one and a half millimeters. The “Heights” used are the same as in the previous section.

Fig. 29 Extension labels and their values

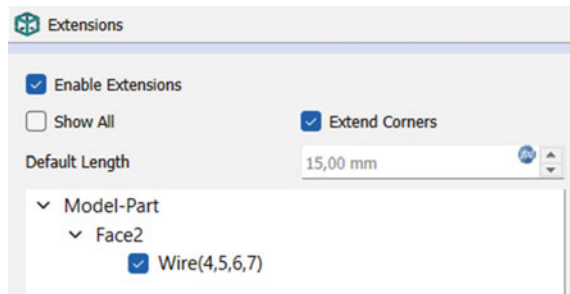


Fig. 30 Depth labels and their values

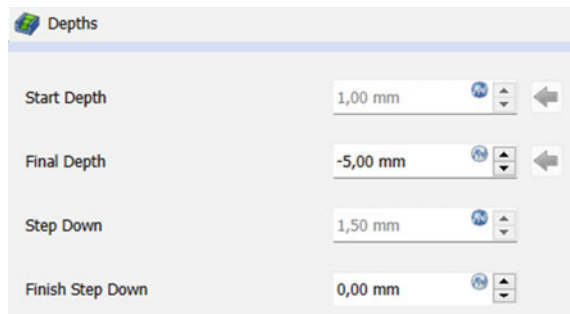


Fig. 31 Roughing operation parameters

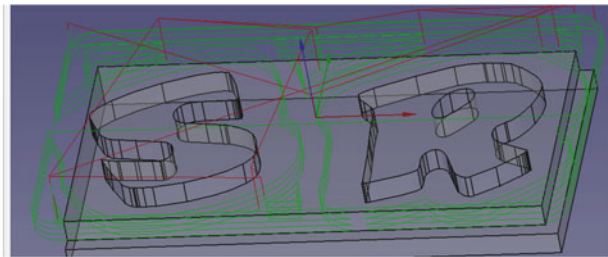
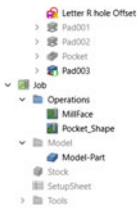
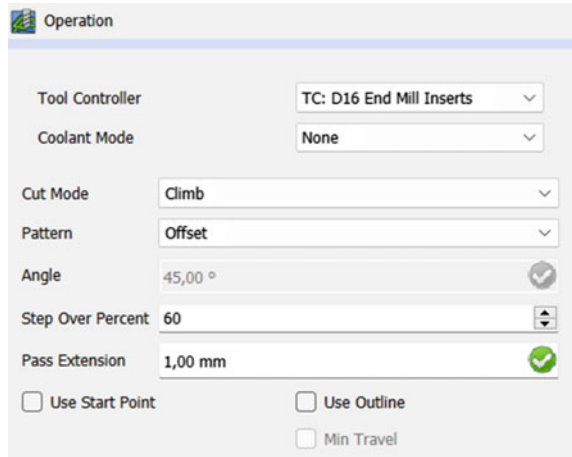


Fig. 32 Rough pocket paths

Finally, the label “Operations” has the configuration shown in Fig. 31.

It is necessary to leave a millimeter of separation to the letters to leave material for the final finishing pass. That is, the value defined in “Pass Extension”. Pressing “Apply” and “Ok”, the rough paths are defined as shown in Fig. 32.

5.4.5 Profile Operation of the Lateral Faces

This operation is necessary to mill the profile previously defined for alignment. The same $\phi 16$ end mill is used. The “Base Geometry” is defined by these two edges as shown in Fig. 33 up. The depths are “Start Depth” of -5 mm, “Final Depth” of -10 mm and “Step Down” of 1.5 mm. Setting up those values, the profile paths are defined as shown in Fig. 33 down.

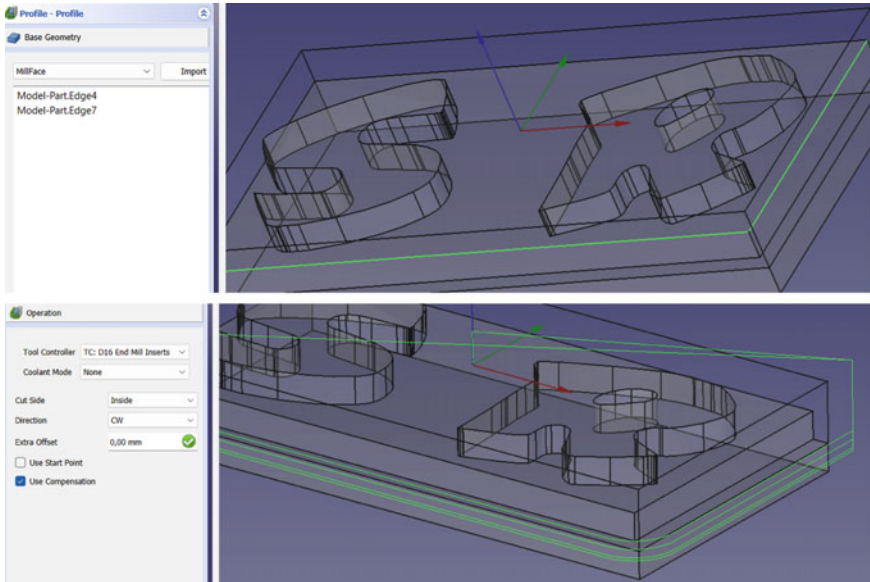


Fig. 33 Profiling: **Up** edges used for defining the base geometry, **Down** profile paths

5.4.6 Finish Operation for the Profile of the Letters

The $\varnothing 16$ mm mill used for the rough operation cannot reach the narrow spaces of the design. Thus, it is necessary to use a tool with a smaller diameter (a $\varnothing 4$ mm HSS end mill). The geometry used will be the top faces of the design (Fig. 34 up). The “Depths” values are milling between $Z = +1$ and $Z = -5$, with a “step Down” of 1.5 mm. None “Finish Step Down” it is needed. Additionally, by setting up those values, the profile paths are defined (Fig. 34 down).

5.4.7 Mill Pocketing of the R Hole

With the same $\varnothing 4$ mm HSS end mill, the milling processes of the electrode tool needs to be finished. The operation is a “pocket shape” The base geometry is the surface at the bottom of the hole (Fig. 35 up). The definition of the operation is shown in Fig. 35 down.

5.5 CAM Simulation

When all the operations are defined, it is possible to calculate all the paths of the tools as shown in Fig. 36.

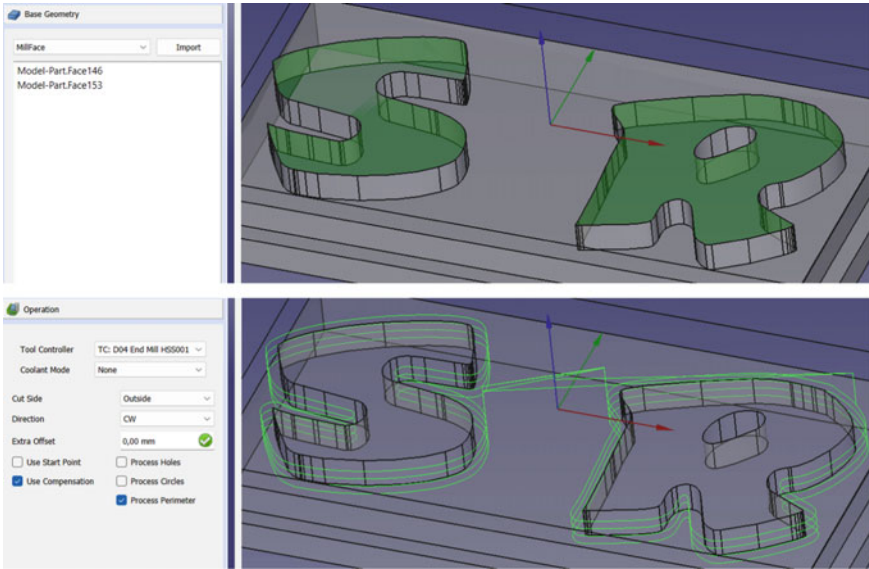


Fig. 34 Finish operation: **Up** base geometry for the profile finish operation, **Down** profile paths for the finish operation

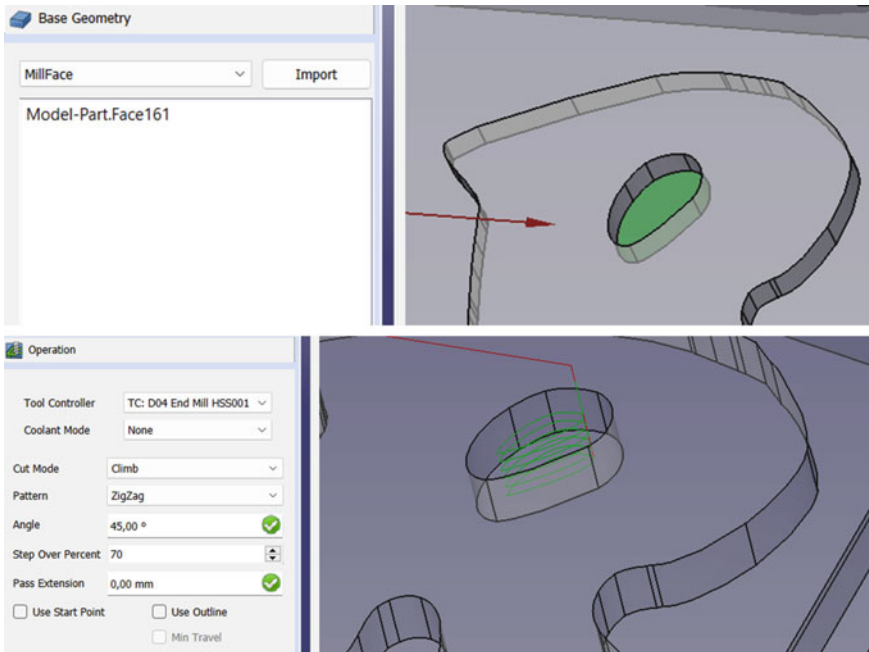


Fig. 35 Milling the hole operation: **Up** base geometry for the R hole pocket, **Down** milling the hole

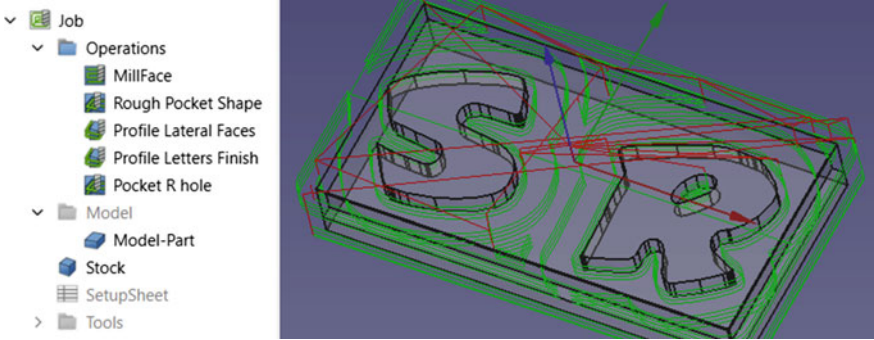


Fig. 36 Milling operations paths

The order of operations can be modified in the “Job Edit” window using the label “Workplan” and the up and down arrows (Fig. 37).


Simulations can help the user revise whether the trajectories of the tool are correct or not. CAM simulation of all trajectories can also be performed in FreeCAD by pressing the “CAM Simulator” icon . A random position during simulation can be seen in Fig. 38.

Fig. 37 Workplan edition

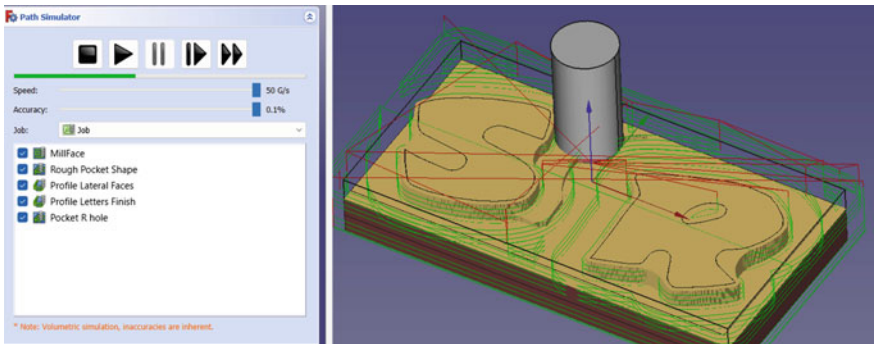
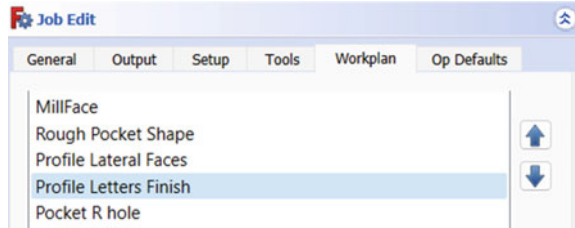



Fig. 38 CAM simulator progression

5.6 *Post-Processing*

Post-processing programs allow generating the gcode that milling centers need to perform machining operations. In this case, the post-processing will allow obtaining the gcode required to mill the electrode. To obtain this code, it is necessary to return to the “Job Edit” window using the label “Output” (Fig. 39 up). In this window, it is required to write the output file name (RS.gcode), the processor type (Grbl post-processor) and the work coordinate systems (G54). Grbl is a no-compromise, high-performance, low-cost alternative to parallel-port-based motion control for CNC milling. To machine this tool, a Microcut M760 vertical milling machine with a Fagor 8065 numerical control that works fine with the Grbl G-code lines is used. Finally, by pressing the post-process icon , the gcode is saved in the output file designed and shown in a pop-up window (Fig. 39 down).

5.7 *Development of Milling in Machines*

To validate the post-processed CNC program before sending it to the milling machine, using the Fagor free simulator. This program emulates the one that works on the milling machine.

First, it is necessary to load the tools using in the real machine (Fig. 40). In this case, the tool numbers are 09, 15, and 18 that must be consistent with the ones previously used in FreeCAD. The dimension of the stock should be also included with the same values as those previously used. The stock used shall be copper 102 mm long and 52 mm wide, slightly more than needed for the workpiece.

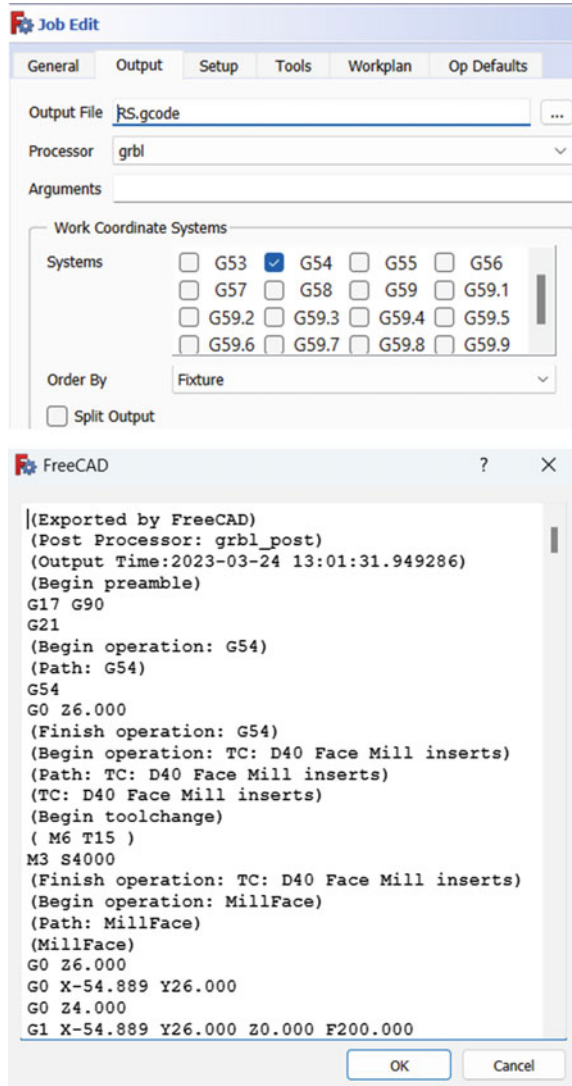
When the stock and tools are properly setup, it is possible to open the CNC file in the Fagor editor (Fig. 41).

The post-processed program only needs two changes to run perfectly, marked with the white arrow:

- G21 (units in mm) in this machine is G71.
- The tool selection is disabled in the code because of the parentheses. Thus, the user must check that the tool selection is in accordance with the tools inserted in the machine-tool and, if so, just erase the parenthesis from the code. These parentheses are used only to introduce comments in the program.

Additionally, the origin defined in the machine with G54 in the upper left-hand position due to the grip on the clap should be moved. For this purpose, an incremental zero offset using G158 in the code (orange arrow in Fig. 41) is applied. In this sense, the CNC adds the offset to the active G54 at a time to consider the position of the clamp as shown in Fig. 42. In this case, the offset was of 51 mm in the X axis and 26 mm in the Y axis.

Fig. 39 Gcode generation:
Up output job edition, **Down**
Gcode generated



CNC Fagor also allows performing simulations of the machining process. Thus, the last step before sending the code to the milling machine and executing it is to execute the simulation as shown in Fig. 43.

After verifying that the program works as expected, the program can be opened in the machine where it is also possible to run the same simulation (Fig. 44).

After all checks and gripping the stock material on the clamp, the machining process is started as shown in Fig. 45.

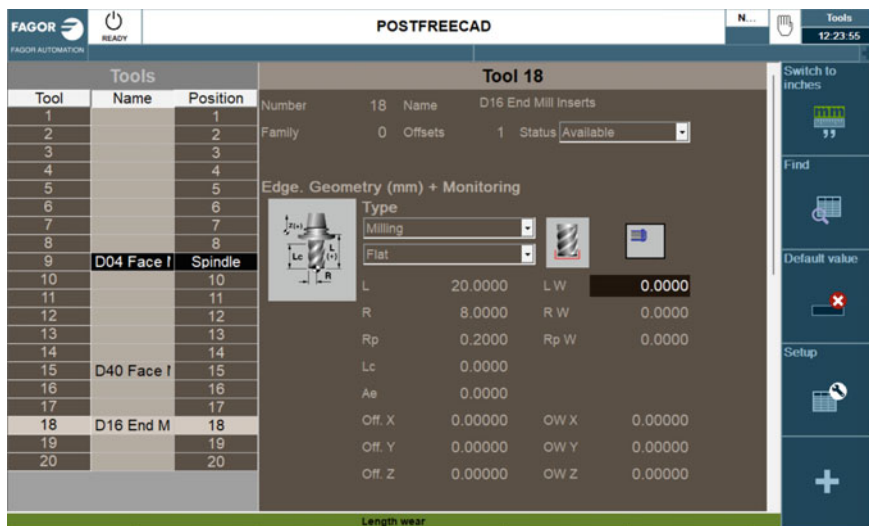


Fig. 40 Machine/simulator tools table

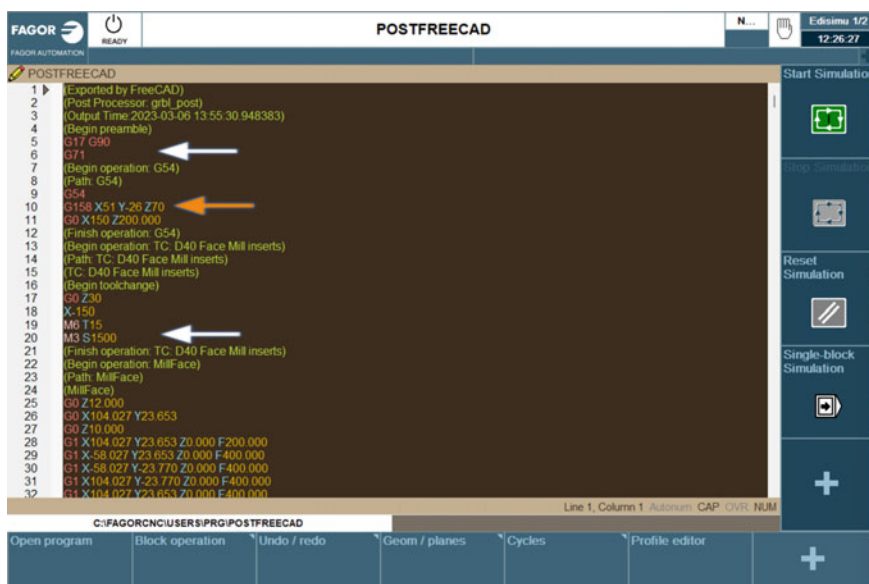


Fig. 41 Opening and editing the program

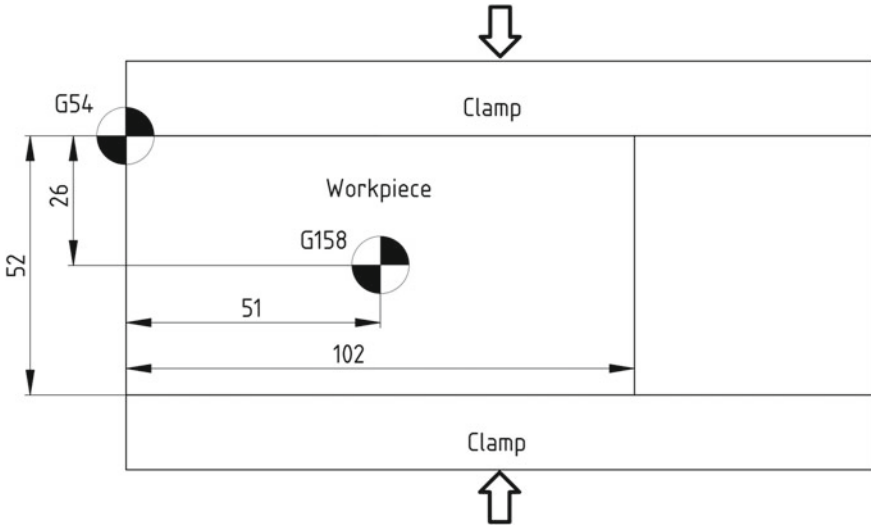


Fig. 42 Zero offset with G158

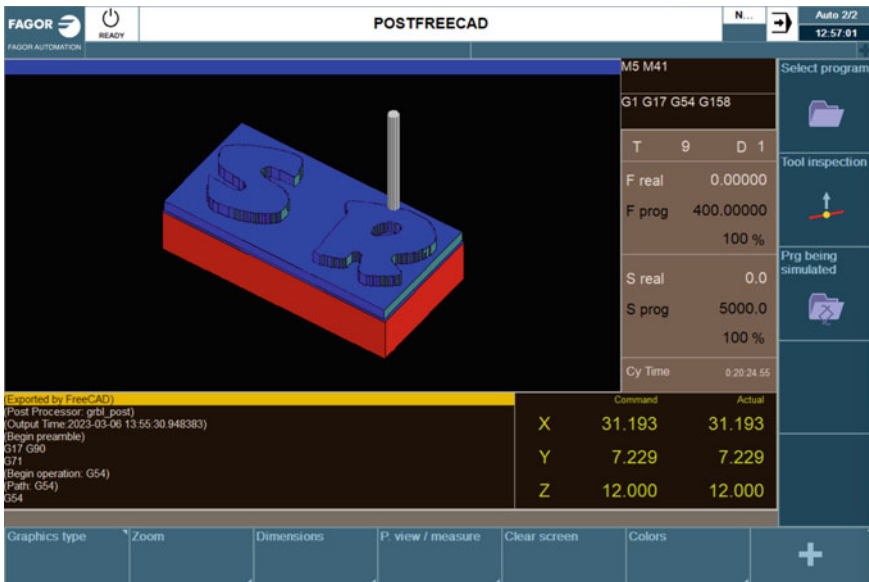


Fig. 43 Simulating the program in the computer



Fig. 44 Simulating the program in the milling machine

To complete the manufacturing of the electrode, a handle is needed to place the electrode in the EDM machine. One easy way to do it is by manufacturing the handle using a lathe (Fig. 46). The material used to do this handle is aluminum with good machinability.

5.8 Processes in the EDM Machine

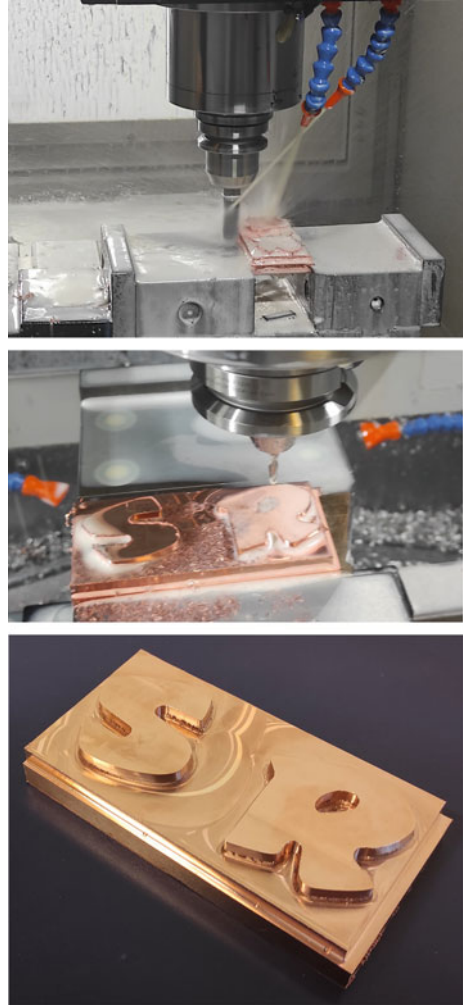
5.8.1 Parallelism of Electrode Front to Machine Axis

Later, the electrode is fixed to the clamp in the machine. For that purpose, it is necessary to align the frontal face of this tool with the XY plane of the machine (Fig. 47). Using a dial indicator and a couple of screws in the clamp, the orientation in both axes is modified. After the first axis is aligned, the same must be done with the second one.

5.8.2 Alignment of the Side Edge of the Tool

Once the previous step was performed, the electrode was parallel to the worktable of the EDM machine, but it was not aligned with the axis. The error of alignment of the electrode with the rotation around the handle must be avoided. The dial indicator will be on the machined step. In this case, it is only needed to move the X-axis because the other machined face is perpendicular to the first as shown in Fig. 48.

Fig. 45 Electrode machining: **Up** executing the program in the milling machine, **Center**) Finishing the workpiece/electrode, **Down** Cu electrode finished



5.8.3 Clamping the Part

The clamping method for the workpiece requires to also consider the alignment of the part. This can be made using a dial indicator as it was done for the electrode (Fig. 49). The workpiece used is a steel part in a parallelepiped shape of $100 \times 50 \times 8$ mm. The material is SJ275.

Fig. 46 Manufacturing of the handle: **Up** turned handle in the lathe after machining, **Down** handle fixed to electrode

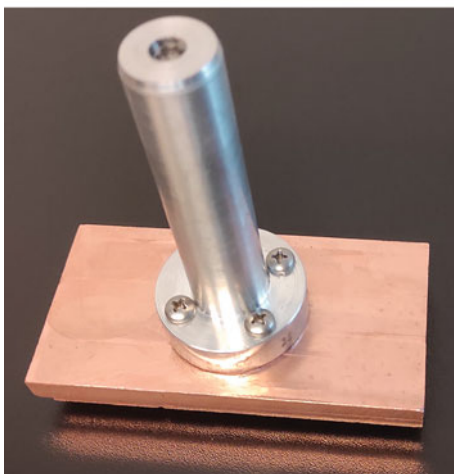


Fig. 47 Parallelism of the electrode front

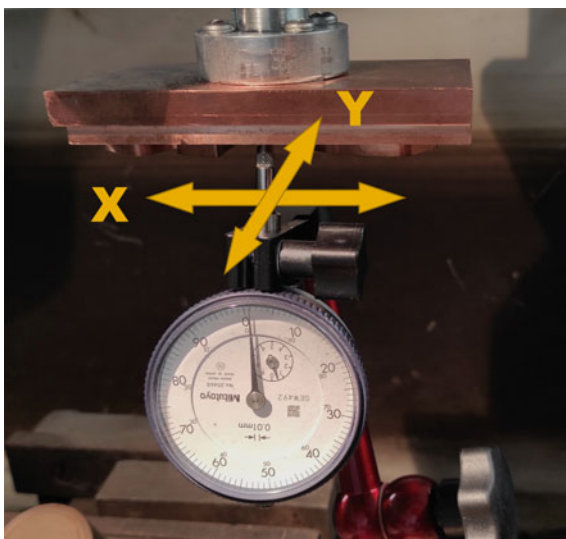


Fig. 48 Alignment by rotating the electrode



Fig. 49 Alignment of the workpiece



5.8.4 Workpiece Positioning

By touching the electrode and the workpiece in the three axes, the optimal positioning is defined. The touch is detected by the electrical continuity between the workpiece and the electrode. Figure 50 shows the movement of the electrode to set the zero in the X-axis touching the lateral side machined in the electrode and the flank of the workpiece. When electrical continuity is detected, a zero in the measurement system is established. Then, the electrode is moved over the workpiece to correctly position the letter of the electrode according to the measures in this axis. For example, in Fig. 51 the measures in the X-axis for the double protuberance of the electrode are shown.

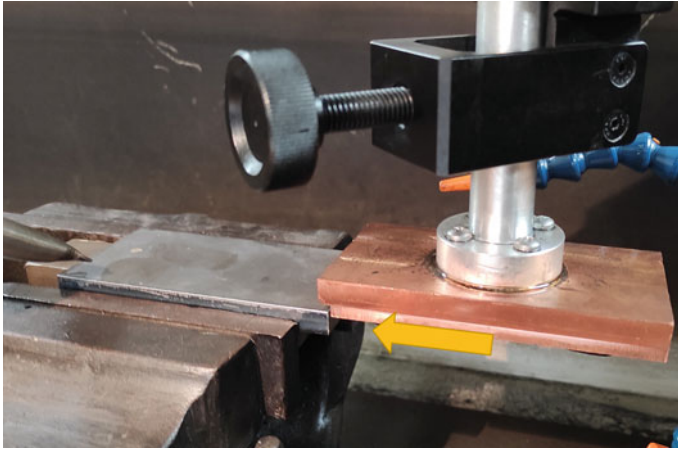
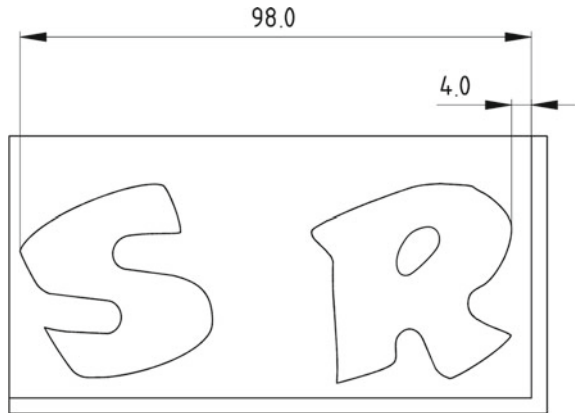


Fig. 50 Setting zero on the X-axis

Fig. 51 Positioning electrode protruding in the X-axis



5.8.5 Cleaning Method

The gap between the workpiece and the electrode must be cleaned throughout the process to optimize the discharge channel, remove the detached metal particles, and provide space for the formation of contact points between the electrode/tool and the workpiece. In this case, a cleaning method by external flow using two nozzles to supply a pressure dielectric fluid to the gap is used. The details of the cleaning setup can be seen in Fig. 52. In addition, the tool will perform an oscillating movement up and down that will allow, for a few tenths of a second, the electrode to move away from the area to be eroded approximately one millimeter, enough to clean the area.



Fig. 52 Starting the EDM process: verifying the cleaning method

5.8.6 Electrodischarge Manufacturing Process

According to the EDM parameters selected in Table 1, the process starts after the tank is full of dielectric fluid. In the Z-axis, 2.5 mm in two cavities will be machined, following the indications in Fig. 9. Two tool motions must be performed. After a couple of hours for each cavity, the process is completed. After removing the workpiece from the EDM machine and cleaning it, obtaining the final part as shown in Fig. 53. Moreover, a model manufactured using clay allows showing the positive part of the piece.

6 Outcomes

The outcome of the activity will be a part machined by EDM following the design displayed in Fig. 1.

7 Deliverables and Assessment

Each student must make a final report that includes all steps using his initial design.

The evaluation will be through the delivery of that final report and its public defense.

Fig. 53 Finished part (up) and part modeled with clay



8 Conclusions

The activity started with a simple design on paper. This drawing would be the starting point to obtain a cavity in a mold, and that objective has been fulfilled by following the steps described. By delving into these sections, students will gain a comprehensive understanding of how EDM, CAM, and open-source software can be harnessed collectively to revolutionize manufacturing processes, opening up new possibilities for innovation and growth.

Study of Quality Parameters for Abrasive Waterjet Cutting of Metals



Bogdan-Alexandru Chirita , Eugen Hergehelegiu , Maria-Crina Radu , and Nicolae-Catalin Tampu 

1 Introduction

1.1 Evolution of Water Jet Cutting Method

Water has shaped nature with its eroding power for millions of years. Waterjet cutting has been used in the mining field since the end of the nineteenth century in Russia and New Zealand (Engemann, 1993; Summers, 2003). In 1950, high-pressure water jets were used for woodcutting. In 1987, Mohamed Hashish was awarded the patent for “Method and apparatus for forming a high-velocity liquid abrasive jet”, which is the basis for the current abrasive waterjet (AWJ) machining technologies (Hashish, 1987). Nowadays AWJ, a non-conventional machining technology, is used extensively in numerous industries for cutting various materials with low machinability, such as glass, ceramics, concrete, metals, composites, etc.

Abrasive waterjet machining uses the kinetic energy of a highly pressurized waterjet mixed with abrasive particles to produce a controlled erosion of the processed material in order to generate a cut along a contour (Hashish, 2015).

1.2 Advantages and Disadvantages

The main advantages of AWJ are:

- There is no heat generation, which is useful compared to other processing methods where the material has a heat affected zone where the mechanical and chemical

B.-A. Chirita (✉) · E. Hergehelegiu · M.-C. Radu · N.-C. Tampu
Department of Industrial Systems Engineering and Management, Faculty of Engineering, “Vasile Alecsandri” University of Bacau, Calea Marasesti 157, 600115 Bacau, Romania
e-mail: chib@ub.ro

properties are modified. The water quickly absorbs the heat resulting from the interaction between the abrasive particles and the material.

- Material loss is low due to the small width of the cut.
- There are no burrs and surface hardening.
- It can be used for processing various materials, even hard ones: stainless steel, titanium alloys, aluminum, brass, stone, granite, marble, ceramics, glass, plastics.
- No additional processing is required for finishing.
- CAD /CAM control leads to precision work.
- The cutting speed is high.
- The machining forces are small, and vibration is low.
- Intricate shapes can be obtained.
- Machine programming is simple and fast.

The main disadvantages of AWJ are:

- There is no possibility for simultaneous processing of multiple parts, which increases the costs.
- The equipment is expensive.
- The precision decreases for thicker parts due to the tailback and burr development.
- Water may oxidize metals or degrade some materials.
- There is a high level of noise during AWJ.
- It depends on water quality.

2 Background

The AWJ system is composed of the following main components (Fig. 1): water filtering subsystem, the ultrahigh pressure pumps, the cutting head, the motion system, the catcher tank, and the ancillaries.

2.1 Water Filtering Subsystem

As the waterjet may reach pressures up to 600 MPa and supersonic speeds up to 900 m/s, the water used in AWJ must meet the quality criteria presented in Table 1. Industrial waters may sometimes cause equipment to malfunction, due to the presence of solid particles. For example, if the concentration of calcium carbonate is too high, it can obstruct the cutting head, which is why several water treatment methods can be used. The simplest method uses resin filtering that replaces calcium salts with sodium salts. The second method is reverse osmosis, which removes the contaminants at the molecular level by forcing the water through a semipermeable membrane. The third method uses ionization, which replaces the negative ions (chlorides, sulphates) with positive, hydroxyl ions and sodium and calcium ions are replaced with hydrogen. It was observed that ionization is the most effective treatment to improve the service

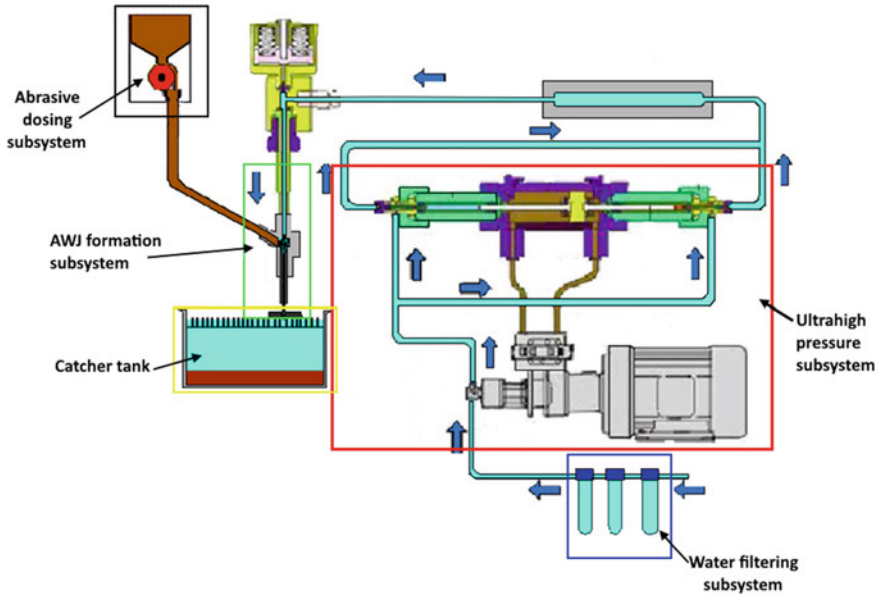


Fig. 1 AWJ system diagram

Table 1 Water requirements for AWJ

Attribute	Requirements
Total dissolved solids (TDS)	< 500 mg/l
Total hardness	< 25 mg/l
Fluorine	< 250 mg/l
Iron	< 2 mg/l
Manganese	< 1 mg/l
Turbidity	< 5 NTU
Free chlorine	< 1 mg/l
pH	6.5–7.5

life of the AWJ parts. Experiments have shown that reverse osmosis can enhance service life up to 190 h, whereas filtering may expand the service life with up to 78 h.

2.2 Ultrahigh Pressure Subsystem

This is used to increase water pressure from the ambient value to the high values necessary in the process using multistage pumps. High pressure values require the use of hydraulic pressure intensifiers from where the water passes into an attenuator

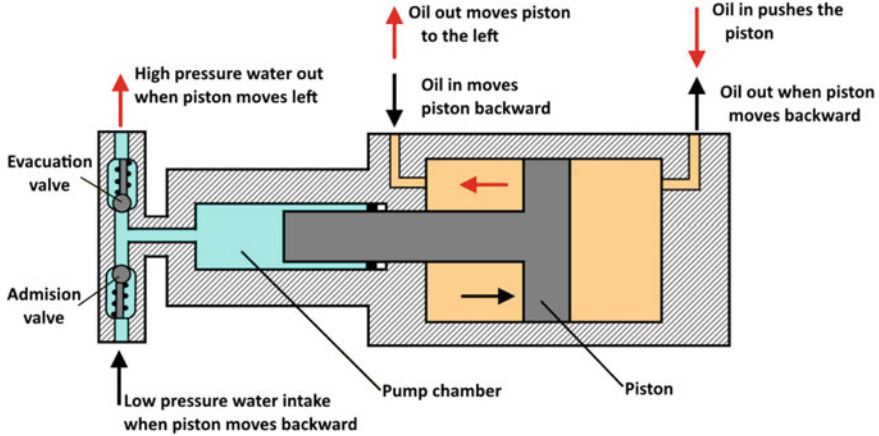


Fig. 2 Pressure multiplier

to reduce the influence of the cyclic pressure variations determined by the intensifier functioning. The intensifier is made of two cylinders with diameter ratios from 1/10 to 1/25. On the larger side, the pressure on the hydraulic plunger is 5–35 MPa and because of the diameter ratio, in the second cylinder the pressure can rise to 400 MPa (Fig. 2). To assure a continuous functioning, two or more pressure intensifiers can be coupled in parallel (Fig. 3).

2.3 Jet Formation Subsystem

- (a) **Waterjet.** Waterjet cutting principle is based on the effects of a thin jet of water has upon a material at high pressure and high flowing speed. Waterjet cutting is considered a form of micro erosion. During this process, a large volume of water is forced through a small diameter nozzle. The constant high pressure water flow interacts with a small area of the material causing micro-cracks at the impact. The water removes the detached particles, so the micro-cracks are exposed to erosion and propagate until a full cut is obtained. The system used for the formation of the waterjet is presented in Fig. 4. An important aspect is the coherency of the waterjet. The structure of the waterjet contains an initial coherent flow which gradually spreads and turns into droplets. A more coherent waterjet packs an increased power density, so it is more efficient.
- (b) **Abrasive waterjet.** Cutting is achieved using a waterjet mixed with an abrasive material. The mixing and homogenization take place in the mixing chamber of the cutting head and the kinetic energy is transferred in the focalization tube (Fig. 5). AWJ can be used to cut a large variety of materials, following various contour shapes, as an alternative to other technologies, such as laser or plasma cutting.

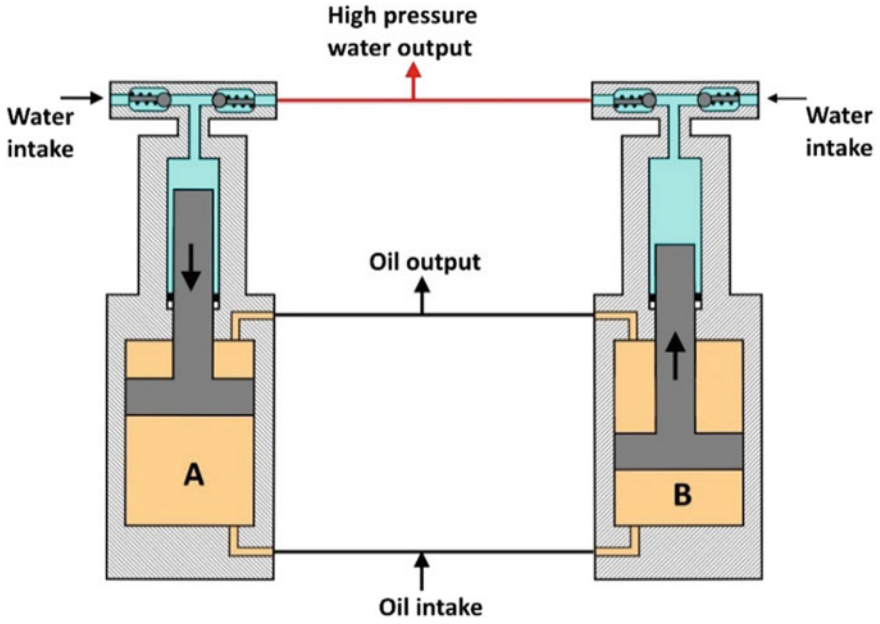
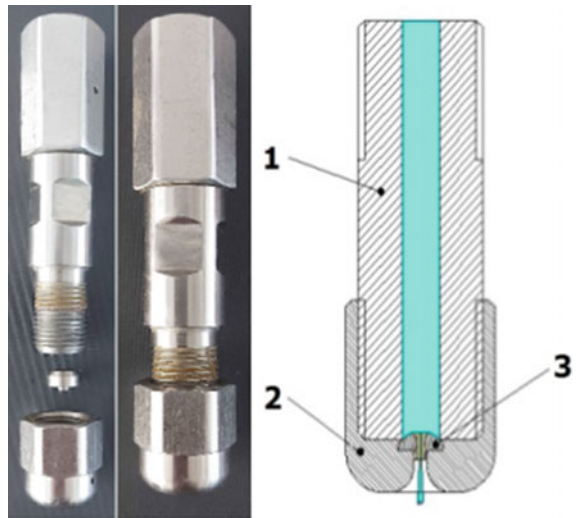


Fig. 3 Parallel pressure multipliers

Fig. 4 Waterjet cutting head: high pressure tube (1), clamping nut (2), nozzle (3)



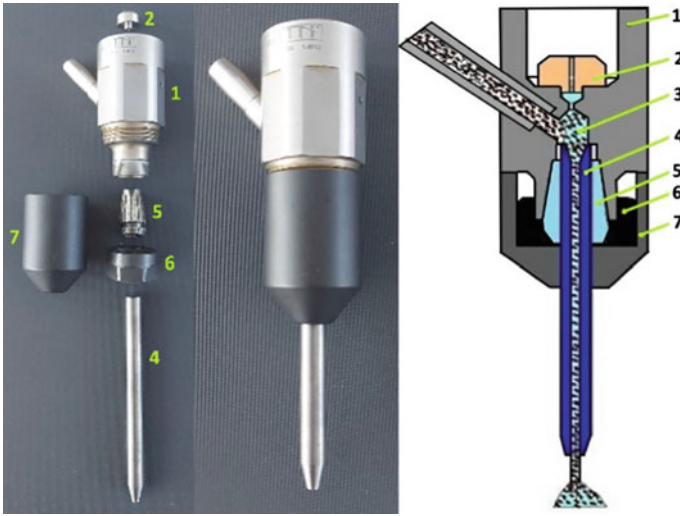


Fig. 5 Abrasive waterjet cutting head: casing (1); nozzle (2), mixing chamber (3), focalization tube (4), collet (5), clamping nut (6), protective case (7)

2.4 The Catcher Tank

This is used to collect the mixture of water, abrasive particles, and processed material because only 10% of the total jet energy is consumed during cutting. The rest of the energy is absorbed by a container (tank) that may use different construction solutions: a bed of 0.15–0.3 m thick made of steel or ceramic balls (Fig. 6a), a layer of water 0.5–1 m deep (Fig. 6b), or plates made of corrosive resistant materials (Fig. 6c).

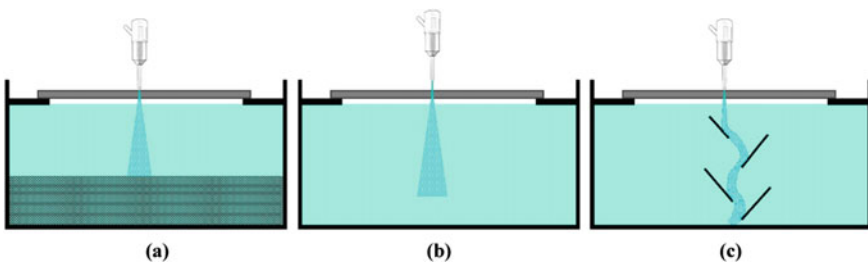
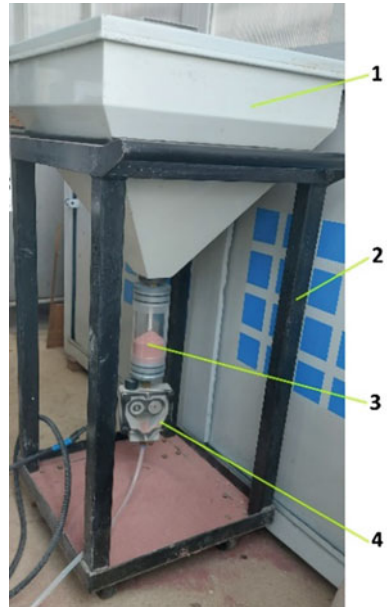


Fig. 6 Jet energy amortization system

Fig. 7 Abrasive dosing:
hopper (1), hopper stand (2),
control cylinder (3),
dispenser (4)



2.5 Abrasive Material Dosing System

The abrasive material dosing system is composed of a hopper and a metering valve. This valve measures and controls the abrasive flow, with possibility to set values within an interval of 1–999 g/min. It is recommended that the distance between the dosing system and the cutting head should be minimum. The dosing system has the following components: the hopper where the abrasive material is contained, a control cylinder to see when the abrasive runs out, and the dispenser that is connected to the numerical controller (Fig. 7).

2.6 The Motion System

The motion system is used to control the position of the cutting head, which is necessary to perform the cutting. CAD/CAM software and CNC controllers are used to create the paths and to interpolate the motion of the machine.

Table 2 Abrasive materials and hardness properties

Abrasive material	Hardness	
	Mohs	Knoop
Aluminum oxide	8–9	2.100
Garnet	7.5	1.350
Fine granite particles	8	–
Olivine	5.5	1.100
Silicon carbide	9.15	2.500
Sand	–	700
Granulated steel	–	400–800
Copper slag	–	1.050
Glass powder	5.5	400–600
Zirconium	–	1.300

Fig. 8 Microscope image of garnet abrasive particles

2.7 Abrasive Materials Utilized for AWJ

AWJ uses various types of abrasive materials, such as: aluminum oxide, garnet, glass, fine particles of granite, silicon carbide, sand, steel beads, copper slag aggregate, olivine, etc. Abrasive materials are classified using criteria such as hardness, structure, shape, grain dimensions. Table 2 presents the most used materials and their hardness.

A microscopic image of garnet granules is presented in Fig. 8 and the material properties are in Table 3.

2.8 Kerf Geometry

According to ISO/TC 44 N 1770 standard (2010), kerf geometry is characterized by the following parameters (Fig. 9):

- Li—entrance width of cut

Table 3 Abrasive material properties—garnet produced by Barton International (Barton.com, 2023)

Properties	Observations
General description	<ul style="list-style-type: none"> – Combination of almandine $\text{Fe}_3\text{Al}_2(\text{SiO}_4)_3$ and pyrope $\text{Mg}_3\text{Al}_2(\text{SiO}_4)_3$ (silicates) – Homogenous minerals – No chemical emissions – Aluminum and iron ions may be partially replaced by calcium, magnesium and manganese: $\text{Ca}_3\text{Fe}_2(\text{SiO}_4)_3$, $\text{Mn}_3\text{Al}_2(\text{SiO}_4)_3$
Chemical composition	<ul style="list-style-type: none"> – Silica (SiO_2) 41.34% – Ferrous oxide (FeO) 9.72% – Ferric oxide (Fe_2O_3) 12.55% – Aluminum oxide (Al_2O_3) 20.36% – Calcium oxide (CaO) 2.97% – Magnesium oxide (MgO) 12.35% – Manganese oxide (MnO) 0.85%
Hardness	7–9 on Mohs scale
Power	Hard to break
Granules shape	Sharp edges with irregular shape
Splitting (cleavage)	Pronounced lamination, the cleavage plane is irregular
Color	Rose red
Stripes	White
Transparence	Transparent
Gloss	Vitreous
Specific gravity	3.9–4.1 g/cm^3
Refractive index	1.83
Facet angle	37° and 42°
Crystallization	Cubic (isometric) rhombic dodecahedron, tetragonal or combinations
Melting temperature	1315 °C
Magnetism	Variable magnetic attraction
Moisture absorption	Inert, nonhygroscopic
Pathologic effect	No
Harmful emissions	No

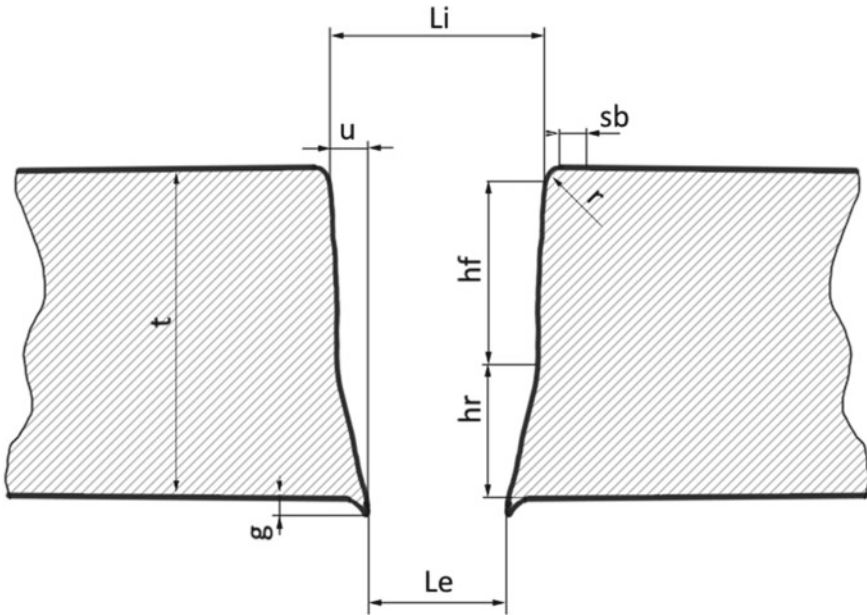


Fig. 9 Terms defining kerf geometry

- Le —exit width of cut
- g —burr
- hf —fine cut
- hr —remaining surface
- u —perpendicularity
- r —edge radius
- sb —beam affected zone
- t —workpiece thickness.

2.9 AWJ Process Parameters

AWJ process is controlled by a series of input parameters that can be classified into the following categories: hydraulic parameters, cutting parameters, abrasive parameters, material parameters, mixing parameters (Jegaraj & Babu, 2005; Natarajan et al., 2020; Sisodia et al., 2023).

The hydraulic parameters refer to:

- *Water jet pressure.* This gives the kinetic energy necessary to cut through the material. The depth of jet penetration is directly proportional to the pressure. It

was also observed that higher pressure improves surface quality and reduces water and abrasive consumption.

- *Nozzle diameter.* The depth and width of the cut are dependent on the nozzle diameter. Larger nozzle diameters increase the depth of the penetration and the width of the cut, also.

The abrasive parameters refer to:

- *Abrasive flow rate.* The rise of the abrasive flow rate increases the depth of jet penetration to a certain extent. However, it was observed that overdosing of the abrasive leads to an agglomeration of the mixing chamber that decreases the abrasive kinetic energy. The optimum amount of abrasive material depends upon the water jet pressure, nozzle diameter, the length and inner diameter of the focalization tube.
- *Abrasive material.* Various materials are used, as mentioned earlier, but garnet is the most common.
- *Abrasive particles sizes and shapes.* The size of the abrasive particles (mesh number) reflects on the removal speed. A smaller mesh number means that the abrasive has a larger granule size and higher removal speed. This is also associated with higher surface roughness. Medium and smaller grains (#60 to #200) are used for cutting metal, glass, or composite materials.

The mixing parameters refer to the *focalization tube length* and *inner diameter*. The jet coherency is improved when the tube dimensions increase to a critical size. The depth of the jet penetration improves when the tube length is increased, as the abrasive particles require a certain acceleration distance. However, if the length is too high, the friction between the tube walls and the abrasive particles can lower the speed, thus reducing the AWJ efficiency. Usually, the length to diameter ratio varies from 50 to 100. The inner diameter of the focusing tube has a similar influence. The inner diameter varies in the 0.5–1.3 mm range, while the length is up to 150 mm. A ratio of 3:1 between the tube inner diameter and the nozzle diameter is recommended (Hashish, 2015).

The cutting parameters refer to:

- *Standoff distance.* This is the distance between the nozzle and the upper surface of the processed part. A higher standoff distance will reduce the depth of the cut, increase surface roughness and the kerf taper. Larger standoff distances can be used when the water jet is more coherent. Typically, the standoff distance varies between 1 and 5 mm.
- *Traverse speed.* This is the relative speed between the cutting head and the part. Lower traverse speeds are associated with a higher quality of the cut because of the more intense interaction between the AWJ and the material. Higher traverse speeds lead to reduced penetration of the jet, with higher surface roughness and increased kerf taper.

- *Inclination angle*. This is the angle between the part surface and the flow direction of the AWJ and can be modified by tilting the cutting head. It can be used in the machining of soft, fragile materials, or to affect the kerf taper formation.

3 Objectives

The current paperwork has the following objectives:

- Acquire by the students of general notions related to AWJ.
- Capacity to use the equipment and the programming software.
- Development of skills concerning:
 - AWJ process planning—realization of part contour, choosing the process parameters, resource planning, machine programming, choosing of the quality parameters.
 - Conducting the experimental test.
 - Checking of the parts.
 - Drawing conclusions.

4 Resources and Organization

4.1 AWJ Machine

The AWJ cutting machine used in the experimental study is KNUTH Hydro-Jet Eco 0615 with the main technical features as follows: the cutting range 1510×610 mm; operating pressure 1500 bar; water jet cutting mode without and with abrasive mix; displacement mode on X and Y axis—automatically, on the Z axis—manually; maximum feed rate 4 m/min; displacement precision on X axis $\pm 0.03/300$ mm; displacement precision on Y axis $\pm 0.02/300$ mm; repeatability on x axis $\pm 0.02/300$ mm; repeatability on y axis $\pm 0.02/300$ mm; motor power 7.5 kW; water flow 2.4 l/min.

The machine is composed of the following main units (Fig. 10):

- The water tank (1) and the cutting head (2) (Fig. 10a).
- The water pressure system (3) (Fig. 10b).
- The dosing system (Fig. 10c).
- The control and command unit contains the NC controller, the hand panel, and the wheel panel (Fig. 10d).

The hand panel contains the buttons for interacting with the NC command and two potentiometers to override the technological parameters (traverse speed, waterjet pressure) (Fig. 11).

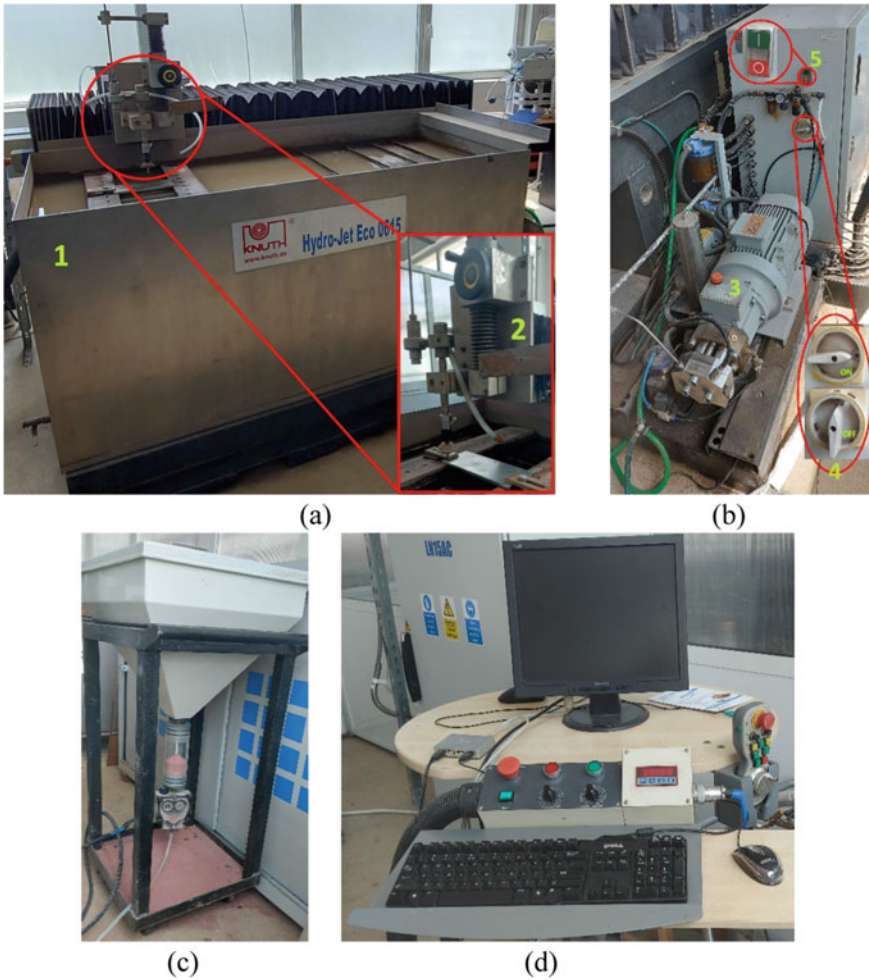


Fig. 10 AWJ cutting machine: water tank and the cutting head (a), ultra high-pressure pump and powering buttons (b), abrasive dosing (c), machine control and command (d)

The handwheel is used for the manual operation of the machine and contains the following elements (Fig. 12): the wheel for the manual displacements (1), NC Start button (2), NC Stop button (3), Jog– minus direction (4), Jog+ positive direction (5), Sand button to start abrasive flow (6), Pump button to start up the pressure pump (7), Pressure button to start the high pressure pump (8), axis selection switch (9), position increment switch (10), Emergency stop button (11), handwheel enable switch (12) on both sides.



Fig. 11 Machine hand panel: Emergency button (1), NC stop (2), NC start (3), Reset (4), Feed rate override (5), Pressure override (6), High pressure display (7)

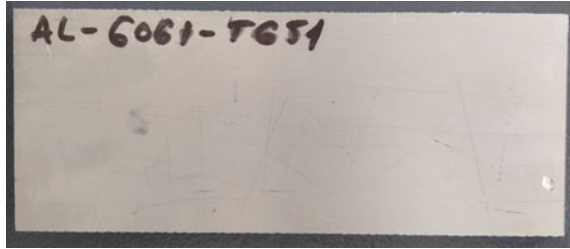
Fig. 12 Machine handwheel



4.2 Material Processed

The part was cut from a $200 \times 70 \times 6$ mm aluminum alloy plate (Fig. 13). Al6061-T651 is a widely used aluminum alloy due to its general characteristics, such as a very good strength-to-weight ratio, good machinability and weldability, high corrosion resistance, and heat treatability. Anodization gives a protective layer for finished parts. Its applications are various and include aeronautical components, couplings, marine fittings and hardware, electrical connectors and components, hydraulic pistons, valves, appliance fittings, decorative hardware, camera parts, bike frames, etc. Chemical composition of Al6061-T651 is presented in Table 4, while mechanical properties are in Table 5.

Fig. 13 Aluminum alloy plate



4.3 The Part

The part chosen for this work combines the most often used geometrical features to exemplify the use of AWJ technology for cutting exterior and interior contours. The part contains straight and circular edges to form the exterior shape whereas the interior contour is a circle (Fig. 14).

5 Session Development

5.1 Turn On/Off the AWJ Cutting Machine

The procedure to turn on/off the AWJ cutting machine is described in the diagram from Fig. 15.

5.2 Job Creation

The AWJ cutting procedure, or the job as denoted by the software, can be divided into two main sections. The first section contains the steps necessary to create the numerical program that the machine uses to cut the contour of the part, whereas the second section contains the steps for the actual AWJ cutting using the NC code.

The software used to set up and control the machine is PACut (Fig. 16a). At the start, the initial screen of the program (Fig. 16b) displays some general information, and the user must click the **PACut** button from the right-side, which opens a new window with the job options (Fig. 17).

The job option window contains three choices:

- New job is used for the creation of a new AWJ cutting project.
- Job list is the database that contains previous AWJ cutting programs, which can be reused or edited.
- Exit when the user wants to quit the program.

Table 4 Chemical composition of Al6061-T651

Element	Al	Cr	Cu	Fe	Mg	Mn	Si	Ti	Zn	Others, each	Others, total
%	95.8–98.6	0.04–0.35	0.15–0.4	Max 0.7	0.8–1.2	Max 0.15	0.4–0.8	Max 0.15	Max 0.25	Max 0.05	Max 0.15

Table 5 Mechanical properties of Al6061-T651

Brinell hardness	Elasticity	Yield strength	Ultimate tensile strength	Elongation at break
95	68.9 GPa	276 MPa	310 MPa	17%

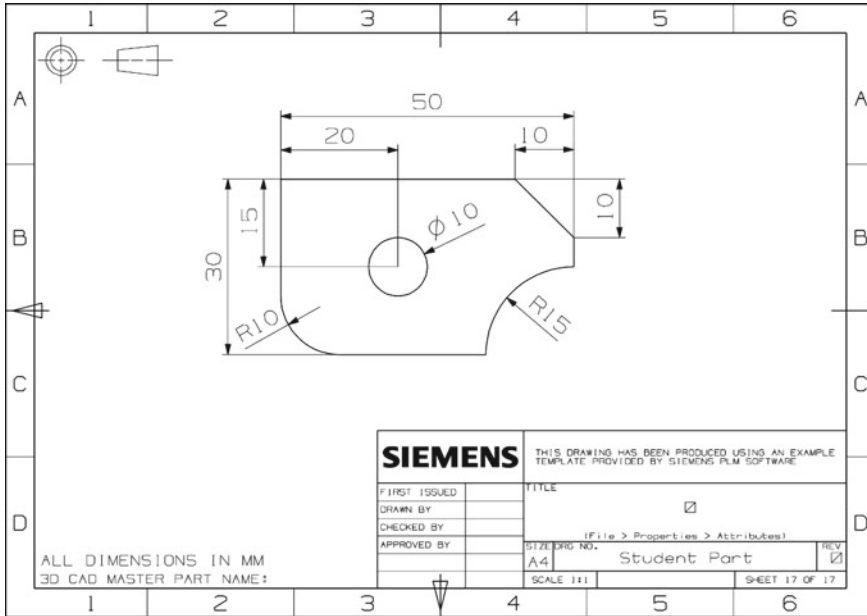


Fig. 14 Part drawing

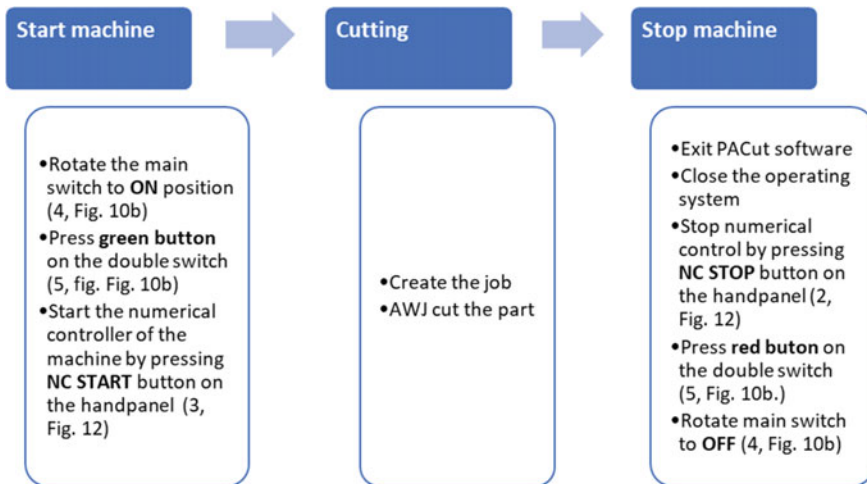


Fig. 15 AWJ cutting machine power on/off procedure

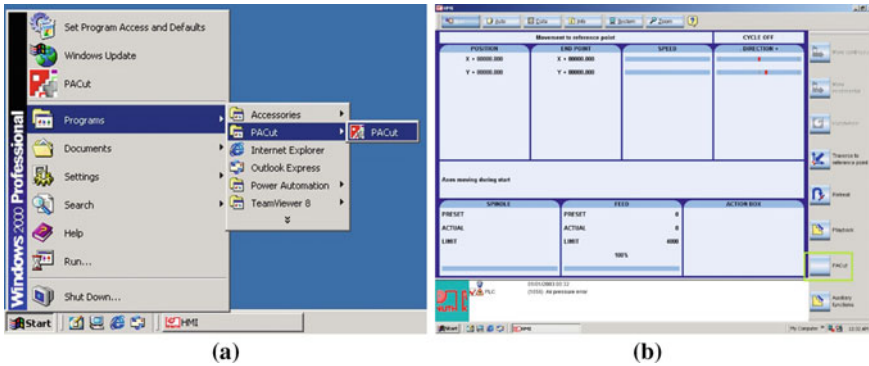


Fig. 16 Program start (a), start screen (b)

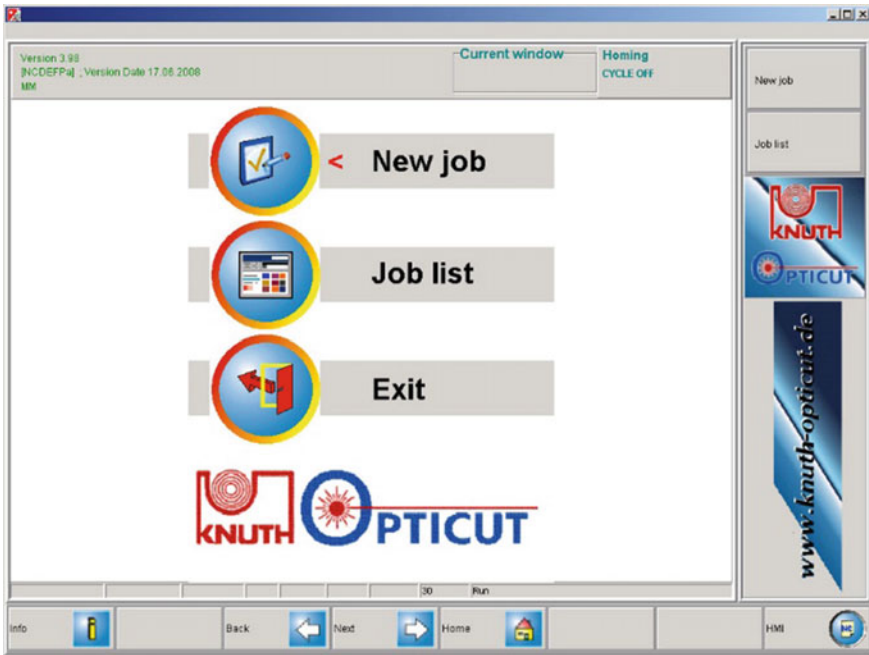


Fig. 17 Job options

For the current work a new job must be created, which opens the interface related to the sheet database (Fig. 18). The sheet database contains inputs from previous works, while also allowing the user the possibility to create new ones. Next, a new sheet is defined by clicking the button *New database entry* from the right-side panel. In the newly opened window (Fig. 19) the user must provide the following information:

- The material field in which the user specifies the material that the part is made of. The current job is carried out using an aluminum alloy Al6061.
- The thickness field in which the user must specify the thickness of the part to be cut. For this job the part will be cut from a plate with a 6 mm thickness.
- Width and height are used to provide the dimensions of the plate used to cut the part from. The plate for this job is 70 × 200 mm.
- Speed is used to specify the value of the cutting head speed, also known as the traverse speed. For the current project, the value of the traverse speed is 50 mm/min.
- Cutting path offset is the distance between the jet axis (focalization tube axis) and the theoretical contour of the part. The value of the offset is a little larger than the radius of the focalization tube internal hole to take into consideration the spread of the jet, so the value was set to 0.6 mm.
- Number of sheets refers to the number of sheets stacked together when one wants to manufacture multiple parts with only one cut. This number is limited by the sheet thickness and the risk that the jet does not penetrate through the entire thickness of the stack. For the current job a single plate is used, therefore the value of the number of sheets is 1.

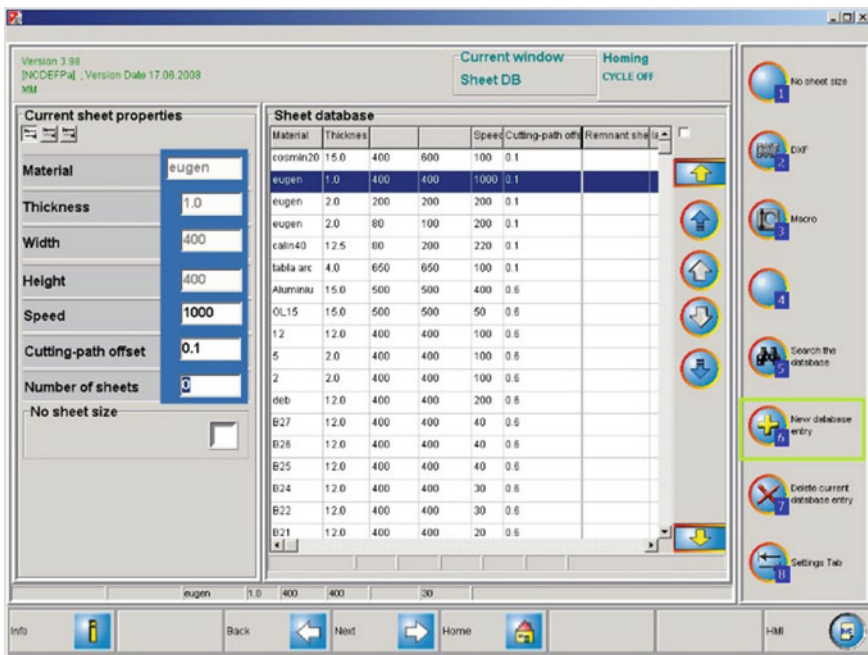


Fig. 18 Sheet database interface

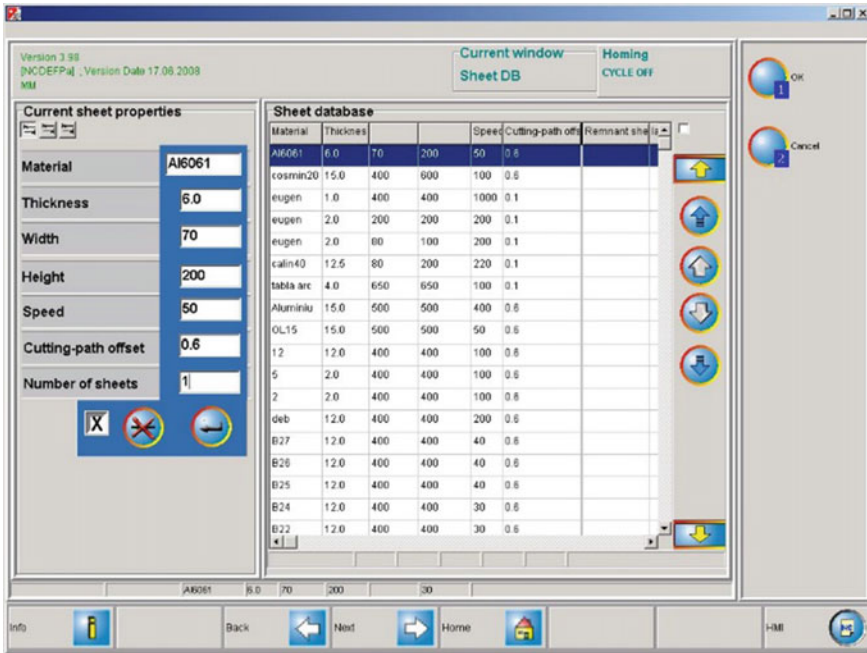


Fig. 19 Creation of a new sheet for the job

Next step of the setup process is to choose the technological parameters, which are accessed by clicking on the third button in the Current sheet properties. In the program interface, the user must introduce values for the following parameters (Fig. 20):

- Abrasive is working as a logical operator with two values: 0 when the cutting is executed only with pressured water, without abrasive, and 1 when the cutting is done with AWJ. For the current job, the parameter is set to 1, since metal cutting requires the use of abrasive material.
- Low pressure sets the minimum pressure of the water jet. For this job, the value is set at 1500 bar.
- Piercing pressure sets the value of the water jet pressure during the initial penetration in the material. For this job, the value is set also at 1500 bar.
- Piercing time sets the time interval used by the AWJ to cut the initial penetration hole into the material. For the current job, the time was set at 8 s.
- Piercing diameter is the diameter of the piercing hole, which was set at 1 mm.
- Cutting pressure sets the pressure of the water jet during the cutting process. For superior cutting quality, this value was set at 1500 bar.
- Sand value sets the value for the abrasive flow rate. In the current job, this parameter was set at 300 g.

To save the values of the parameters, click on the *Save ramp* button (Fig. 20). Next, click on the button *Make a new database entry* to add the newly defined material

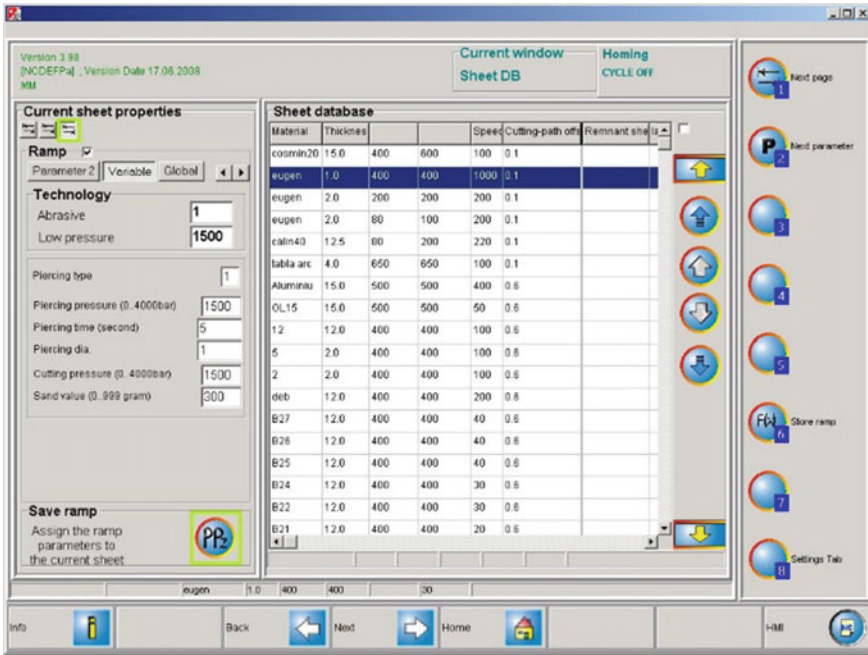


Fig. 20 Technological parameters

to the existing database. After that, the user must click the button *Next* situated at the base of the screen to pass to the subsequent step where the geometry of the cutting contour is defined (Fig. 21).

There are two ways to define the cutting contour, which represents the shape of the part. The first one is to use the drawing module of the PACut software. The second one is to design the part using an external dedicated CAD software and export it to a dxf format file that can be imported afterwards in PACut.

This second way is used to further define the cutting contour into the job. For this, the user must click the button *6 Load DXF file from disk* (Fig. 22) that opens a navigation window to the desired dxf file (Fig. 23). Opening the file brings the contour into the software and the user must click the button *Next* to set up the tailoring of the contour on the sheet or the plate from which the part is cut. The cutting may be executed either on external or internal contours with various shapes, such as polygonal, circular, or combined. The cutting must start and end at certain distances from the contour (lead in and lead out) to avoid damaging the shape of the part.

Using this interface (Fig. 24) the user can set the following parameters:

- The orientation angle defines the angular position between the contour and the plate. Depending on its shape and dimensions, contour rotation can ensure a higher degree of material usage.



Fig. 21 Adding the material in the database

- The lead-in and lead-out size, which defines the length of the paths of the cutting head at the beginning (green arrow representation) and at the end of the cutting (red arrow representation), respectively, when external contours are executed. For the current job, the lead-in (entrance distance) was set at 3 mm, while the lead-out (exit distance) is 2 mm.
- For the internal circular contour, similar values were assigned to the lead-in distance (3 mm) and the lead-out distance (2 mm) of the cut.
- There are various strategies to approach the beginning and the end of the cutting paths: either straight, or tangential to the contour.

After clicking the button *Next*, a new interface opens. If multiple parts are to be cut from the sheet, the user can define a matrix of contour distribution with the desired number of lines and columns. For the current job only one part is cut, as represented in Fig. 25. In addition, in this interface the NC code is saved with an assigned name (*StudentPart*) by clicking button *1 Save NC program to job list*.

This concludes the first section of the AWJ cutting procedure.

The subsequent steps are related to the second section of the process, where the NC program is loaded into the machine controller and the part is cut out using the AWJ.

Thus, the next step is to find the NC program in the Job list (Fig. 17). There are two possibilities, one is by scrolling the list, the other is to use the Search function.

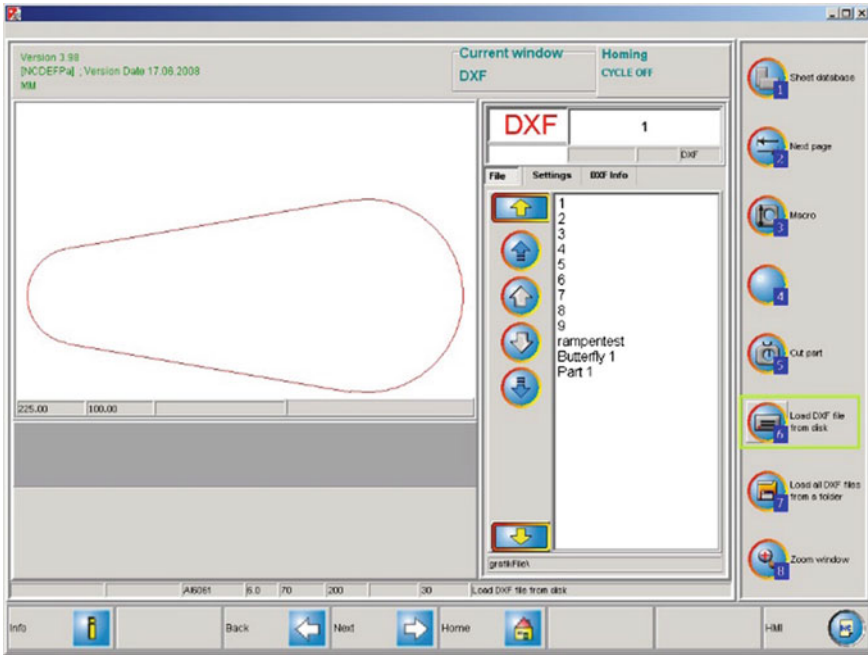


Fig. 22 Definition of the cutting contour

After the program loads, the main characteristics are displayed on screen (Fig. 26). Click the button *Next* to enter the cutting program.

The interface displays the contour of the part together with the lead in and lead out distances. It is necessary to set the point of origin for the path of the cutting head: click 5 *Manual* button (Fig. 27a), then 1 *Move machine* button (Fig. 27b) to establish the position of the origin point. The coordinates of the origin point must be introduced and after that click on 4 *Shown position = start position* button, then 6 *Move machine to start point* button (Fig. 28). On the machine handwheel click on the *START* button to move the cutting head in the machine origin point. After another click on the *START* button from the handwheel to move the cutting head in the starting position for cutting (Fig. 12). Click *Back* button to return to the previous screen. The standoff distance is set manually to 3 mm by using a gauge block (Fig. 29). Press the *Start cutting* button (Fig. 27a) and then *START* button on the handwheel and the machine will start cutting the programmed contour (Fig. 30).

During the operation, the position of the cutting head can be followed in real time on the screen (Fig. 31).

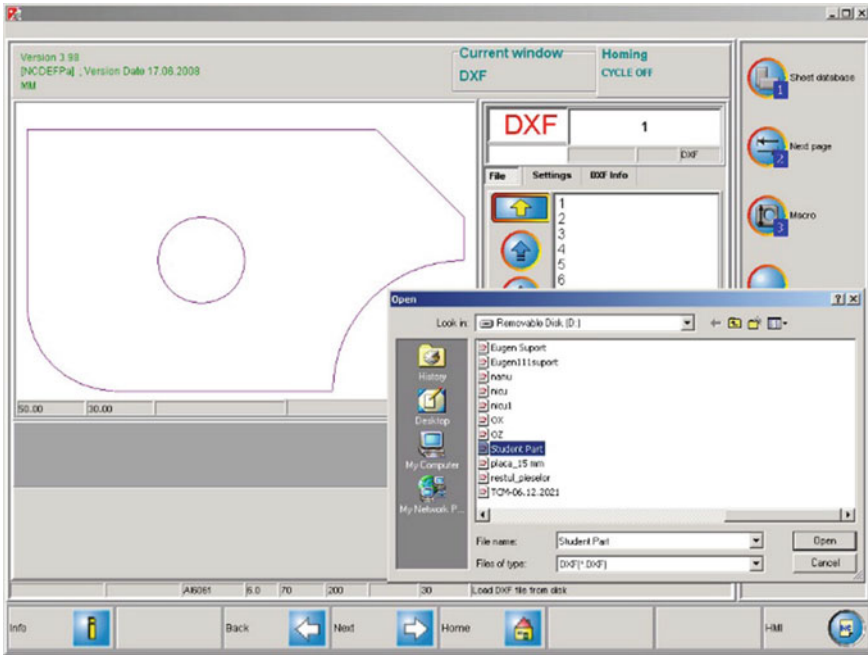


Fig. 23 Import the contour from the dxf file

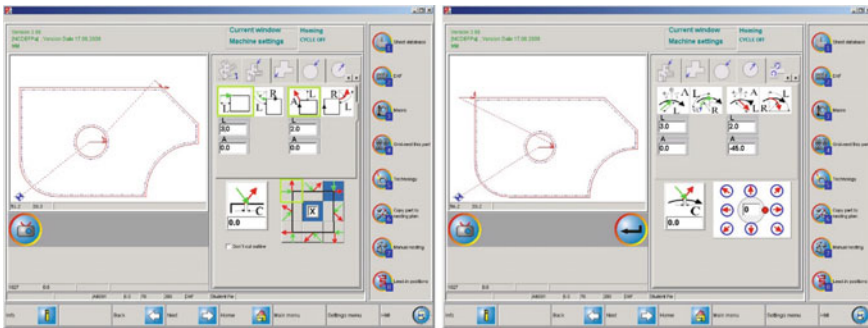


Fig. 24 Setting of the cutting path

6 Outcomes

The part obtained from the AWJ cutting process is presented in Fig. 32.

The quality of the part is assessed by examining the following elements: dimensional accuracy, contour defects, kerf angle, and kerf surface aspect.

The dimensions of the part can be measured using various instruments but, for this work, a profile projector was chosen. Profile projectors, also known as optical

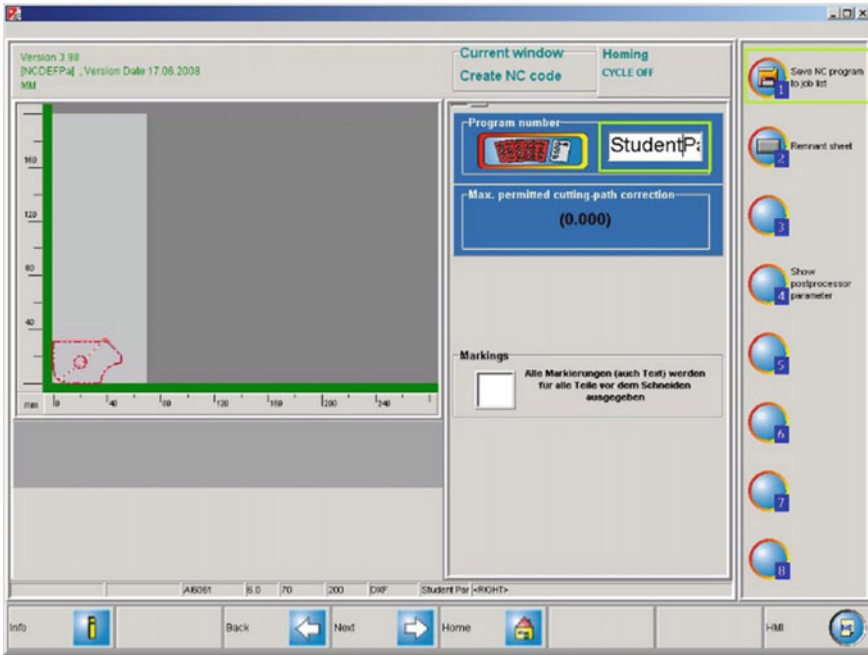


Fig. 25 Save NC program to the job database

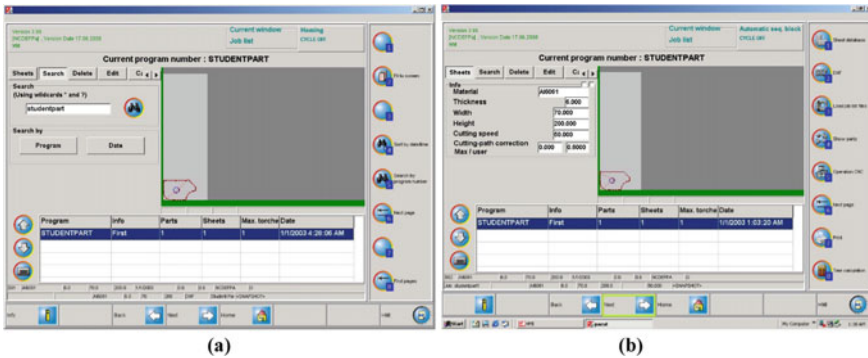


Fig. 26 Loading an NC program from the Job list

comparators, use a light source to illuminate a part placed on a table to obtain a shadow that is projected on a screen. A special optical system (telecentric) is used to obtain accurate measurements of the objects by projecting a shadow with constant size and no warping irrespective of the position on the table.

A Mitutoyo PH-A14 profile projector (Fig. 33) was used as it can measure the linear and circular dimensions of the part, but it also allows highlighting the

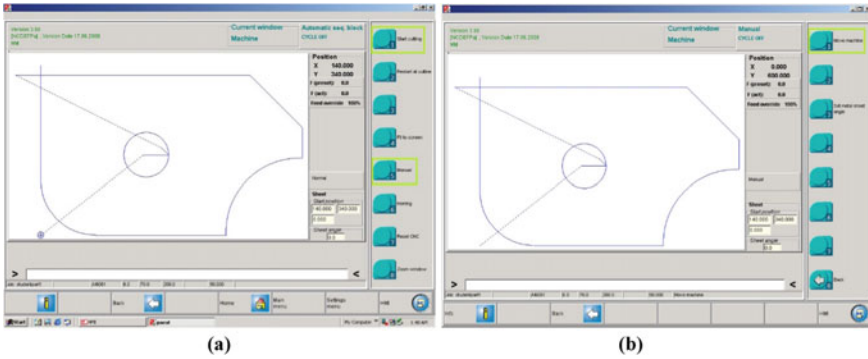


Fig. 27 The cutting head path

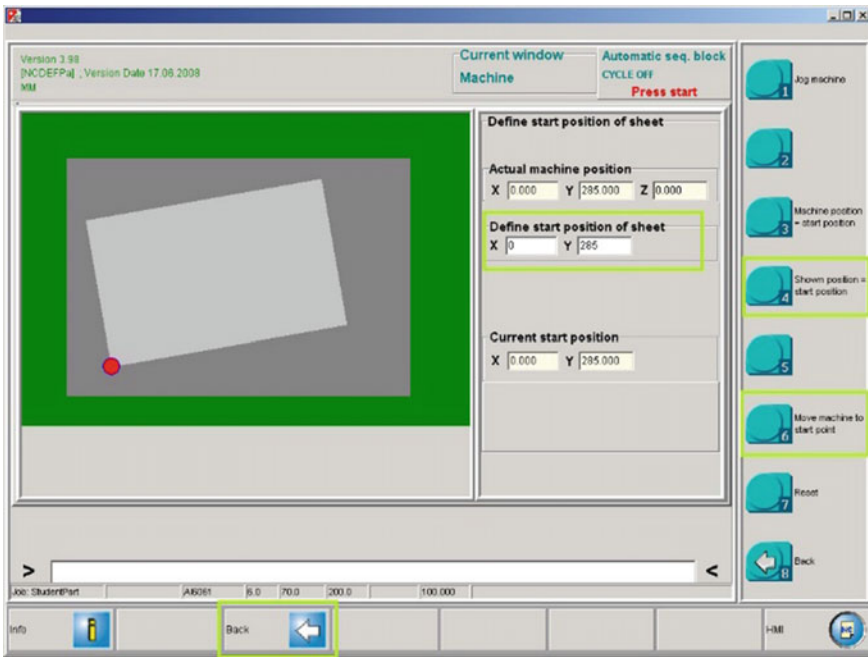


Fig. 28 Setting the origin point

shape defects due to the $10\times$ magnification factor. This is an inverted-reversed projector, meaning that the projected image is flipped both vertically and horizontally compared to the position of the object. It has a digital counter to measure absolute and incremental displacements or coordinates in a range of 200×100 mm.

The screen has a rectangular scale printed on it and an additional scaled dial can be mounted for more complex measurements. By aligning the shadow with the scale,

Fig. 29 Setting the standoff distance



Fig. 30 AWJ cutting progress

the dimensions of the part can be measured from the movement of the table in the cartesian XY coordinates that are displayed on the digital counter. Some dimensions can be determined directly, when the movements are recorded along a single axis, whereas other dimensions require calculations if the movements are on both axes.

The distance between two points in a cartesian XY system, $A(x_A, y_A)$ and $B(x_B, y_B)$, can be calculated using the equation:

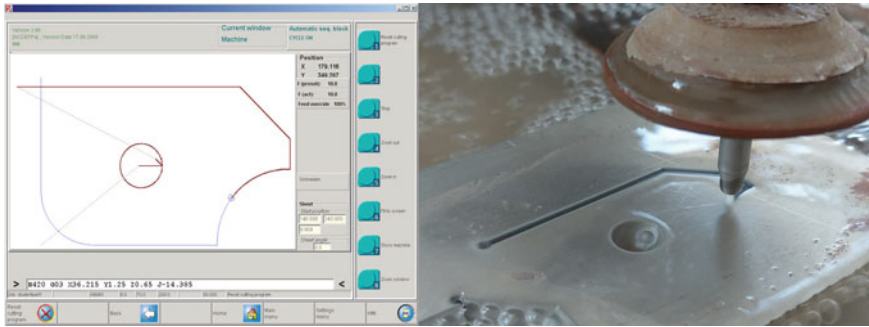


Fig. 31 Monitorization of the cutting head position

Fig. 32 AWJ cut part



$$\Delta_{AB} = \sqrt{(x_B - x_A)^2 + (y_B - y_A)^2} \tag{1}$$

6.1 Dimensional Accuracy

The following dimensions were measured: the length of the part L , the width of the part w , the arc radius R_1 , shoulder radius R_2 , chamfer dimensions l_1 and l_2 , and the hole diameter \varnothing (Fig. 34). Each measurement was repeated three times and the average value was considered the effective dimension.

For the measurement of the length of part L , the part was aligned with the screen grid and the displacement was recorded on the digital counter. The recorded values and the average length are presented in Table 6. A similar approach was used to measure the width w and chamfer dimensions, l_1 and l_2 (Fig. 35).

For the measurement of arc radius, the contour was first centered (Fig. 36a) and the point was assigned as origin $O(0,0)$. By measuring the coordinates for a series of

Fig. 33 Mitutoyo PH-A14 profile projector



Fig. 34 Part dimensions

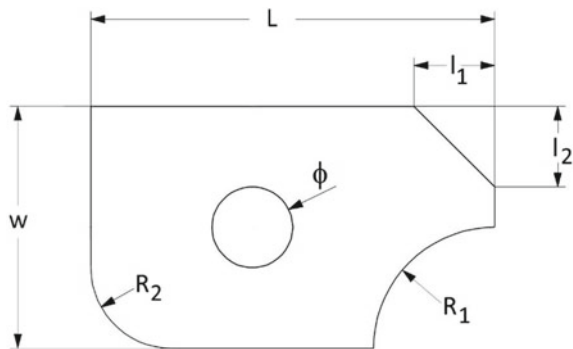


Table 6 Linear dimensions measurement

Verified dimension [mm]	Nominal value	Measurement			Average	Error
		1	2	3		
Length L	50	49.95	49.92	49.93	≈ 49.93	0.07
Width w	30	29.91	29.92	29.92	≈ 29.92	0.08
Chamfer l ₁	10	9.93	9.95	9.93	≈ 9.94	0.06
Chamfer l ₂	10	10.06	9.99	10.07	≈ 10.04	-0.04



Fig. 35 Measurement of part dimensions

points on the circumference, the radii were calculated using the equation mentioned previously and the average value is the arc radius (Table 7).

Shoulder radius was measured using the additional dial for radii and angle measurement (Fig. 36b). The part was first aligned with the axes, then the table was moved until there was the best overlap between the contour and the circular marks of the dial. The radius is calculated as the average value of the displacements and the reading on the dial (Table 8).

For the hole measurement (Fig. 37) three diameters were measured in different directions and the results were averaged (Table 9).

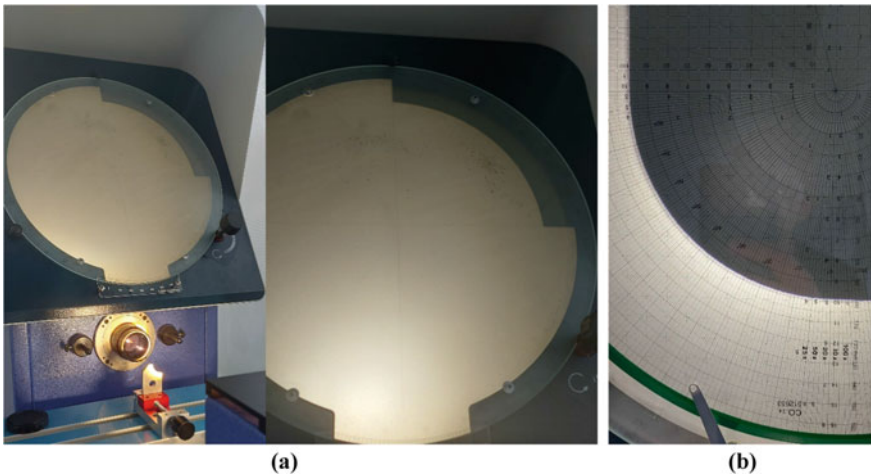


Fig. 36 Radii measurement

Table 7 Arc radius R₁ measurement

Point coordinates	Radius	Average radius [mm]	Nominal radius [mm]	Error
(14.915, 0)	$\sqrt{(14.915 - 0)^2 + (0 - 0)^2} = 14.915$	14.98	15	0.02
(0, 15.075)	$\sqrt{(0 - 0)^2 + (15.075 - 0)^2} = 15.075$			
(14.205, 4.59)	$\sqrt{(14.205 - 0)^2 + (4.59 - 0)^2} = 14.92$			
(9.86, 11.26)	$\sqrt{(9.86 - 0)^2 + (11.26 - 0)^2} = 14.97$			
(4.41, 14.355)	$\sqrt{(4.41 - 0)^2 + (14.355 - 0)^2} = 15.02$			

Table 8 Shoulder radius measurement

Verified dimension	Nominal value	Measurement			Average	Error
		1	2	3		
Radius R ₂ [mm]	10	9.885	9.865	9.90	≈ 9.88	0.12

Fig. 37 Hole diameter measurement

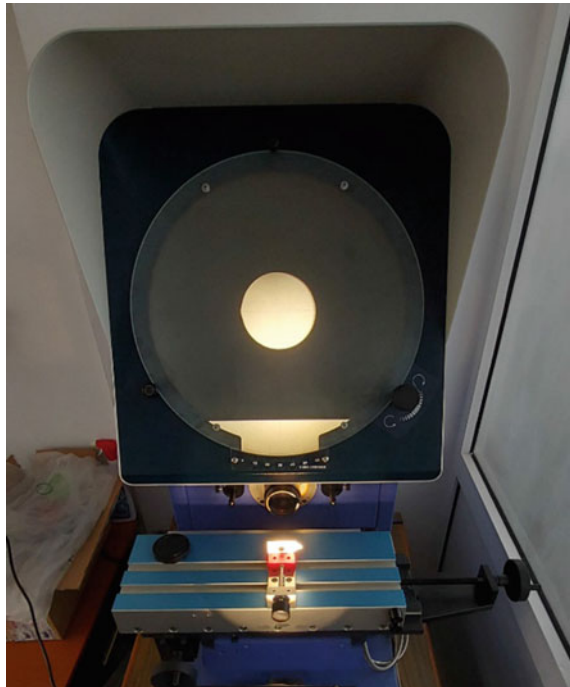


Table 9 Hole diameter measurement

Verified dimension	Nominal value	Measurement			Average	Error
		1	2	3		
Hole diameter \varnothing [mm]	10	10.16	10.21	10.18	≈ 10.18	- 0.18

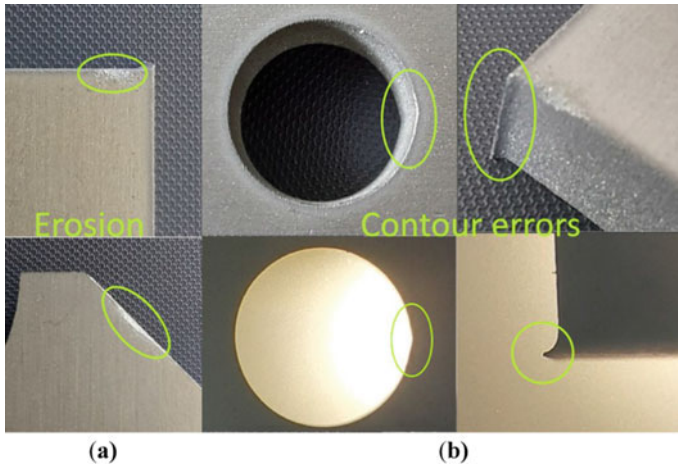


Fig. 38 Defects of AWJ cut parts

6.2 Contour Defects

A series of contour defects can be observed on the part:

- Erosion of the edge produced by the abrasive (Fig. 38a);
- Contour shape errors, such as the roundness deviation of the hole, caused by the prolonged action of the AWJ at the beginning and the end of cutting, or the burr remained at the end of the exterior contour cutting (Fig. 38b).

6.3 Kerf Angle

Kerf angle occurs in AWJ cutting due to the difference between the widths of cut at entrance and exit, respectively. This is caused by the loss of energy of the waterjet and is influenced by various factors, such as the material being processed, the waterjet pressure or the traverse speed. Kerf angle is important when vertical cuts are required. The angle was measured (Fig. 39) and the results are in Table 10.

Fig. 39 Kerf angle

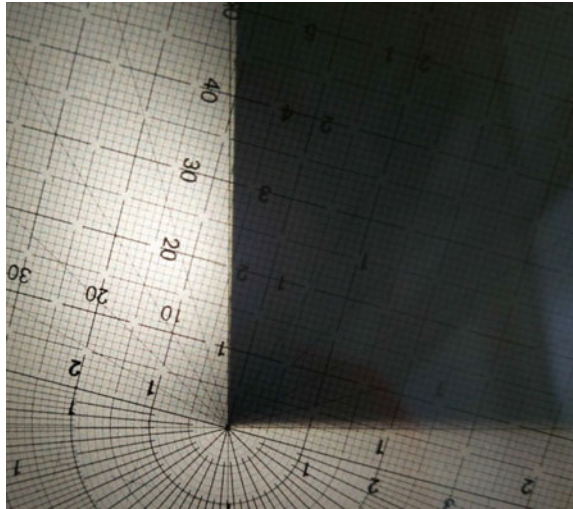


Table 10 Kerf angle

Verified dimension	Nominal value	Measurement			Average	Error
		1	2	3		
Kerf angle α [°]	0	1° 10'	1° 6'	1° 8'	1° 8'	1° 8'

6.4 Kerf Surface Aspect

The surface of the cut (kerf surface) is an important element for the quality of the part. Visual examination of the surface reveals the two areas (Fig. 40):

- the fine cut area (1) that has a smoother aspect because the abrasive particles had higher energy and removed the material by abrasion;
- the rough cut area (2) that has more striations because the material is removed by erosion.

Surface roughness Ra was measured in the middle of the kerf surface using a Mitutoyo SJ-201 roughness meter (Fig. 41) and the results are presented in Table 11.



Fig. 40 Kerf surface

Fig. 41 Surface roughness measurement

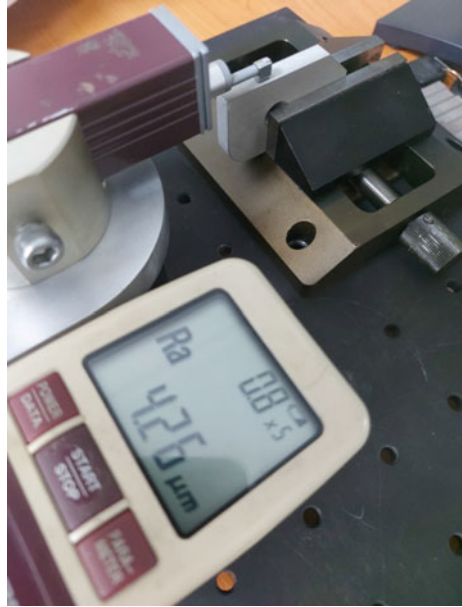


Table 11 Surface roughness

Parameter	Measurement					Average
	1	2	3	4	5	
Surface roughness Ra [μm]	4.36	4.38	4.26	4.13	4.27	4.28

7 Deliverables and Assessment

7.1 Quiz—Knowledge Testing

1. Explain the working principle of the hydraulic pressure intensifier.

.....

2. Choose the advantage of AWJ cutting:

- (a) It depends on water quality
- (b) There is no heat affected zone on the material
- (c) Reduced levels of noise during operation

3. What is the role of the water filtering subsystem

- (a) Reduces the concentration of calcium carbonate
 - (b) Removes debris from the used water
 - (c) Increases the pressure of the water jet
4. What is the value of the pressure created by the intensifier?
- (a) up to 35 MPa
 - (b) up to 100 MPa
 - (c) up to 400 MPa
 - (d) up to 1000 MPa
5. What is the purpose of the catcher tank?
- (a) Movement of the part during processing
 - (b) Collect the residual water and abrasive particles
 - (c) Provide water for the AWJ machine
6. What is the speed of the waterjet in AWJ Machining?
- (a) 200 m/s
 - (b) 400 m/s
 - (c) 900 m/s
 - (d) 1200 m/s
7. What is the recommended length to diameter ratio for the focalization tube?
- (a) 4–20
 - (b) 20–50
 - (c) 50–100
 - (d) 100–150
8. What are the typical values of the interior diameter of the focalization tube?
- (a) 0.1–0.3 mm
 - (b) 0.5–1.3 mm
 - (c) 0.2–2 mm
 - (d) 1–2.5 mm
9. What is the standoff value range in AWJ Machining?
- (a) 0.1–1 mm
 - (b) 1–2 mm
 - (c) 1–5 mm
 - (d) 2–10 mm
10. Name the disadvantage of the AWJ Machining:
- (a) It can only cut simple contour shapes
 - (b) Precision of the cut reduces when material thickness increases
 - (c) It is only suitable for soft materials
 - (d) AWJ increases surface hardening

7.2 Quiz Answers

1. The intensifier is made of two cylinders with diameter ratios from 1/10 to 1/25. On the larger side the pressure on the hydraulic plunger is 5–35 MPa and because of the diameter ratio, in the second cylinder the pressure can rise to 400 MPa.
2. (b) There is no heat affected zone on the material
3. (a) Reduces the concentration of calcium carbonate
4. (c) up to 400 MPa
5. (b) Collect the residual water and abrasive particles
6. (c) 900 m/s
7. (c) 50–100
8. (b) 0.5–1.3 mm
9. (c) 1–5 mm
10. (b) Precision of the cut reduces when material thickness increases

7.3 Measurement Results

Students are required to fill the part drawing with the dimensions obtained after measuring the part by themselves (Fig. 42).

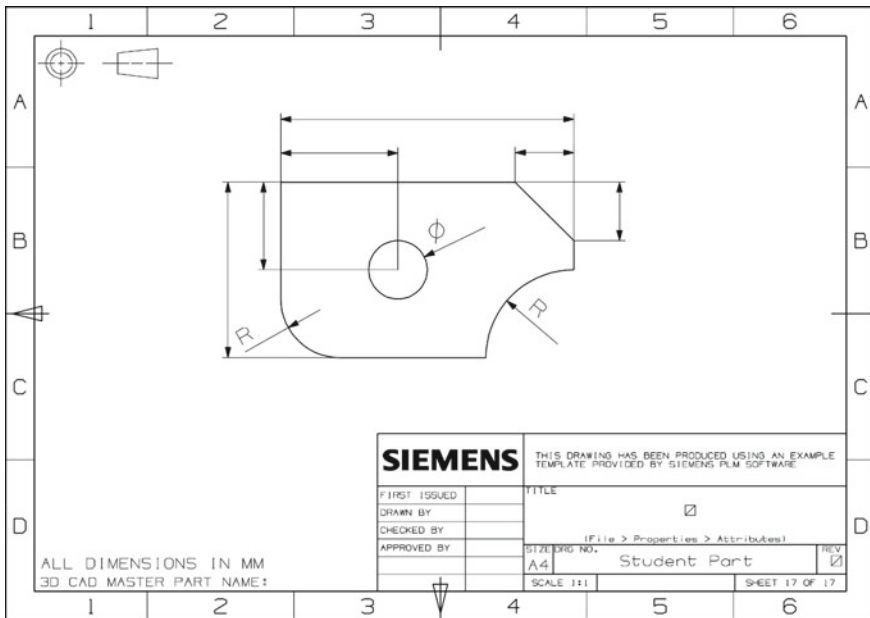


Fig. 42 Measurement report

Observations:

Students are required to mention any observations concerning the aspect and the quality of the part.

.....

.....

.....

.....

.....

8 Conclusions

This chapter introduces waterjet cutting: the principle of operation, the construction of waterjet cutting machines, the abrasive materials used, kerf geometry and the processing parameters. The purpose of the chapter is to provide students with the basic capabilities for programing and operating the waterjet cutting equipment. A systematic tutorial is provided for creating a specific machining technology, programing the machine, and executing the AWJ cutting operation. A method of controlling the quality of the processed part is also presented. The chapter ends with a knowledge test quiz.

References

Barton.com. (2023). *Technical data and physical characteristics ADIRONDACK HPX garnet abrasives*. <https://www.barton.com/wp-content/uploads/2021/04/Technical-Data-ADIRONDACK-HPX.pdf>

Engemann, B. K. (1993). *Schneiden mit Laserstrahlung und Wasserstrahl - Anwendung, Erfahrungen*. Verlag GmbH.

Hashish, M. (1987). Method and apparatus for forming a high velocity liquid abrasive jet. US Patent: Vol. 4,648,215.

Hashish, M. (2015). Waterjet machining process. In A. Y. C. Nee (Ed.), *Handbook of manufacturing engineering and technology* (pp. 1651–1686). Springer London.

ISO/TC 44 N 1770: Water jet cutting—Geometrical product specification and quality (2010). <https://farsungroup.com/assets/farsun-group-waterjet-iso.pdf>

Jegaraj, J. J. R., & Babu, N. R. (2005). A strategy for efficient and quality cutting of materials with abrasive waterjets considering the variation in orifice and focusing nozzle diameter. *International Journal of Machine Tools and Manufacture*, 45(12–13), 1443–1450.

Natarajan, Y., Murugesan, P. K., Mohan, M., & Liyakath Ali Khan, S. A. (2020). Abrasive water jet machining process: A state of art of review. *Journal of Manufacturing Processes*, 49, 271–322.

Sisodia, V., Gupta, S. K., Salunkhe, S., Murali, A. P., & Kumar, S. (2023). An experimental investigation on machining of hardened AISI 440C stainless steel using abrasive water jet machining process. *Journal of Materials Engineering and Performance*.

Summers, D. A. (2003). Waterjetting technology. In *Waterjetting technology* (1st ed.). CRC Press.

Introduction to Computed Tomography: Application to the Inspection of Material Extruded Tensile Testing Specimens



Marcos Alonso, Eugenio López, David Álvarez, and Diego Carou

1 Introduction

The growth of additive manufacturing has rapidly changed the way in which many industries approach their fabrication methods. Additive manufacturing was born as a rapid prototyping process, quickly expanding into many different areas. Although the technology has come a long way in recent years, increased progress and investigation are still necessary to reach the required quality manufacturing standards by the industry (Khosravani & Reinicke, 2020).

In the last decades, different printing technologies were developed, and, to create a common ground for manufacturers and users, the ISO/ASTM 52900 includes the standards for additive manufacturing. Printing covers a wide range of applications, mainly using plastic materials such as polylactic acid (PLA) and acrylonitrile butadiene styrene (ABS), among others. Many makers, researchers, and industries use this technology to create prototypes, small series of parts, and mass-production products.

Material extrusion technology has as a drawback its inability to provide tight dimensional tolerances (Mou & Koc, 2019). Manufacturing failures are substantial when printing (Petsiuk & Pearce, 2020), and the reliability of the process depends on the setting and printing parameters (Mohanty et al., 2022). Moreover, the geometry of the specimen differs from the computed-aided design model (CAD model) to be printed because of inadequate bonding of filament layers or the appearance of voids

M. Alonso · D. Carou (✉)

Departamento de Deseño na Enxeñaría, Escola de Enxeñaría Aeronáutica e do Espazo,
Universidade de Vigo, Ourense, Spain
e-mail: diecapor@uvigo.es

E. López

Instituto de Agroecoloxía y Alimentación, Facultad de Ciencias, University of Vigo, 32004
Ourense, Spain

D. Álvarez

CINTECX, Universidade de Vigo, EEI, ENCOMAT Group, 36310 Vigo, Spain

of different nature: raster gap voids, partial neck growth voids, sub-perimeter voids, intra-bead voids, and infill voids (Tao et al., 2021). When printing, these voids can be formed in a non-uniform way. Both negative and positive air gaps can appear in different locations generating non-uniform structures (Phillips et al., 2022). Thus, the mechanical strength of the printed parts decreases (Dickson et al., 2017).

The actual geometry of the printed part specimen determines its mechanical strength. Thus, the analysis of the accuracy and reliability of the printed specimens regarding their CAD models will allow for a greater knowledge of the technology and a better understanding of the behavior of the specimens when subjected to mechanical testing. In addition, understanding the printing process and its relation to mechanical properties can help optimize the weight of the part-saving material while achieving the tensile strength requirement (López et al., 2022).

Outcomes of the printing process, such as the dimensional tolerance, surface quality, and mechanical properties, heavily depend on the selection of the printing parameters (Pérez et al., 2018; Prabhakar et al., 2021). Many of these parameters are interrelated, making it difficult to identify an optimum setting (Kristiawan et al., 2021). In general, the printing parameters can be sorted into three main groups: geometric (nozzle size, filament size), processing (melting temperature, bed temperature, printing speed), and structural (layer thickness, infill geometry, infill density, raster angle, raster gap) (Prabhakar et al., 2021).

The printing process is subjected to many factors that may affect the specimen's geometry. Thus, the user can select, for instance, different top and bottom layer configurations, the number of walls, infill density and patterns, and layer thickness. This selection will lead to different geometries with critical features such as the distance between the printing paths, defined by the raster model of the part, width, and the crossroads between printing paths (Zhang et al., 2021). Moreover, it is important to note that the printing orientation is critical for determining the contour of the part as it defines the relative position of the bottom, top, and wall geometries around the middle cross-section of the specimens (Birosz et al., 2022). There is a body of research focused on the study of the geometry of the printing parts to optimize mechanical strength while diminishing mass and printing time as, for instance, was done by Schmitt et al. (2020) in a study of ABS printed components for the automotive sector. Chacón et al. (2017) studied the build orientation, layer thickness, and filament feed rate. The first conclusion they drew was the anisotropy; build orientation greatly affects the anisotropy of the mechanical properties such as ductility or the failure behavior of the pieces. The on-edge and horizontal orientations provide the biggest influence on the strength and strain values. For example, the upright configuration's tensile strength turned out to be 78 % lower. Regarding layer thickness, no major changes were observed for the on-edge and horizontal orientations. With the upright configuration, the strength increased with the higher layer thickness. Printing speed had a minimum effect on mechanical properties. However, the upright position showed a slight decrease in strength with the feed rate. The lower tensile strength of the upright specimens was also identified by Cerda-Avila et al. (2020) when using PLA. Fontana et al. (2022) analyzed the layer height and infill density. The most important conclusion was that layer height had more relevance than infill density

when referring to pure mechanical strength. Leite et al. (2018) report focused on infill density, extrusion temperature, raster angle, and layer thickness. The strength and stress data increased with infill density. With the rise of extrusion temperature, the layer adhesion improves, but in some cases, with the decrease of viscosity, there was a distortion of the expected shape, resulting in oval-shaped layers. The raster angle was found to vary the distribution of stress throughout the piece. Finally, Lanzotti et al. (2015) reported that the number of perimeters that define the thickness of the contour has a bigger influence than the layer height on the value of the strain at failure.

2 Background

Quality in additive manufacturing is of great importance and the parts must guarantee that they meet the desired ‘repeatability, reproducibility, reliability and preciseness’ as stated by Kim et al. (2018). The quality of the parts depends on the decisions made during the whole printing process: design process, printing process, post-process, and evaluation process (Kim et al., 2018). Throughout the years, many types of destructive and non-destructive tests have been used for part evaluation. Although visual inspection is the most common method due largely to its simplicity, the internal geometry of the specimens requires proper inspection. In this sense, for instance, 2D X-ray imaging (Ng et al., 2022) and X-ray tomography (Rifuggiato et al., 2022) were studied to evaluate defects in ABS-printed parts.

Computed tomography belongs in the non-destructive testing technology category, referring to all methods and techniques for product quality assurance and inspection without destroying the part. CT consists of an X-ray source that ejects photons transmitted through an object and captured by an X-ray detector (Cantatore & Müller, 2011). This technology provides great results in many applications, such as finite element method (FEM) validation, internal defects data, porosity evaluation, or dimensional analysis. CT helps to determine the integrity of a component or structure and measure different product characteristics. Cost and time reduction are two main reasons for expanding non-destructive testing processes regarding destructive methods. Computed tomography gained popularity in many different industries, such as electronics, medicine, food, archaeology, aerospace, and automotive (Kalender, 2006; Khosravani & Reinicke, 2020).

As additive manufacturing expands more and more, the demand for evaluation and control of these parts has risen. Computed tomography was used for the first time for medical purposes back in the early 1970s; appearing the first Dimensional CT measurements in the 1990s in sectors such as the automotive and the medical (El-Katatny et al., 2010; Kruth et al., 2011; Losano et al., 1999). A comprehensive review of the application of CT was presented by Thompson et al. (2016).

The data obtained from CT scans can be grouped into four groups:

- Defect detection: several types of defects can appear in 3D printed parts that can change the mechanical behavior of the parts (Holzmond & Li, 2017). It has been reported that pores inside the specimens can have a crucial role in the fatigue behavior of the parts (Leuders et al., 2013). CT scans are also used to inspect the raw material to prevent failure before printing (Bond et al., 2014).
- Dimensional evaluation: CT is typically used for linear measurements, wall thickness, and comparing the CAD model with the printed part. A high-quality scan and a calibrated system are needed to perform accurate measurements. Although CT scanning can provide internal measurements that would be impossible to obtain with other methods, such as CMM (coordinate measuring machine), optimizing parameters is needed to reduce uncertainty.
- Density measurement: these procedures are used for raw materials and final products. The possibility of obtaining the three-dimensional arrangement of pores via X-ray scanning represents a very accurate measurement and a clear advantage of this method over other previously used procedures (Spierings et al., 2011). CT can provide the volumetric density of the printed parts. By measuring the density and comparing it to the bulk density of the material used, it is possible to know the porosity.
- Surface roughness analysis: the surface roughness examination of 3D printed components with CT is a relatively new practice that has already been tested and proven to be effective (Snyder et al., 2015). It is very useful for analyzing the internal surfaces of the printed parts. It has also been proven that the resolution and magnification of surface topography have a visible effect on the results of these measurements (du Plessis et al., 2013).

In this chapter, we apply these rapid-growing technologies to inspect the printing results of several specimens using different printing parameters in material extrusion. Understanding the differences between the actual geometry of the printed specimen against the CAD model is critical when assessing the mechanical behavior of the parts.

3 Learning Objectives

The objectives aimed at the practical sessions are the following:

- To enhance understanding of the material extrusion process.
- To be able to analyze the different printing parameters and their influence on the outcome of the process.
- To become acquainted with tensile testing standards.
- To recognize the significance of non-destructive testing and, particularly, computed tomography.
- To acquire skills to analyze parts using CT technology.
- To evaluate the results of the process and compare them against the expected ones.

4 Resources and Organisation

This section describes the materials and equipment used. The filament used for printing was polylactic acid (PLA) manufactured by Smart Materials 3D of 2.85 mm in diameter, the printer was the Ultimaker 3Extended desktop printer, and the software was the Ultimaker Cura.

Computed tomographies were obtained with a YXLON FF20 cone beam CT equipped with a 190 kV X-ray transmission tube and a VAREX (Varex Imaging Inc.) flat panel detector with a pixel matrix 2880 by 2800 and CsI scintillation screen (YXLON, 2018). Reconstruction of 3D images was performed by the Siemens CERA-API software running on a workstation with 2x INTEL XEON GOLD 6126 processors at 2.6 GHz and 2x NVIDIA Quadro P6000 GPUs. Reconstructed 3D images were processed with Avizo 3D version 2021.1 (FEI, ThermoFisher Scientific) for image processing, quantification, and analysis.

The session is organized for groups of undergraduate engineering students. Because of the available space around the CT machine and computer, small groups of 3–4 students should be arranged. The time required for carrying out the activities is large. So, homework and processing time without supervision are recommended to take advantage of time. In this regard, students are required to create the g-codes at home. Subsequently, the printing can be done in the lab, so that the instructor, ensuring all required materials are available, can then bring the specimens to the session. Therefore, the session properly requires a two-to-three-hour slot per group. Finally, the instructor will gather all results and present them to the students in a convenient way: a detailed document or a wrap-up presentation of likely 30 min.

5 Session Development

As previously mentioned, preliminary steps are necessary to obtain the tensile testing specimens. In this first stage, the students should design the printing specimen using CAD software at home according to UNE 166005:2012 (AENOR, 2012). This standard requires printing specimens in three orientations: horizontal H , on-edge E , and vertical V . Thus, two alternative CAD models can be generated: H or E and V . The H or E are identical models for printing at horizontal and on-edge orientations, and the V model is aimed for the upright orientation only. The instructor should require groups to print the two geometries in the three orientations to compare them at the end.

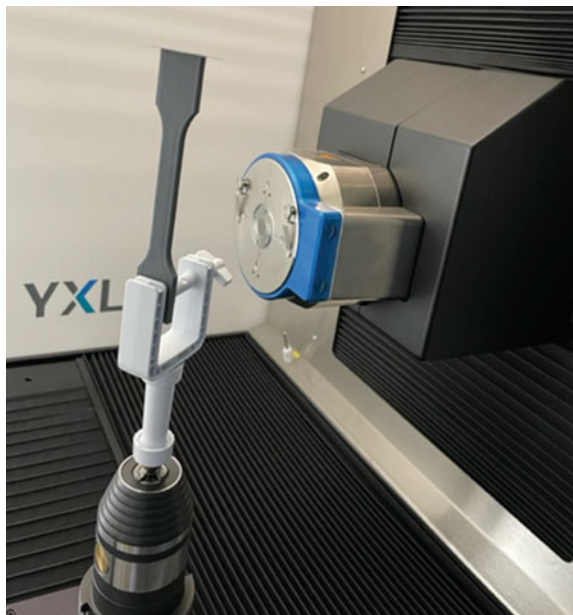
In addition to the build printing orientation, other factors are relevant to defining the geometry of the specimen. Material extrusion is especially suited to work with pieces not fully solid. In this sense, the infill density and the number of perimeters are critical parameters to define the internal structure of the printed specimen. The same occurs for both the top and bottom thickness.

Table 1 Process parameters used as experimental factors

Parameter	Value
Layer height (mm)	0.25
Wall thickness (mm)	0.65
Top and bottom thickness (mm)	0.5
Infill density (%)	40
Infill pattern	Grid
Printing temperature (°C)	210
Bed temperature (°C)	60
Printing speed (mm/s)	30
Build orientation	Vertical

For simplicity, the following steps are described for one specimen, the vertical one. This specimen has a contour completely defined by the wall thickness in the middle section, which is the relevant section for tensile testing. The specimen was printed with an infill of 40 % (in volume) and a wall thickness of 0.65 mm (2 perimeters): the outer wall of the perimeter had a width of 0.35 mm, while the inner one had a 0.3 mm width. Table 1 shows the full breakdown of process parameters. The printing temperature was 210 °C, and the bed temperature was 60 °C. The printing speed was fixed at 30 mm/s.

Once the specimen is printed, it is time to scan it using the CT machine. A circular scan was done on the specimens fitted upright for optimal performance (Fig. 1).

Fig. 1 Positioning of the test specimen on the CT inspection cabin

The voltage and current intensity of the X-ray source can be optimized to enhance the contrast of images. For PLA, being an organic polymer with a low opacity to X-rays, the contrast was optimized by decreasing the voltage to 90 kV with a current intensity of 50 μ A. In addition, the photon flux density on the detector was increased by shortening the X-ray source to the detection panel distance. The distances between the X-ray source to the specimen and the X-ray to the detection panel were 200 and 500 mm, respectively. No X-ray filters were used. With this setup, the instrument calculates the resolution automatically, resulting in a voxel size of 0.06 mm. The number of projections can be calculated using the rule of $\pi/2 \times$ number of pixels of the specimen projected along the X-axis of the detector panel. For most images, the grayscale range had over 30,000 levels. Finally, the reconstruction is fully automated after the scanning is finished. The main parameters used for scanning can be seen in Table 2.

Before analysis, the images were aligned and trimmed to select a region of interest in each specimen (Fig. 2). The region of interest closely captures the portion of material active in the tensile stress tests. Once this operation is completed, the software generates rendered volume representations to inspect the image quality (Fig. 3).

The geometry data was obtained from the binarised images. Binarisation is the key procedure to separate the PLA material from the air-filled void space using an optimal threshold grey level. Several automated thresholding algorithms and interactive thresholding were tested. The most consistent thresholding over all specimens was obtained with an interactive threshold over a rescaled grayscale by reducing the 30,000 to 255 levels. This reduction in the number of grey levels makes it easier to perform a repeatable eye-naked supervised segmentation and detect the air-PLA interface (Fig. 4). The blue pixels over the rescaled greyscale background represent an initial guess of the threshold value above the optimal value because it does not cover all the PLA pixels.

The thresholding value for the PLA-air interface is not the same for all the printed specimens that one could print because it depends on their respective thickness, fill density, and printing orientation. The air-filled void space ranges from zero to threshold minus one, and the PLA ranges from the threshold value to 255. The grey scale threshold used was 85 for this analyzed vertical specimen.

Table 2 CT scan parameters

Characteristic	Value
Type of scan	Circular
Voltage (kV)	90
Intensity (μ A)	50
Distance from source to the specimen (mm)	200
Distance from source to panel (mm)	500
Voxel size (mm)	0.06
Image dimensions (voxels)	582 \times 759 \times 2594

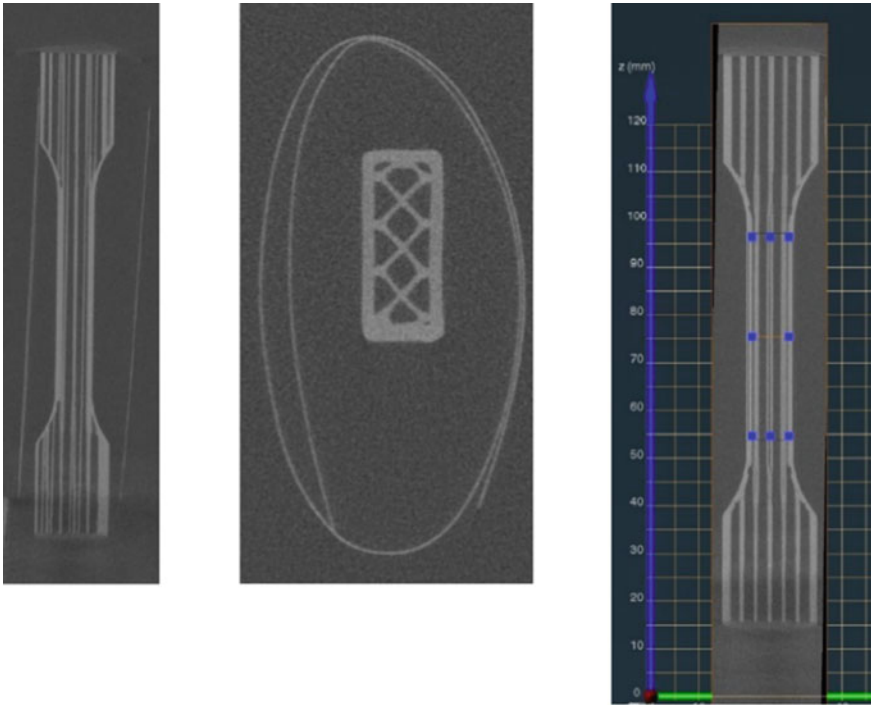
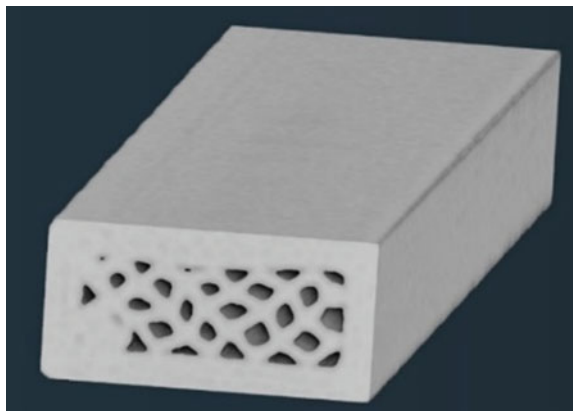


Fig. 2 Slices of the unprocessed CT images. Left: front view; Center: top view. The surrounding line is a paper envelope used as a reference to test the contrast and resolution; Right: alignment process of the raw image and extraction of the sub-volume inside the rectangle defined by the small blue squares. The outside of the rectangle was discarded for image analysis

Fig. 3 Volume rendering representation of a specimen printed with the vertical orientation



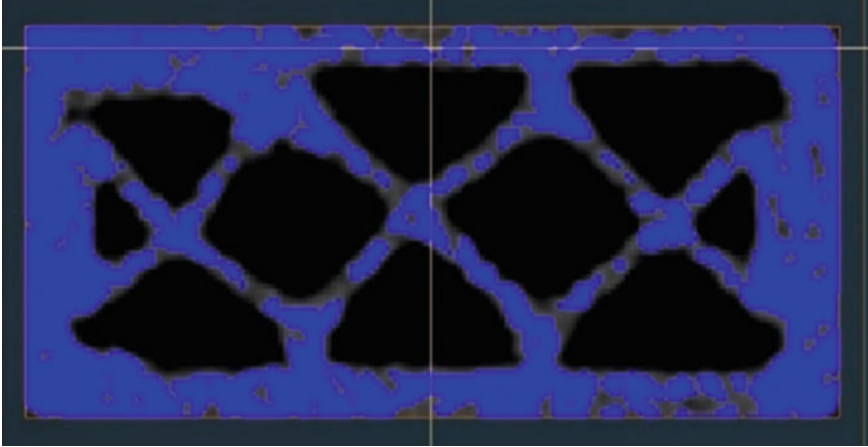


Fig. 4 Caption of the manual thresholding process on an orthogonal slice of the CT image in Avizo-3D

The image resulting from the binarisation is a binary 3D matrix with a value of 1 for every voxel with a grey level that lies in the threshold interval and a 0 for every voxel with other grey levels.

The software computes the volume fraction of an image and outputs a spreadsheet with several results, including the following measures:

- Total volume: complete volume of the image based on the voxel size and the work units.
- Label volume: volume of the selected variable (in this case, PLA) based on the voxel size and the work units.
- Volume fraction: the proportion of the image occupied by the PLA that represents the total infill density of the test specimen.
- Dimensional volumes can be expressed in mm^3 and voxel counts, given that one voxel represents $2.16 \times 10^{-4} \text{ mm}^3$.

6 Outcomes

The analysis of the vertical specimen through CT results in a table of values, as represented in Table 3.

The expected values from the CAD models fed into the 3D printer using the g-code were compared with their corresponding printed specimens. Thus, the objective is to compare the CT volume fraction against a CAD volume fraction obtained from the CAD model.

The procedure to calculate the CAD volume fraction is as follows. First, the area of the transversal section of the *V* model, the transversal section turns out to be 5 mm

Table 3 Volume fraction of PLA in the printed part and calculated parameters resulting from the CT image analysis

Test specimen	Volume fraction	Label volume (mm ³)	Total volume (mm ³)	Label voxel count	Total voxel count
Vertical	0.65	1221	1877	7.09E+06	1.09E+07

× 10 mm. After this, the model was divided into two different zones. The first belongs to the perimeters assumed to be 100 % solid, and the other is the infill, in which the amount of PLA depends on the infill density. The calculated CAD volume fraction (Table 4) is the total PLA occupied volume divided by the total volume. Thus, we obtain a volume fraction to compare to the value obtained from CT measurements.

To compare the CAD volume fraction with the CT volume fraction, it is noteworthy that the volume baselines are different. Because of the methodology used for creating the CT subvolume discarded a small part of the borders as shown in Fig. 2 right, the CT volume fraction uses a smaller volume than that of the CAD model (50 mm²). In this sense, it is required to recalculate the perimeter of the CAD model to have the same volumes. Thus, the internal geometry is maintained, but the total volume is recalculated using the cross-section of the CT subvolume, i.e. $h * b_1$, whose values are those obtained during the subvolume extraction of each specimen. Table 5 lists the dimensions of the extracted volumes, the recalculation of the transversal areas, and both the CAD and CT volume fractions. Moreover, the relative error is also shown.

From the values in Table 5, it is possible to understand that the theoretical section is smaller than the one measured by computed tomography. The relative error reaches almost 20 %. Thus, the difference is noticeable. The characteristics of the machine and setup might play an important role in the quality of the extrusion process. In any case, the inspection by computed tomography gives designers information for optimizing the process, specifically material use for attaining the expected tensile strength.

Table 4 CAD volume fraction results

Test specimen	Perimeter area (mm ²)	Interior PLA area (mm ²)	Total PLA area (mm ²)	Total area (mm ²)	CAD volume fraction
Vertical	17.81	12.88	30.69	50	0.61

Table 5 Corrected % of error between CAD model and calculated volume fractions

Test specimen	CAD cross-section (mm ²)	h (mm)	b_1 (mm)	Corrected cross-section (mm ²)	Corrected CAD volume fraction	CT volume fraction	Relative error %
Vertical	50	4.51	9.40	42.40	0.54	0.65	+ 19.47

7 Deliverables and Assessment

Due to the session being resource and time-intensive, the deliverables of the lab session are just the results of the CT analysis for one specimen per group. The instructor guides this analysis all the time.

8 Conclusions

The lab session on computed tomography allows students to understand non-destructive testing and their potential applications in manufacturing. In this sense, the students learn how to print tensile testing specimens, understand how the printing process works, the fundamentals and basic operations of computed tomography, and assess the quality of printing with computed tomography.

Acknowledgements The authors thank the support given by the Spanish Ministry MCINU EQC2018–004965-P, FEDER 2014-2020 Project for carrying out the computed tomography analysis.

References

- AENOR. (2012). UNE 116005. AENOR.
- Birosz, M. T., Ledenyák, D., & Andó, M. (2022). Effect of FDM infill patterns on mechanical properties. *Polymer Testing*, *113*, 107654.
- Bond, L., Gray, N., Margetan, F., Utrata, D., & Anderson, I. (2014). NDE for adding value to materials from metal powder processing. In *Proceedings of the 2014 World Congress on Powder Metallurgy and Particulate Materials* (pp. 1944–1959), Orlando.
- Cantatore, A., & Müller, P. (2011). Introduction to computed tomography. DTU Mechanical Engineering.
- Cerda-Avila, S. N., Medellín-Castillo, H. I., & Lim, T. (2020). An experimental methodology to analyse the structural behaviour of FDM parts with variable process parameters. *Rapid Prototyping Journal*, *26*(9), 1615–1625.
- Chacón, J., Caminero, M., García-Plaza, E., & Núñez, P. (2017). Additive manufacturing of PLA structures using fused deposition modeling: Effect of process parameters on mechanical properties and their optimal selection. *Materials & Design*, *124*, 143–157.
- Dickson, A. N., Barry, J. N., McDonnell, K. A., & Dowling, D. P. (2017). Fabrication of continuous carbon, glass and Kevlar fibre reinforced polymer composites using additive manufacturing. *Additive Manufacturing*, *16*, 146–152.
- du Plessis, A., Meincken, M., & Seifert, T. (2013). Quantitative determination of density and mass of polymeric materials using microfocus computed tomography. *Journal of Non-destructive Evaluation*, 413–417.
- El-Katatny, I., Masood, S. H., & Morsi, Y. S. (2010). Error analysis of FDM fabricated medical replicas. *Rapid Prototyping Journal*, *16*(1), 36–43.

- Fontana, L., Minetola, P., Iuliano, L., Rifuggiato, S., Khandpur, M. S., & Stiuso, V. (2022). An investigation of the influence of 3D printing parameters on the tensile strength of PLA material. *Materials Today: Proceedings*, 57, 657–663.
- Holzmond, O., & Li, X. (2017). In situ real time defect detection of 3D printed parts. *Additive Manufacturing*, 17, 135–142.
- ISO/ASTM 52900 additive manufacturing—General principles—Terminology (2022).
- Kalender, W. A. (2006). X-ray computed tomography. *Physics in Medicine and Biology*, 51(13), R29–43.
- Khosravani, M. R., & Reinicke, T. (2020). On the use of X-ray computed tomography in assesment of 3D-printed components. *Journal of Nondestructive Evaluation*, 39, 1–17.
- Kim, H., Lin, Y., & Tseng, T.-L. B. (2018). A review on quality control in additive manufacturing. *Rapid Prototyping Journal*, 24(3), 645–669.
- Kristiawan, R. B., Imaduddin, F., Ariawan, D., Ubaidillah, & Arifin, Z. (2021). A review on the fused deposition modeling (FDM) 3D printing: Filament processing, materials, and printing parameters. *Open Engineering*, 11(1), 639–649
- Kruth, J. P., Bartscher, M., Carmignato, S., Schmitt, R., De Chiffre, L., & Weckenmann, A. (2011). Computed tomography for dimensional metrology. *CIRP Annals*, 60(2), 821–842.
- Lanzotti, A., Grasso, M., Staiano, G., & Martorelli, M. (2015). The impact of process parameters on mechanical properties of parts fabricated in PLA with an open-source 3-D printer. *Rapid Prototyping Journal*, 21(5), 604–617.
- Leite, M., Fernandes, J., Reis, L., Vaz, M., & Deus, A. (2018). Study of the influence of 3D printing parameters on the mechanical properties of PLA. In *Proceedings of the 3rd International Conference on Progress in Additive Manufacturing (Pro-AM 2018)*. Nanyang Technological University.
- Leuders, S., Thöne, M., Riemer, A., Niendorf, T., Troster, T., Richard, H., & Maier, H. (2013). On the mechanical behaviour of titanium alloy TiAl6V4 manufactured by selective laser melting: fatigue resistance and crack growth performance. *International Journal of Fatigue*, 48, 300–307.
- López, V. M., Carou, D., & Cruz, S. F. A. (2022). Feasibility study on the use of recycled materials for prototyping purposes: A comparative study based on the tensile strength. *Proceedings of the Institution of Mechanical Engineers, Part B: Journal of Engineering Manufacture*, 237(5), 801–811.
- Losano, F., Marinsek, G., Merlo, A. M., & Ricci, M. (1999). Computed tomography in the automotive field. Development of a new engine head case study. In *DGZfP Proceedings BB 67-CD*, 65–73.
- Mohanty, A., Nag, K. S., Bagal, D. K., Barua, A., Jeet, S., Mahapatra, S. S., & Cherkia, H. (2022). Parametric optimisation of parameters affecting dimension precision of FDM printed part using hybrid Taguchi-MARCOS-nature inspired heuristic optimisation technique. *Materials Today: Proceedings*, 50(5), 893–903.
- Mou, Y. A., & Koc, M. (2019). Dimensional capability of selected 3DP technologies. *Rapid Prototyping Journal*, 25(5), 915–924.
- Ng, F. L., Tran, T. Q., & Liu, T. (2022). A methodology to develop part acceptance criteria model using non-destructive inspection technique for FDM printed part. *Materials Today: Proceedings*, 70, 310–316.
- Pérez, M., Medina-Sánchez, G., García-Collado, A., Gupta, M., & Carou, D. (2018). Surface quality enhancement of fused deposition modeling (FDM) printed samples based on the selection of critical printing parameters. *Materials*, 11(8), 1382.
- Petsiuk, A. L., & Pearce, J. M. (2020). Open source computer vision-based layer-wise 3D printing analysis. *Additive Manufacturing*, 36, 101473.
- Phillips, C., Kortschot, M., & Azhari, F. (2022). Towards standardising the preparation of test specimens made with material extrusion: Review of current techniques for tensile testing XE “Tensile testing.” *Additive Manufacturing*, 58, 103050.

- Prabhakar, M. M., Saravanan, A. K., Lenin, A. H., Ieno, I. J., Mayandi, K., & Ramalingam, P. S. (2021). A short review on 3D printing methods, process parameters and materials. *Materials Today: Proceedings*, 45(7), 6108–6114.
- Rifuggiato, S., Minetola, P., Stiuso, V., Khandpur, M. S., Fontana, L., & Iuliano, L. (2022). An investigation of the influence of 3D printing defects on the tensile performance of ABS material. *Materials Today: Proceedings*, 57(2), 851–858.
- Schmitt, M., Mehta, R. M., & Kim, I. Y. (2020). Additive manufacturing infill optimisation for automotive 3D-printed ABS components. *Rapid Prototyping Journal*, 26(1), 89–99.
- Snyder, J., Stimpson, C., Thole, K., & Mongillo, D. (2015). Build direction effects on microchannel tolerance and surface roughness. *Journal of Mechanical Design*, 137(11), 111411.
- Spierings, A., Schneider, N., & Eggenberger, R. (2011). Comparison of density measurement techniques for additive manufactured metallic parts. *Rapid Prototyping Journal*, 17(5), 380–386.
- Tao, Y., Kong, F., Li, Z., Zhang, J., Zhao, X., Yin, Q., Xing, D., & Li, P. (2021). A review on voids of 3D printed parts by fused filament fabrication. *Journal of Materials Research and Technology*, 15, 4860–4879.
- Thompson, A., Maskery, I., & Leach, R. K. (2016). X-ray computed tomography for additive manufacturing: A review. *Measurement Science and Technology*, 27(7), 072001.
- YXLON. (2018). YXLON FF20 CT.
- Zhang, B., Nasereddin, J., McDonagh, T., von Zeppelin, D., Gleadall, A., Alqahtani, F., Bibb, R., Belton, P., & Qi, S. (2021). Effects of porosity on drug release kinetics of swellable and erodible porous pharmaceutical solid dosage forms fabricated by hot melt droplet deposition 3D printing. *International Journal of Pharmaceutics*, 604, 120626.

Optimization of the Turning Process by Means of Machine Learning Using Published Data



Francisco de Arriba-Pérez , Silvia García-Méndez , Diego Carou ,
and Gustavo Medina-Sánchez 

1 Introduction

Turning is one of the main subtractive manufacturing processes used in industry. Despite the availability of other options, turning usually starts with cylindrical bars. Several metallic materials, such as aluminum, steel, and titanium, can be turned. The process is of high complexity, and the cutting mechanism involves high temperatures and mechanical loads. Accordingly, the quality of the machined surface is one of the key issues. Moreover, surface integrity is a critical aspect since it affects the functional performance of the components in aspects such as fatigue, creep, corrosion, and wear resistance (Liao et al., 2021).

Conventionally, researchers try to optimize machining processes using experimental approaches based on the Design of Experiments (DoE). In this sense, they perform experimental plans, record the results, and analyze them by statistical methods (Lauro et al., 2016). However, this approach is costly and time-consuming.

In the last years, Artificial Intelligence (AI) and, mainly, Machine Learning (ML) have emerged as valuable tools for analyzing large amounts of data in a wide variety of

F. de Arriba-Pérez (✉) · S. García-Méndez
Grupo de Tecnoloxías da Información,atlanTTic, Universidade de Vigo, Vigo, Spain
e-mail: farriba@gti.uvigo.es

S. García-Méndez
e-mail: sgarcia@gti.uvigo.es

D. Carou
Departamento de Deseño na Enxeñaría, Escola de Enxeñaría Aeronáutica e do Espazo, Ourense,
Universidade de Vigo, Ourense, Spain
e-mail: diecapor@uvigo.gal

G. Medina-Sánchez
Departamento de Ingeniería de los Procesos de Fabricación, Universidad de Jaén, Jaén, Spain
e-mail: gmedina@ujaen.es

use cases [Natural Language Processing—NLP (Bashir et al., 2021), sports (Nguyen et al., 2022), health (Ngiam & Khor, 2019)].

The sensorization of the Industry 4.0 environment and the need to parameterize the performance of the equipment have led to the exchange of information between intelligent objects for subsequent processing (Jasperneite et al., 2020). The need for parameterization has encouraged the implementation ML techniques for the optimization of different industrial processes (Carou et al., 2022).

Ti6Al4V is the most generally used alpha–beta alloy (Alam et al., 2023) and, specifically, it has been extensively used in research in machining. Titanium alloys are difficult-to-cut materials because their increased strength and hardness generate high temperatures during machining and accelerate tool wear (Revuru et al., 2017). The importance of titanium alloys can be understood when attending to their applications in sectors such as aerospace, automotive, biomedical, military, petrochemical, and sports (Pushp et al., 2022). Thus, many published studies can provide experimental results of surface roughness in turning the Ti6Al4V alloy to feed ML algorithms.

This chapter presents a guideline for developing a lab session in which the students will learn how to use ML to optimize the parameters in titanium alloys' turning process using only published data. SMOreg, Decision Stump, and Random Forest algorithms are compared, and the results are evaluated using proper metrics.

2 Background

The material removal mechanism in turning varies from rough to finish turning (Derani & Ratnam, 2021). In this sense, Fig. 1 shows the ideal cutting of both processes. The major flank plays an essential role in the cutting in rough turning. However, the cutting occurs in the region dominated by the tool nose radius in the finishing process.

The quality of the surface is conventionally assessed by analyzing the roughness of the surface. It is generally accepted that surface roughness is mainly affected by the feed movement of the cutting tool and the tool nose radius. This relationship was modeled by Knight and Boothroyd (Knight & Boothroyd, 2019). In this sense, the theoretical arithmetical average value (Ra) can be calculated using Eq. 1, in which f is the feed rate and re the tool nose radius:

$$Ra = 0.0321 \frac{f^2}{re} \quad (1)$$

The ideal surface roughness cannot easily be achieved because of the complexity of the actual turning process. Several factors affect the cutting process; therefore, the results usually vary from the theoretical ones. In this sense, external and internal loads (mechanical, thermal, chemical) may cause changes (anomalies) to the work-piece during machining. Among these anomalies, changes in surface topography are relevant (Liao et al., 2021).

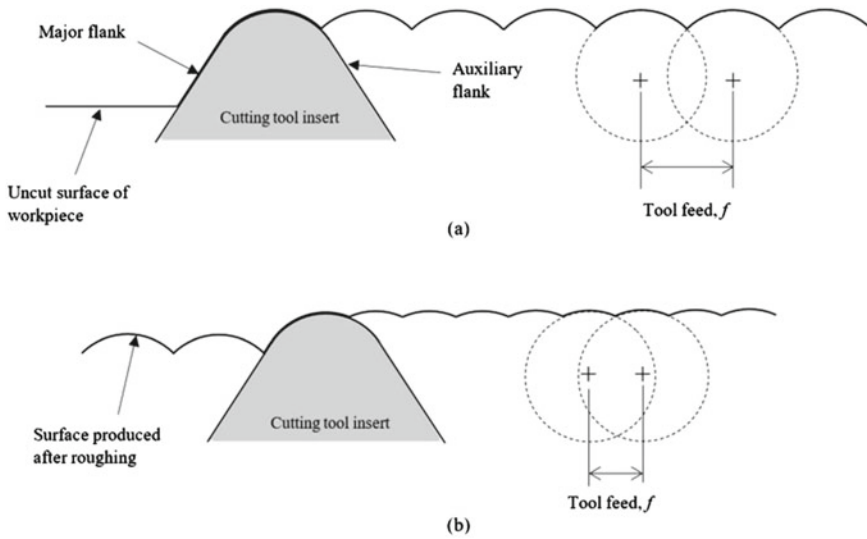


Fig. 1 Surface profile in rough turning (up) and finish turning (down). Permission granted by Derani and Ratnam (Derani & Ratnam, 2021)

Several researchers have tried identifying the main factors that may affect the turning process. Those related to the tool, workpiece, cutting parameters, and cutting phenomena are recognized among them. Some of these factors are classified and listed in Fig. 2, enabling an understanding of the complex nature of turning. However, when conducting turning experiments, feed rate (Anurag & Sahoo, 2022) and tool nose radius (Schultheiss et al., 2015) are critical for surface roughness, thus confirming the model established by Eq. 1.

Cutting tool parameters	Cutting parameters	Workpiece properties	Cutting phenomena
<ul style="list-style-type: none"> • Tool material • Tool overhang • Tool shape • Nose radius 	<ul style="list-style-type: none"> • Dry • Wet • Process kinematics • Depth of cut • Feed rate • Cutting speed • Tool angle 	<ul style="list-style-type: none"> • Workpiece diameter • Workpiece length • Workpiece hardness • Workpiece mounting 	<ul style="list-style-type: none"> • Accelerations • Surface roughness • Chip formation • Friction • Wear • Cutting force variation

Fig. 2 Factors affecting the turning process (Serra & Chibane, 2010)

ML is an alternative approach to using traditional experimental and statistical techniques for surface roughness prediction. These models allow detection patterns even in scenarios where there is no linearity between the features and the variable to be predicted (target feature) (Thongpeth et al., 2021). These techniques are generally divided into supervised and unsupervised. In the former supervised approach, an annotated data set, either by human experts or automatically labeled, is exploited. The data for training the model are called features, while the prediction is called target. The ultimate objective is to discover hidden patterns in the features that allow to understand the relationship between them and the target. Conversely, the unsupervised approach involves discovering clusters, that is, closely related entries in an unlabeled data set using a certain distance metric. This academic practice will focus on studying supervised ML models.

As previously mentioned, to predict the target value, supervised ML models need to be trained using labeled data. In particular, the most popular supervised models use different mathematical approaches to obtain these patterns. In this line, regressors or the features of the Support Vector Machine (SVM) system are used based on the intersection of hyper-planes. Another usual technique uses Decision Trees. These methods generate branches based on the input features. More in detail, each fork generates a new branch in which a different feature is evaluated. These classifiers aim to divide the problem into subgroups by a range of values defining a category. These previous approaches can be combined, creating meta classifiers, as in the popular Random Forest algorithm, which combines n Decision Trees (Witten et al., 2016).

ML techniques vary depending on the type of feature of the target: (i) numerical or (ii) categorical. In the first case, the target feature corresponds to real numerical values (e.g., measurements gathered from sensors, probabilities, etc.), and the classifier must be configured to act as a regressor. Conversely, when the target feature is categorical, the classifier is trained to detect patterns characteristic of each category. This chapter focuses on the first scenario (Subasi, 2020).

3 Learning Objectives

This session will help students:

- To be familiar with the evaluation of surface roughness in turning.
- To identify factors that potentially may affect surface roughness.
- To understand the foundations of ML.
- To compare various ML algorithms and evaluate their suitability using proper metrics.
- To apply ML in a data set and extract information for defining the setup and optimizing the results of the turning process.

4 Resources and Organization

The session was specially designed for groups of 10–20 undergraduate engineering students. A slot of 2 h is recommended for developing the session.

Hardware and software requirements are not highly demanding. Thus, they are adequate for implementation in conventional lab spaces. The main requirements are listed below:

- Operating system: Windows 10 64 bits.
- Processor: Intel i3.
- RAM: 8 GB DDR4.
- Disk: 10 GB of free space.
- Software for data analysis: Weka.¹ This free available, portable, and easy-to use software provides a comprehensive collection of data analysis techniques for preprocessing and modeling. Moreover, it provides visualization tools such as the graphical user interface.

One computer per student is required since students will have to follow the steps introduced by the instructors and then carry out their analysis.

There exist two alternatives to obtain data for the analysis. Firstly, to gather the data set from published data. Secondly, to obtain the data set by direct measurements on turned samples in the workshop. In addition, the two strategies can be combined, as shown by García-Martínez et al. (2023) for the material extrusion process, where data is gathered from the literature and by direct measurements. The approach to follow in this lab session will require only published data. However, this lab session might be enhanced, including complimentary experimental turning tests and surface roughness measurement.

The data set required for developing the session will be gathered without making any distinction between the application of the process (i.e., finishing or roughing).² Based on that, the students will be provided with a data set of experimental results published in the literature on turning off the Ti6Al4V alloy. The data set³ proposed includes 138 values (103 for training and 35 for testing) of the *Ra* output (Amrita et al., 2022; Chen et al., 2017; Mia et al., 2019). The machining parameters used for obtaining these values included: cutting speed (m/min), feed rate (mm/rev), depth of cut (mm), and an individual column for each cooling technique.⁴ The output is the *Ra* (μm). This data set will be used for training the model.

¹ Available at https://waikato.github.io/weka-wiki/downloading_weka (accessed Dec. 14, 2023).

² Note that this chapter is just an introduction to the methodology, not an in-depth research study.

³ Available at <http://bit.ly/3CeWoD3> (accessed Dec. 14, 2023).

⁴ Most studies do not include specific details of the tools. Thus, it is sometimes impossible to have relevant data such as tool nose radius or other turning parameters.

5 Session Development

The instructor will present the background and learning outcomes to the students and the following steps within the experimental pipeline in a practical use case using Weka and a train data set. The practice is expected to last one hour and a half. After that, students will test their knowledge with the test data set.

The ML process is divided into six fundamental stages: (i) data analysis, (ii) feature engineering, (iii) feature selection, (iv) classification, (v) hyperparameter optimization, and (vi) evaluation.

5.1 Data Analysis

Data analysis represents the initial and essential step to ensure the high quality of the input data. The analyses consist of:

- **Feature mapping.** Categorical and nominal features are transformed into numeric features. Accordingly, ML models exploit numerical values to infer relevant behavior patterns based on distances, error minimization, correlations, etc. To perform feature mapping with spreadsheets, additional numerical columns must be created for each textual one, considering the ordering of the possible values.

Using Weka, students must click the *Explorer* option and select the data set to be loaded (in *csv* or *arff* format, the latter used by Weka). In the Filter functionality, a list of possible filtering options will be displayed, as shown in Fig. 3. The filtering options must be selected under the path *filters/unsupervised/attribute*. Typically, *StringToNominal* or *OrdinalToNumeric* are exploited. If the option *StringToNominal* is used, the data set will be saved using the *Save* option in *arff* format. Note that the unsupervised filter is unrelated to the classification task. It executes a specific rule that transforms a column from one type to another. Finally, students must open the file and modify the features to numeric format as in Listing 1.

- **Interpolate missing data.** Several options exist to ensure that the input data have no empty values: average, minimum, maximum, etc. The selection of the strategy depends on the classification problem. Particularly, the *ReplaceMissingValues* filter in the path *filters/unsupervised/attribute* replaces the missing values with the average. Other replacements than the average can be obtained with a formula in a spreadsheet.
- **Homogenize experimental data.** It ensures the input data is aligned among the different sources used regarding feature name, normalization, or binarization. Firstly, the same column name must be used in a spreadsheet or *csv* file. Note that the transformations must be applied in all new data sets students create.

Listing 1 Nominal to numeric transformation

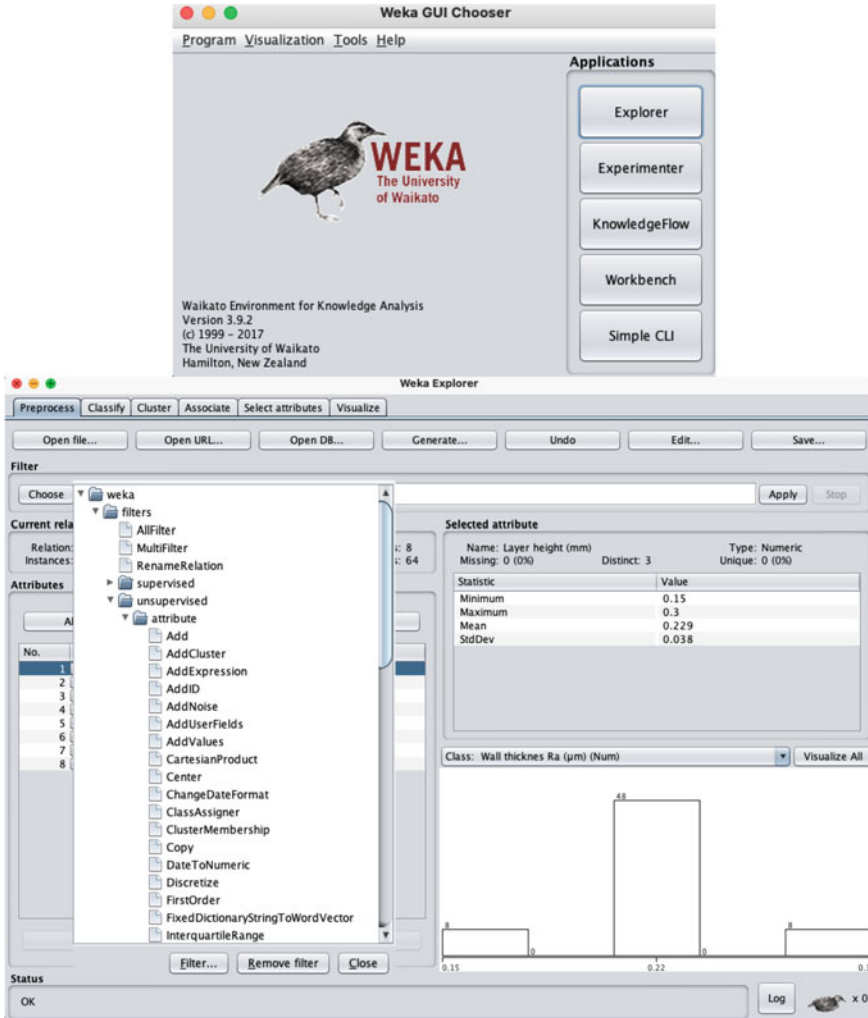


Fig. 3 Weka interface to choose a feature transform approach

@attribute 'Cutting speed (m/min)' {40,60}
@attribute 'Cutting speed (m/min)' numeric

5.2 Feature Engineering

In data science, the final goal is to generate knowledge from the data (Moreno-Mateos & Carou, 2022), i.e., engineer features: accumulated values (e.g., from time series), the difference between two features, statistical values (e.g., quartiles). This

process also applies to changes in the existing data, for example, by creating a new feature by establishing ranges for the values of another feature. These changes can be done through simple functions created on spreadsheets at the end.

5.3 Feature Selection

Once the input data were analyzed and the features were engineered, it was the turn to select the most representative features to train the ML models. There exist two main options in the literature: (i) statistical thresholding and (ii) model-based selection. Both approaches allow to the detection of non-duplicate feature values and highly correlated features concerning the target and are complemented by visual representation of the most relevant features. Moreover, in the model-based selection approach, a model is used to infer from a training subset the most relevant features. It serves a dual purpose: (i) reduction of the training samples, which results in more efficient models, and (ii) classification performance improvement by removing unrelated or misleading features that may lead to incorrect predictions.

Initially, in *Select attributes—Weka tab*, students must select the *Ranker* method as *Search Method* under the path *attributeSelection/Ranker* and *CorrelationAttributeEval* as *Attribute Evaluator* under the path *attributeSelection/CorrelationAttributeEval*. The latter evaluator shows results between -1 and 1 . The closer to the extremes, the more correlated the features are with the target and, therefore, more representative.

For the second analysis, students must use *ClassifierAttributeEval*, as indicated in Fig. 4. A tree-based classifier such as *trees/RandomForest* offers competitive performance in most scenarios. This evaluator uses a measure similar to correlation. However, its values will not be bounded. In this sense, the greater the absolute value's relevance. To launch the test, students must select the target feature from the list displayed above the *Start* button, by default the last column of the data set, and press this button. Given the results, students can move to *Preprocess* tab and remove certain features during exportation using the *Remove* button.

5.4 Classification

The models used for classification will be selected depending on the data's nature and the experimental plan's needs or limitations. Moreover, baseline models are used for comparative purposes. In this lab practice, the following algorithms will be exploited⁵:

⁵ However, the Weka tool provides numerous types of classifiers, the student is encouraged to explore other alternatives.

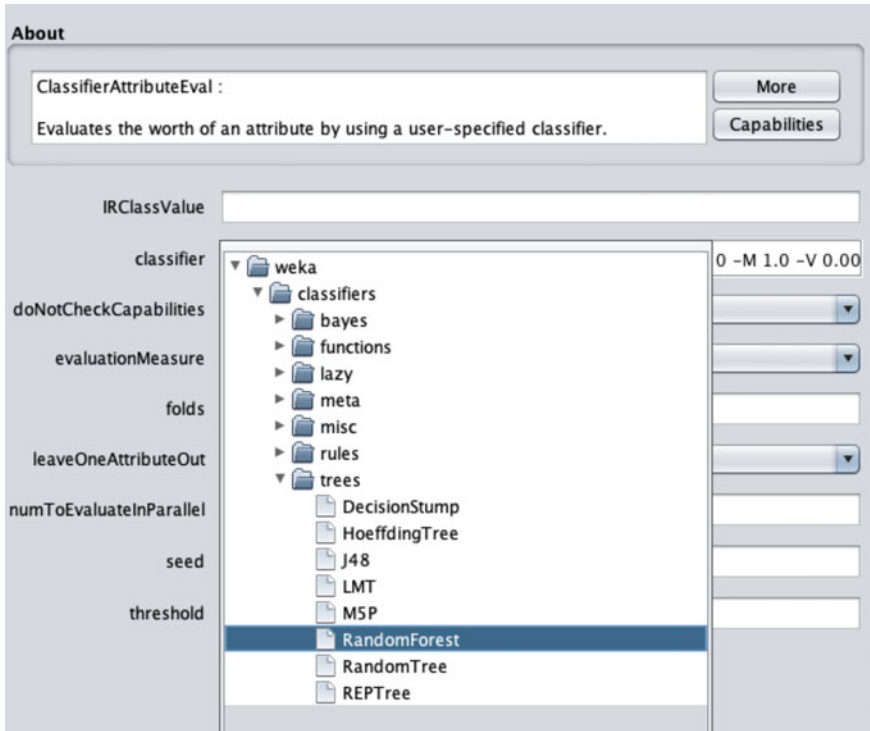


Fig. 4 Weka interface to choose a feature selection approach

- SMOreg⁶ (Assim et al., 2020). It is a regression implementation of SVM.
- Decision Stump (DS⁷) (Uskov et al., 2021). It is a basic tree model.
- Random Forest (RF⁸) (Schonlau & Zou, 2020). It is a more complex tree-based model since it is composed of n trees.

To test classifiers on the experimental data set, students must select the *Classify* tab and choose the model by pressing the *Choose* button. The models available are in *functions/SMOreg*, *trees/DecisionStump*, and *trees/RandomForest*.

⁶ Available at <https://weka.sourceforge.io/doc.dev/weka/classifiers/functions/SMOreg.html> (accessed Dec. 14, 2023).

⁷ Available at <https://weka.sourceforge.io/doc.dev/weka/classifiers/trees/DecisionStump.html> (accessed Dec. 14, 2023).

⁸ Available at <https://weka.sourceforge.io/doc.dev/weka/classifiers/trees/RandomForest.html> (accessed Dec. 14, 2023).

5.5 *Hyperparameter Optimization*

The last process before training and testing consists of identifying the classifiers' optimal hyperparameters. Accordingly, each classifier model has default initialized attributes that can be modified to improve performance. In line with the above, a subset of the complete data set is extracted to avoid bias and different configurations of the classifiers are tested. To select the parameters of the classifiers, students should pick the model on the right of the *Choose* button. A very common parameter to modify in the RF classifier is the *numIterations*, as can be seen in Fig. 5. In data sets larger than the one used, for example, its effect and improvement in the results are usually notable when iterating n times in search of the optimal configuration. It must be considered that the execution time and resources consumed will increase the larger this value is.

5.6 *Evaluation*

Traditional evaluation methods divide the data set into partitions for training and testing, like 50%-50%, 60%-40%, 70%-30%, or 80%-20%. However, this approach only ensures that the entire data set is tested and that the chosen partitions do not produce biased results in the evaluation metrics. Consequently, the most appropriate method for evaluation to avoid over-fitting and minimize over- and underestimation is cross-validation (Berrar, 2019).

Cross-validation uses different partitions of the experimental data set over multiple iterations for training and testing the models. The latter creates a more realistic evaluation plan. The traditional tenfold cross-validation technique shuffles the experimental data set and divides it into segments of equal length, using 9 for training and 1 for testing, without overlapped testing partitions. This process is repeated 10 times. In the end, the overall evaluation metrics are averaged.

To experiment with *Classify* tab following the train/test split procedure, *Percentage split* must be selected. The latter value corresponds to the part of the data set dedicated to training, and the rest will be used for testing. If the experimental data set is split into train and test partitions, students can use the *Supplied test set* option. In addition to the fact that both data sets must match in terms of columns, column names, and data typology, it is recommended that both the train and test files have been previously saved in *arff* format and loaded into Weka.

To use cross-validation, students must select *Cross-validation* and choose the number of folds. Exploit the *Use training set* option to check that the data set is not randomized. If, when running Weka with this option enabled, the results are far from 80%, it means that the model cannot find patterns even when trained and evaluated with the same data set. To launch the first test, choose the target variable from the list displayed under *More options* and press the *Start* button.



Fig. 5 Weka interface to modify the hyperparameters of the RF model

Since the ML models will be used as regressors, the most appropriate evaluation metrics are the relative absolute error (RAE, Eq. 2) and the mean absolute percentage error (MAPE, Eq. 3) instead of the accuracy, precision, and recall computed when these models are used as classifiers. The models act as regressors because the target value is numeric and may present infinite feasible values.

The RAE metric measures the model’s adaptability regarding feature-target value changes. More in detail, it computes the average-percentual deviation between the predicted value and the expected one. Moreover, the utilization of the MAPE metric is preferred due to the anticipated high sparsity in surface roughness values. More in detail, the MAPE metric assesses the same deviation (i.e., between predicted and

actual values) but is normalized to the actual values rather than the average as in the case of the RAE.

The correlation variable and RAE will be printed in the display window by default. To select new metrics, click on the *More options* button and *Evaluation metrics* as shown in Fig. 6. Note that the MAPE metric is not included. Therefore, students must use a spreadsheet to calculate it. To export the prediction in the *Classifier evaluation* options window, click on *Output predictions* and select *csv*. When executing, the id of the instance, the real value, the predicted value, and its difference will be printed on the screen, each parameter separated by commas. The student can select this data, copy and paste it to a *csv* file and open it with a spreadsheet application.

$$RAE(\%) = 100 \frac{\sum_{i=1}^n |f_i - a_i|}{\sum_{i=1}^n |\bar{a} - a_i|} \tag{2}$$

being f_i forecast values, and a_i actual values.

$$MAPE(\%) = \frac{100}{n} \sum_{i=1}^n \left| \frac{f_i - a_i}{a_i} \right| \tag{3}$$

The results using the cross-validation method with the proposed data sets are presented in Table 1. The behavior of RF is superior in all metrics. RF correlates 0.96

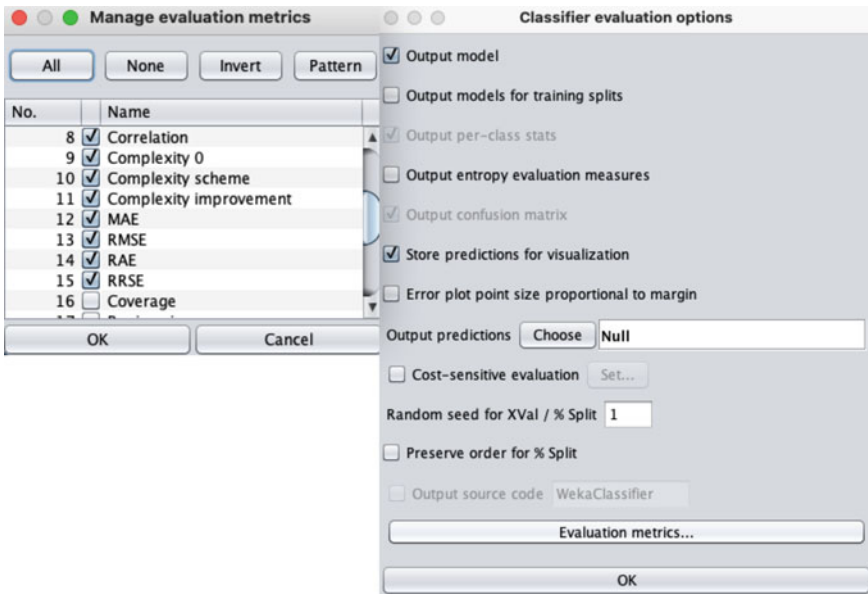


Fig. 6 Weka interface to choose the evaluation metrics

Table 1 Result values for the selected ML models using tenfold cross-validation technique

	SMOreg	DS	RF
Correlation	0.84	0.88	0.96
RAE (%)	55.99	53.56	31.12
MAPE (%)	36.28	35.63	19.82

Table 2 Result values for the selected ml models using Supplied test set option

	SMOreg	DS	RF
Correlation	0.87	0.88	0.98
RAE (%)	48.45	56.86	32.32
MAPE (%)	21.47	25.58	12.69

with the surface roughness target feature. Moreover, a MAPE value of 19.82% represents a deviation between actual and predicted values lower than 20%. In contrast, the 31.12% of RAE metric is expected because the actual and predicted measures are not close to the mean. For this reason, the MAPE measure is a more accurate metric in this type of problem.

6 Outcomes

Once the instructors have delivered the guidelines to the students, they are expected to use the test data set. Students must use the original data set to train the model and the test data set to validate it using *Supplied test set* option. Verify that this data set has the same column names and types, or solve any problem following the steps described in Sect. 5.1. The next step will be to analyze the information and select the relevant features. Moreover, they must evaluate the three proposed classification models using the evaluation metrics provided by Weka and including the RAE and MAPE results obtained. They are expected to discuss performance differences among the classifiers. Students can improve the latter performance using hyper-parameter tuning and checking their effect on the evaluation metrics. The results with all features and with the default configuration are shown in Table 2. As in the same case of cross-validation, RF performs better than the rest of the classifiers. The student shall make as same discussion analyses as in the above experiment.

7 Deliverable and Assessment

At the end of the session, students must deliver a summary of the techniques and tools used for data analysis, feature engineering, and selection (e.g., interpolate missing data, homogenize experimental data, etc.). Additionally, this summary must include

the features engineered and selected and their relevance. Results must be displayed in a table containing the correlation values, the RAE, and the MAPE metrics for each classifier used. Moreover, an additional table with the results obtained with hyper-parameter tuning must be included. A deliverable template is provided to the students.⁹

8 Conclusions

The present chapter provides an example of the use of ML to analyze published data to optimize the turning conditions of Ti6Al4V alloy. The main conclusions of the chapter are the following:

- The main mechanisms that generate the surface roughness in turning are well known. The ideal surface roughness profile primarily depends on the feed rate and tool nose radius.
- The actual surface roughness differs from the ideal values. Thus, the setup for turning cannot be arranged using only feed rate and tool nose radius.
- ML is suitable for analyzing complex relationships between multiple factors and outcomes, especially when large data sets are available.
- The students will learn how to use and apply ML methods in manufacturing. Specifically, they will create a setup for the turning process of Ti6Al4V alloy using as the outcome, the surface roughness.

Acknowledgements This study was partially supported by Xunta de Galicia grants ED481B-2021-118 and ED481B-2022-093, Spain.

References

- Alam, S. T., Tomal, A. A., & Nayeem, M. K. (2023). High-speed machining of Ti-6Al-4V: RSM-GA based optimization of surface roughness and MRR. *Results in Engineering*, 17, 100, 873–100, 883.
- Amrita, M., Kamesh, B., & Sree, K. L. S. (2022). Multi-response optimization in machining Ti6Al4V using graphene dispersed emulsifier oil. *Materials Today: Proceedings*, 62, 1179–1188.
- Anurag, K. R., Sahoo, A. K., et al. (2022). Comparative performance analysis of coated carbide insert in turning of Ti-6Al-4V ELI grade alloy under dry, minimum quantity lubrication and spray impingement cooling environments. *Journal of Materials Engineering and Performance*, 31, 709–732.
- Assim, M., Obeidat, Q., & Hammad, M. (2020). Software defects prediction using machine learning algorithms. In *Proceedings of the International Conference on Data Analytics for Business and Industry: Way Towards a Sustainable Economy* (pp. 1–6). IEEE.

⁹ Available at <http://bit.ly/3X45Wdr> (accessed Dec. 14, 2023).

- Bashir, M. F., Arshad, H., Javed, A. R., et al. (2021). Subjective answers evaluation using machine learning and natural language processing. *IEEE Access*, 9, 158, 972–158, 983.
- Berrar, D. (2019). Cross-validation. In *Encyclopedia of bioinformatics and computational biology* (pp. 542–545). Elsevier.
- Carou, D., Sartal, A., & Davim, J. P. (2022). *Machine learning and artificial intelligence with industrial applications*. Springer.
- Chen, Y., Sun, R., Gao, Y., et al. (2017). A nested-ANN prediction model for surface roughness considering the effects of cutting forces and tool vibrations. *Measurement*, 98, 25–34.
- Derani, M. N., & Ratnam, M. M. (2021). The use of tool flank wear and average roughness in assessing effectiveness of vegetable oils as cutting fluids during turning—A critical review. *The International Journal of Advanced Manufacturing Technology*, 112, 1841–1871.
- García-Martínez, F., Carou, D., de Arriba-Pérez, F., et al. (2023). Toward datadriven research: preliminary study to predict surface roughness in material extrusion using previously published data with machine learning. *Rapid Prototyping Journal*, 29(8), 1640–1652.
- Jasperneite, J., Sauter, T., & Wollschlaeger, M. (2020). Why we need automation models: Handling complexity in Industry 4.0 and the internet of things. *IEEE Industrial Electronics Magazine*, 14(1), 29–40.
- Knight, W. A., & Boothroyd, G. (2019). *Fundamentals of metal machining and machine tools*. CRC Press.
- Lauro, C. H., Pereira, R. B. D., Brandão, L. C., et al. (2016). *Design of experiments—Statistical and artificial intelligence analysis for the improvement of machining processes: A review*. Springer.
- Liao, Z., la Monaca, A., Murray, J., et al. (2021). Surface integrity in metal machining—Part I: Fundamentals of surface characteristics and formation mechanisms. *International Journal of Machine Tools and Manufacture*, 162, 103, 687–103, 737.
- Mia, M., Gupta, M. K., Lozano, J. A., et al. (2019). Multi-objective optimization and life cycle assessment of eco-friendly cryogenic N₂ assisted turning of Ti-6Al-4V. *Journal of Cleaner Production*, 210, 121–133.
- Moreno-Mateos, M. A., & Carou, D. (2022). *A note on big data and value creation*. Springer.
- Ngiam, K. Y., & Khor, I. W. (2019). Big data and machine learning algorithms for health-care delivery. *The Lancet Oncology*, 20, 262–273.
- Nguyen, N. H., Nguyen, D. T. A., Ma, B., et al. (2022). The application of machine learning and deep learning in sport: Predicting NBA players' performance and popularity. *Journal of Information and Telecommunication*, 6, 217–235.
- Pushp, P., Dasharath, S., & Arati, C. (2022). Classification and applications of titanium and its alloys. *Materials Today: Proceedings*, 54, 537–542.
- Revuru, R. S., Posinasetti, N. R., Vsn, V. R., et al. (2017). Application of cutting fluids in machining of titanium alloys—a review. *The International Journal of Advanced Manufacturing Technology*, 91, 2477–2498.
- Schonlau, M., & Zou, R. Y. (2020). The random forest algorithm for statistical learning. *The Stata Journal: Promoting Communications on Statistics and Stata*, 20(1), 3–29.
- Schultheiss, F., Hägglund, S., & Ståhl, J. E. (2015). Modeling the cost of varying surface finish demands during longitudinal turning operations. *The International Journal of Advanced Manufacturing Technology*, 84, 1103–1114.
- Serra, R., & Chibane, H. (2010). Effects of cutting parameters during turning 100C6 steel. In *EPJ Web of Conferences* (pp. 1–8).
- Subasi, A. (2020) *Practical machine learning for data analysis using Python*. Elsevier.
- Thongpeth, W., Lim, A., Wongpairin, A., et al. (2021). Comparison of linear, penalized linear and machine learning models predicting hospital visit costs from chronic disease in Thailand. *Informatics in Medicine Unlocked*, 26, 100, 769–100, 776.
- Uskov, V. L., Bakken, J. P., Putta, P., et al. (2021). Smart education: Predictive analytics of student academic performance using machine learning models in weka and Dataiku systems. In *Proceedings of the Smart Innovation, Systems and Technologies Conference* (pp. 3–17).
- Witten, I. H., Frank, E., Hall, M. A., et al. (2016). *Data mining: Practical machine learning tools and techniques*. Morgan Kaufmann.

Creating Accessible Interactive Training Materials in Manufacturing Engineering



Şener Karabulut  and Şirin Okyayuz 

1 Introduction

In today's educational landscape, the profound impact of educational technologies on teaching and learning approaches is undeniable. Technological innovations and changes have significantly reshaped the perspectives and methodologies employed by educators. Educational institutions now face the imperative task of reevaluating the where, what, when, and how of student learning to ensure the continuous delivery of high-quality education. Improving the quality of education necessitates enhancements in instructional methods, increased student engagement, the creation of conducive learning environments, in addition to the adoption of innovative learning techniques. Key elements that underscore successful education emphasize the shift from passive to active learning and the dynamic integration of technology into the educational process.

Furthermore, the utilization of digital technology fosters collaborative knowledge production within pedagogical and social contexts, enabling students to share their experiences. This educational paradigm not only mandates the integration of technology but also sets the stage for the emergence of new disciplines and pedagogical tools that offer engaging and motivating opportunities to address the challenges posed by education in the digital era.

Furthermore, a profound relationship exists between vocational and technical education, technology, and scientific research, given that the attributes of the workforce continually evolve in response to changes in production methods, tools, and equipment used in various industries.

Ş. Karabulut (✉)

Department of Mechanical Program, Hacettepe University, 06935 Ankara, Turkey

e-mail: senerkarabulut@hacettepe.edu.tr

Ş. Okyayuz

Department of Translation and Interpreting, Hacettepe University, 06800 Ankara, Turkey

e-mail: sirinokyayuz@hacettepe.edu.tr

The manufacturing industry stands as a testament to ongoing technological advancements and the ever-evolving demands of the market. To remain competitive and nurture a highly skilled workforce, organizations must commit resources to continuous training and development initiatives. Online training has emerged as an especially advantageous and cost-effective method for enhancing the skills of personnel in the field of manufacturing engineering.

In the contemporary landscape, characterized by an inclusive and diverse workforce, ensuring the accessibility of training materials within the manufacturing industry is of paramount importance. This accessibility extends to all employees, including those who are Deaf and Hard of Hearing (HoH). The objective of this chapter is to outline the essential principles and strategies required for the creation of interactive training materials that are not only inclusive but also tailored to the specific needs of individuals within the Deaf and HoH community who are employed in the metal industry.

Expanding employment and professional training opportunities for individuals who are deaf and HoH (DHH) has become a prominent issue on the global agenda. In response to this concern, various countries have enacted laws and provided incentives to encourage the employment of DHH individuals. On the other hand, individuals who are DHH face challenges in adapting to and effectively communicating within their workplace. Additionally, these employees aspire to advance in their careers, but the lack of accessible training materials tailored to their needs hinders their progress. The issue of DHH employment is not resolved solely through recruitment; if on-the-job training fails to meet the desired quality, the full potential of disabled individuals cannot be realized. This situation poses a problem for both employers and the disabled workforce (Erdiken, 2005). Therefore, it is crucial to provide training and advancement opportunities that are accessible to individuals who are DHH (Fenge & Subaşıoğlu, 2019). Kalkan and Karabulut (2021) reported that approximately 67% of disabled individuals working in this sector have hearing impairments, with communication problems being the most significant difficulty encountered in their professional lives (41.6%).

The research in the field summarized above highlights that there is a vital need for accessible vocational digital training for the DHH. Accessibility may be defined as an approach and implementation that ensures that people are not excluded from using something based on experiencing a disability (Duggin, 2016). Thus, in terms of training material the written resources provided need to be comprehensible for the present and future DHH workforce. Studies on literacy rate and reading speeds of the DHH indicate that technical texts would not meet the training needs of the DHH. For example, İlkbaşaran (2015) stresses the importance of presenting written texts and sign language content simultaneously. Several studies have reported that the level of literacy among DHH students is often behind those of hearing (Kyle & Harris, 2006, 2010). Other studies confirm that DHH individuals do not attain average reading skills and speeds at the expected levels when compared to their peers (see Güldenöğlü & Miller, 2014). Antia et al., (2005, p. 244), argue that “although large numbers of DHH students are educated in general-education classrooms educators continue to express concern that the quality of their learning in general-education

classrooms might be less than optimal for communication access and interaction”. The use of sign language and plain language in training are tried and tested methods used to eliminate these disadvantages (Myers & Martin, 2021; Schriver, 2017).

2 Creating Accessible/Digital Training Materials

2.1 *Creating Online Training Materials in Manufacturing Engineering to Develop Effective Training Materials*

Figure 1 shows the development of an online training materials process. This structured approach ensures that the online training program is well-defined, engaging, effective, and adaptive to the learners’ needs.

- **Identify training objectives (1):** Begin by defining the training objectives. Understand the skills and knowledge that students need to acquire or improve upon. Align these objectives with the overall training goals to ensure that the training program contributes to the institution’s success.
- **Assess learning needs (2):** Conduct a thorough assessment of the learning needs of your students. This can be done through surveys, interviews, or analyzing performance gaps. Understanding the specific requirements of your workforce will enable you to tailor the training content accordingly.
- **Choose the right format (3):** Online training offers various formats, such as interactive modules, videos, webinars, or gamified learning. Select the format that best suits the training objectives and the preferences of students.
- **Content development (4):** Create engaging and relevant content that aligns with the learning objectives. Ensure that the material is easy to understand and accessible to all students. To enhance learning, incorporate multimedia elements like videos, infographics, and interactive quizzes.
- **Make use of a learning management system (LMS) (5):** Invest in a powerful LMS to deliver, oversee, and monitor the training program. An LMS facilitates content organization, student progress monitoring, and training effectiveness evaluation.
- **Encourage interactivity and collaboration (6):** Foster a collaborative learning environment by incorporating discussion forums, group activities, or virtual classrooms. Encourage students to interact with each other and share knowledge and experiences.
- **Provide flexibility (7):** Students have different learning styles and schedules. Ensure that the training program allows flexibility for learners to progress at their own pace. This will promote higher engagement and knowledge retention.
- **Assess and evaluate (8):** Regularly assess the effectiveness of the training program. Use quizzes, assessments, and feedback surveys to gather insights into the program’s impact. Analyze the data to identify areas for improvement.

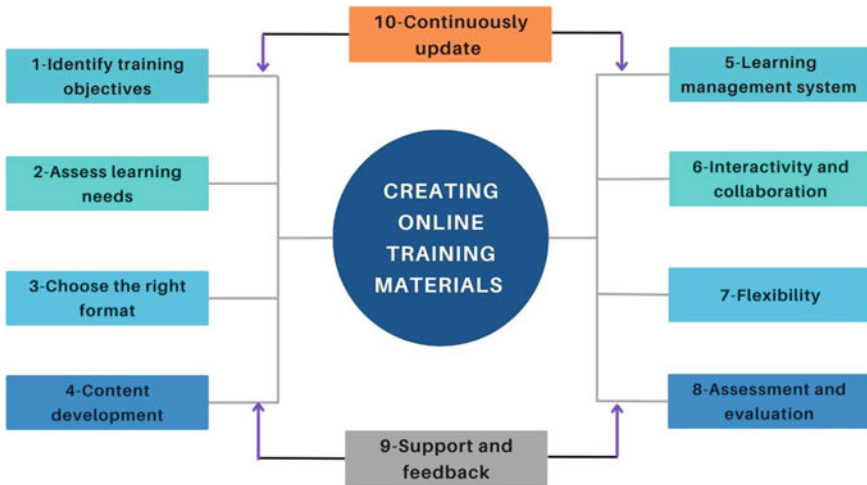


Fig. 1 Development of an online training materials process

- **Continuously update content (9):** Keep the training content up-to-date to reflect changes in the industry, technologies, or organizational practices. Outdated content can hinder the effectiveness of the training program.
- **Offer incentives and recognition (10):** To motivate students to participate actively in the training, consider offering incentives or recognition for completing the program or achieving specific milestones.
- **Support and feedback (11):** Provide adequate support to students throughout the training process. Address any technical issues promptly and be receptive to feedback to improve the overall training experience.

2.2 *The Development of a Technical Sign Language Repertoire (TSLR)*

2.2.1 **The Sign Language Barrier in Technical Fields**

The development of accessible interactive training materials involves considering various components to ensure that the training is inclusive and effective for a diverse audience. Figure 2 depicts the components accessible interactive training materials process. The process of creating a technical sign language repertoire (TSLR) is a response to a significant challenge faced by Deaf and HoH individuals in technical professions (Fig. 3). In many cases, established sign language systems lack specialized signs for tools, machines, devices, and technical processes used in specific work

environments. This deficiency in technical sign language can lead to communication problems and hinder the career growth and job satisfaction of Deaf and HoH professionals. This endeavor needs to be undertaken by a group of experts as outlined below:

Field professionals (team): Deaf and/or HoH individuals with on-the-job experience in the field where the TSLR is being developed.

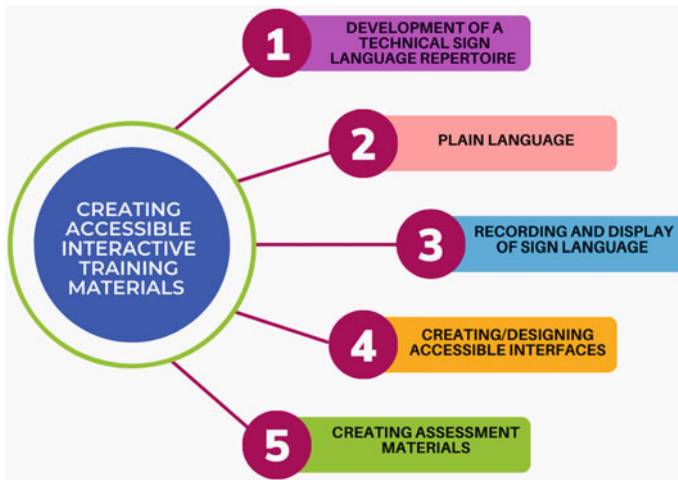


Fig. 2 Creating accessible interactive training materials process



Fig. 3 Schematic representatives of technical sign language process

Linguist: A deaf sign language expert proficient in the designated sign language at a C2 level (based on the Common European Framework of Reference for Languages—native level).

Technical sign language repertoire: Sign language equivalents for tools, machinery, devices, technical procedures, etc., that a professional can use in a predetermined work environment.

Process: The process of developing the repertoire as outlined below.

Engineers: Team composed of hearing experts (mechanical engineers) who compile a list of personnel to be addressed within the endeavor and prepare and revise written drafts in the technical language to be used.

End-users (recipients): Present and future employees and anyone who uses the sign language in question; represent the ultimate users. Final users may also include all users of the specified sign language (the sign language community).

Application: Mobile application and website through which TSLR is shared with the end-users.

2.2.2 Need for Developing TSLR

The need to develop TSLR arises in two different situations:

(a) *Lack of signs corresponding to technical terminology*

In work processes, deaf and hard-of-hearing individuals working in technical environments may encounter communication issues when there are no sign language equivalents for components, parts, elements, etc., used in their work. Most institutional and other educational programs are designed for hearing individuals, and professional interactions primarily occur through spoken language. Additionally, accessible education for deaf and hard-of-hearing individuals is often lacking. Consequently, these individuals may not possess the necessary contextual knowledge to perform their jobs professionally, which negatively affects work quality. Furthermore, they may be unable to pursue professional development in such work environments. In such cases, it is imperative to provide these groups with the same opportunities as their peers, which can only be achieved through clear communication flow with hearing colleagues within the group.

(b) *Existing signs not widely known or used*

In many cases, deaf and HoH individuals employed in a specific work environment may have developed a set of signs related to their jobs. It is necessary to ensure the sustainability of this naturally evolving repertoire and create a system for transferring these signs to professionals in similar fields. This not only enhances efficiency in professional communication but also contributes to the development of technical sign language vocabulary.

2.2.3 Building TSLR Development Team and Choosing Members

Creating an effective TSLR development team is critical to the success of the training. The team should reflect diversity in age, gender, and educational background to ensure a comprehensive approach to TSLR creation.

Team members:

Team members are crucial in designing and conducting the process, so their qualifications are of utmost importance. Figure 4 depicts the team members and deaf linguists during the development of TSLR. These individuals should possess the following qualities:

- Capability to represent professionals in the field effectively.
- Ability to create a draft repertoire using predetermined rules and steps directed by a professional linguist.
- Openness to guidance and collaborative work throughout the process.
- Team Selection:

Team selection should include individuals who can generate sign language inputs, considering the following criteria:

- Representation of diverse demographics (age, gender, education, etc.).
- Preliminary screening based on language skills and proficiency in sign language by the linguist.
- Voluntary participation.
- Availability of technical resources (computer, screen, internet, etc.) and time.
- Providing detailed information about the process, purpose, steps, and outputs to all participants to ensure they are on the same page.

Professional linguist: A deaf sign language expert with native-level proficiency. This individual guides the team through the development process, providing linguistic expertise. The linguist operates in tandem with the development team, forming a



Fig. 4 a TSLR development team members, b deaf linguist

collaborative partnership essential for the successful development of the TSLR. To achieve this, they should have access to a diverse array of aids and resources, all aimed at streamlining and enhancing the development process.

Deaf and HoH experts: Individuals with practical experience in the field who understand the technical nuances. Their input is invaluable for accurate sign creation.

Engineers: Hearing technical experts responsible for drafting initial technical language input. They collaborate closely with the team to provide the foundational technical content.

Volunteers: Team members must volunteer and have the necessary resources and time commitment for the training. Clear communication about the purpose, steps, and expected outcomes is vital to ensure alignment.

The role of a professional linguist is pivotal in the development of a TSLR (Technical Sign Language Resource). Their responsibilities encompass several crucial tasks:

Terminology mining: The linguist works closely with engineers, utilizing a pre-determined list of technical concepts. Their primary goal is to identify and incorporate accepted terminology into the TSLR, ensuring that it aligns seamlessly with the training objectives.

Arbitration: In situations where multiple signs are proposed for a single technical element, the linguist becomes the ultimate decision-maker. They assess and select the most appropriate sign based on linguistic criteria and clarity, maintaining the integrity of the TSLR.

2.2.4 Support Materials for Linguists (and the Team)

The linguist works with a pre-defined “concept list” provided by engineers and may expand the lists with inputs from the team when necessary. The linguist should identify and define the established terminology inputs from the team (extracting terminology from the team). In cases where multiple signs are developed to refer to a single item or component, the linguist should mediate. The arbitration activity carried out by the linguist should result in selecting the most linguistically and functionally suitable option.

In the context of the details provided above, since the linguist also acts as a sort of team educator, it is crucial to equip this expert and provide assistance in carrying out their role. In this context, the following aspects are significant:

- Providing the linguist with a standard list of machine elements and their explanations (prepared in plain and accessible language, along with other resources) is essential. This is considering that the linguist is not an engineer, and this professional is a member of the Deaf community.

- If there is no groundwork laid for the linguist to internalize or access the information using accessible resources, linguists and engineers should facilitate communication for the linguist by engaging an expert sign language interpreter in the field.
- Visual resources should be provided to the linguist to ease the process of terminology preparation and development.
- The provision of technical or other visual drawing types is crucial. Terminology and input development activities cannot be carried out solely using written materials.

2.2.5 Rules to Be Observed by Linguists Throughout the Process

The sign selected for a machine element should be a “natural sign” in the respective sign language (at the language level) and should be adoptable by users at the national level.

Any signs already in use by the team should be added to the repertoire.

Sign language options developed for machine elements in other sign languages can be considered reliable and effective sources. Therefore, the linguist needs to research these signs in other sign languages.

To determine and gain acceptance for the most common and acceptable option, the team should be divided into smaller working groups under the guidance of the linguist.

The linguist should ensure that the developed signs are acceptable to the broader Deaf community, both structurally and contextually. The linguist should coordinate team efforts with other Deaf community representatives.

The linguist should confirm that all sign language and other materials (finger spelling, visual support materials, written information, etc.) to be included in the application and website providing access to information are complementary and accessible to end-users.

In the process of generating input, linguists have three reference sources at their disposal: (a) visual support used to refer to an element or concept, (b) finger spelling of the element or concept, and (c) plain language text that provides input regarding the function or concept. The linguist must decide on the communication channel (online, in-person, via Skype, Zoom, etc.) through which the process will be conducted and determine the type of communication flow (focus group, semi-structured Q&A, etc.). Furthermore, the linguist should ascertain the most effective ways to utilize these resources to provide the necessary input.

If the linguist presents the element using finger spelling and the team can collectively identify and agree upon a sign language equivalent, there may be no need for written or visual aids. In such a case, it can be deduced that the machine element is well-understood, and the sign language equivalent has been efficiently determined.

If the team cannot identify a sign language equivalent for the machine element, or if multiple options exist in this context, the linguist may explore other avenues:

- Using provided visual supports to uncover signs that evoke the most associations and discussing them with the team.
- Displaying sign language equivalents in other sign languages to facilitate more effective team deliberation.
- Presenting plain language text describing the element's function with functional explanations and collaborating with the team to develop a sign that conveys a connotative meaning.

Linguists have a broader vocabulary due to their specialization, particularly in the field of technical terminology development. Therefore, several aspects fall within the linguist's area of expertise:

- Ensuring that the developed sign does not overlap with other technical signs (terminology autonomy).
- Ensuring that the sign is easily distinguishable.
- Providing specific meaning to the terminology, in contrast to a mere word.
- Making the terminology expandable for communication use.
- Addressing a hierarchical classification when developing terminology (if the element pertains to a machine, machine component, tool, etc.). Upper-level terms (classification) should be defined and added to the terminology repository when necessary.

The process of creating a new term typically involves the following steps:

- Proposal for term creation.
- Verification of the term.
- Validating the term for use.
- Introducing the term into usage.

It is essential to evaluate whether the developed terminology and discourse align with the goals of end-users and to confirm its relevance to the objectives, employers' needs, and the team's work cycle.

3 The Importance of Utilizing Plain Language

Accessibility endeavors, by their very nature, demand the involvement of professionals possessing a diverse array of skill sets, educational backgrounds, and expertise. In light of this diversity, the use of plain language emerges as a pivotal tool, one that not only accommodates the multifaceted contributors but also serves as a catalyst for coherent communication and enhanced comprehension.

Plain language, at its core, can be defined as language that is clear, concise, organized, and tailored to the specific audience it addresses. While there may not exist a universal guide applicable to plain language across all languages and contexts, there are what can be referred to as "fundamental attributes" of plain language. Individuals entrusted with the task of crafting plain language models must possess a

profound understanding of the concept's principles and objectives. They must then adeptly adapt these principles to their respective languages and contexts, ensuring that plain language remains effective and impactful.

Plain language offers a host of benefits, both tangible and abstract:

- **Efficiency in Information Transfer:** The use of plain language expedites the dissemination of information, ensuring the prompt and effective conveyance of the intended message.
- **Broadening the Reach of Your Message:** By employing plain language, the message extends its accessibility to a broader audience, surmounting potential communication barriers that might hinder understanding.
- **Reduced Likelihood of Misinterpretation:** The inherent clarity within plain language serves to reduce the probability of misinterpretation. Consequently, less time is expended on elucidating textual content, especially when it encompasses instructional elements. This streamlined approach leads to a more efficient understanding and adherence to directives by the end-users.

When it comes to crafting descriptions of machine parts using plain language, several key considerations should guide your approach:

- Tailor your language to the specific audience you are addressing, avoiding reliance on personal preferences or specialized jargon.
- Structure your sentences to ensure they are easily comprehensible to individuals from diverse backgrounds and varying levels of expertise.
- If the use of technical terms is unavoidable, provide clear explanations at the initial introduction of these terms to enhance overall clarity and understanding.
- Prioritize the use of commonly recognized synonyms, particularly when dealing with less familiar terminology or concepts.
- Steers clear of circular definitions, a practice that involves refraining from incorporating elements from the term itself when providing its definition. Maintain consistency and ensure comprehensive understanding by including any term or machine element used in the definition of another machine element within the Technical Sign Language Development (TSLD) list. This practice promotes a cohesive and standardized approach throughout the content.

By adhering to these principles and recognizing the value of plain language, you can effectively bridge the gap between complex technical information and end-users with diverse backgrounds, ultimately enhancing accessibility and comprehension in your training.

4 Recording and Displaying Sign Language Materials

In the intricate world of sign language, the process of recording videos demands a distinct blend of skills, the utilization of specialized tools, and meticulous planning. In this chapter, we pave the way for effective sign language video creation.

4.1 *The Art of Sign Language Narration*

At the heart of sign language video production lies the pivotal role of the narrator. This individual is entrusted with the responsibility of not only conveying messages through the medium of sign language but also ensuring that the content is lucidly comprehensible. The narrator stands as a linchpin in content validation and linguistic adaptation, weaving together the intricacies of language, culture, and communication. A truly qualified narrator possesses a rich tapestry of attributes, including:

- **Being Deaf or HoH:** This attribute bestows upon the narrator a unique ability to convey not just linguistic nuances but also cultural subtleties, offering a deeper layer of authenticity to their communication.
- **Fluency in Sign Language:** Proficiency in generating sign language text with fluency is essential. The narrator's capacity to articulate complex concepts with grace and clarity is foundational.
- **Primary Use of Sign Language:** Sign language is not just a tool but a natural medium of communication for the narrator. It is their native language, the very essence of their expression.
- **A Role Model within the Deaf Community:** The narrator serves as more than just a communicator does; they are a beacon within the Deaf community, inspiring others through their mastery of sign language and cultural alignment.
- **High Proficiency in Common Written Language:** A deep command of written language allows the narrator to bridge the gap between the Deaf and hearing worlds.
- **Educational and Professional Background:** A robust foundation in linguistics, language teaching, and sign language interpreting equips the narrator with the knowledge and skills needed to navigate the intricacies of communication.
- **Deaf Community Engagement:** Prior experience in working within the Deaf community provides valuable insights into the community's dynamics and needs.
- **Cultural Awareness:** A nuanced understanding of Deaf culture and the Deaf community enriches the narrative and ensures cultural sensitivity.
- **Regular Interaction:** Consistent engagement with members of the Deaf community fosters a connection that is reflected in the narrator's communication.
- **Translation Proficiency:** The ability to seamlessly translate written materials into sign language, and vice versa, is an indispensable skill.
- **Media Production Expertise:** Proficiency in visual-audio production, design, and editing guarantees the creation of engaging and informative sign language videos.
- **Quality Control Skills:** A narrator must possess the ability to review, verify, and monitor the final product, ensuring its accuracy and adherence to standards.

4.2 The Collaborative Power of the Sign Language Coach and Team

A well-coordinated team is imperative to elevate the quality of sign language videos. The sign language coach plays a vital role in assisting the narrator during video preparation, while the sign language team serves as the guardians of authenticity and clarity. Here is a glimpse into their roles:

Sign language coach:

The sign language coach offers guidance and support to the narrator during the preparation of sign language videos. Proficiency in local sign language and sign language translation is paramount for this role.

Sign language team:

Comprising representatives of the Deaf community, the sign language team evaluates and approves the recordings crafted by the narrator. These individuals are highly skilled in sign language usage, serving as role models for the community. They possess the competence to assess and approve the use and presentation of sign language in videos.

The technical expert:

For the orchestration of a flawless recording, a technical expert is required. Their role involves meticulous consideration of technical recommendations to optimize the recording process. Here is a glimpse into their realm:

4.3 Technical Recommendations

Camera format

Ideally, the person operating the camera should be well-versed in sign language, facilitating seamless communication with the narrator.

The choice of a digital camera reigns supreme due to its user-friendly interface, superior quality, and expansive storage capacity, which is ideal for lengthy recordings.

To capture the essence of sign language with precision, the camera should boast ample storage to accommodate 60 min of video.

High-resolution filming capabilities are essential, as they offer the flexibility to fine-tune quality during post-production, ensuring that the final product is a masterpiece of clarity.

The camera should allow manual adjustments to aperture and shutter speed whenever possible, affording greater creative control.

Manual focusing capabilities are preferred to ensure that the narrator remains the focal point.

The option for manual white balance adjustment, whether through automatic or manual settings, enhances color accuracy and consistency.

Narrator's attire

Attire plays a significant role in ensuring visual clarity for Deaf and HoH individuals who may have visual impairments.

Narrators are advised to wear clothing that starkly contrasts with their skin tone, offering easy visual distinction. Options include dark colors such as black, brown, navy, and dark green, or light shades like off-white or various tones of orange.

Simplicity is key, with plain colors that accentuate the narrator's hands and face, promoting visibility.

Patterns or stripes should be eschewed, and clothing with low V-neck or round-neck designs is preferable.

Though not obligatory, long-sleeved tops that extend to the wrists can enhance visibility.

Consideration should be given to hairstyles, jewelry, and clothing that do not obscure the face and hands, with cultural sensitivities considered.

The recording is an intricate process that combines linguistic prowess, technical finesse, and cultural sensibilities. Additional elements of the recording process, from lighting techniques to studio setup and beyond are important all in pursuit of crafting sign language videos with precision and impact.

Lighting

Adequate lighting is essential to ensure clear visibility of the narrator. During video capture, care should be taken to minimize shadows caused by the narrator, equipment, and other elements. Lighting should create sufficient contrast between the screen, the narrator, and the background. Natural lighting is recommended. Attention should be paid to potential shadows. When using artificial lighting, two methods are available:

'Three-point' lighting: One primary light is positioned approximately 45 degrees to the right or left of the narrator and 45 degrees downward to illuminate their face and body. Fill lights are placed behind and in front of the main light at the camera's height, and a back light is positioned slightly above the narrator, creating a backlight that reflects off the screen.

Flat lighting: Two lights are positioned in opposite directions behind the camera to illuminate the entire area and eliminate shadows.

Studio and equipment

- Availability of a film studio.
- Recording studio.
- 1 digital professional camera.
- 1 tripod.
- 1 computer.
- Broadcast preparation software.
- Video compression software.
- A screen (green or blue).

- Studio layout plan indicating the necessary distance between the camera, narrator, reflectors, screen, and more.

4.4 Recording and Video Capture

Here are some points to watch out for during recording and video capture. The camera should be at eye level. The narrator should directly address the viewer. Signs should be fully visible on the camera (the narrator's hand movements should be visible upwards, downwards, and to the sides). The sign area should be covered—most sign languages require visibility from below the waist to above the head and at least one elbow's width to the sides. The camera should not be moved; it should remain in the same position throughout recording. The area where the narrator can sign should be defined. The signing area should be determined. To maintain quality, manual focus may need to be used instead of automatic focus. Manual zoom or specific camera placement may be necessary. The distance between the screen, narrator, and camera should be less than 2 m. The narrator should appear natural and not look at an assistant or divert attention from the camera.

The narrator should have a thorough understanding of the material, maintaining fidelity to the written source. The translation team should focus on creating accurate sign language translations at the conceptual level rather than literal word-by-word translations.

Recording in small segments may be preferable to ease editing and maintain a natural flow.

Additional responsibilities

- Ensure the studio is clean and available.
- The camera should be fully charged or plugged in during recording.
- Lights should be operational, and necessary cables should be set up.
- The technical coordinator, narrator, support team, and cameraperson should all be present in the studio simultaneously.
- Arrive at the studio one hour before recording to prepare equipment.
- Short test footage should be captured before the actual recording begins.

Post-production process

The narrator should be clearly visible on screen, allowing viewers to see all movements and facial expressions.

Facilitating the identification and use of sign language videos is essential (see above stated suggestions for accessible website and app design).

5 Designing for Inclusive Accessibility: Considerations for Creating Mobile App Interfaces

5.1 *Choosing the Right Training Delivery Method*

In the journey of creating an effective training program, the initial step involves selecting the most suitable training delivery method. This decision is pivotal and must be made after a careful evaluation of various factors, including the training objectives and the composition of the target audience. Different organizations may adopt diverse approaches, tailored to their specific requirements and the nature of the content they wish to convey. Here, we explore several training delivery methods:

Microlearning: A revolutionary training approach characterized by its succinctness. Microlearning offers short, focused, and bite-sized learning modules, typically spanning a brief 3–5 min. Designed to deliver just-in-time information, it is tailored for those with busy schedules and a need for swift access to specific knowledge or skills. Its adaptability across various devices makes it a convenient choice for on-the-go learners.

Mobile learning (mLearning): In the age of ubiquitous mobile devices, mLearning courses are designed exclusively for smartphones and tablets. More comprehensive than microlearning, yet shorter than traditional training courses, mLearning offers flexibility. Learners can access training content anytime, anywhere, catering to the modern, mobile lifestyle.

Blended learning: This innovative approach seamlessly melds both online and face-to-face training components. Students can engage in online modules at their own pace while also benefiting from in-person training sessions. Blended learning provides the flexibility of self-paced learning combined with the invaluable advantages of human interaction with instructors and peers. It shines particularly when dealing with intricate subjects that necessitate additional guidance or hands-on practice.

Other training delivery methods: Beyond the aforementioned methods, various alternatives exist, such as traditional instructor-led training (ILT), virtual instructor-led training (VILT), simulation-based training, and gamified learning. Each method carries its own set of strengths and weaknesses, and the choice should be made following the specific training objectives, learner preferences, and available resources. The selection of the appropriate training delivery method is pivotal, for it can significantly enhance the training program's effectiveness and ensure a captivating and impactful learning experience.

5.2 *Selecting the Ideal Training Delivery Platform*

With the training delivery method decided, the next crucial step is to choose the appropriate training delivery platform. This platform serves as the digital foundation for your online training program and must align seamlessly with your institution's needs. Here, we outline the key features that an exemplary training delivery platform should encompass:

Single sign-on (SSO): Simplifying the user experience, SSO enables users to access the training platform using their existing credentials from other systems, eliminating the hassle of multiple usernames and passwords.

Cloud hosted solution: Embracing the benefits of the cloud, a cloud-based platform offers scalability, accessibility from anywhere with an internet connection, automatic updates, and reduced IT infrastructure costs.

Offline access: Recognizing that some learners may contend with limited or intermittent internet access, the platform should provide the option to download training modules for offline access, ensuring continuous learning even in challenging connectivity scenarios.

White label: Personalization is key, and a white-label solution allows you to brand the training platform with your institution's logo, colors, and themes, creating a cohesive and bespoke learning environment in line with your organization's identity.

Content security: Security is paramount for safeguarding sensitive training content and user data. The platform should feature robust security measures to protect against unauthorized access and data breaches.

Responsive interface: To accommodate various devices, including desktops, laptops, tablets, and smartphones, the platform must be responsive and adaptable, ensuring learners can access training content seamlessly on their preferred devices.

Ease of management: User-friendliness extends to administrators and trainers as well. An intuitive interface simplifies content management, making it easy to upload, organize, and manage training content.

Collaboration features: Fostering a collaborative learning environment, the platform should offer social learning features, discussion forums, and peer-to-peer interaction, facilitating knowledge sharing among learners.

Interactive widgets: Engaging learners further, interactive elements such as quizzes, simulations, and gamified activities enhance learner engagement and knowledge retention.

Analytics: Robust analytics and reporting capabilities are vital for tracking learner progress, assessing the training program's effectiveness, and identifying areas for improvement.

Integration with existing learning and development platforms: Streamlining the training process, seamless integration with existing HR and learning management systems (LMS) enables efficient data exchange.

The careful consideration of these features empowers organizations to select a fitting training delivery platform. It aligns with their training goals, enhances user experience, and bolsters the overall success of the online training program.

5.3 Enhancing Engagement with Interactive Features

Creating an online training program that captivates learners and enhances knowledge retention involves the strategic incorporation of interactive features into the content. These interactive elements not only boost learner engagement but also contribute to better retention of knowledge. Here are some interactive features to consider:

Page curl: This effect emulates the physical act of turning pages, evoking the feel of a traditional book or manual. It adds a touch of familiarity and enriches the overall user experience.

Text highlight: Allowing learners to highlight critical text passages directs their attention to essential information, enhancing comprehension.

Bookmark: Learners can mark specific pages or sections for quick reference, facilitating the revisiting of crucial content without the need to navigate through the entire module.

Annotation: Empowering learners to add personal notes and annotations directly within the content fosters personalized learning and allows them to jot down key takeaways and ideas.

Text search: The capability to search for specific terms or topics within the content saves time and simplifies the process of finding relevant information.

Font change: Offering options to adjust font size and style accommodates various reading preferences, ensuring a comfortable reading experience for all learners.

Share option: Enabling learners to share specific content or notes with colleagues encourages a collaborative learning environment and promotes knowledge sharing.

Interactive quizzes and assessments: Incorporating interactive quizzes, simulations, and assessments throughout the training module reinforces learning, encourages active participation, and helps learners gauge their understanding of the material.

Multimedia integration: The integration of multimedia elements like videos, audio clips, animations, and infographics introduces variety to the content and keeps learners engaged.

Gamification elements: Gamified elements such as badges, points, and leaderboards add an element of enjoyment to the learning experience, motivating learners to complete the training program.

By integrating these interactive features into the training modules, organizations can craft a dynamic and engaging learning experience that sustains student interest, motivation, and active participation in the training process.

5.4 Inclusive Accessibility Design

Inclusive accessibility design represents a commitment to creating designs that cater to users with disabilities. It acknowledges the diverse skills, habits, and preferences of individuals with disabilities, ensuring they can access products or services on an equal footing with their non-disabled counterparts. This approach encompasses linguistic, presentational, and content-based considerations, promoting an inclusive and accessible digital environment. Figure 5 shows a sample accessible mobile application interface.

Designing in line with the principles of inclusive accessibility entails leveraging various resources, including:

Literature and research: Insights gleaned from existing research and practices in the field.

Previous designs for similar audiences: Drawing inspiration from past designs targeted at the same disability group.

Input from disabled individuals: Gathering information and validation from individuals with disabilities involved.

Experiences of accessibility advocates: Tapping into the experiences of experts in the field of inclusive accessibility.

5.5 Exploring the Dimensions of Inclusive Accessibility

Defining the target audience: Identifying the target audience is crucial. However, it's essential to recognize that the size and characteristics of this audience can vary significantly. Design decisions for a broad audience encompassing all deaf and hard-of-hearing individuals will differ from those targeting a specific subset, such as a particular age group employed in a specific workplace. Therefore, depending on the nature of the task:

- Obtaining audience insights from organizations representing a broad spectrum of deaf and hard-of-hearing individuals.

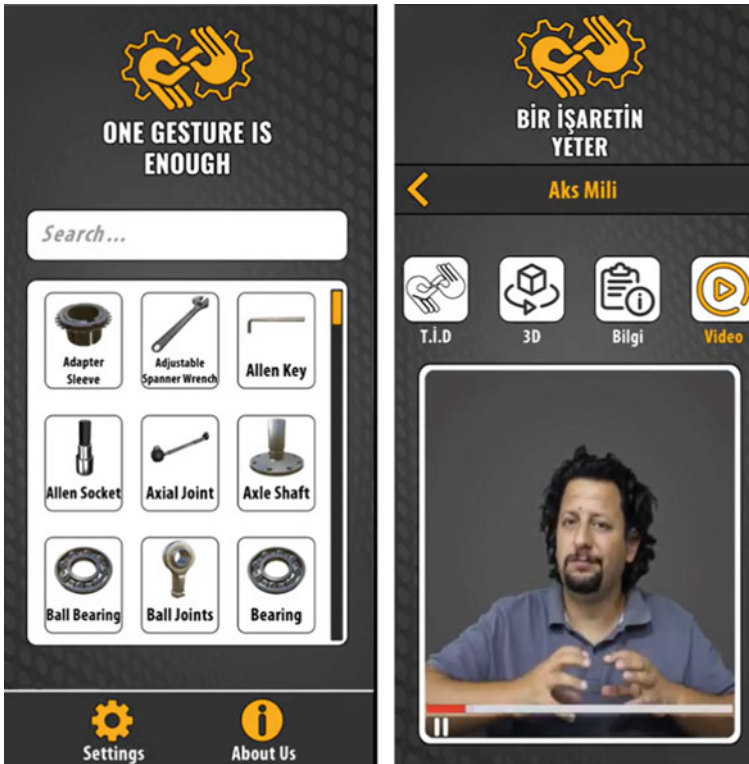


Fig. 5 Designing accessible mobile application interface

- Alternatively, when dealing with smaller, more defined groups (such as age groups or educational backgrounds), take a sample segment from that group.

Proceed with consideration for both the limitations and capabilities of the disabled individual.

When the target audience encompasses multiple profiles: In cases where the target audience includes various profiles, prioritize design based on the skills and limitations of the most disadvantaged group. While aiming to cater to this group might not fulfill the “wants” of all other users, it ensures that the service or product remains accessible and usable for everyone.

5.6 Misconceptions About Design Elements

Assuming familiarity with common online features: It is a misconception to assume that the target audience is already familiar with every online feature because

many applications follow the “design for all” or “universal design” principles. In reality, while some applications may aim for inclusivity, they do not always succeed, and others are designed without considering accessibility at all.

Neglecting details: Inclusive accessibility often hinges on the fine details. Design teams often make routine decisions, particularly regarding aesthetics and engineering design. However, in most cases, a product’s accessibility hinges on the details.

Misjudging perception abilities: It is a significant fallacy to assume that deaf and hard-of-hearing individuals have lower perceptual abilities compared to the general population. When non-deaf individuals observe limited interactions and gaps in knowledge during communication with deaf individuals, they may inadvertently fall prey to misconceptions.

It is important to remember that, historically, the majority of systems, services, and products worldwide have been designed with non-disabled individuals in mind. Accessibility for deaf and hard-of-hearing individuals was often added as an afterthought, resulting in mixed success. For instance, movies were initially designed for hearing audiences, and subtitles or sign language interpretation were later included. However, in some cases, the addition of these features did not ensure accessibility, as the extensions were not designed with accessibility in mind from the start.

5.7 *A Shift in Design Perspective*

While we focus on designing for the deaf and HoH audience, the necessity of adopting a different design perspective from day one must be underlined. In all interface designs for inclusive accessibility, it is vital to embed this mindset from the outset. The most significant risk here is progressing without consulting the user base. Unintentional mistakes can occur when designers proceed without a deep understanding of the user population.

Deaf and HoH individuals living in a world not designed for them have developed superior “accessibility skills” for coping. They navigate a world where communication has been a challenge since birth. Thus, their “accessibility skills” often surpass those of the average non-disabled user.

Universal standards for inclusive accessibility: While there are universal standards for inclusive accessibility design, it is crucial to remember that the realities of disabled individuals vary by country, language, culture, and target audience. Different socio-economic strata in each society typically house disabled individuals. Due to this, their access to education and the workforce can vary, introducing additional constraints. The degree of constraint varies according to the realities of the broader society. For instance, in many countries, deaf and hard-of-hearing individuals participate in “inclusive education,” sharing classrooms with their hearing peers. However, the success of this system relies on proper implementation. If deaf and HoH children

are exposed to the same educational system and curriculum as their peers (such as a teacher verbally explaining a topic and asking students to read from textbooks for reinforcement), this places the deaf child at a disadvantage. They would not have access to the primary mode of communication, spoken language. Furthermore, the materials given for reading may not be in their “primary communication language”. Consequently, while inclusive education works well in some countries where the groundwork has been laid correctly, in others, the same success has not been achieved.

Considering these factors, universal standards can serve as a starting point, but customized designs are essential, considering country, language, culture, and target audience.

Reading skills among deaf and HOH individuals: A widespread misconception is that the reading skills of deaf and HoH individuals are on par with those of average individuals. Particularly, there is an assumption that a deaf individual who has received a certain level of education would have grasped written language just as fluently. Two factors should be considered here:

- Due to educational disadvantages, these individuals often have lower reading and writing skills compared to the average population.
- When deaf and hard-of-hearing individuals read a written language, they do not read it in the same way as hearing individuals.

Deaf individuals often use sign language as their primary mode of communication, and it has its unique grammar, structure, and vocabulary. While there may be similarities with other languages, some elements diverge. For example, written Turkish is built upon spoken Turkish, with numerous suffixes added to the verb (tense, condition, etc.). In sign language, there are no suffixes; everything is conveyed through the signing itself. If a suffix is attached to a verb in written Turkish, the deaf individual will not have a corresponding concept in their sign language. Therefore, analyzing and decoding every suffix to understand meaning is not part of their linguistic repertoire. This is further compounded by the system’s design and educational shortfalls.

5.8 Diversity Within the Deaf and Hard-of-Hearing Audience

Deaf and hard-of-hearing users are not a homogeneous group: A prevalent misconception is that all deaf and hard-of-hearing users are uniform in their needs. However, this group of users is incredibly diverse. Their abilities and limitations can vary greatly, and design decisions should accommodate this diversity. For instance, a user with limited literacy skills may rely solely on sign language videos for information, while another user may be a proficient reader who prefers written text.

The importance of cultural sensitivity: Deaf and hard-of-hearing individuals often belong to distinct linguistic and cultural communities. Consideration of these cultural differences is vital when designing accessible interfaces. What might work for one community may not be suitable for another.

Consider the use of color: Color plays a significant role in design. For users relying on sign language or written text, color can be a valuable tool for conveying information. However, it is essential to ensure that color is not the sole means of conveying information, as this can exclude users with color blindness or other visual impairments.

Language and text: Written content must be made accessible to deaf and hard-of-hearing users. Language should be simple and easy to understand. Additionally, consider offering both sign language videos and written text to cater to a broader audience.

Support visual elements with text: When using visuals, ensure that they are accompanied by text or sign language to convey information effectively. Icons and images should be designed to be clear and easily understandable.

Consider user viewing habits: In your screen or interface design, take into account the typical viewing habits of your users. Highlight sign language or written text prominently for deaf and hard-of-hearing users.

Text formatting and fonts: Use accessible fonts and font sizes to improve readability. The choice of font size and style can significantly affect the user experience.

Training and awareness: Training your design team and stakeholders in the principles of inclusive accessibility is essential. Increasing awareness about inclusive accessibility is a fundamental step toward achieving it.

6 Creating Assessment Materials

Conducting a training needs analysis (TNA) is a crucial first step in the online training program creation process. It involves assessing the workforce's skills, knowledge, and performance gaps. By conducting a TNA, you can identify the specific training needs of your students and determine the reasons for creating a new training program. Some common reasons for conducting a TNA and building a new training program include:

- (a) **Inadequate Current Training:** The existing training program may not meet the required standards or may be outdated, necessitating the development of a new, improved program.
- (b) **Uncovered Topics:** The current training program might not cover all the essential topics or skills needed by students in their roles.
- (c) **Training Program Ineffectiveness:** Students may feel that the existing training program is not helping them learn or develop the necessary competencies effectively.
- (d) **New Skills or Technologies:** The introduction of new skills, technologies, or processes in the organization may require specialized training, prompting the need for a new program.

- (e) **Changing Training Objectives:** Evolving training goals may demand training programs aligned with the new objectives.

6.1 Language(s) to Be Used and Sensitivity to Language Structures

By understanding the specific needs and reasons behind creating a new training program, trainers can design a targeted and effective learning experience for students. When addressing the needs of the deaf and HoH community, it is paramount to recognize that this is not a homogeneous group with uniform educational backgrounds or language proficiencies. Therefore, in evaluating the accessibility of educational materials or testing comprehension, special considerations should be taken into account.

Presenting Questions in Both Languages: In order to cater to the diverse language preferences within the community, it is advisable to present questions in both sign language and written form whenever feasible. This ensures that individuals can engage with the content in a way that suits their language proficiency.

Special Attention to Exceptional Cases: Questions posed in sign language may occasionally contain exceptional cases where the answer is inherently embedded within the question. It is essential not to overlook these instances, as they can provide a holistic understanding of language comprehension.

Keep Questions Short and Simple: Crafting questions in a concise and straightforward manner is crucial. Utilizing plain language, as outlined in the Plain Language Guidelines, should be the preferred approach. This simplification enhances accessibility and comprehension for all.

6.2 The Process and Team for Developing Assessment Materials

When developing measurement and assessment materials tailored for the deaf and HoH, assembling a proficient team with specific expertise is crucial for ensuring the effectiveness and accessibility of these materials.

Subject Matter Expert: This expert possesses an in-depth understanding of the content and can strategize how questions should be formulated based on the material to achieve the desired educational outcomes.

Assessment Specialist: This professional focuses on the assessment process and evaluates questions in terms of assessment quality. They ensure that an adequate

number of questions align with educational objectives and that the assessment serves its intended purpose.

Accessibility Expert: A consultant with expertise in creating questions that are accessible in terms of formats, modalities, and perceptual levels for deaf and HoH individuals.

Deaf Linguist and Sign Language Expert: An expert who can review questions and confirm their accessibility for the target audience, particularly in sign language.

Sign Language Interpreter: An integral member of the team who facilitates effective communication among team members and individuals from the deaf and hard of hearing community.

6.3 Steps in Developing Measurement and Assessment Materials

Identification of Intended Learning Outcomes: Begin by clearly outlining the intended learning outcomes to serve as a foundation for question creation.

Determination of Question Types: Categorize question types as headings based on the intended learning outcomes, ensuring alignment.

Creating Questions: Questions are formulated by extracting relevant information from sources following the predetermined question types. It is essential to ensure that no question's answer is concealed within another question or answer choice.

Language and Presentation Check: Thoroughly review question sentences, focusing on language clarity and accessibility. Confirm that both written and sign language versions of questions are available.

Review of Questions: Questions are revised and refined based on feedback and assessments.

Pilot Group Testing: Before finalization, questions undergo testing with a pilot group to assess their clarity and effectiveness.

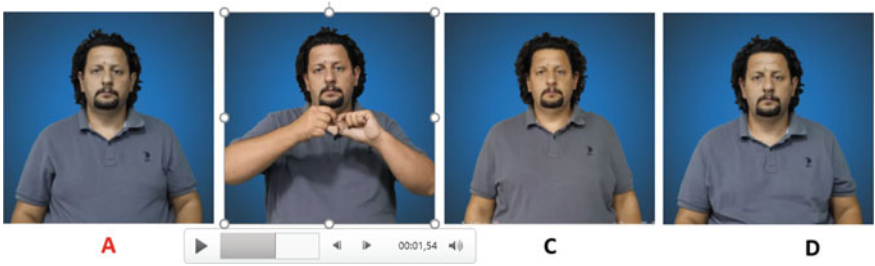
Measurement and Assessment Process: The actual measurement and assessment process can be conducted through various means, whether face-to-face or online, to evaluate learners' comprehension and knowledge retention.

Sample questions:

Picture from video: **Question1: What is the sign shown in the video?**



Video from name: **Question 2:** Taps are tools used to create screw threads. It is used to create threads inside the guide hole. Look at the videos. Which is the tap?



Picture from video: **Question3:** What is the sign shown in the video?



Video from the picture: **Question 4:** The micrometer seen in the picture. Look at the videos. Which one is micrometer?



By following these comprehensive steps and assembling a dedicated team of experts, you can ensure that the learning experience for deaf and HoH individuals is not only accessible but also effective in achieving educational objectives.

7 Conclusions

The development of accessible digital training materials and Technical Sign Language Repertoire (TSLR) is pivotal for promoting inclusivity in technical professions, particularly for the Deaf and HoH.

We began by outlining a systematic approach to creating online manufacturing engineering training materials, emphasizing aligning objectives, assessing learner needs, choosing formats, and utilizing learning management systems. Interactive elements, flexibility, regular assessments, content updates, and incentives were highlighted as vital for success.

The creation of TSLR addresses challenges faced by Deaf and HoH individuals in technical fields, including a lack of specialized signs. We discussed two scenarios: the absence of signs and formalizing existing ones, stressing the importance of a diverse development team and the linguist's role.

Plain language use was underscored for accessibility, focusing on clarity and conciseness, tailoring language, optimizing sentence structure, and explaining technical terms.

Lastly, we explored recording and displaying sign language materials, emphasizing skilled narrators, collaborative efforts with coaches and teams, and technical expertise.

In essence, accessible training materials and TSLR promote inclusivity, bridging gaps, and empowering individuals. Our exploration covered various aspects of effective online training programs, from delivery methods and platforms to engagement strategies, accessibility design, designing for the Deaf and HoH, and measurement materials. These principles enable organizations to create inclusive training, fostering continuous learning and success.

References

- Antia, S. D., Reed, S., & Kreimeyer, K. H. (2005). Written language of deaf and hard-of-hearing students in public schools. *Journal of Deaf Studies and Deaf Education*, 10, 244–255.
- Atayurt Fenge, Z. Z., & Subaşıoğlu, F. (2019). Dünyada ve Türkiye’de İşitme Engellilik: Zaman Çizelgesi. *Ankara Üniversitesi Dil ve Tarih-Coğrafya Fakültesi Dergisi*, 59, 1188.
- Duggin, A. (2016). *What we mean when we talk about accessibility*. *Accessibility in government*. <https://accessibility.blog.gov.uk/2016/05/16/what-we-mean-when-we-talk-about-accessibility-2/> (accessed December 14, 2023).
- Erdiken, B. (2005). Anadolu Üniversitesi Engelliler Yüksekokulundan mezun olmuş işitme engelli öğrencilerin istihdamı, iş durumu ve ayrımcılık. *Öz-Veri Dergisi, TC Başbakanlık Özürlüler İdaresi Başkanlığı*, 2(1), 377–503.
- Güldenöğlü, B., & Miller, P. (2014). İşiten ve İşitme Engelli Okuyucuların Kelime İşleme Becerilerinin Karşılaştırmalı Olarak İncelenmesi, 29, 18–38.
- İlkbaşaran, D. (2015). *Literacies, mobilities and agencies of deaf youth in Turkey: Constraints and opportunities in the 21st century* (Unpublished doctoral dissertation), The University of San Diego.

- Kalkan, Ö. K., & Karabulut, Ş. (2021). Türkiye’de Metal Sektöründe Çalışan SağırlaİlişkinBir DuruAnalizi. *Sosyal Politika Çalışmaları Dergisi*, 53, 941–1062.
- Kyle, F. E., & Harris, M. (2006). Concurrent correlates and predictors of reading and spelling achievement in deaf and hearing school children. *Journal of Deaf Studies and Deaf Education*, 11, 273–288.
- Myers, B., & Martin, T. (2021) Why plain language? Linguistic accessibility in inclusive higher education. *Journal of Inclusive Postsecondary Education*, 3(1).
- Schriver, K. A. (2017). Plain language in the US gains momentum: 1940–2015. *IEEE Transactions on Professional Communication*, 60, 343–383.

Index

A

Abrasive materials, 224, 227–229, 231, 240, 257
Abrasive Waterjet (AWJ), 221–224, 226, 228, 230–232, 235, 237, 240, 242, 244, 252, 255, 257
Abrasive waterjet cutting, 226
Accessibility, 6, 76, 290, 298, 299, 304, 305, 307, 309, 311–313, 316
Accessible interactive materials, 289, 292, 293
Accessible materials, 312
Additive manufacturing, 3, 9, 22, 105, 106, 115, 153–155, 167, 170, 259, 261
Aerospace, 22–26, 51, 81, 261, 274
Algorithm, 265, 274, 276, 280
Alignment, 12, 17, 91, 141, 157, 158, 178, 186, 192, 199, 205, 213, 214, 216, 266, 296, 300, 313
Analysis of Variance (ANOVA), 112–114
Analytical analysis, 51, 57, 60, 73
Ashby diagram, 25, 29, 32, 36, 37
Attention Deficit Hyperactivity Disorder (ADHD), 8–10, 17, 18
Autism Spectrum Disorder (ASD), 8–10, 17, 18

B

Bloom's taxonomy, 4, 14, 17, 54, 55

C

CAM programming, 154, 155, 157, 174–176
CAM simulation, 200, 206, 208

Casting, 22, 32, 34, 117–119, 126, 127, 129, 151, 153–156, 159–161, 165, 172, 174, 177, 180
Clamping, 40, 45–47, 87, 88, 90, 138, 214, 226
CNC, 151, 154, 155, 159–161, 174–177, 180, 187, 209, 210, 227
Computed tomography, 261–263, 268, 269
Computer-Aided Design (CAD), 6, 17, 67, 109, 110, 152, 153, 155, 169, 185–188, 193, 194, 222, 227, 241, 260, 262, 263, 267, 268
Computer Aided Manufacturing (CAM), 152–155, 161, 174–176, 185, 193, 200, 208, 222
Conceptual design, 151, 155–158, 182
Coordinate Measuring Machine (CMM), 151, 155, 178, 180, 262
Creativity, 1, 3, 8, 55, 76, 153, 179, 180
Critical thinking, 1, 3, 17, 23, 36, 37, 54, 55, 76, 104
Cross-section, 61, 63, 132, 133, 136–138, 147, 260, 268
Cryogenic tank, 28
Cutting force, 131–139, 141–143, 145–148

D

Data analysis, 277, 278, 285
Deaf, 290, 292–297, 300–302, 307, 309–313, 315, 316
Deaf and Hard of Hearing (DHH), 290, 292–294, 296, 302, 307, 309–313, 315, 316
Defects, 40, 99, 100, 102–104, 160, 246, 252, 261, 262

Design, 1–10, 14, 15, 17, 27–29, 34–36, 39, 40, 44, 46, 53, 57, 76, 77, 83, 87, 106, 107, 109, 112–115, 126, 151–156, 158, 159, 163, 166, 168, 179, 185–187, 189, 191, 193, 196, 197, 199, 206, 218, 219, 263, 273, 300, 302, 303, 307–312

Design of Experiments (DoE), 106, 109, 111, 112, 115, 273

Design sprint, 2–5, 7, 14, 15, 17

Dimensional accuracy, 117–119, 132, 135, 138, 139, 147, 244, 248

Dynamometer, 138, 139, 147

E

Electrodes, 185, 187, 191–194, 196, 199, 200, 206, 209, 213–217

Electro Discharge Machining (EDM), 185–187, 192, 197, 213, 218, 219

Extrusion, 60–65, 69, 71–74, 77, 261, 268

F

Finite Element Method (FEM), 39, 40, 42, 46, 47, 50, 51, 57, 65, 72, 261

Forming, 8, 22, 49–60, 63, 65, 66, 68, 70, 75–77, 118, 127, 129, 133, 140, 221, 295

Fuel tank, 25, 26, 31

G

Group discussion, 26, 102

H

Handout, 24, 101

Hard of hearing, 290, 294, 307, 309–311, 313

Homework, 42, 263

Human-centered design, 2–5, 7, 14, 17

I

Ideal surface roughness, 274, 286

Ideal work method, 52, 53, 60, 63, 65, 73–75

Image processing, 188, 263

Inclusivity, 18, 309, 316

Injection, 22, 39–42, 44, 46, 47, 81, 83, 84, 86, 87, 92, 95–98, 100–104, 155, 187

Injection molding machine, 82, 96, 100, 104

Innovation, 2–5, 8, 17, 153, 179, 219, 289

Inspection, 155, 161, 164, 177–180, 182, 259, 261, 264, 268

Internal geometry, 261, 268

Investment casting, 117–119, 126–128

K

Kerf, 228, 230–232, 244, 252, 253, 257

L

Lost wax, 127

M

Machine learning, 273

Machining, 22, 117, 119, 131, 132, 135, 137–142, 147, 151, 154, 156, 159–161, 174, 175, 177, 180, 186–188, 191, 209, 210, 214, 215, 221, 232, 255, 257, 273, 274, 277

Material extrusion, 105, 154, 159, 259, 262, 263, 277

Material selection, 21–26, 29, 30, 32, 33, 35–37

Mean Absolute Percentage Error (MAPE), 283–286

Milling, 132, 154, 155, 159, 161, 163, 174–177, 200–204, 206–210, 213, 214

Mobile app, 294, 304, 307, 308

Mold-filling, 46, 47

Molding, 22, 40, 41, 47, 81, 83, 84, 101–104

Monitoring, 6, 15, 17, 131, 135, 291

Multi-objective optimization, 21

N

Net Promoter Score (NPS), 6, 16, 18

Non-conventional machining, 221

Numerical analysis, 57, 65, 66, 69, 74, 76

O

Online training materials, 291

Opensource, 6, 17, 185, 186, 188, 219

Oral presentation, 15, 68, 75, 76, 179, 181

P

Part accuracy, 117, 244

Part quality, 40
 Plain language, 291, 297–299, 312, 316
 Polishing, 126, 127, 129, 192
 Post-processing, 65–67, 175, 209
 Problem-solving, 1, 2, 3, 17, 23, 36, 55, 103, 152, 155
 Product design, 2, 3, 17, 43, 154
 Product Lifecycle Management (PLM), 151, 152, 154, 155, 158, 163, 167
 Project-Based Learning (PBL), 55, 76, 151–153, 155, 156, 182
 Prototype, 2, 4–9, 11, 12, 17, 105, 151, 178, 186, 259
 Prototyping, 9, 10, 13, 105, 151, 259

Q

Quality control, 151, 154, 155, 157, 161, 300
 Quiz, 254, 256, 257, 291, 305, 306

R

Random forest, 274, 276, 281
 Relative Absolute Error (RAE), 283–286
 Rubric, 14, 15

S

Service-learning, 2–5, 17
 Sign language, 290–303, 309–313, 316
 Simulation, 39, 40, 42, 43, 51, 57, 65–68, 73, 76, 77, 152, 175, 200, 206, 208, 210, 304–306

Slab method, 51, 53–55, 63, 65, 69, 71, 72, 76
 Slicing, 11, 12, 109, 113, 169
 Sketch, 6–8, 10, 11, 14, 17, 110, 114, 156, 158, 160, 194–199
 Surface roughness, 106, 109, 110, 112–114, 118, 123, 124, 129, 231, 254, 262, 274, 276, 285, 286
 Sustainable Development Goals (SDGs), 4, 5, 17

T

Technical sign language, 292–294, 296, 299, 316
 Tensile testing, 262–264, 269
 3D printing, 6, 9, 11, 13, 17, 108, 113
 Torsional strength, 109
 Technical Sign Language Repertoire (TSLR), 292–296, 316
 Turning, 117–120, 126–128, 132, 137, 139–141, 143, 148, 154, 155, 159, 160, 174–177, 273–277, 286, 306
 2-stroke piston, 156, 158, 159

W

Waterjet, 221, 222, 224–226, 232, 252, 255, 257
 Wax, 117, 119–122, 124–128
 Worksheet, 24, 101